

**UNCLASSIFIED**

---

---

**AD 297 214**

*Reproduced  
by the*

**ARMED SERVICES TECHNICAL INFORMATION AGENCY  
ARLINGTON HALL STATION  
ARLINGTON 12, VIRGINIA**



---

---

**UNCLASSIFIED**

2

NOTICE: When government or other drawings, specifications or other data are used for any purpose other than in connection with a definitely related government procurement operation, the U. S. Government thereby incurs no responsibility, nor any obligation whatsoever; and the fact that the Government may have formulated, furnished, or in any way supplied the said drawings, specifications, or other data is not to be regarded by implication or otherwise as in any manner licensing the holder or any other person or corporation, or conveying any rights or permission to manufacture, use or sell any patented invention that may in any way be related thereto.

63-2-5

CATALOGED BY ASTIA  
AS AD NO. 297211

**U S A R M Y**  
**TRANSPORTATION RESEARCH COMMAND**  
**FORT MUSTIS, VIRGINIA**

TCREC Technical Report 62-3B

**FLEXIBLE-WING CARGO GLIDERS**  
**VOLUME II**

Task 9R38-01-017-72  
Contract DA 44-177-TC-779

September 1962

PREPARED BY

RYAN AEROSPACE  
A Division of The  
RYAN AERONAUTICAL COMPANY  
San Diego, California

297 214



ASTIA  
MAR 1 1963  
TISIA

## DISCLAIMER NOTICE

When Government drawings, specifications, or other data are used for any purpose other than in connection with a definitely related Government procurement operation, the United States Government thereby incurs no responsibility nor any obligation whatsoever; and the fact that the Government may have formulated, furnished, or in any way supplied the said drawings, specifications, or other data is not to be regarded by implication or otherwise as in any manner licensing the holder or any other person or corporation, or conveying any rights or permission, to manufacture, use, or sell any patented invention that may in any way be related thereto.

## ASTIA AVAILABILITY NOTICE

Qualified requesters may obtain copies of this report from

Armed Services Technical Information Agency  
Arlington Hall Station  
Arlington 12, Virginia

This report has been released to the Office of Technical Services, U. S. Department of Commerce, Washington 25, D. C., for sale to the general public.

The information contained herein will not be used for advertising purposes.

The findings and recommendations contained in this report are those of the contractor and do not necessarily reflect the views of the U. S. Army Mobility Command, the U. S. Army Materiel Command, or the Department of the Army.

Contract DA 44-177-TC-779

TCREC 62-3B  
VOLUME II

FLEXIBLE WING CARGO GLIDERS  
DESIGN CRITERIA AND AERODYNAMICS

Ryan Report No. 61B114(A)  
15 September 1962

Prepared by  
Ryan Aeronautical Company  
San Diego, California

U. S. ARMY TRANSPORTATION RESEARCH COMMAND  
FORT EUSTIS, VIRGINIA

HEADQUARTERS  
U. S. ARMY TRANSPORTATION RESEARCH COMMAND  
TRANSPORTATION CORPS  
Fort Eustis, Virginia

TCREC-ADS 9R38-01-017-72

SUBJECT: Flexible-Wing Cargo Glider

TO: See Distribution List

1. The work described in this report was accomplished by Ryan Aeronautical Company for the U. S. Army Transportation Research Command, Fort Eustis, Virginia, under the terms of contract DA 44-177-TC-779. The report covers an investigation of the use of the Flexible-Wing concept for aerial cargo delivery.

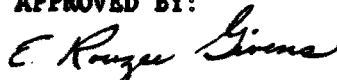
2. The conclusions made by the contractor are concurred in by this Command.

3. Based upon the facts presented in the report, proposals have been solicited and a contract will be awarded for a Flexible-Wing configuration of a 1,000-pound payload capability, which may be towed and/or dropped from existing Army aircraft. The program includes the detailed design, fabrication, and flight testing of the Flexible-Wing vehicle. The major objective of the program is to ascertain the feasibility of the Flexible-Wing concept and to provide information necessary for the development of an aerial cargo delivery system.

FOR THE COMMANDER:

  
EARL A. WIRTH  
CWO-4 USA  
Adjutant

APPROVED BY:

  
E. ROUZEE GIVENS  
Project Engineer, USATRECOM

## PREFACE

For the convenience of the reader, this report is divided into Volumes I and II. This is Volume II, and presents design data, structural description, loads and stress analysis, weights and balances, towing and control system, aerodynamics, performance, and stability and control data.

Volume I, under separate cover, presents only the highlights of the report as a Final Program Summary.

These two volumes have been prepared as the Final Report of a study program conducted for the U. S. Army Transportation Research Command by the Ryan Aeronautical Company. The study was accomplished to determine the design, performance and functional parameters of towed air logistic gliders of the flexible (or Rogallo) wing concept. The study was authorized under Contract No. DA 44-177-TC-779, dated 21 June 1961.

The study program produced designs for four basic configurations of towed gliders having payload capabilities of 250, 1,000, 4,000 and 8,000 pounds each. Alternate versions of the 250 and 1,000 pound configurations were also developed to provide capability of air dropping the vehicle from the AC-1 Caribou aircraft for point delivery of logistic materiel.

## CONTENTS

	<b>Page</b>
<b>PREFACE</b>	<b>iii</b>
<b>LIST OF ILLUSTRATIONS</b>	<b>v</b>
<b>LIST OF SYMBOLS</b>	<b>viii</b>
<b>I. AERODYNAMICS AND PERFORMANCE</b>	
<b>Summary</b>	<b>1</b>
<b>Method of Approach</b>	<b>4</b>
<b>Technical Discussion</b>	<b>12</b>
<b>Conclusions</b>	<b>88</b>
<b>II. STABILITY, CONTROL AND DYNAMICS</b>	
<b>Summary</b>	<b>89</b>
<b>Method of Approach</b>	<b>91</b>
<b>Technical Discussion</b>	<b>114</b>
<b>Conclusions</b>	<b>138</b>
<b>III. DESIGN CRITERIA AND STRUCTURAL DESCRIPTION</b>	
<b>Summary</b>	<b>139</b>
<b>Method of Approach</b>	<b>144</b>
<b>Technical Discussion</b>	<b>146</b>
<b>Loads and Stress Analysis</b>	<b>149</b>
<b>Conclusions</b>	<b>168</b>
<b>Weights and Balance</b>	<b>169</b>
<b>IV. CONTROL AND TOWING SYSTEM DATA</b>	
<b>Summary</b>	<b>197</b>
<b>Method of Approach</b>	<b>200</b>
<b>Technical Discussion</b>	<b>201</b>
<b>Hydraulic Actuator, Valve, and Accumulator Size</b>	<b>210</b>
<b>Conclusions</b>	<b>235</b>
<b>V. APPENDIX</b>	
<b>A. Results of Wing Membrane Fabric Test</b>	<b>241</b>
<b>B. Digital Computer Program for Flexible Wing         Cargo Glider Landing Flare Calculations</b>	<b>249</b>
<b>C. Model Specification - Strength &amp; Rigidity,         Flight Loads</b>	<b>253</b>
<b>D. Model Specification - Strength &amp; Rigidity,         Ground Loads</b>	<b>257</b>
<b>E. References - Part I &amp; II</b>	<b>263</b>
<b>F. Study Drawings</b>	<b>268</b>
<b>VI. DISTRIBUTION</b>	<b>285</b>

## ILLUSTRATIONS

Figure	Page
1 to 13 Thrust Horsepower Required - Towed Gliders incl.	15 to 27
14 to 26 Free-Flight Performance Gliders incl.	28 to 40
27 to 29 Thrust Horsepower - L-20A incl.	41 to 43
30 to 33 Take-off Ground Runs, L-20A and Gliders incl.	44 to 47
34 Glider Landing Distance	48
35 to 37 Rate of Climb, L-20A and Gliders incl.	49 to 51
38 to 49 Mission Profiles, L-20A and Gliders incl.	52 to 63
50 to 52 Take-off Distances, Helicopters with Gliders incl.	64 to 66
53 to 61 Power Required and Available, Helicopters and Gliders incl.	67 to 75
62 to 64 Rate of Climb, Helicopters and Gliders incl.	76 to 78
65 to 73 Mission Profiles, Helicopters and Gliders incl.	79 to 87
74 Axis System Convention	118
75 Longitudinal Geometry	119
76 Center of Gravity Variation with Wing Angle	120
77 Towed Glider Trim Neutral Points, Wing Alone	121
78 Towed Glider Trim Requirements	122
79 Longitudinal Tow Bridle	123
80 Tow Control Static Hinge Moments	124
81 Roll Control Geometry	125
82 Dynamic Stability Variation with Directional Stability	126

7

ILLUSTRATIONS (Cont)

Figure		Page
83	Dynamic Stability During Tow - Effect of Tow Line Length	127
84	Dynamic Stability During Tow - Effects of Attach Points	128
85	Apex Horizontal Hinge-Moment Coefficient vs. Wing Angle of Attack	129
86	Wing Sweepback Angle vs. Wing Lateral Deflection	130
87	Control Hinge Moment Coefficient vs. $\eta$	131
88	Roll Control Hinge Moment Coefficient vs. Wing Deflection	132
89	Roll Control Hinge Moment Coefficient vs. Wing Deflection	133
90	Body Group Expressed as Percent of Gross Weight for Five Towed Configurations	171
91	Body Group Expressed as Percent of Gross Weight for Five Towed Configurations	171
92	Lighting Gear Expressed as Percent of Gross Weight for Five Towed Configurations	172
93	Controls Group Expressed as Percent of Gross Weight for Five Towed Configurations	172
94	Weight Empty Expressed as Percent of Gross Weight for Five Towed Configurations	173
95	Specifications of Transistorized UHF FM Receiver	204
96	Roll Control Power System	205
97	Flare Characteristics - 4,000 and 8,000 Lb. Payload Towed Gliders	209
98	Pitch Change Diagram	214
99	Cylinder Loading - 4,000 and 8,000 Lb. Towed Glider	215
100	Remote Control Box Schematic and Layout Towed Glider	216
101	Electrical Schematic 250 Lb. Towed Glider	217

ILLUSTRATIONS (Cont)

Figure		Page
102	Electrical Schematic 1000 Lb. Towed Glider	218
103	Electrical Schematic 4,000 and 8,000 Lb. Towed Gliders	219
104	3000 PSI Hydraulic Control System - 8,000 and 4,000 Lb. Air Cargo Gliders	220
105	L-20 Aircraft Modifications	223
106	Tow Bridle of H-23D Helicopter	225
107	H-23D Helicopter Modifications	227
108	Tow Bridle of HU-1A Helicopter	229
109	HU-1A Helicopter Modifications	231
110	Tow Bridle of H-34 Helicopter	233
111	H-34 Helicopter Modifications	237
112	Helicopter/Glider Relationship - Towed Cruise Configuration	239
113	Results of Weatherometer Exposure Tests	242
114	Fabric Tests	243
115	Test Load vs. Elongation	244
116	Test Load vs. Elongation	245
117	Test Load vs. Elongation	246
118	Test Load vs. Elongation	247
119	Test Load vs. Strain	248
120	8,000 Lb. Glider, Study	269
121	8,000 Lb. Glider, Study	271
122	250 Lb. Glider, Study	273
123	1,000 Lb. Glider, Study	275
124	250 Lb. Glider - Air Drop Deployment	277

ILLUSTRATIONS (Cont)

Figure		Page
125	1,000 Lb. Glider - Air Drop Deployment	279
126	1,000 Lb. Glider - Air Drop with Cable Suspension	281
127	Landing Gear Liftoff System	283

LIST OF SYMBOLS

W	Weight
Tol	Integration Tolerance
T	Tow, lbs.
$\alpha_T$	Angle between tow axis & body X-axis
$\alpha_o$	Initial angle of attack
$z_T$	Tow moment arms, ft.
$\epsilon$	Angle, in plane of symmetry, between tow line and relative wind.
$\bar{M}_\alpha$	Longitudinal stability, dimensionalized
$\bar{M}_g$	Pitch damping, dimensionalized
$\bar{L}_\alpha$	Lift-Curve slope, dimensionalized
W	Gross Weight
$W_{max}$	Maximum gross weight
$I_y$	Pitching moment of inertia
$I_x$	Roll moment of inertia
$I_z$	Yaw moment of inertia
$I_{xz}$	Product of inertia
p	Atmospheric density
g	Acceleration due to gravity
K/	Velocity conversion factor for f.p.s.
s	Reference area
$\Delta t$	Time increment
Sref	Coefficient reference area
$C_L$	Lift coefficient
$C_D$	Drag coefficient

$V_S$	Termination velocity
$V_I$	Initial velocity
$V_I$	Initial Flight Path Angle
THP	Thrust Horsepower
DV	True Airspeed
W	Gross weight in pounds
S	Ground tow
W	Gross weight of A/C
F	Acceleration force
V	Velocity in ft./sec.
T.O.	(subscript) = Take-off
T.D.	Touchdown
$\mu$	Coefficient of friction
L/D	Lift/drag ratio
$\lambda_u$	Length of upper bridle
$\lambda_l$	Length of lower bridle
$\lambda$	Total bridle length
$V_e$	Airspeed, FPS, EAS
$U_{de}$	Gust velocity, FPS, EAS
m	Slope of Curve
$K_W$	Gust factor
S	Wing Area, Sq. Ft.
c	Average chord ft. (area/span)
H	Hinge Line
Pf	Pilot induced force
$C_{n\beta}$	Rate of change of yaw moment, Coeff. due to slide slip.

$\Lambda$	Wing sweepback angle
$\phi$	Wing deflection angle
$C_{l\beta}$	Rate of change of rolling moment Coeff. with respect to side slip
$dc_n/dQ_L$	Longitudinal state stability margin
$\Lambda LE$	Leading edge sweep angle
$C_{y_B}$	Rate of change of sideforce Coeff. w/side slip
$C_y$	Sideforce Coeff.
$C_{\eta_P}$	Rate of change of yawing moment $C_{off}$ with respect to velocity about the longitudinal axis.

## I. AERODYNAMICS AND PERFORMANCE

### SUMMARY

The data contained herein presents the results of the study which relates to the performance of the towed air logistics gliders. Four basic configurations, with payload capacities of 250, 1,000, 4,000 and 8,000 lbs. each, were analyzed for towing and free-flight modes. Performance and flight characteristics of Army aircraft used for towing, both for tow and free of tow regimes, were also analyzed; and analysis of an air drop configuration of 1,000 lb. payload capacity was made, with ejection and deployment time and motion study included. The towed paraglider in each of the configurations presented is highly compatible with helicopter tow. Use, however, of the L-20A fixed wing airplane for tow of the 250 lb. and 1,000 lb. payload vehicle is operationally suitable, but is deficient for STOL requirements. Optimum cruise speed and maximum range of the L-20 and paraglider combination do not occur for the paraglider wing loadings considered in this study.

The analysis of the air drop configuration of the 1,000 lb. payload vehicle showed that ejection and deployment from the AC-1 (Caribou aircraft) can be accomplished satisfactorily. The study indicates that best results are obtained with ejection occurring at a horizontal velocity of the carrier airplane of 200 knots and at an altitude above terrain of 1500 ft.

The study was based on assumption that the L-20A airplane and the H-23D helicopter would be the towing aircraft for the paragliders having payloads of 250 lb. and 1,000 lb. The HU1-B helicopter was considered as the towing aircraft for the 1,000 lb. and 4,000 lb. payload vehicles. The H34 helicopter was considered as the towing aircraft for the 1,000, 4,000 and 8,000 lb. payload vehicles.

The paraglider configurations studied can be considered to have an average lift/drag ratio of 3.5. The lift/drag parameter was established for wing loadings of 5, 6 and 7 lbs/ft<sup>2</sup>. It was found that maximum lift/drag occurred for each configuration at true airspeeds of 50 to 60 knots. The data herein will show that the wing loading affects the combination of the towing aircraft and the paraglider with respect to mission radius and towing airspeed. The wing loadings of the paraglider must be matched with the cruise speed of the towing vehicle. In the case of the L-20, as the tow aircraft, an increase of from 5 to 7 lbs/ft<sup>2</sup> in wing loading will increase the maximum radius of the combination by 5%. Therefore, to obtain maximum radius, the wing loading for this combination should be increased beyond the parameters studied.

Take-off and landing distances with helicopter tow for all of the configurations are comparable to established STOL requirements of 500 feet over a 50 ft. obstacle. The data shows that the L-20A airplane as a tow aircraft is not within the established STOL requirements. Take-off distance of the L-20A with the 1,000 lbs. payload paraglider is 870 feet compared with 560 ft. for the basic airplane without the paraglider. Landing distances of the paragliders are identical for all configurations regardless of weight. These landing distances are 560 ft. on a hard surface with no braking; 225 ft. on soft ground with no braking; and 175 ft. on hard surface with braking. The selection of glide speed on the final glide slope is highly critical and relates directly to the vertical descent velocity at touchdown. By maintaining a glide speed of 60 knots and proper execution of the flare, a zero vertical descent velocity at touchdown will result.

Free flight performance analyses of the paragliders were made for each of the configurations. Free flight or glide profiles were based on wing loadings of 5, 6 and 7 lbs/ft<sup>2</sup>. Body drag was based on a theoretical value for a wing loading of 6 lbs/ft<sup>2</sup>, with data extended for 20% decrease and 20% increase in body drag. Theoretical drag values were used for wing loadings of 5 and 7 lbs/ft<sup>2</sup>. Horizontal range versus release altitude data shows that the maximum range expected for the 1,000

lb. configuration is almost 7 nautical miles when the release altitude is 10,000 ft. Rate of sink data shows that minimum rate of sink in the order of 1500 ft. per minute at a true airspeed of 50 knots will occur in all configurations of similar wing loadings.

## METHOD OF APPROACH

Aerodynamic performance analysis was conducted on towed logistic gliders with payload capacities of 250, 1,000, 4,000 and 8,000 pounds. Since the configurations considered do not belong to a "family", the performance of each design was accomplished individually with no scaling of data between designs. After determining the lift and drag characteristics of the gliders, their free glide performance was calculated. Performance of the combination of various gliders in tow with an L-20A aircraft and H-23D, HU-1B, and H-34A helicopters was computed, and helicopter-glider performance was programmed on the IBM 650 digital computer. A family of wing loading and body drag variations were considered. Unless indicated otherwise, wing loading is 6.0 lbs/ft<sup>2</sup>, and body drag is the median or theoretical value. The major significant results are presented in this report.

### Lift and Drag

A lift and drag analysis of each design was accomplished. Only force characteristics of the Flexible Wing were obtained from unpublished NASA wind tunnel data. These data were for a wing with a flat plan leading edge sweep of 45° and a rigged leading edge sweep with spreader bar of 50°. The wing of each configuration was similar to the tested wing and, therefore, the data could be used directly. The drag of the body and its protuberances and the wing supporting structure was built up from each component by using experimental data and theoretical methods available in Reference 1. The drag coefficients of each component were based on the wing area by the equation

$$C_D = C_{D\pi} \frac{S}{S}$$

where  $S$  = reference area.  $C_D$  = drag coefficient, and the subscript  $\pi$  refers to the component. No subscript refers to the complete configuration. The interference drag of proximity of components was also

considered.

A cable supported wing on the 1,000 lb. payload configuration was briefly investigated. Here again, unpublished wind tunnel data corrected for leading edge radius was used for the wing force characteristics.

The lift and drag of each glider configuration was reduced to thrust horsepower required vs. true airspeed for use in the performance calculations by the equation

$$\text{THP}_{\text{Req}} = \frac{DV}{325}$$

where the drag, D, is in pounds and the flight path velocity, V, is in knots. For use in the IBM 650 helicopter program an equivalent area, f, vs. true airspeed was determined for each configuration using

$$f = C_D S$$

The drag of a 300 ft. nylon tow cable of adequate strength (hence, diameter) for each application was analyzed. From equations of Reference 2, and with a known towline tension and cable weight per foot, the cable sag may be computed. It is important to note that the tractor and towed glider are assumed to be at the same altitude. Using the computed sag and known cable diameter, the drag can be determined from Reference 1. For all configurations the resulting drag of the tow cable was less than one percent of the drag of the towed vehicle at maximum lift/drag ratio. The tow cable drag, therefore, was omitted in all computations and is not discussed in detail here.

#### Free Glide of Towed Gliders

The free glide performance of the gliders included calculation of lift/drag ratios, rates of sink, and maximum horizontal glide ranges. Rate of sink for each configuration was computed using

$$\text{Rate of Sink} = \frac{33,000 \text{ THP}_{\text{Req}}}{W}$$

where W = gross weight in pounds. The glide range in wings level flight is

$$\text{Horizontal Range} = \text{Altitude} \frac{\text{Lift}}{\text{Drag}}$$

Variations in wing loading and body drag were considered.

#### Performance of L-20A Aircraft

The substantiating data report containing the performance curves for the de Havilland L-20A "Beaver" was not available at the time this study was conducted. Only the SAC Charts (Reference 3) were obtained for reference. It was necessary, therefore, to reconstruct the thrust horsepower available and thrust horsepower required from this limited information. Power plant data was obtained from the engine manufacturer in Reference 4. Propeller characteristics, blade section data, and performance equations were obtained from References 5, 6 and 7 to complete the reconstruction of thrust horsepower available and required. Using the derived data, the climbs and missions in the SAC Charts were duplicated with reasonable accuracy to provide the necessary check.

#### L-20A - Towed Glider Take-Off

Only take-off performance of the L-20A as given in the SAC Charts was duplicated, using the following equation from Reference 8:

$$S = \frac{W}{2g} \frac{V_{T.O.}^2}{(F_{V=0} - F_{T.O.})} \log_e \frac{F_{V=0}}{F_{T.O.}}$$

In the above equation S = ground run, W = weight of aircraft, F = accelerating force, V = velocity in ft/sec, and the subscript T. O. = take-off. The same equation was used for the L-20A with a glider in tow. The take-off speed used for the 5.0 and 6.0 lbs/ft<sup>2</sup> wing loading was 45 knots, while 50 knots was used for the glider with wing loading of 7.0 lbs/ft<sup>2</sup>. For take-off it was assumed that the glider accelerated on a hard surfaced runway at maximum lift/drag ratio. At take-off airspeed the wing incidence was increased and the craft lifted off. For all cases the L-20A becomes airborne after the glider.

#### Towed Glider Landing

The landing ground roll, S, was calculated using the empirical equation from Reference 7:

$$S = \frac{0.1022 V_{T.D.}^2}{\mu - (D/L)} \log_{10} \frac{\mu(L/D)}{V_{T.D.}}$$

where  $V_{T.D.}$  = velocity at touchdown in knots,  $\mu$  = coefficient of friction,

and  $L/D$  = lift/drag ratio. Touchdown speed for all gliders was 42 knots. This velocity corresponds to a lift coefficient of 1.0 which is less than the 1.15 maximum. Ground effects were neglected. An IBM 650 digital computer program in two degrees of freedom was initiated for a cursory investigation of the landing flare problems involved. It was determined with the computer program that the gliders could not be flared to contact the ground at zero sink rate from a glide at maximum lift/drag ratio. Under this condition ground contact would occur (under ideal conditions, or initiation of flare from proper altitude) with a sink rate in the order of 7.5 ft/sec. By increasing the glide speed to 60 knots a landing flare initiated at a height of 29 ft. would touch down at zero sink rate.

#### L-20A - Towed Glider Climbs

A take-off gross weight of 4220 pounds for the L-20A was used for climb calculations. This weight is the basic mission take-off weight given in Reference 3 decreased by the internal payload and increased by the addition of a co-pilot. Rates of climb were computed using

$$\text{Rate of Climb} = \frac{33,000 \text{ THP}_{\text{Excess}}}{W}$$

where  $W$  = gross weight of L-20A or the combination of L-20A and towed glider.

#### L-20A - Towed Glider Missions

Radius type missions at sea level, 5,000 ft. and 10,000 ft. were selected for displaying relative performance of the L-20A with various glider configurations in tow. The climb portion of the missions was accomplished at maximum rate of climb. The cruise portion of the missions was computed at 99% of the long range cruise specific range. The 99% figure was used since the increase in cruise airspeed is significant for the 1% penalty in specific range. From the total of 570 lbs. of usable fuel it was assumed that 20 lbs. were used for warm-up and take-off ground run. Landing reserves (53 lbs.) include fuel for 20 minutes long range cruise at sea level and a 5% allowance for variation in individual engine fuel consumption. It was assumed that the towed gliders were released at cruise altitude at the maximum mission radius point.

### Digital Computer Program for Helicopter Analysis

An intricate program has been developed for the IBM 650 digital computer to calculate the power required at the rotor shaft, the flapping coefficients, the torque coefficients, etc., for the helicopters in their towed glider missions. The basis of the computation method is Reference 10. The charts in this reference are superior to earlier work because they include an allowance for stall in the reversed - flow region and contain no small-angle assumptions regarding blade section inflow angles and velocities. The information on the charts is actually computed from the equations in Reference 11 as needed, rather than being obtained from prohibitively large tables.

The power required at the rotor shaft is used in overcoming the rotor profile-drag, the induced and parasite-drag, and in increasing the potential energy of the helicopter in climb. The power equation is non-dimensionalized by thrust coefficient, and is written as follows:

$$\frac{C_P}{C_T} = \frac{C_{p_o}}{C_T} + \frac{C_{p_i}}{C_T} + \frac{C_{p_p}}{C_T} + \frac{C_{p_c}}{C_T}$$

The inputs which are required by the program are given below with values which were assumed to pertain to all three helicopters.

<u>Symbol</u>	<u>Input</u>	<u>Value</u>
a	slope of curve of section lift coefficient against section angle of attack	5.73 per radian
$\bar{c}_l$	average section lift coefficient in reversed velocity region	-1.20
$\bar{c}_{d_o}$	average profile drag coefficient in reversed velocity region	1.10
$\delta_o$	constant in the $C_{D_o}$ expression	0.0087
	$C_{D_o} = \delta_o + \delta_1 \alpha_r + \delta_2 \alpha_r^2$	
$\delta_1$	coefficient of $\alpha_r$ in the $C_{D_o}$ expression	-0.0216

$\delta_2$	coefficient of $\alpha_r^2$ in the $C_{D_o}$ expression	0.4
B	tip-loss factor	0.97
$\eta$	Lock number	15.0
$\sigma$	rotor solidity	
R	blade radius measured from center of rotation, ft	
$\theta_1$	difference between blade root and blade tip pitch angles, positive when tip angle is larger, deg	
$\Omega$	rotor angular velocity, radians/sec.	
W	helicopter gross weight, lb.	
$\rho$	mass density of air, slugs/cu. ft.	
$\gamma$	flight path angle (positive in climb) deg.	
$f_h$	helicopter parasite-drag area, sq. ft.	
$f_t$	towed glider parasite-drag area, sq. ft.	
V	true airspeed along flight path, ft/sec.	

The program is accurate to within 10% as indicated in an attempt to match a NASA example. This is considered adequate for a study of this type.

#### Performance of Helicopters

The correlation of the computed speed performance with the helicopter performance of References 3, 9 and 12 is good since the maximum speeds given in these references were used to derive an equivalent parasite drag area. The climb and range performance were within 10% of agreement with the references.

The following data were used as helicopter input for the performance IBM program.

Helicopter	H-23D	HU-1B	H-34A
Rotor Solidity	.03425	.0506	.0569
Blade Radius, ft.	17.7	22	28
Blade Twist, deg.	-8	-10	-8
Rotor Velocity, rad/sec	38.6	32.8	23.15
Gross Weight, lb. (including two pilots and fuel)	2478	5954	9789
Fuel, lb.	280	1007	1572
%Power Loss (cooling, gear, anti-torque, etc.)	15%	10%	15%

The power required as referred to in this report is power required by the main rotor. It does not include the power lost due to transmission, cooling, anti-torque, etc. Therefore, the power required is compared to a net normal power available which is engine brake (shaft on the HU-1B) horsepower less the losses given in the above table.

#### Performance of Helicopters with Towed Gliders

The digital computer program has been used to generate the performance data for the helicopter-glider combination. The wing loading of all configurations considered with the helicopters was 6.0 lb/ft<sup>2</sup>. The power required curves presented in Figures 53 to 61 define the maximum possible speed at the net normal power available and indicate the best speed for climb. The best climb speed is that at which level flight power is a minimum. For each configuration at a given altitude, runs were made for various climb path angles at the best climb speed. The net normal power available at that altitude then indicated the maximum climb angle. The maximum rate of climb then was simply  $R/C = V_T \sin \gamma$ . The rates of climb were then adjusted where necessary to agree with References 3, 9, and 12 for helicopter alone, and then accordingly for the combinations. The resultant rate of climb data are presented in Figures 62 to 64.

The calculated missions are shown in Figures 65 to 73 at sea level, 5,000 ft., and 10,000 ft. at the speeds for 99% maximum range. The fuel for warm-up and take-off was considered to be the fuel for five minutes of sea level normal rated power. An average rate of climb for

a given configuration determines the time required to climb at maximum normal power and therefore the fuel used. For maximum range, the system would be flown at the speed for which the specific range reaches its peak value. However, the speed was increased about five knots for only a 1% penalty in total range or radius. The gliders were released over destination at cruise altitude and the helicopter alone was returned to home base. The fuel for landing and reserve was considered to be 10% of total usable fuel. The distance traveled with the takeoff and landing fuel allowance was not included in the range capability.

#### Helicopter - Towed Glider Take-Off

The take-off performance of the helicopter - towed glider combination was calculated using the following equation from Reference 9:

$$S = \left( \frac{V}{P} \right) d \left( \frac{MV^2}{2} \right)$$

In the above equation S = ground run of the glider, V = velocity in ft/sec, M = mass of combination in slugs, and P = power available minus power required to maintain forward flight. It is assumed that the helicopter initially lifts off vertically and then accelerates a few feet above the ground until the glider becomes airborne. Similarly to the L-20A - glider take-off, the glider is accelerated on a hard surfaced runway at maximum lift/drag ratio. At a take-off airspeed of 45 knots the glider wing incidence was increased to effect lift-off.

## TECHNICAL DISCUSSION

The Thrust Horsepower Required vs. True Airspeed plots (Figure 3, for example) show that the airspeed for minimum horsepower required increases with increasing wing loading of the glider. It is apparent, therefore, that consideration must be given to matching glider wing loading to tow vehicle cruise airspeed for most efficient operation of the combination. Choice of wing loading also dictates (for a constant body drag) maximum lift/drag ratio, minimum rate of sink, and maximum horizontal glide range. These effects can be noted in Figures 14, 15 and 16. It is interesting to note that approximately the same thrust horsepower is required to tow one 4,000 lb. payload vehicle as for four 1,000 lb. payload vehicles.

The horizontal range plots are for maximum lift/drag ratio wings-level glides. Glides at airspeeds above or below the airspeed for maximum lift/drag ratio or turning maneuvers will result in decreased horizontal range.

Take-off distances of various size gliders in combination with the L-20A (Figures 30 through 33) and helicopters (Figures 50, 51 and 52) appear to be reasonable and operationally feasible. Landing the glider after a free glide, however, may present a minor problem. It was determined that the glider could not be flared to a zero sink rate touch-down from a glide at maximum lift/drag. If a zero sink rate landing is necessary, either a continuous glide at a higher airspeed or a two part landing flare with the initial phase at a higher airspeed may be accomplished.

The selection of proper wing loading for a given tractor-glider combination is evident in the L-20A Mission Profiles (Figure 38, for example). It appears that for maximum mission radius a glider with wing loading greater than  $7.0 \text{ lbs/ft}^2$  is necessary when towed by an L-20A aircraft.

### Aerial Drop Concept

The concept of delivering Flexible Wing towed gliders by dropping them from a de Havilland Caribou transport airplane has been considered. This twin-engine airplane has the capacity for two 1,000 lb. payload or ten 250 lb. towed gliders. Preliminary design drawings of these configurations are included in the Appendix.

The configuration to be used for this application is standard except for the wing structure and erection mechanism. The wing must be collapsible for stowing the gliders aboard the launch aircraft, necessitating incorporation of wing deployment mechanism and actuators.

A drag parachute is to be used to extract the glider through the rear door of the cargo compartment. The size and type of parachute, of course, depends on the drop speed and the desired vehicle velocity for wing deployment. A particular condition which was investigated in this study was the following:

Drop Altitude	1,500 feet
Drop Speed	200 knots
Payload	1,000 pounds
Gross Weight	1,498 pounds

An ideal parachute with a drag coefficient of 1.4 based on a projected diameter of six feet was assumed. An ideal parachute as referred to here implies a chute of zero porosity. For stability considerations, however, it would be advisable to use a chute with a fabric porosity of approximately 150 cubic feet/square feet/minute. This number refers to the cubic feet of air that will pass through one square foot of the cloth per minute under a pressure of 1/2 inch of water. A chute of this porosity requires a blossomed diameter of 6.75 in order to be equivalent to a six foot nonporous chute. A chute with a projected diameter of 6.75 feet has a nominal diameter of about ten feet.

In a typical drop exercise, the operator pulls the chute release cable to initiate drop. The chute pack drops from its attach point located on the aft end of the wing keel which extends beyond the end of the ramp. After a short free fall, the chute pack reaches the end of the rip cord static line and is deployed. When the chute is fully deployed, the drag force breaks the restraint lines (or releases the glider brakes) and releases the glider. Under the conditions considered the drag

chute force is initially 5,370 lb. and will produce a rearward acceleration of 3.6 g's relative to the Caribou. The glider and launch aircraft will separate 0.44 seconds after the restraint cable release.

At this instant a timing mechanism unlocks the wing and allows deployment at a rate controlled by a dynamic pressure sensitive brake. The deployment is effected by the drag chute tension riser which is connected through a pulley system to the spreader bar. When the wing is fully open, the keel slide locks and the drag chute jettisons.

At start of wing deployment, the flight path angle of the glider will be of the order of  $-50^{\circ}$ . Upon wing deployment, the glider will assume a normal flight path and in the same manner as the conventional towed glider.

**THRUST HORSEPOWER REQUIRED VS. TRUE AIRSPEED**  
**ON SEA LEVEL STANDARD DAY**  
**250 LB. PAYLOAD GLIDER**  
**W/S - 6.0 LB/FT<sup>2</sup>**

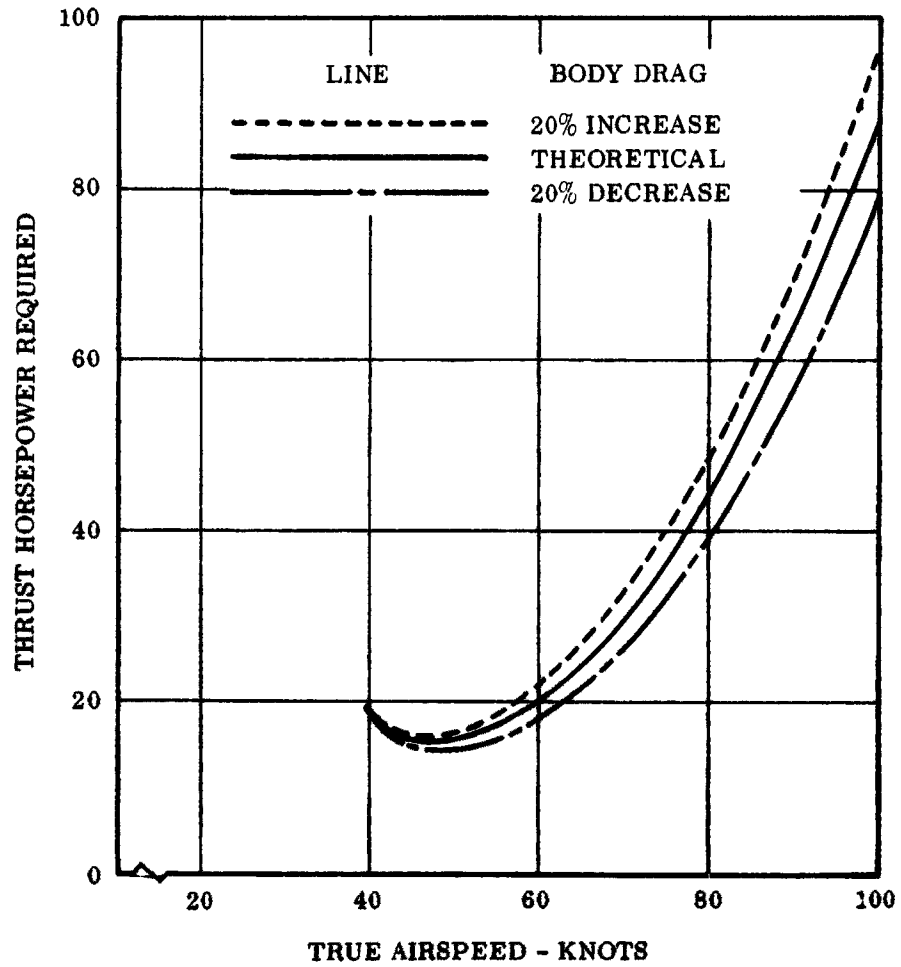


Figure 1 Thrust Horsepower Required - Towed Gliders

**THRUST HORSEPOWER REQUIRED VS. TRUE AIRSPEED**  
**ON STANDARD DAY**  
**250 LB. PAYLOAD GLIDER**  
**W/S = 6.0 LB/FT<sup>2</sup>**

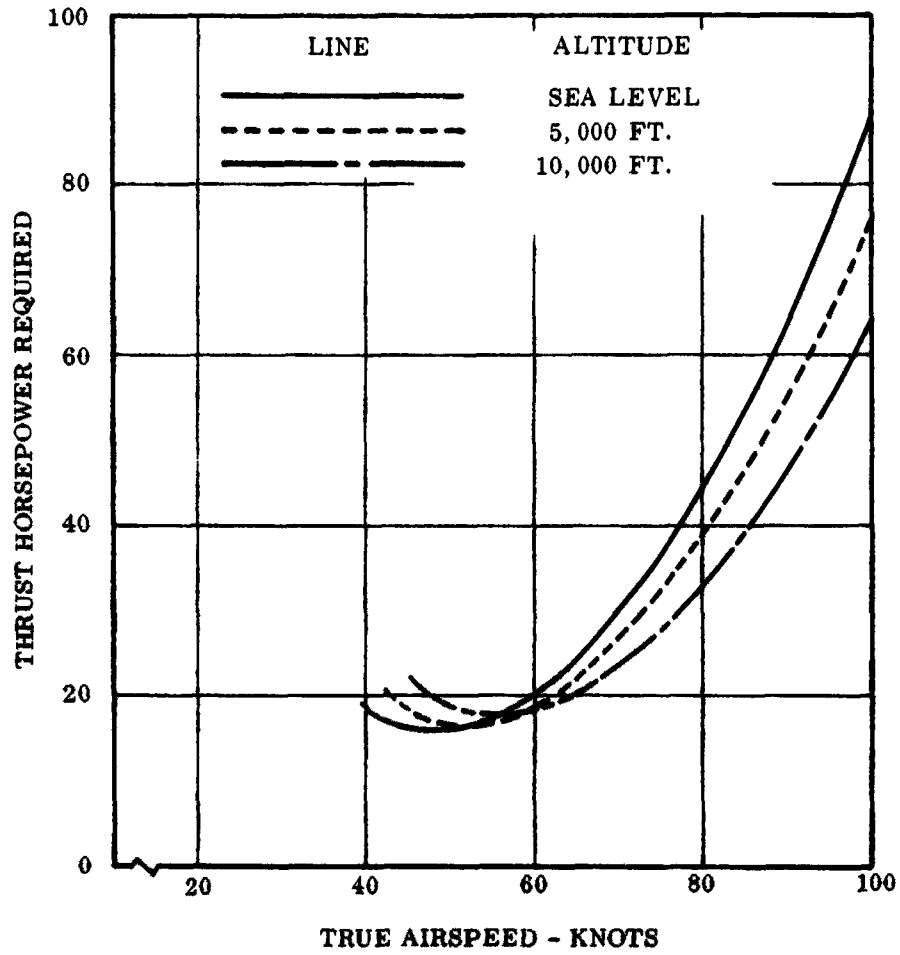
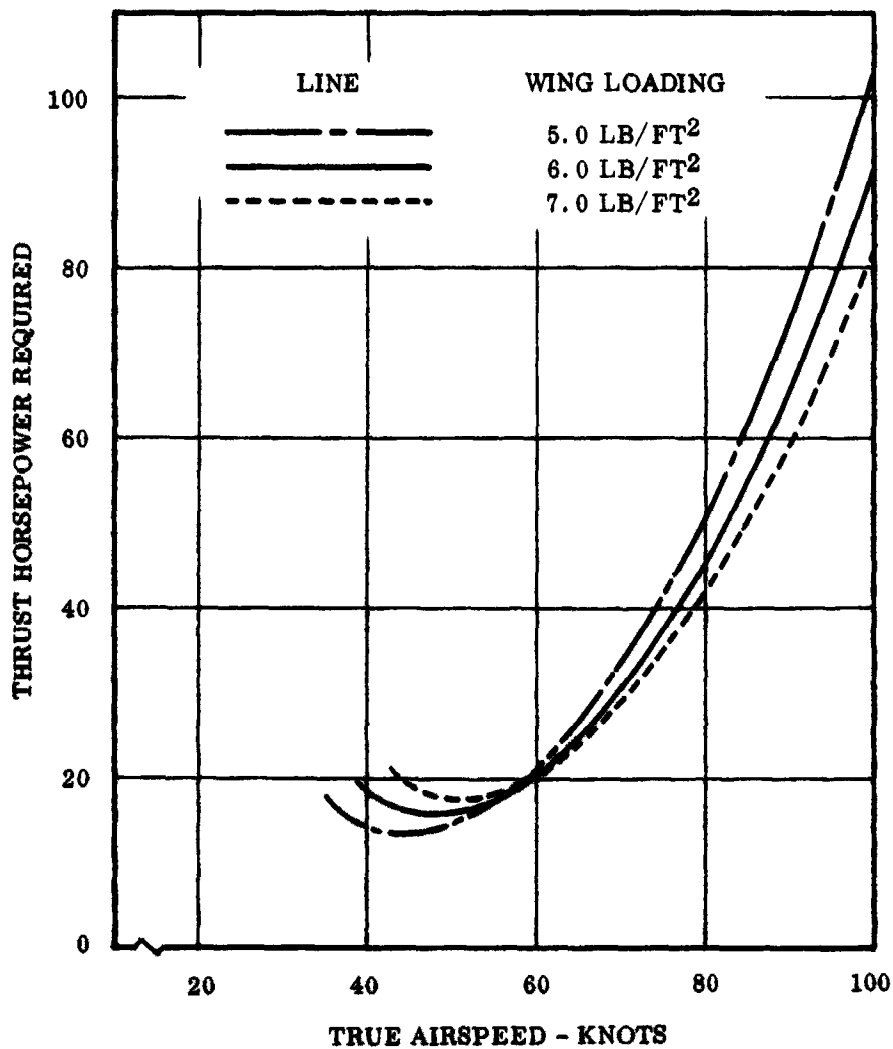


Figure 2 Thrust Horsepower Required - Towed Gliders

7

**THRUST HORSEPOWER REQUIRED VS. TRUE AIRSPEED  
ON SEA LEVEL STANDARD DAY  
250 LB. PAYLOAD GLIDER**



**Figure 3 Thrust Horsepower Required - Towed Gliders**

**THRUST HORSEPOWER REQUIRED VS. TRUE AIRSPEED**  
**ON SEA LEVEL STANDARD DAY**  
**1000 LB. PAYLOAD GLIDER**  
**W/S = 6.0 LB/FT<sup>2</sup>**

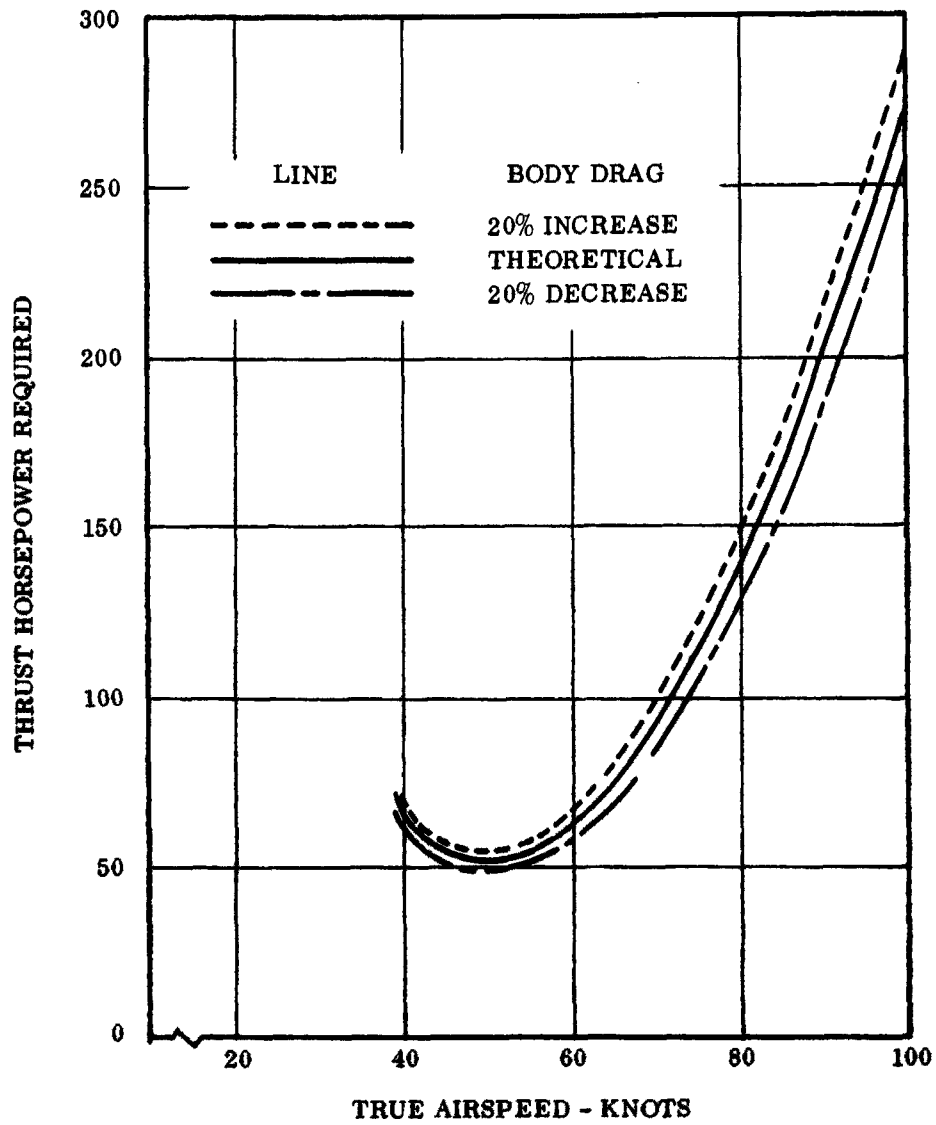


Figure 4 Thrust Horsepower Required - Towed Gliders

**THRUST HORSEPOWER REQUIRED VS. TRUE AIRSPEED**  
**ON STANDARD DAY**  
**1000 LB. PAYLOAD GLIDER**  
**W/S = 6.0 LB/FT<sup>2</sup>**

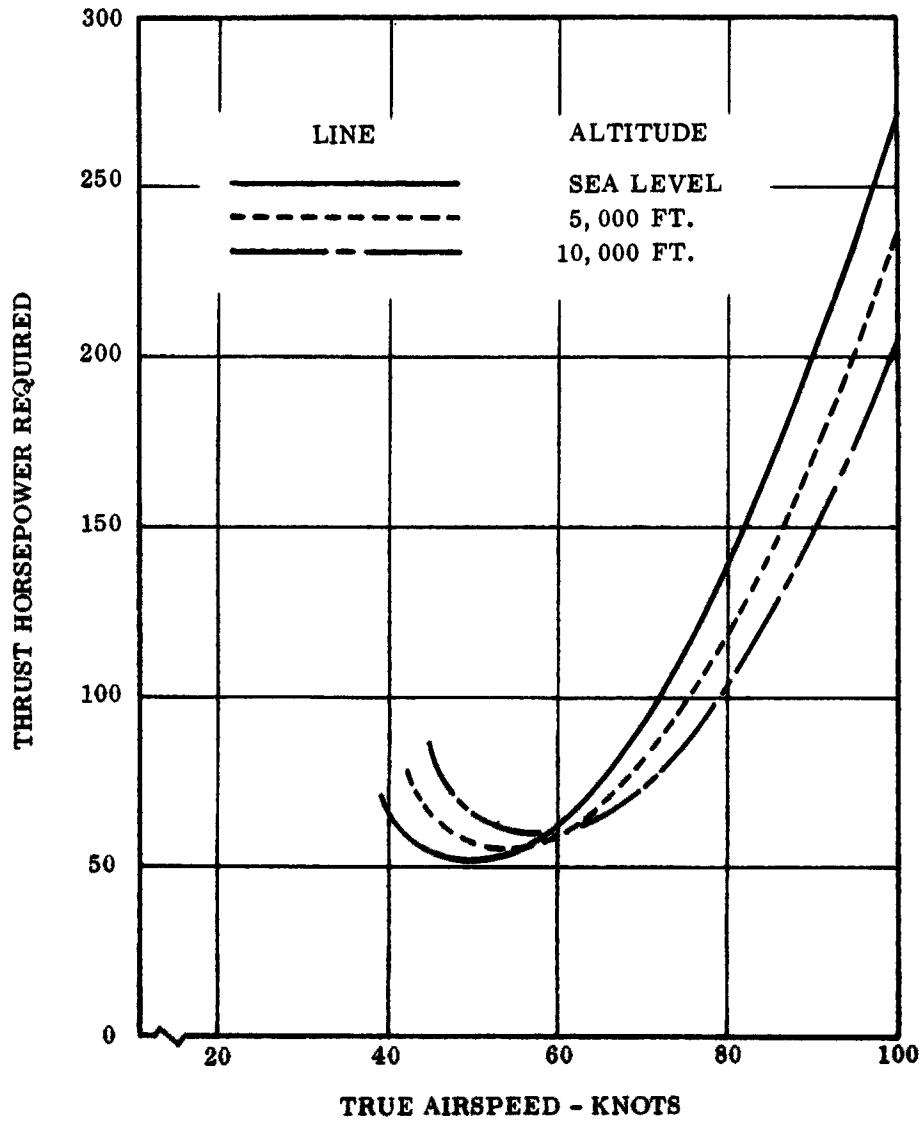


Figure 5 Thrust Horsepower Required - Towed Gliders

THRUST HORSEPOWER REQUIRED VS. TRUE AIRSPEED  
ON SEA LEVEL STANDARD DAY  
1000 LB. PAYLOAD GLIDER

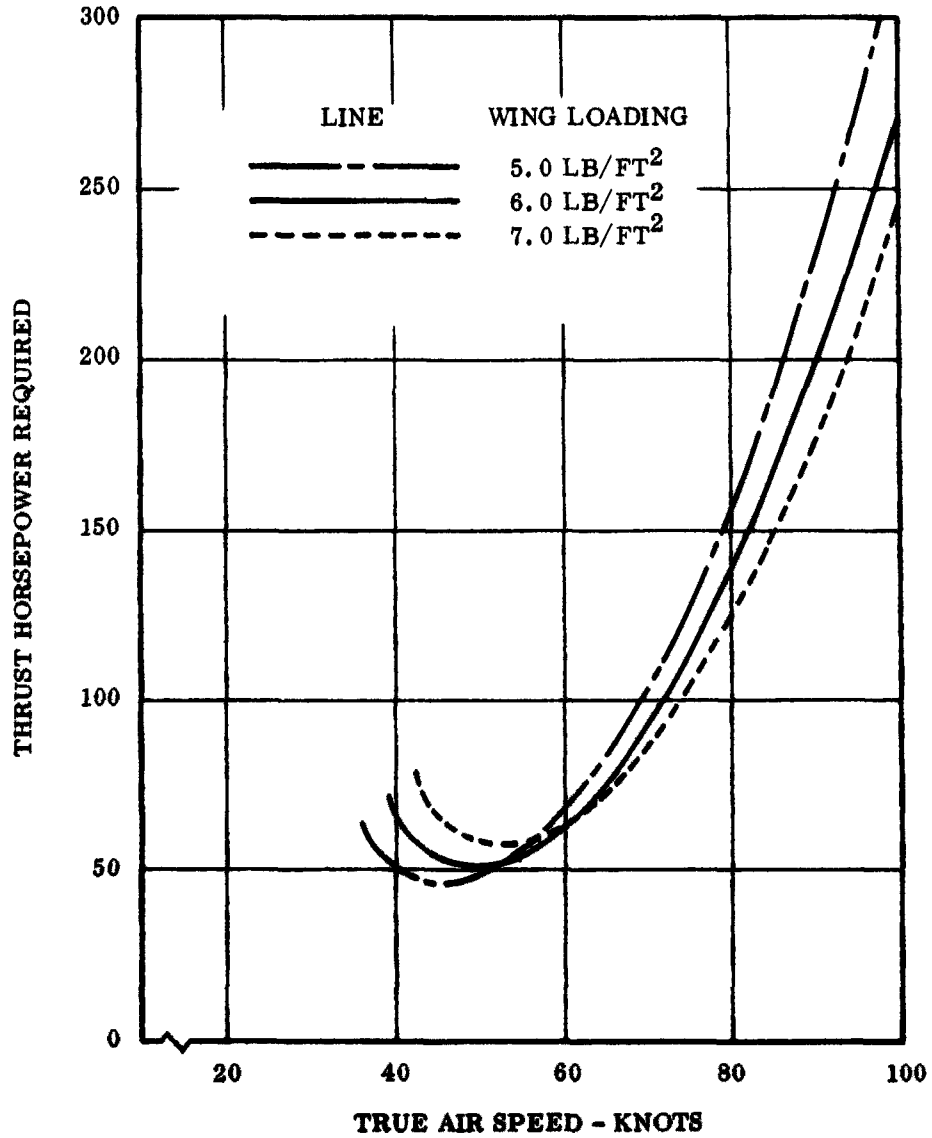


Figure 6 Thrust Horsepower Required - Towed Gliders

**THRUST HORSEPOWER REQUIRED VS. TRUE AIRSPEED**  
**ON SEA LEVEL STANDARD DAY**  
**1000 LB. PAYLOAD GLIDER**  
**W/S = 6.0 LB/FT<sup>2</sup>**

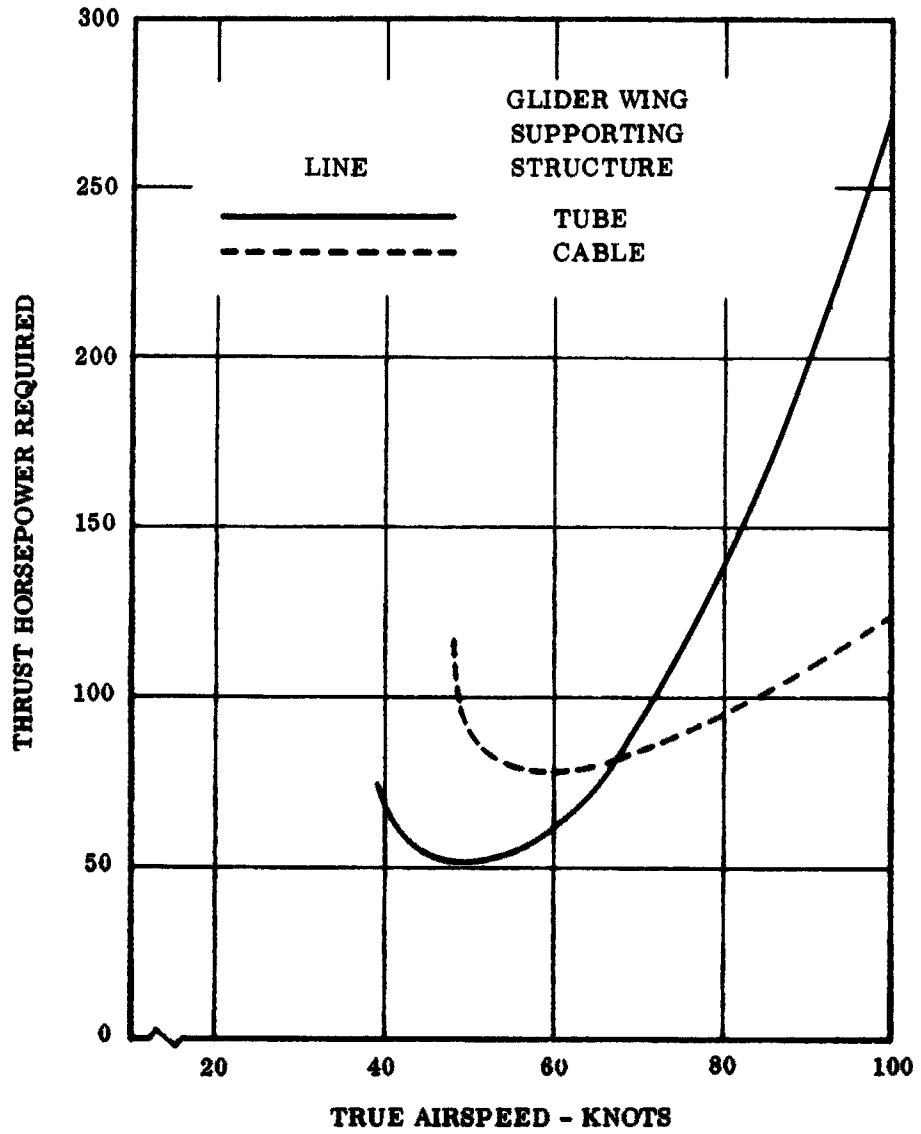


Figure 7 Thrust Horsepower Required - Towed Gliders

**THRUST HORSEPOWER REQUIRED VS. TRUE AIRSPEED**  
**ON SEA LEVEL STANDARD DAY**  
**4000 LB. PAYLOAD GLIDER**  
**W/S = 6.0 LB/FT<sup>2</sup>**

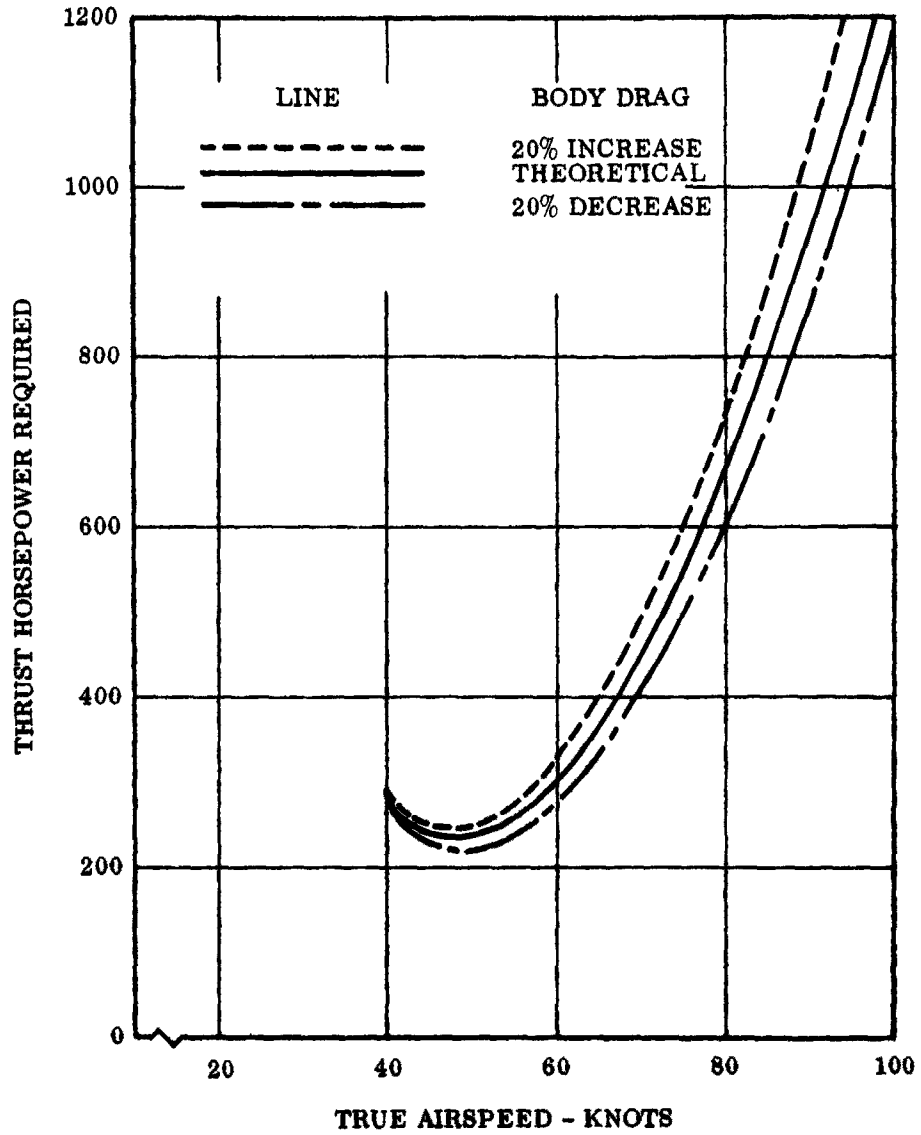


Figure 8 Thrust Horsepower Required - Towed Gliders

**THRUST HORSEPOWER REQUIRED VS. TRUE AIRSPEED**  
**ON STANDARD DAY**  
**4000 LB. PAYLOAD GLIDER**  
**W/S = 6.0 LB/FT<sup>2</sup>**

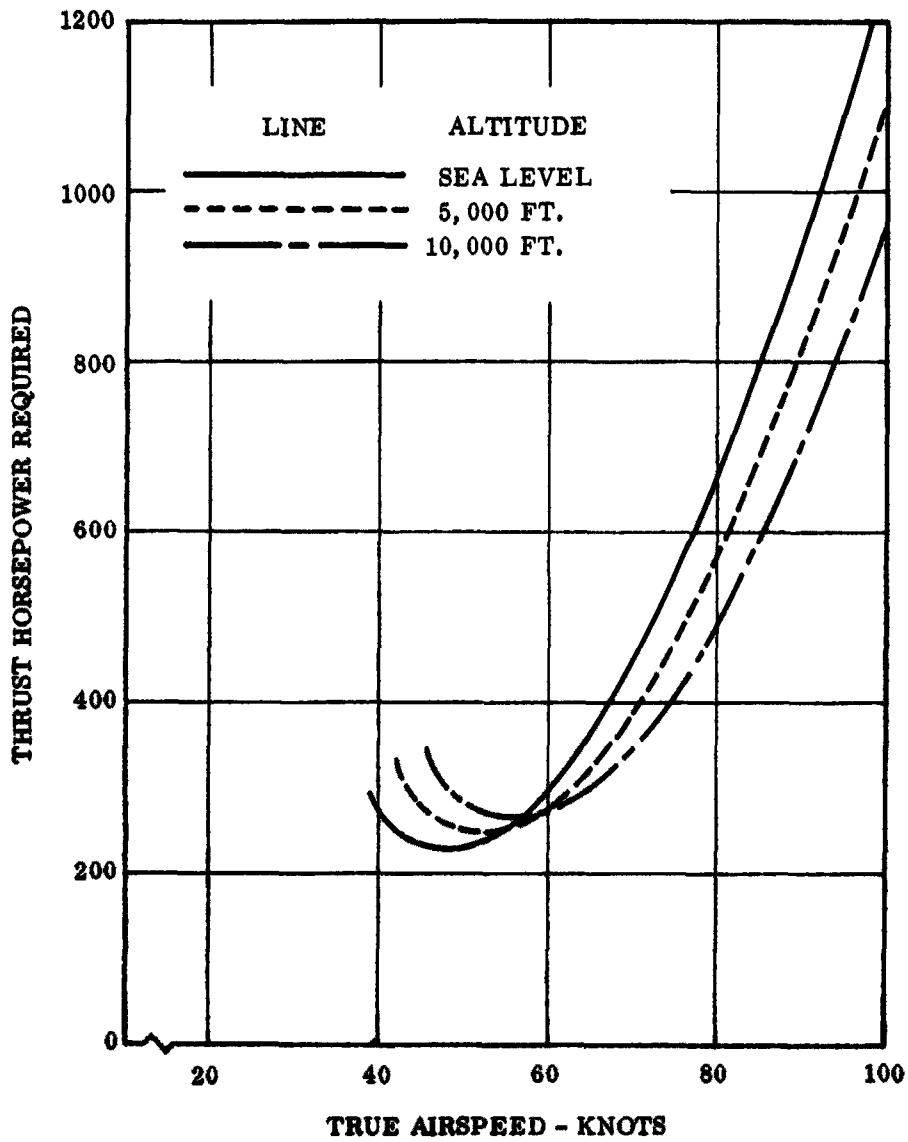
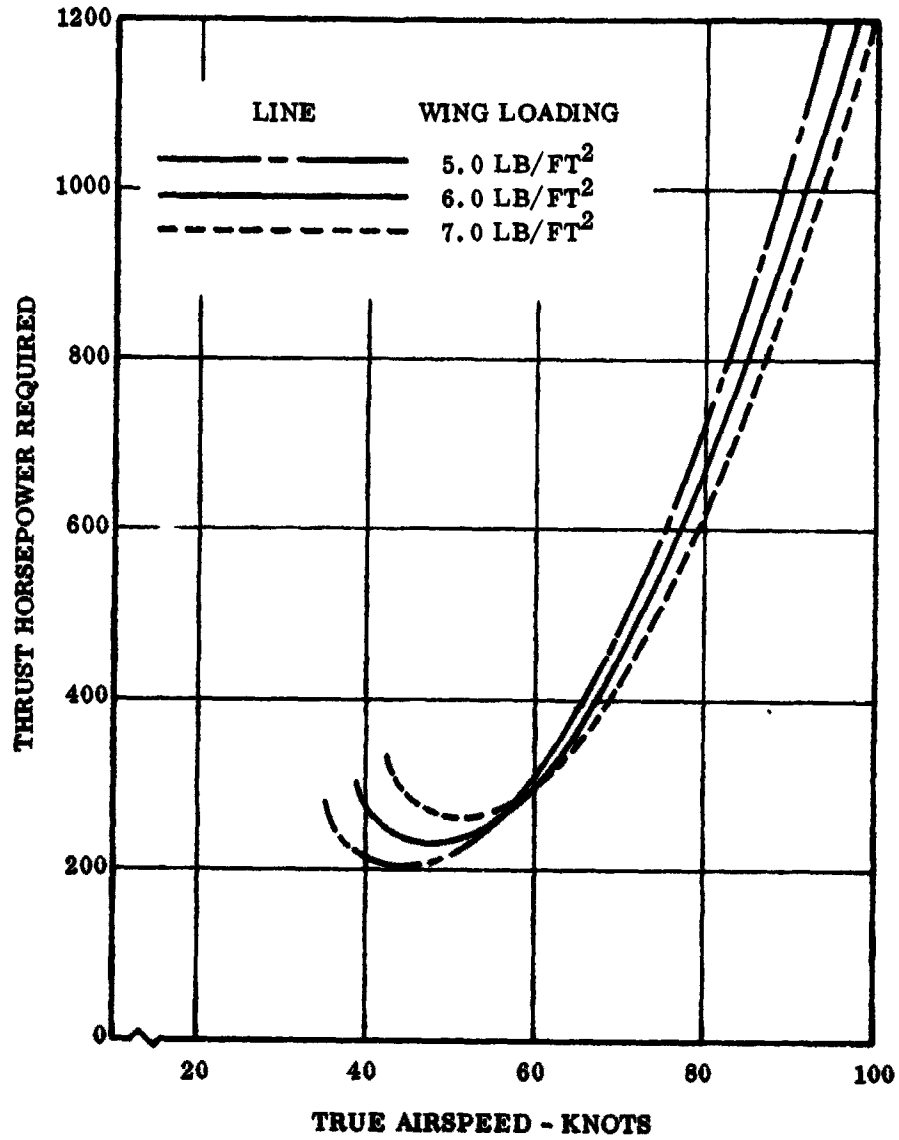


Figure 9 Thrust Horsepower Required - Towed Gliders

**THRUST HORSEPOWER REQUIRED VS. TRUE AIRSPEED  
ON SEA LEVEL STANDARD DAY  
4000 LB. PAYLOAD GLIDER**



**Figure 10 Thrust Horsepower Required - Towed Gliders**

**THRUST HORSEPOWER REQUIRED VS. TRUE AIRSPEED**  
**ON SEA LEVEL STANDARD DAY**  
**8000 LB. PAYLOAD GLIDER**  
 **$W/S = 6.0 \text{ LB/FT}^2$**

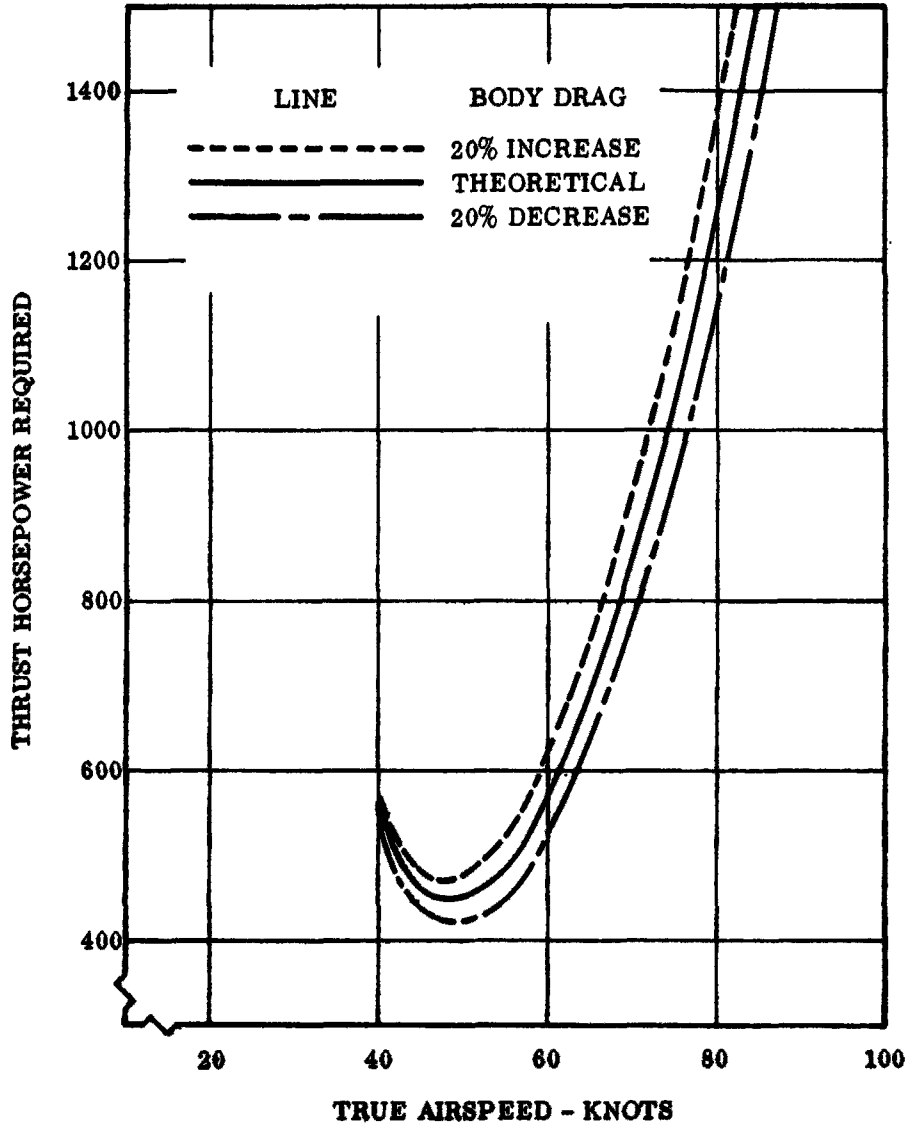


Figure 11 Thrust Horsepower Required - Towed Gliders

**THRUST HORSEPOWER REQUIRED VS. TRUE AIRSPEED**  
**ON STANDARD DAY**  
**8000 LB. PAYLOAD GLIDER**  
 **$W/S = 6.0 \text{ LB/FT}^2$**

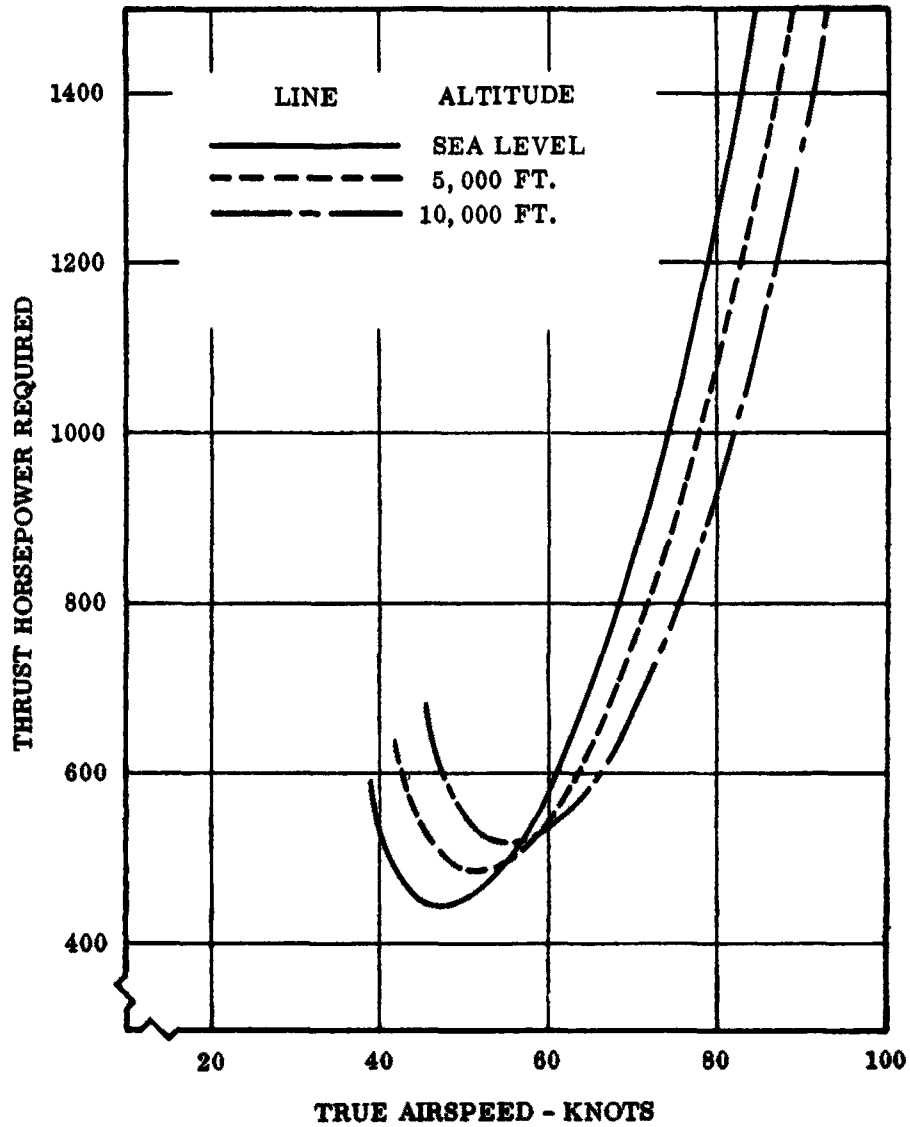
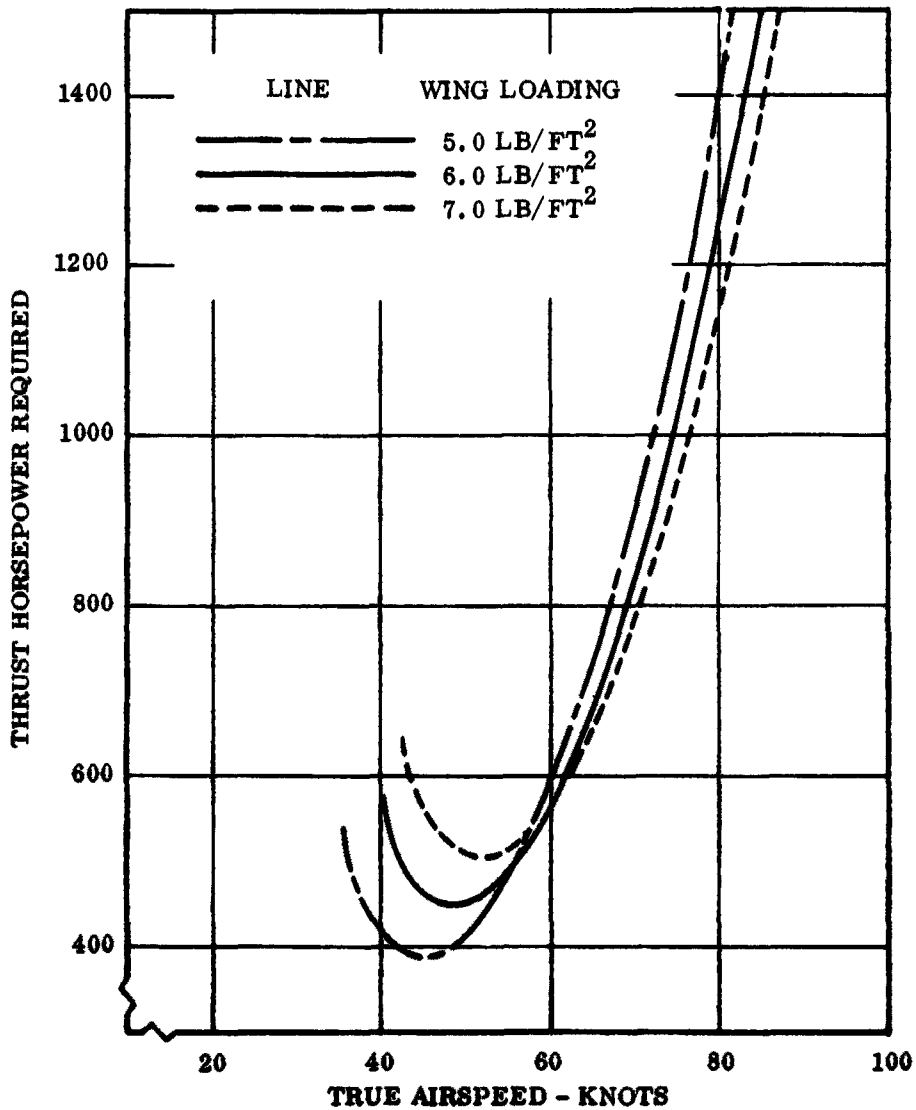


Figure 12 Thrust Horsepower Required - Towed Gliders

**THRUST HORSEPOWER REQUIRED VS. TRUE AIRSPEED  
ON SEA LEVEL STANDARD DAY  
8000 LB. PAYLOAD GLIDER**



**Figure 13 Thrust Horsepower Required - Towed Gliders**

LIFT/DRAG VS. TRUE AIRSPEED  
 ON SEA LEVEL STANDARD DAY  
 250 LB. PAYLOAD GLIDER

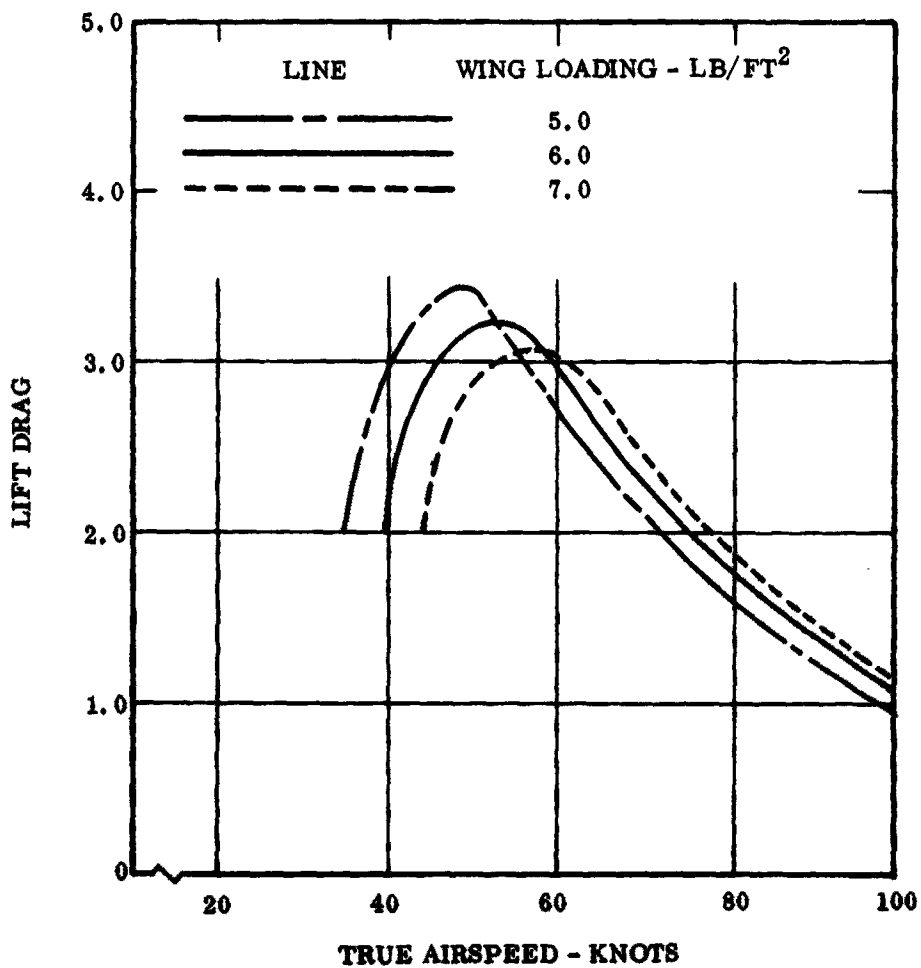


Figure 14 Free-Flight Performance Gliders

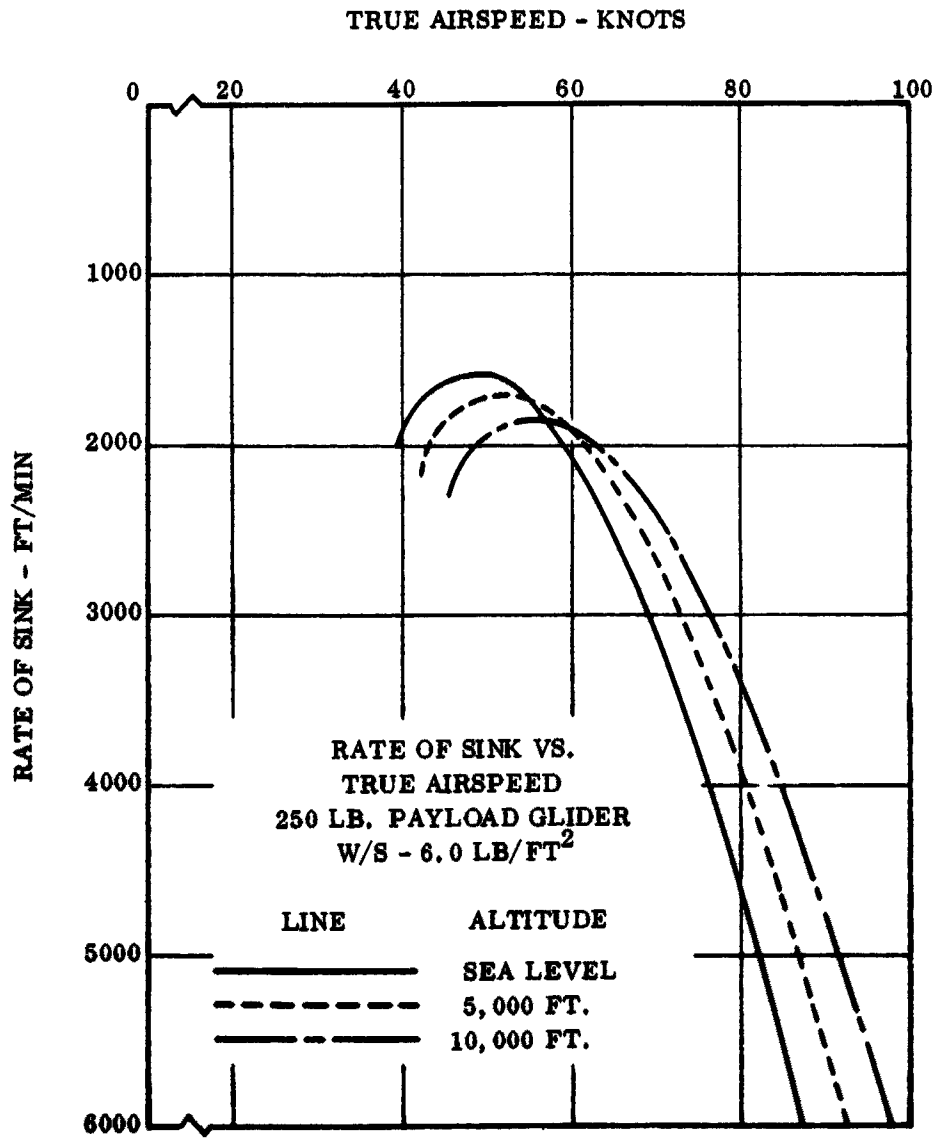


Figure 15 Free-Flight Performance Gliders

HORIZONTAL RANGE VS. ALTITUDE  
250 LB. PAYLOAD GLIDER

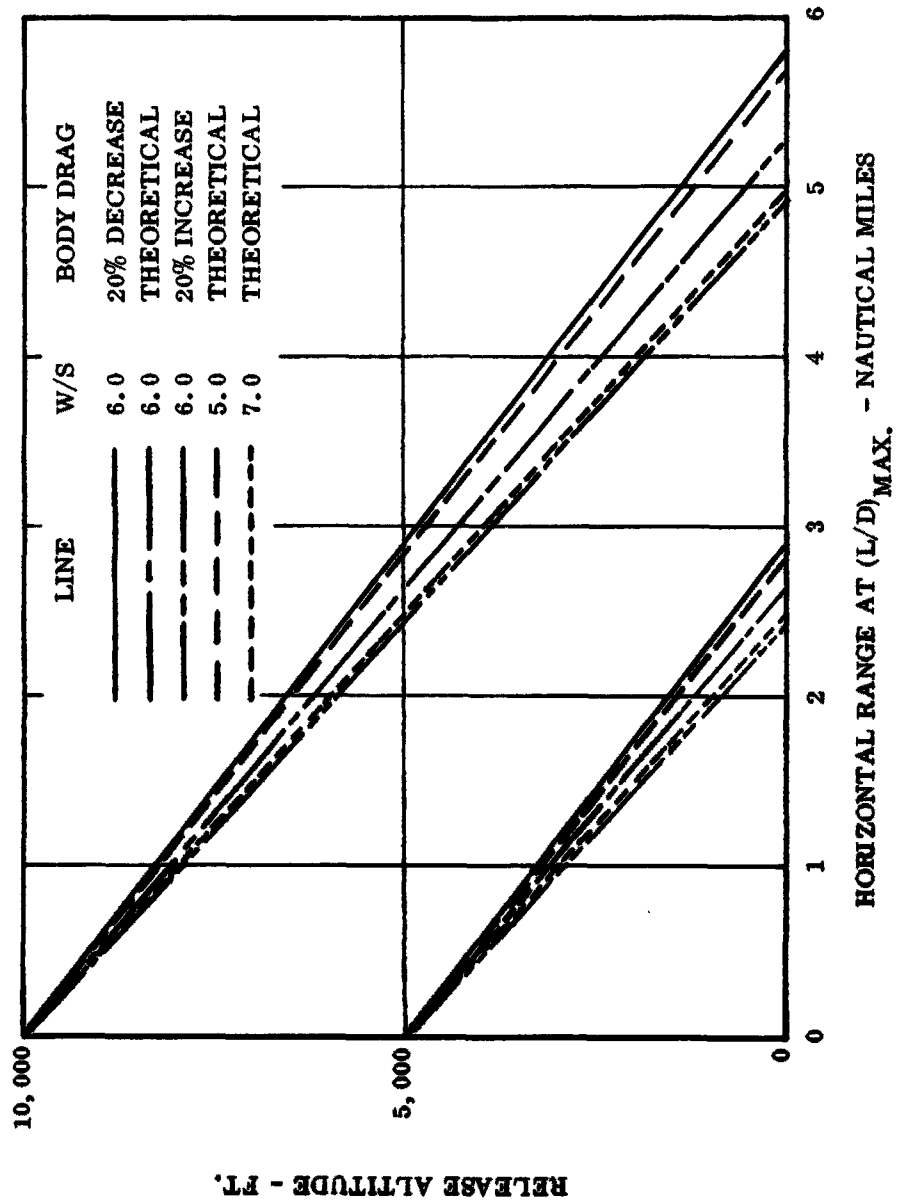


Figure 16 Free-Flight Performance Gliders

LIFT/DRAG VS. TRUE AIRSPEED  
 AT SEA LEVEL STANDARD DAY  
 1000 LB. PAYLOAD GLIDER

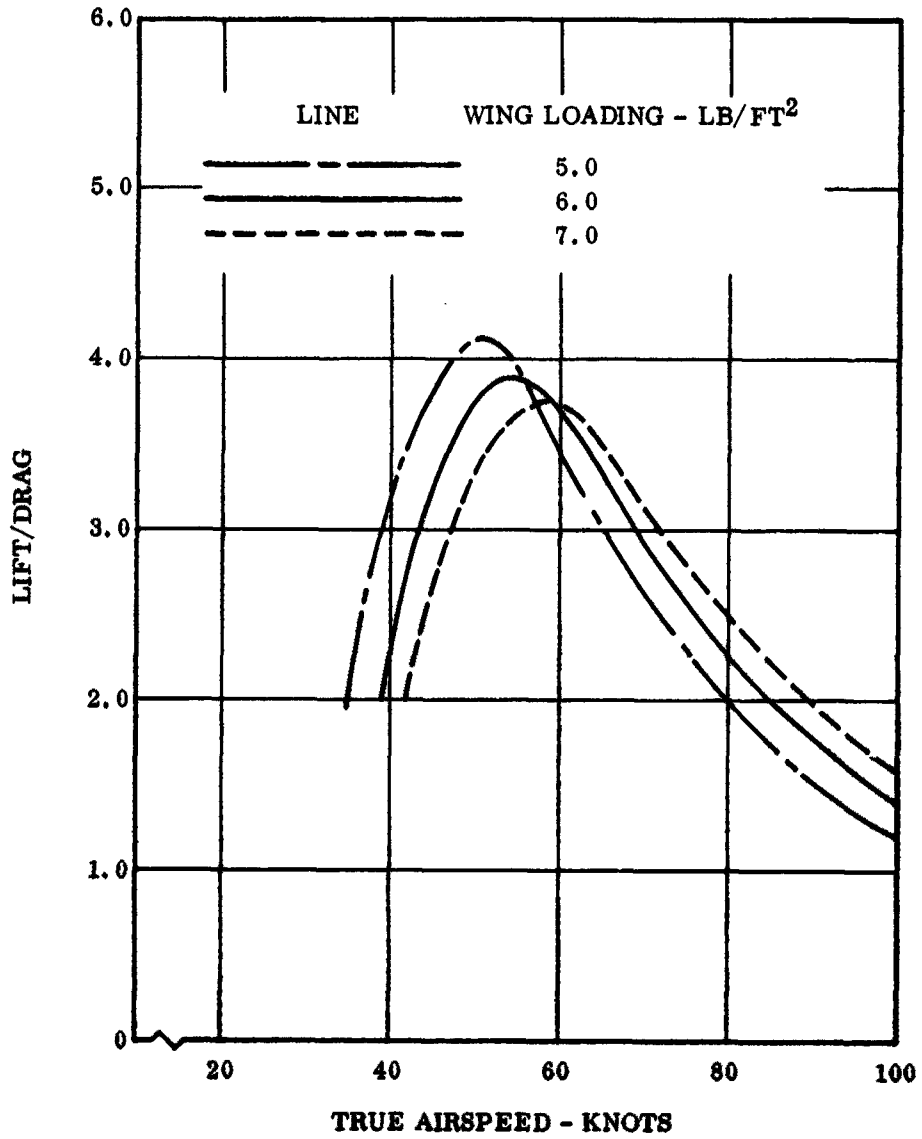


Figure 17 Free-Flight Performance Gliders

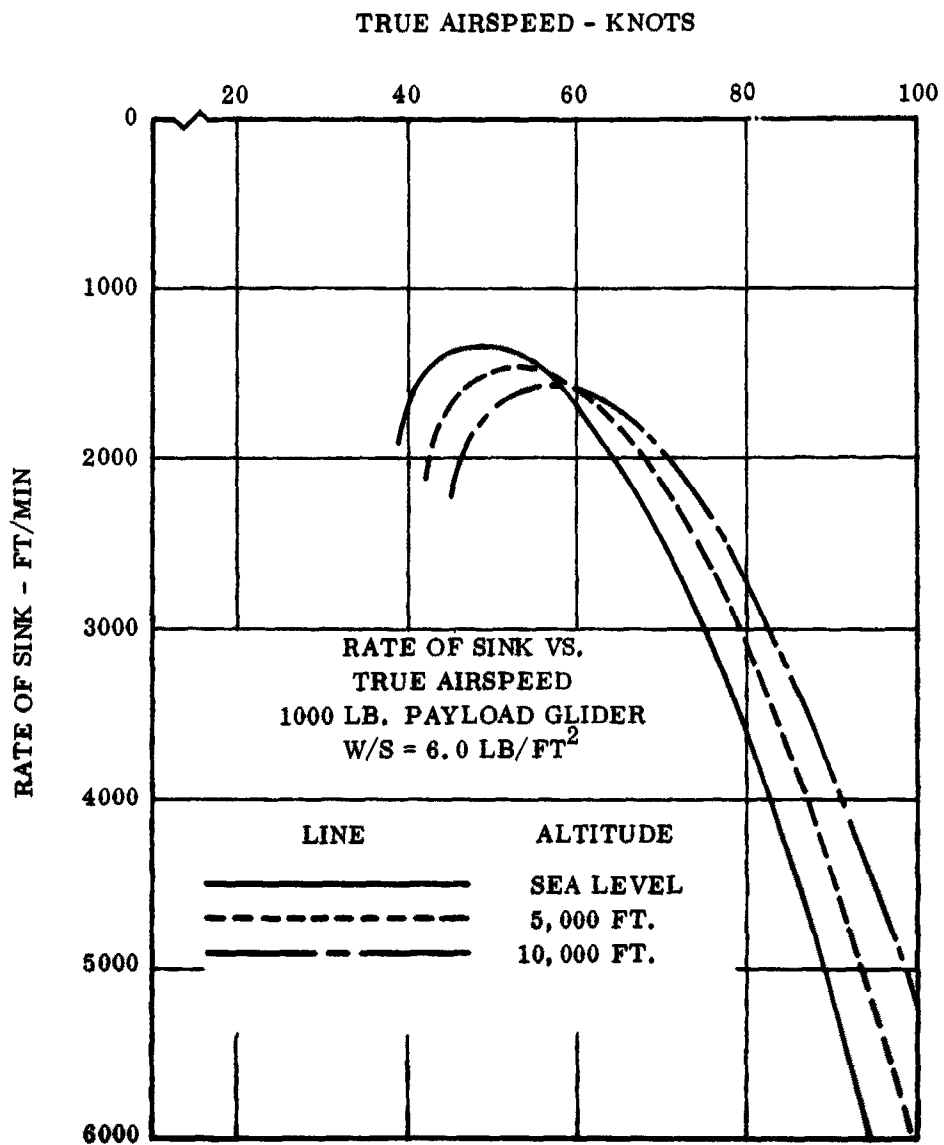


Figure 18 Free-Flight Performance Gliders

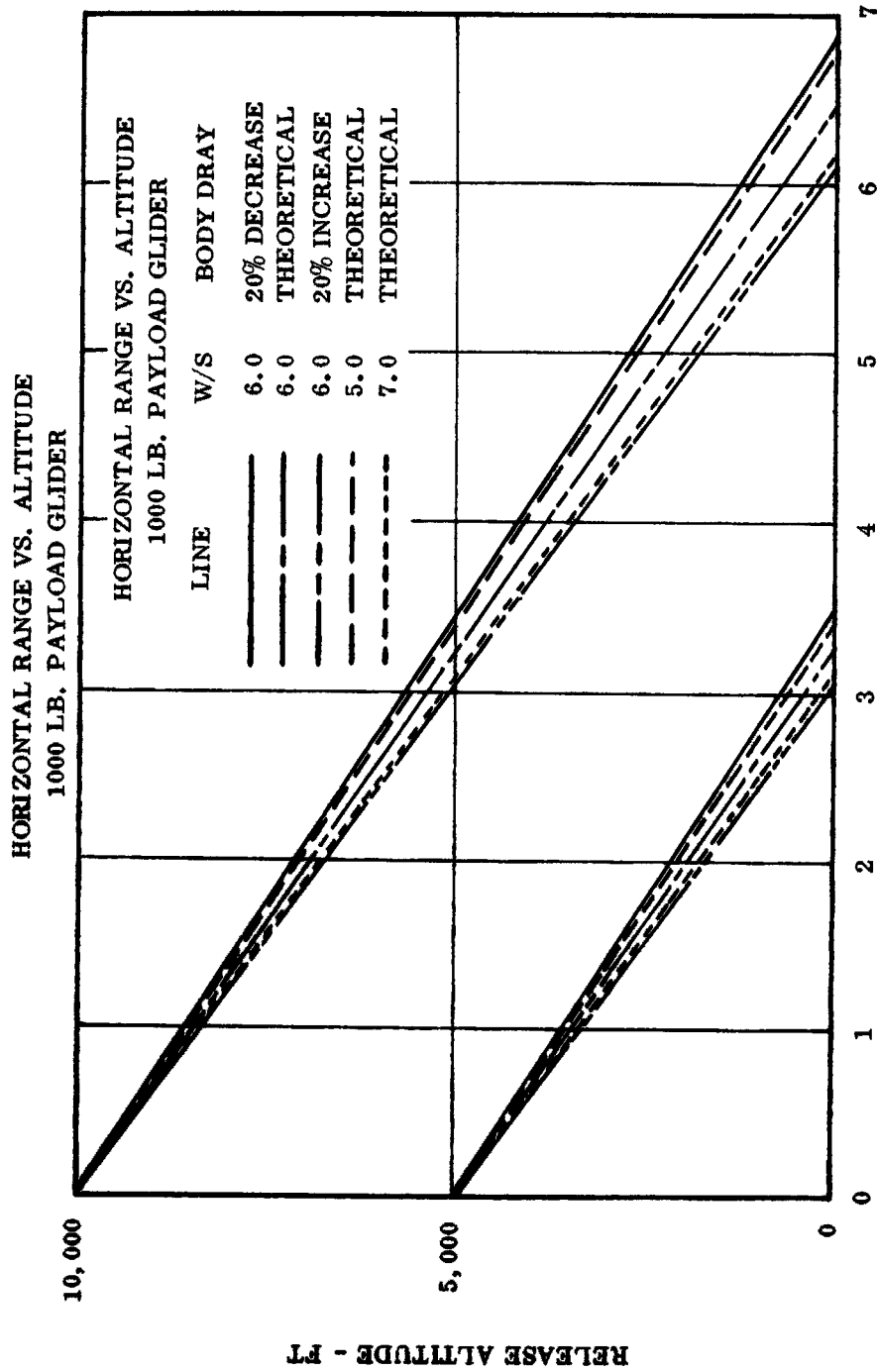


Figure 19 Free-Flight Performance Gliders

LIFT/DRAG VS. TRUE AIRSPEED  
 ON SEA LEVEL STANDARD DAY  
 1000 LB. PAYLOAD GLIDER  
 $W/S = 6.0 \text{ LB/FT}^2$

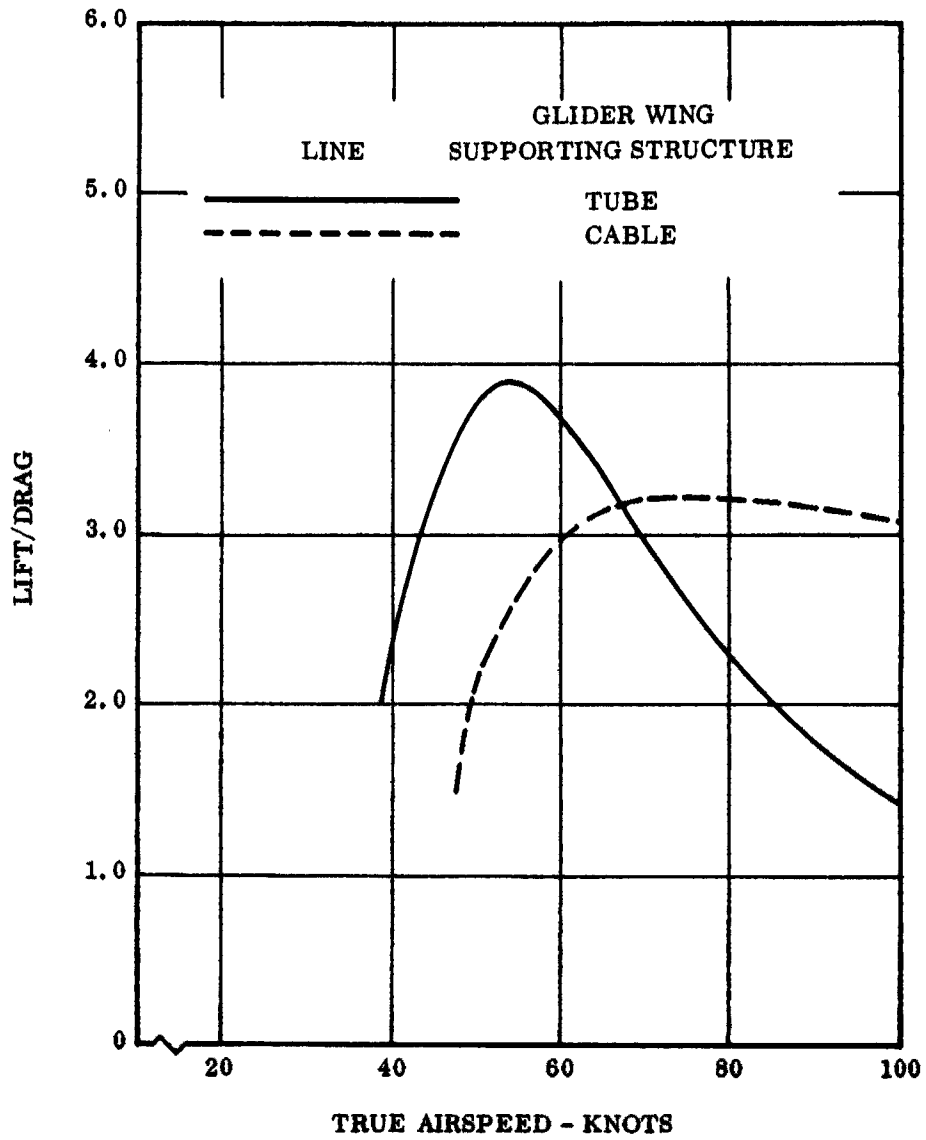


Figure 20 Free-Flight Performance Gliders

LIFT/DRAG VS. TRUE AIRSPEED  
 ON SEA LEVEL STANDARD DAY  
 4000 LB. PAYLOAD GLIDER

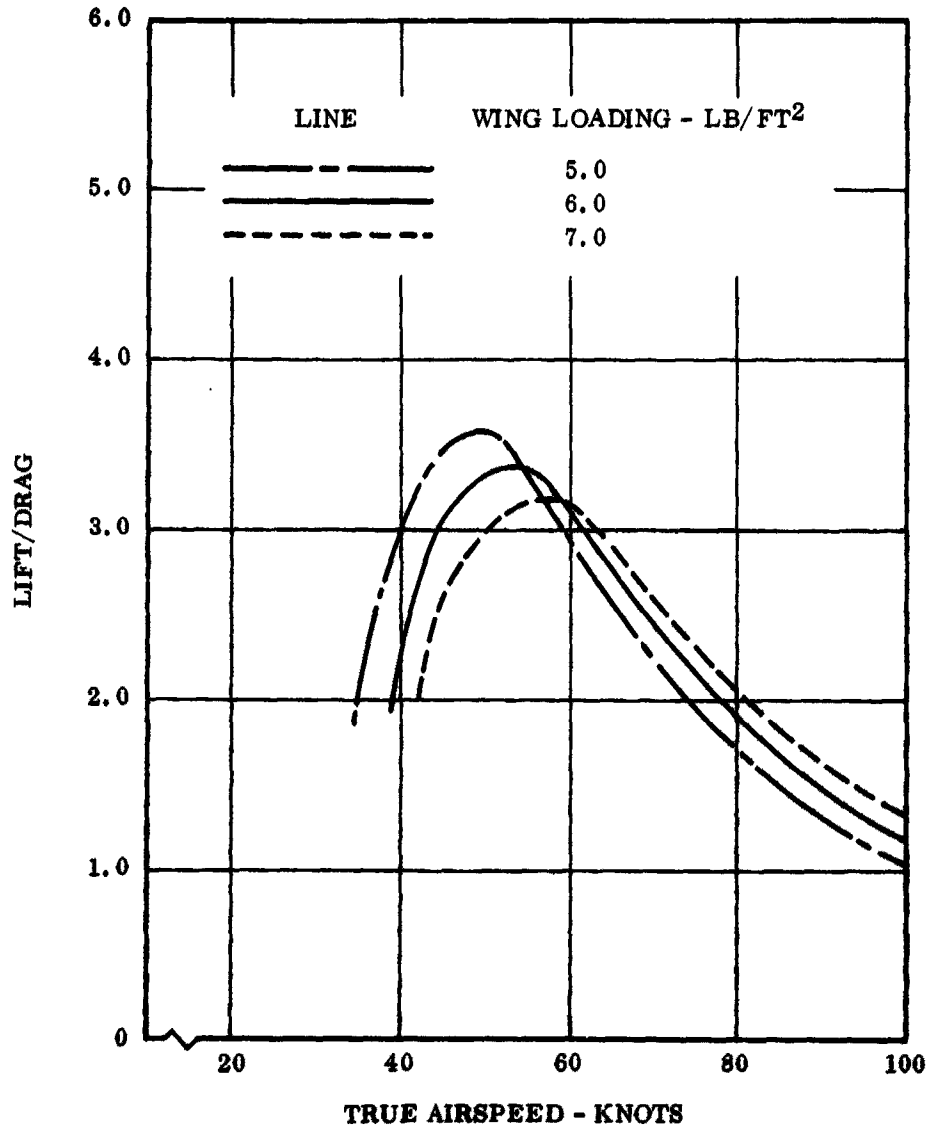


Figure 21 Free-Flight Performance Gliders

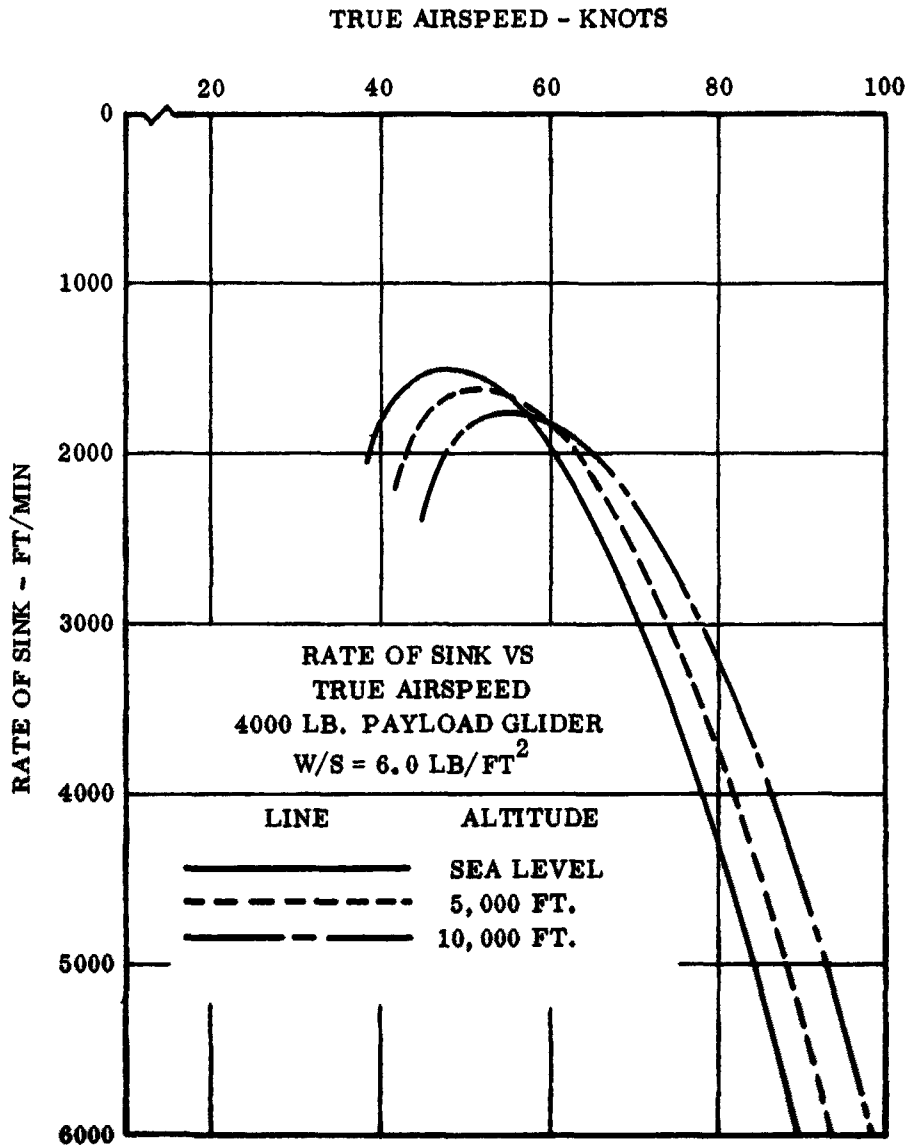


Figure 22 Free-Flight Performance Gliders

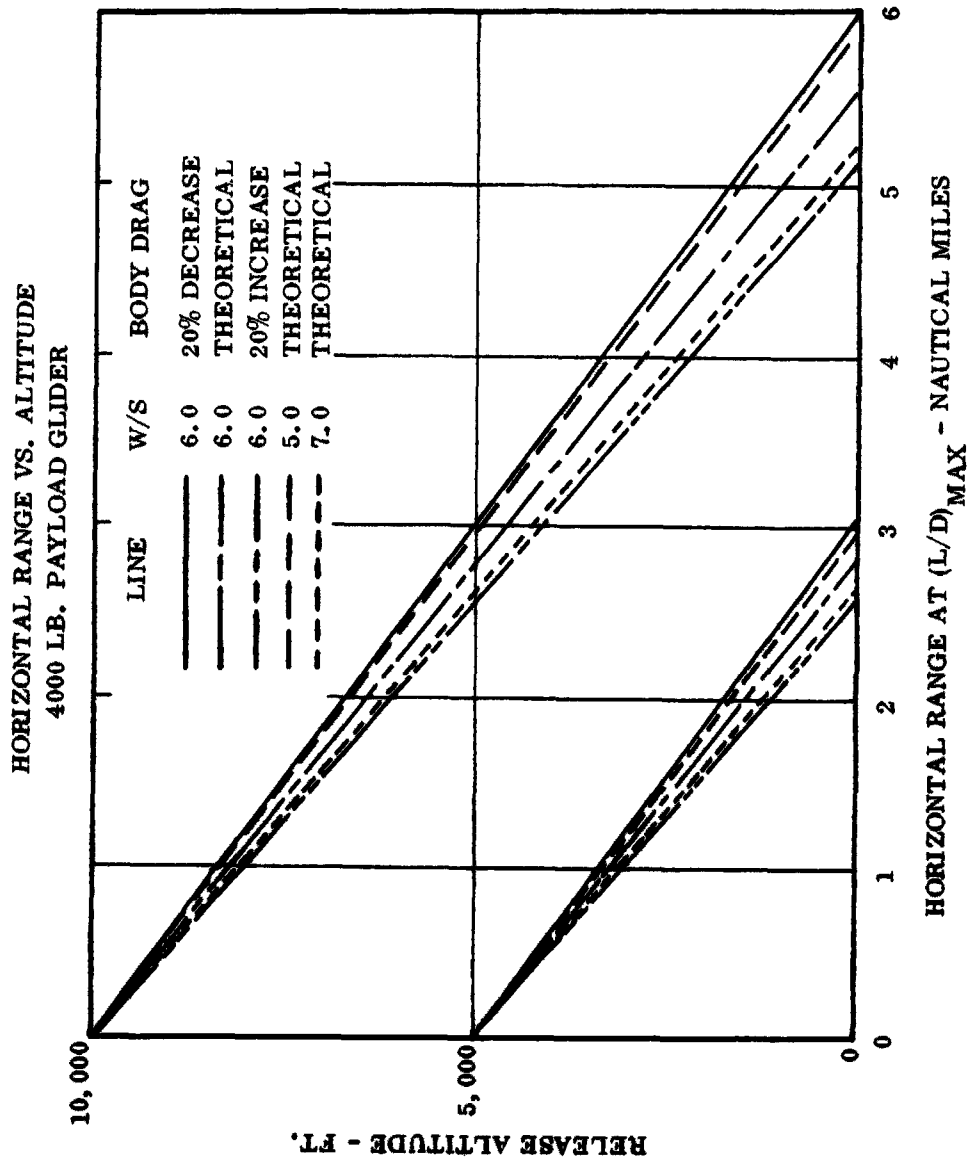


Figure 23 Free-Flight Performance Gliders

LIFT/DRAG VS. TRUE AIRSPEED  
 ON SEA LEVEL STANDARD DAY  
 8000 LB. PAYLOAD GLIDER

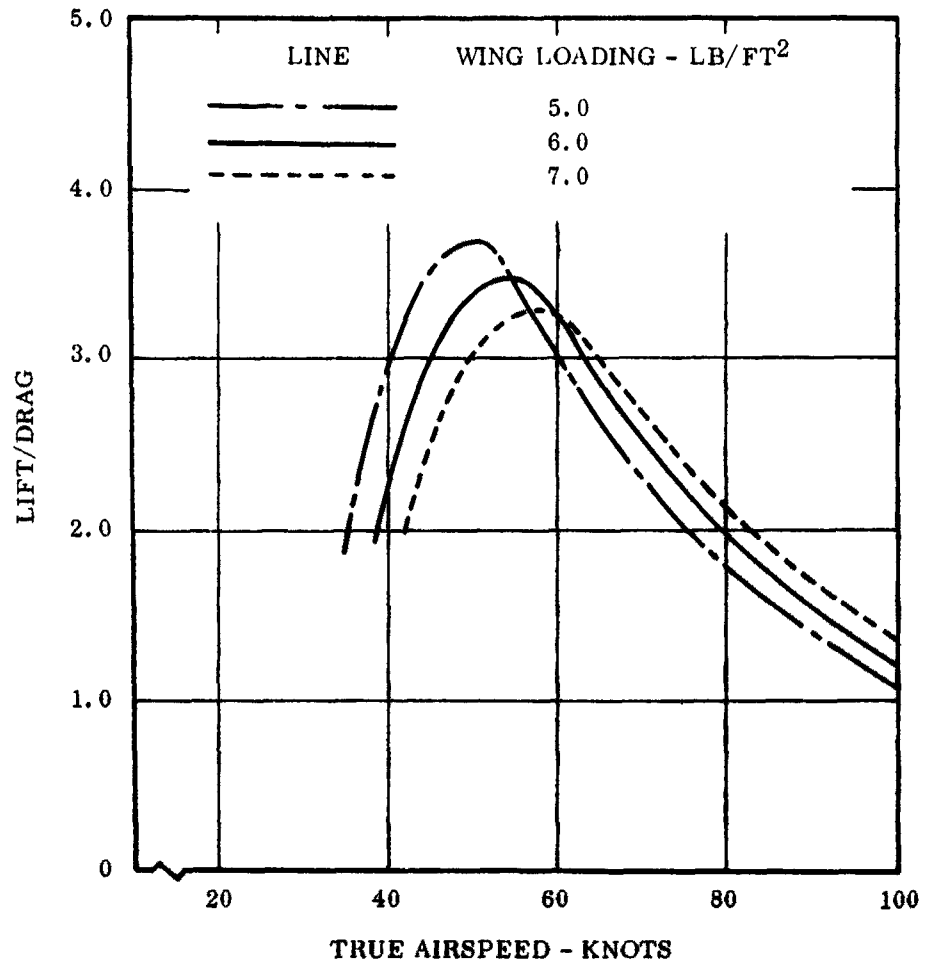


Figure 24 Free-Flight Performance Gliders

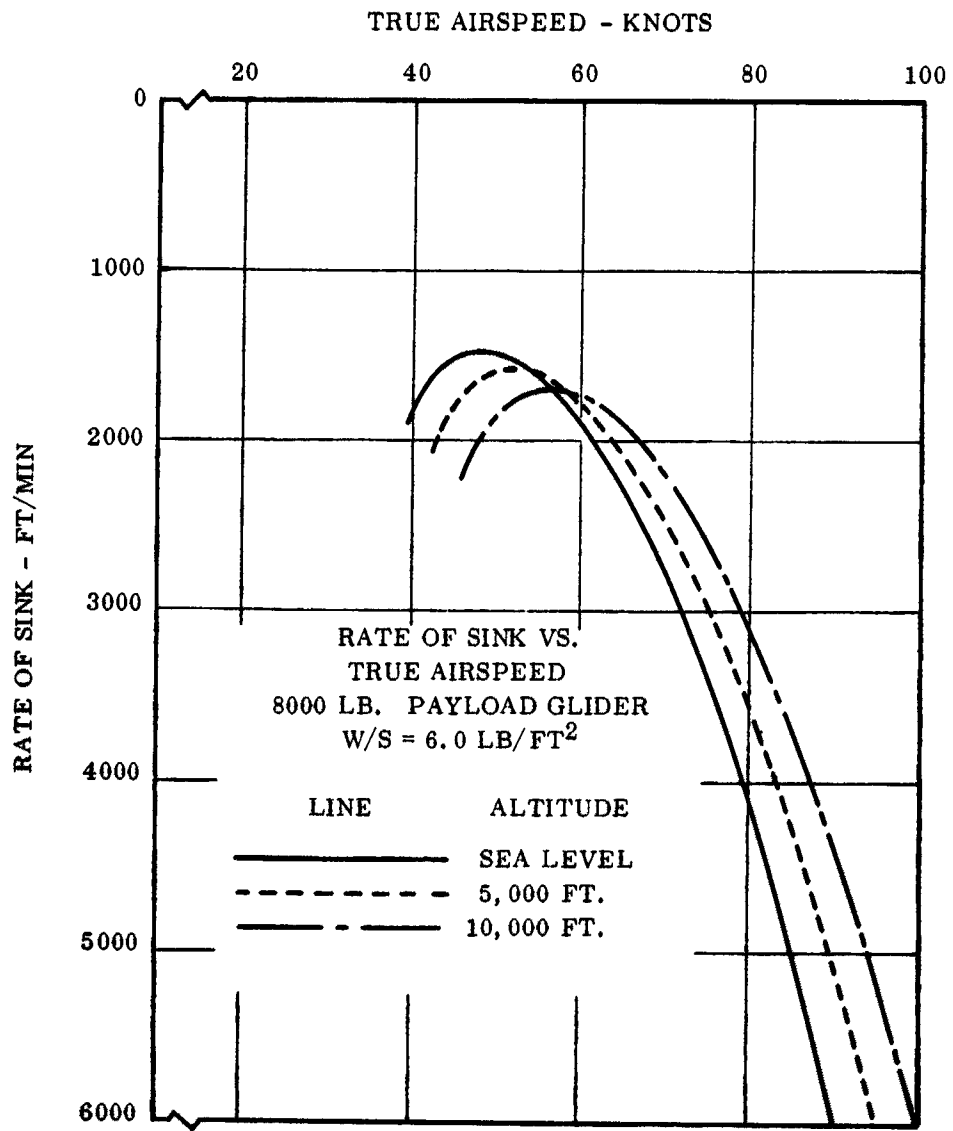


Figure 25 Free-Flight Performance Gliders

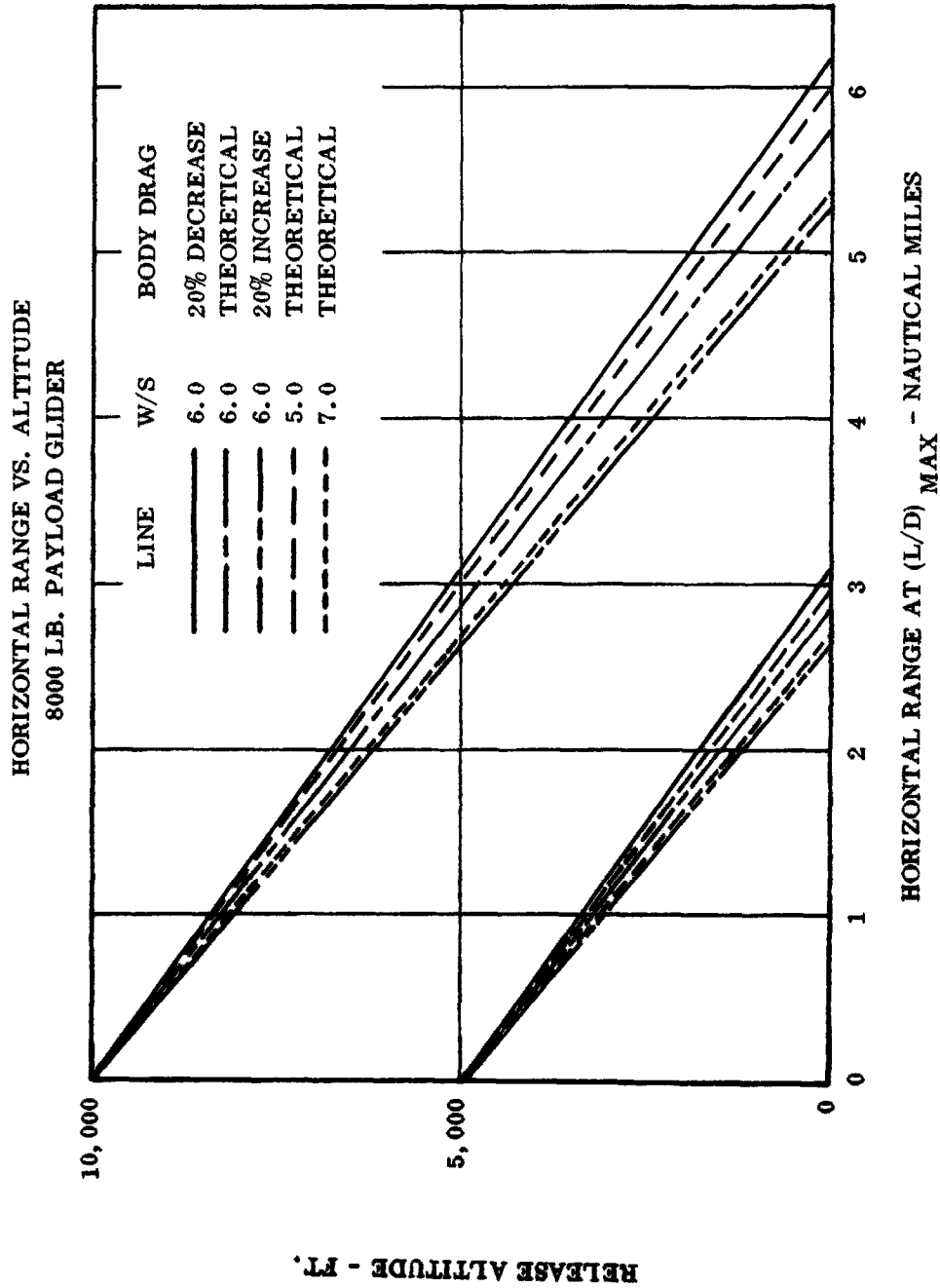


Figure 26 Free-Flight Performance Gliders

L-20A PERFORMANCE  
THRUST HORSEPOWER VS. TRUE AIRSPEED  
SEA LEVEL STANDARD DAY

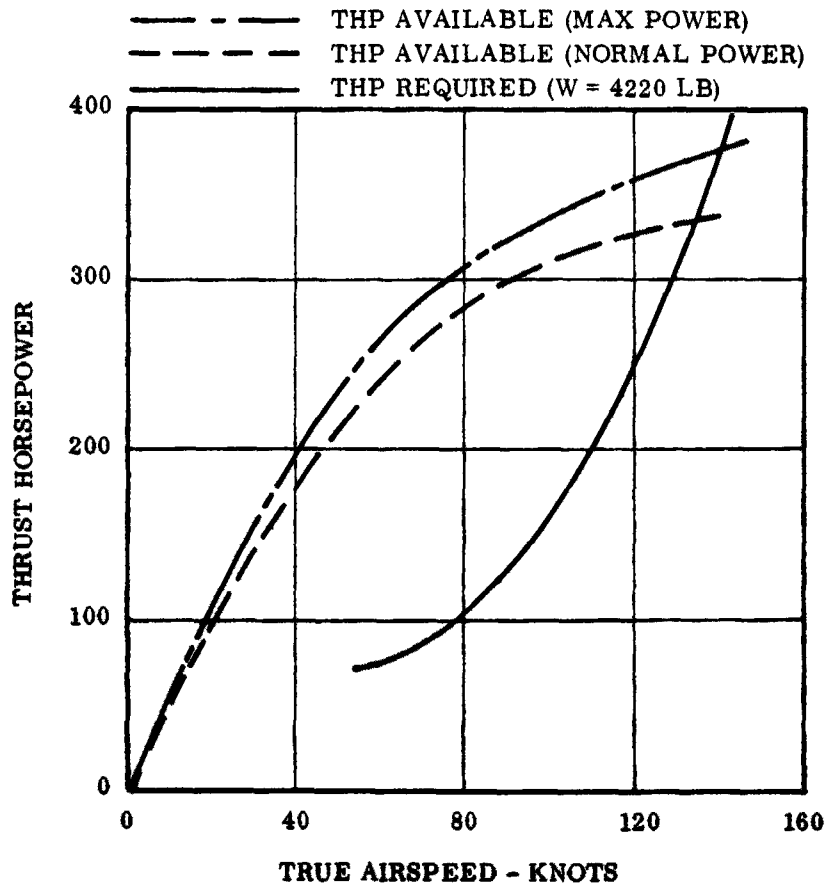


Figure 27 Thrust Horsepower - L-20A

L-20A PERFORMANCE  
THRUST HORSEPOWER VS. TRUE AIRSPEED  
5000 FT. STANDARD DAY

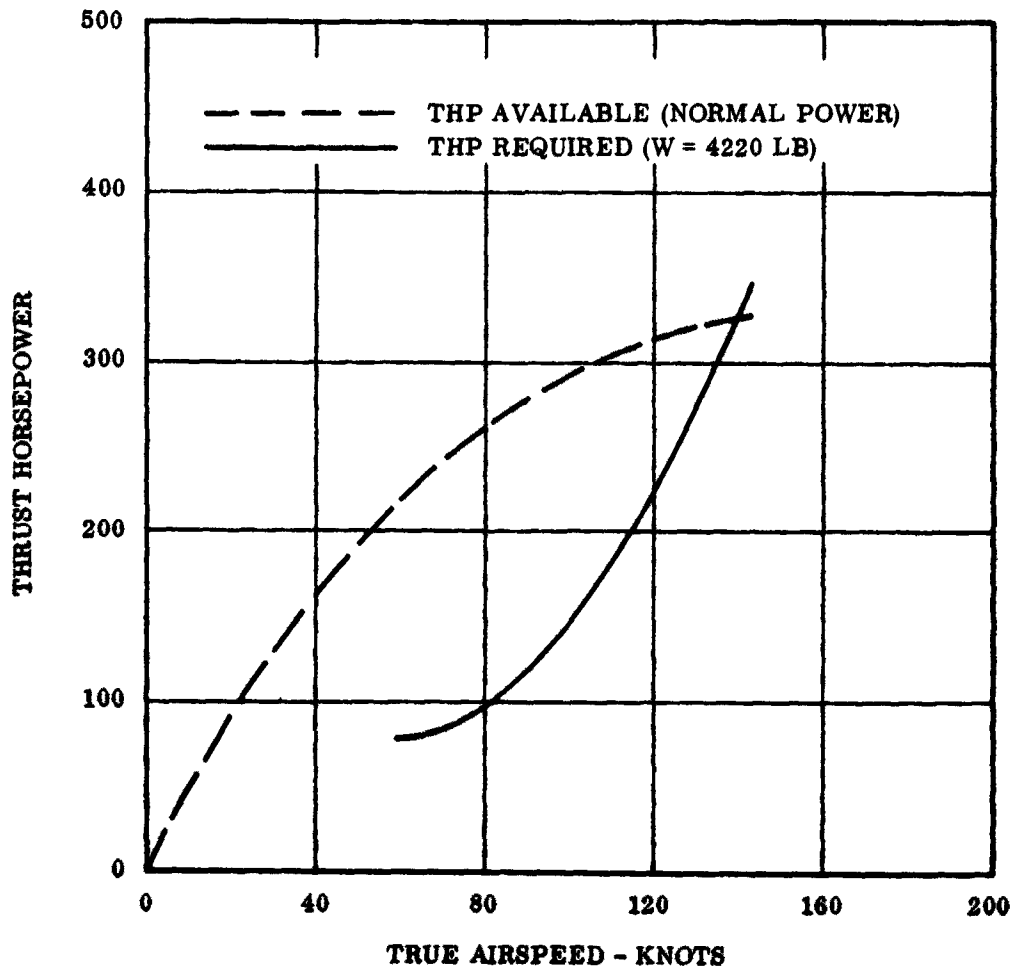


Figure 28 Thrust Horsepower - L-20A

L-20A PERFORMANCE  
THRUST HORSEPOWER VS. TRUE AIRSPEED  
10,000 FT. STANDARD DAY

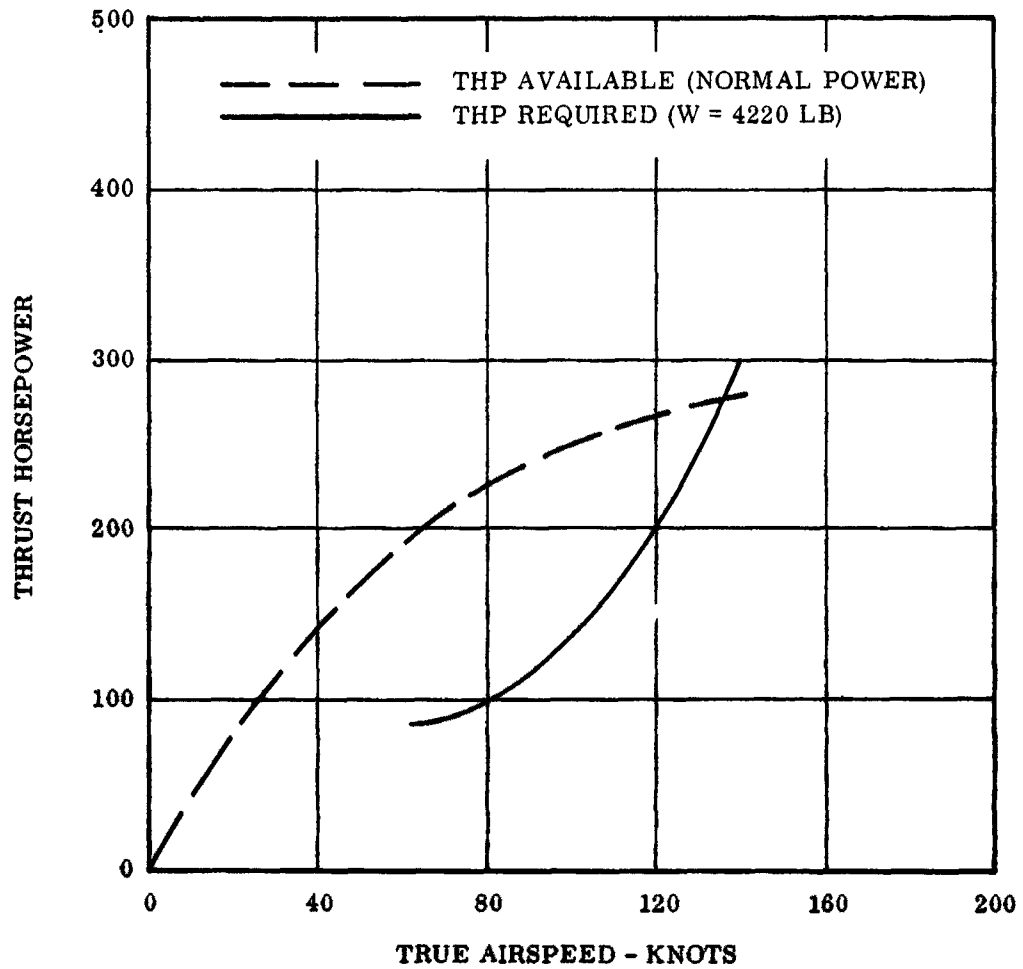


Figure 29 Thrust Horsepower - L-20A

L-20A TAKE-OFF  
GROUND RUN AT SEA LEVEL  
STANDARD DAY

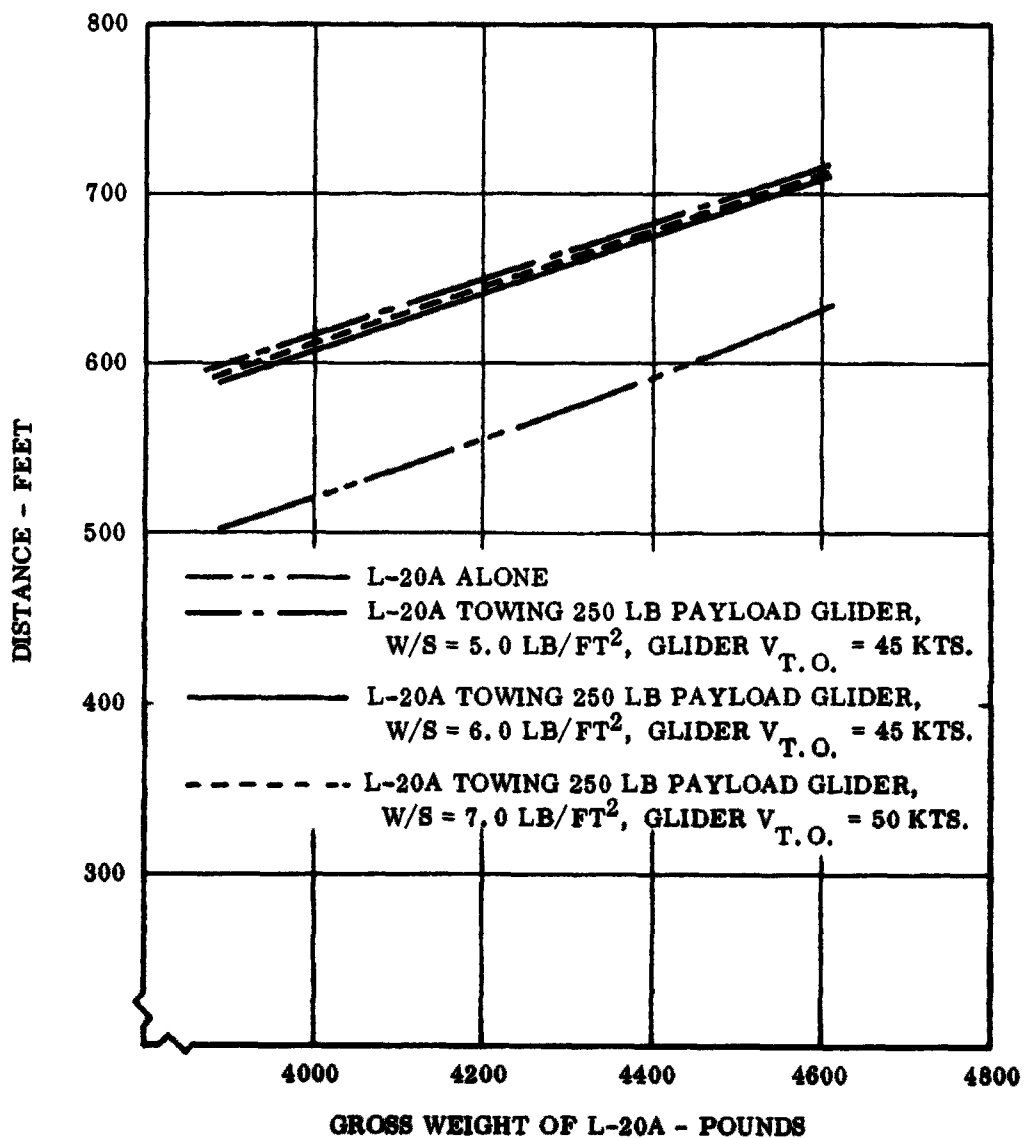


Figure 30 Take-off Ground Runs, L-20A and Gliders

L-20A TAKE-OFF  
GROUND RUN AT SEA LEVEL  
STANDARD DAY  
GLIDER W/S = 6.0 LB/FT<sup>2</sup>

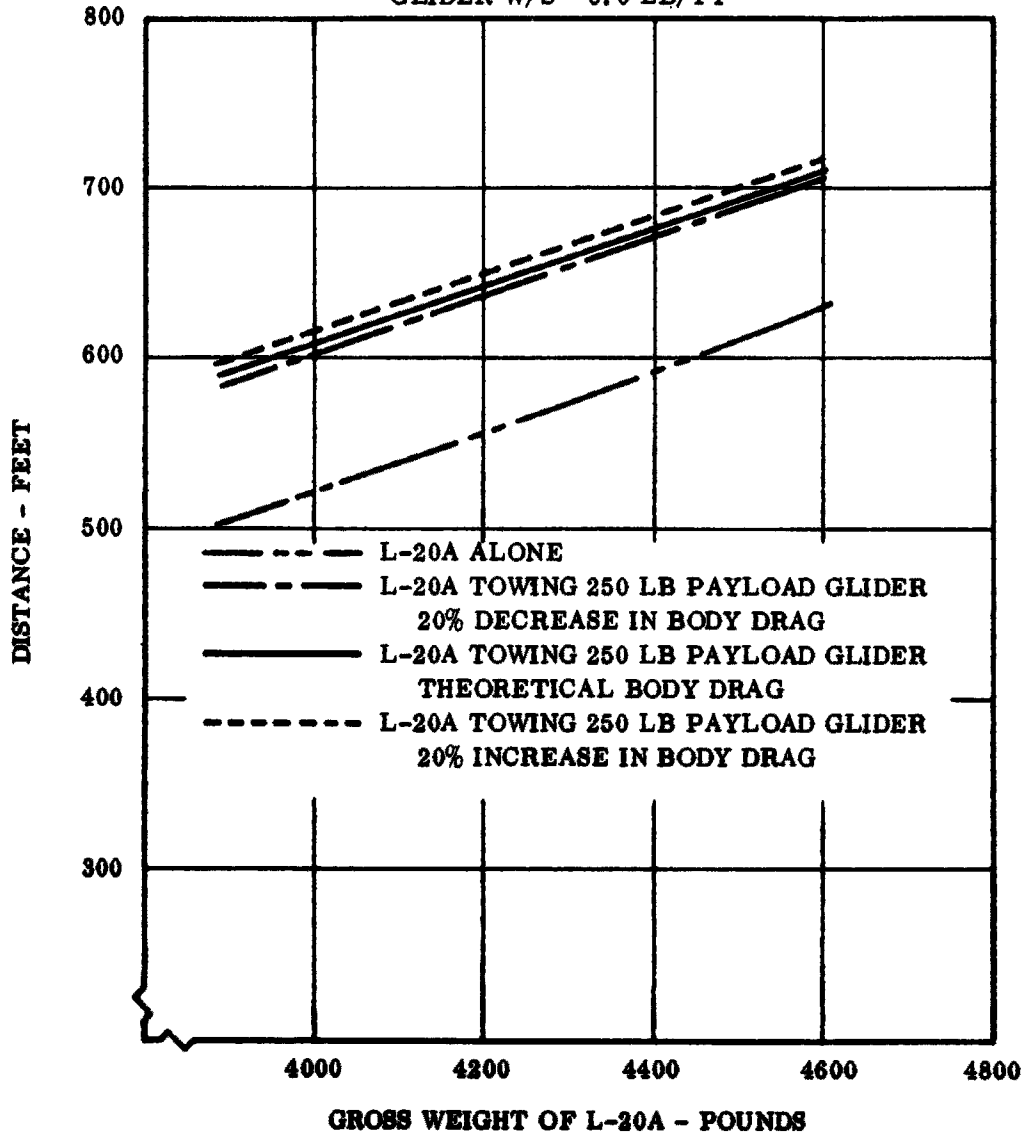


Figure 31 Take-off Ground Runs, L-20A and Gliders

L-20A TAKE-OFF  
 GROUND RUN AT SEA LEVEL  
 STANDARD DAY  
 GLIDER W/S = 6.0 LB/FT<sup>2</sup>

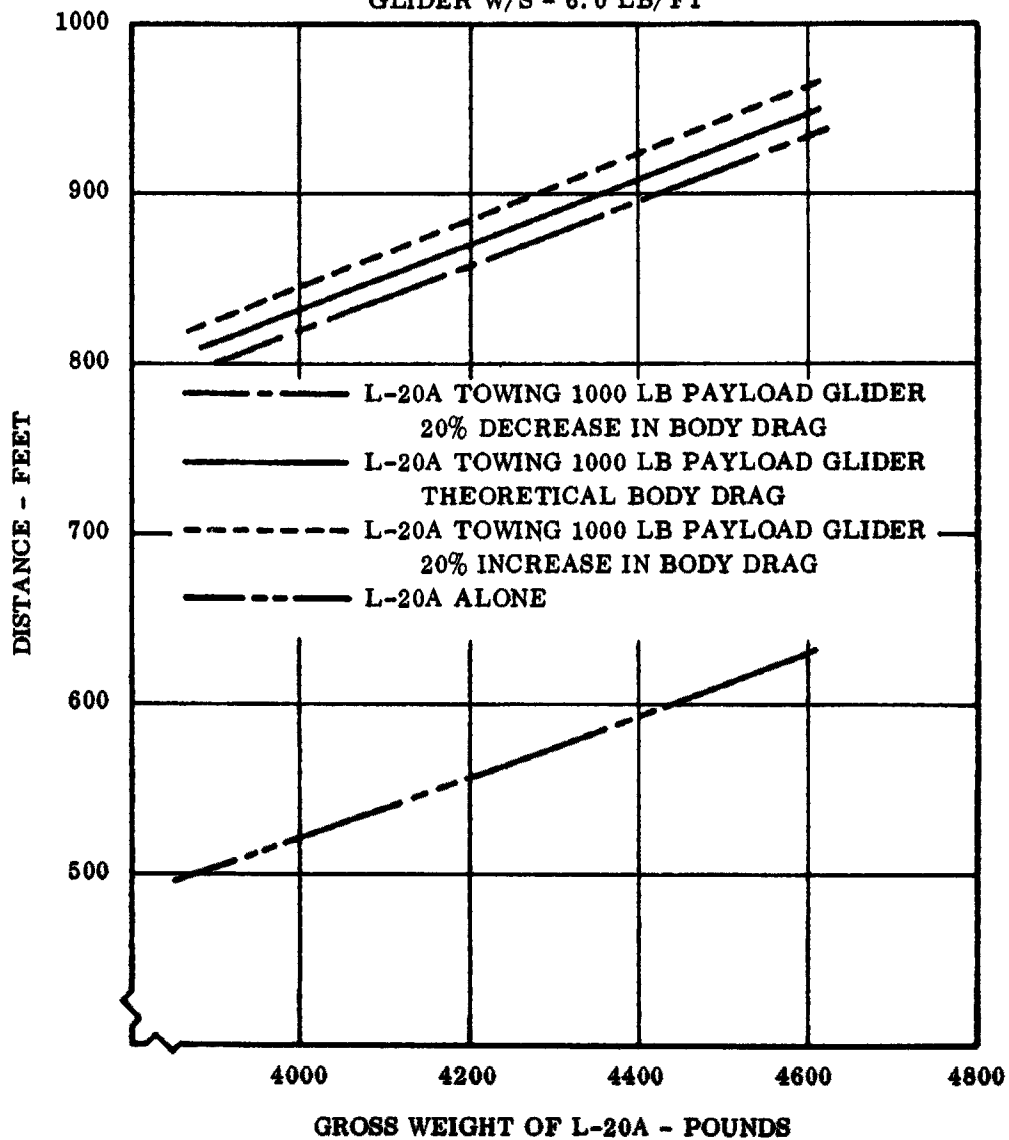


Figure 32 Take-off Ground Runs, L-20A and Gliders

**L-20A TAKE-OFF  
GROUND RUN AT SEA LEVEL  
STANDARD DAY**

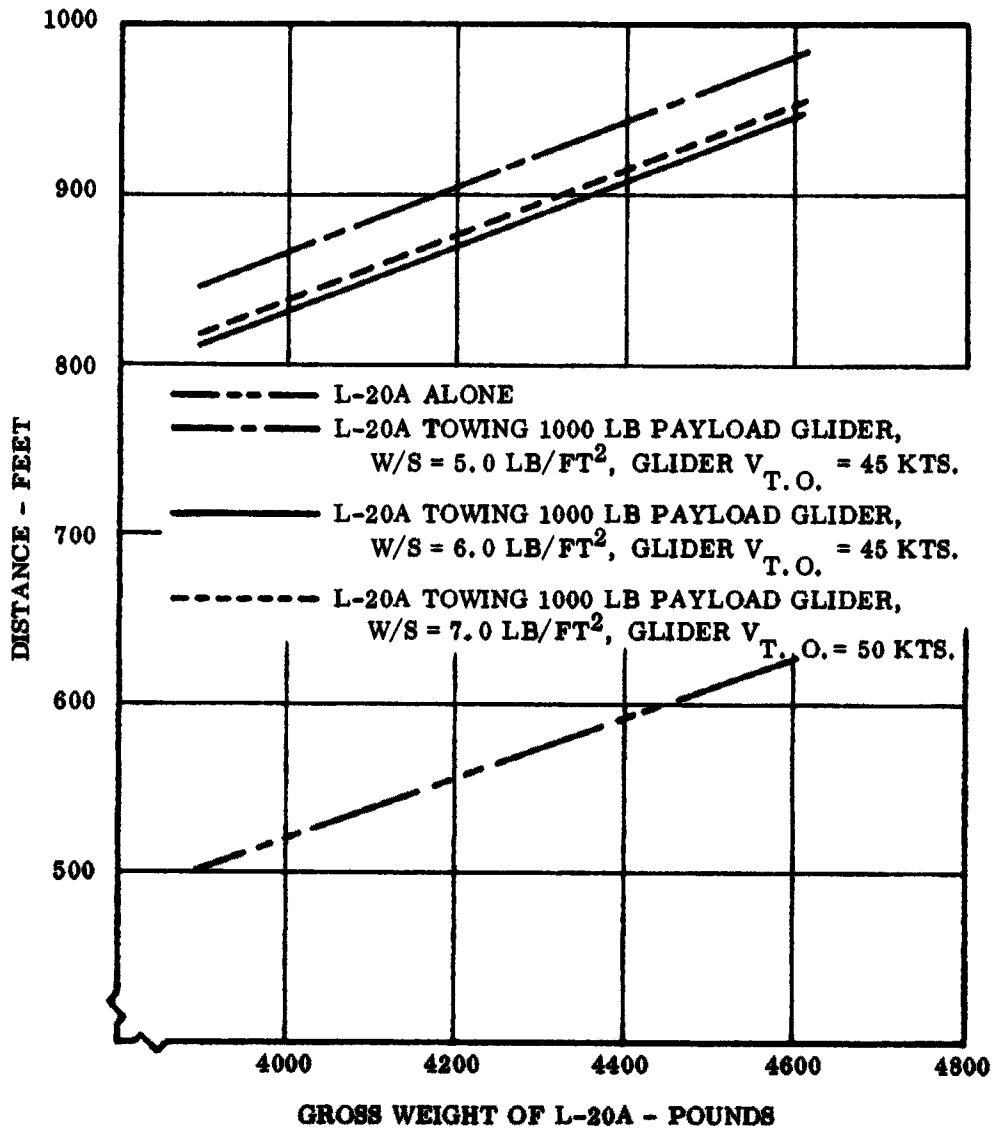


Figure 33 Take-off Ground Runs, L-20A and Gliders

LANDING DISTANCE VS. GLIDER DESIGN PAYLOAD  
SEA LEVEL STANDARD DAY

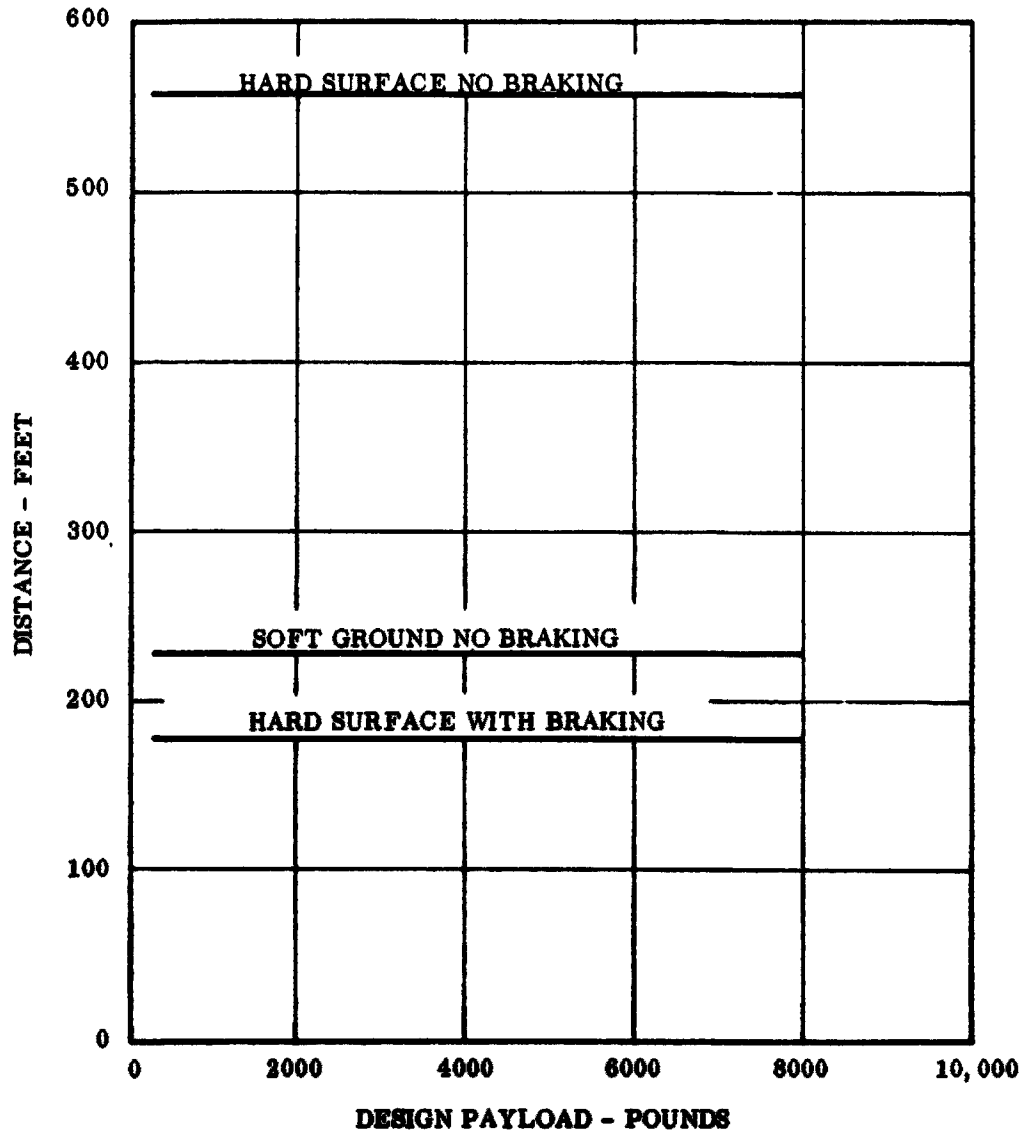


Figure 34 Glider Landing Distance

RATE OF CLIMB VS. TRUE AIRSPEED  
ON SEA LEVEL STANDARD DAY  
L-20A WEIGHT = 4220 LB, GLIDER W/S = 6.0 LB/FT<sup>2</sup>

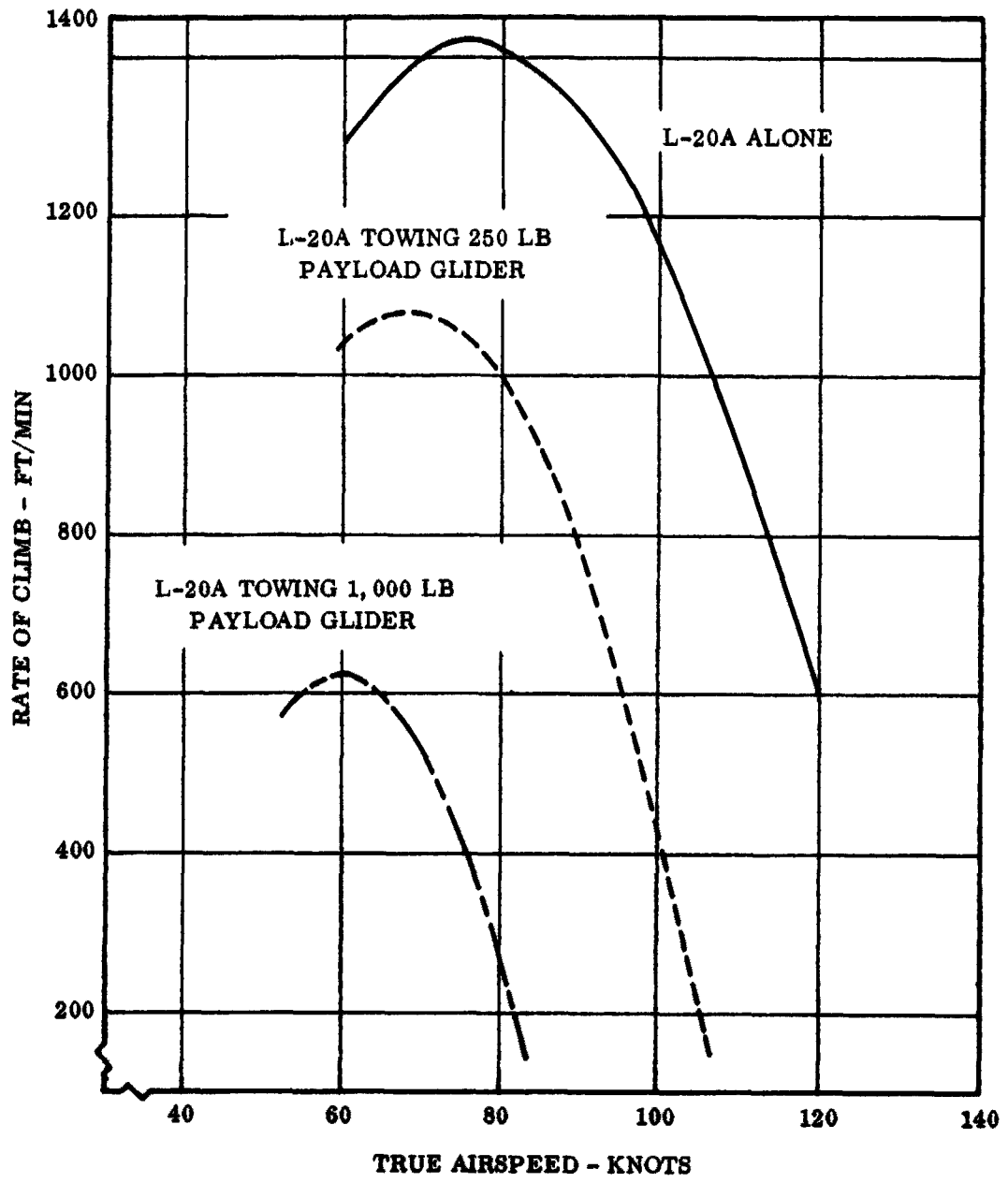


Figure 35 Rate of Climb, L-20A and Gliders

RATE OF CLIMB VS. TRUE AIRSPEED  
ALTITUDE - 5,000 FT, STANDARD DAY  
L-20A WEIGHT = 4,220 LB, GLIDER W/S = 6.0 LB/FT<sup>2</sup>

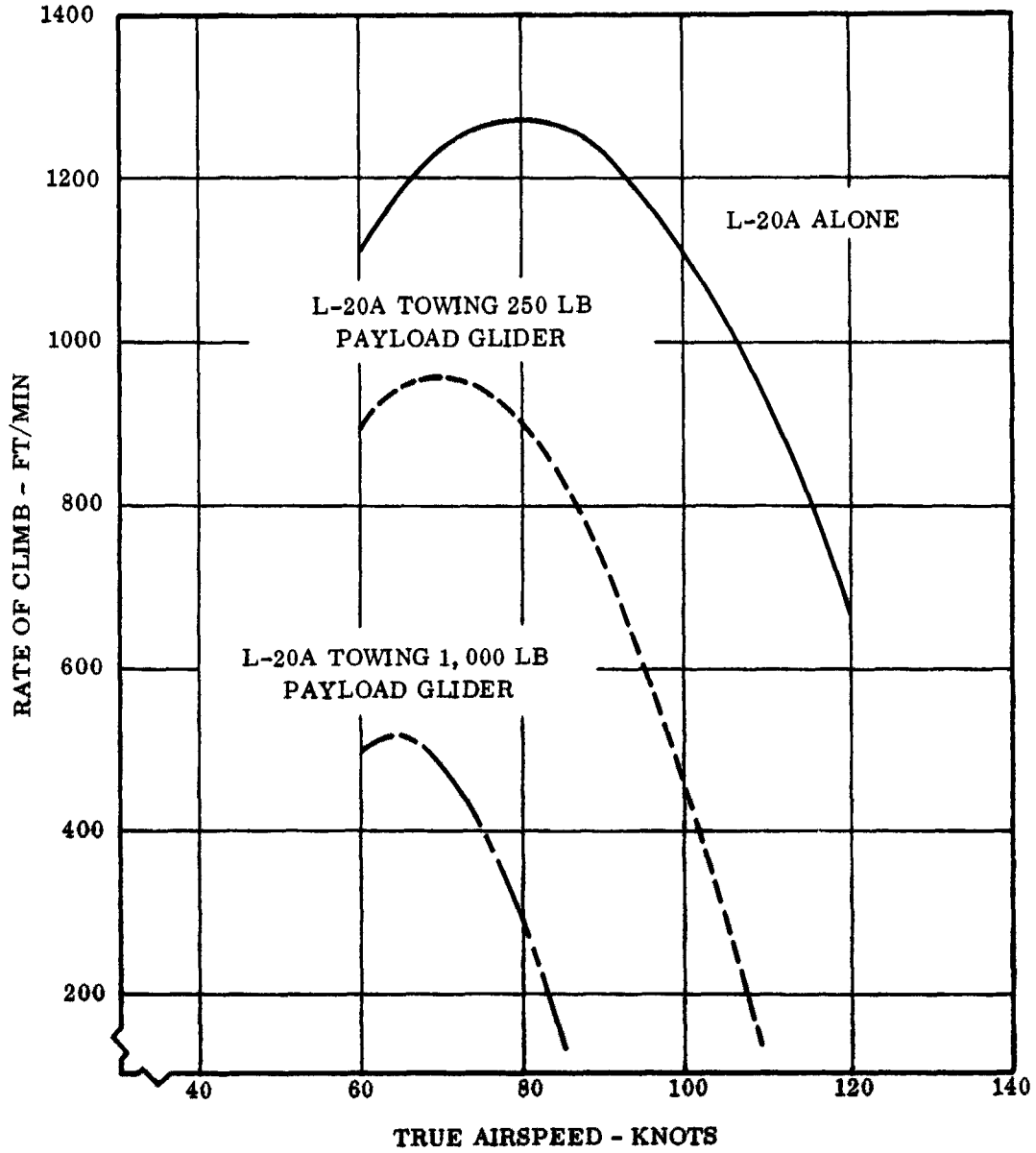


Figure 36 Rate of Climb, L-20A and Gliders

RATE OF CLIMB VS. TRUE AIRSPEED  
ALTITUDE = 10,000 FT, STANDARD DAY  
L-20A WEIGHT = 4220 LB, GLIDER W/S = 6.0 LB/FT<sup>2</sup>

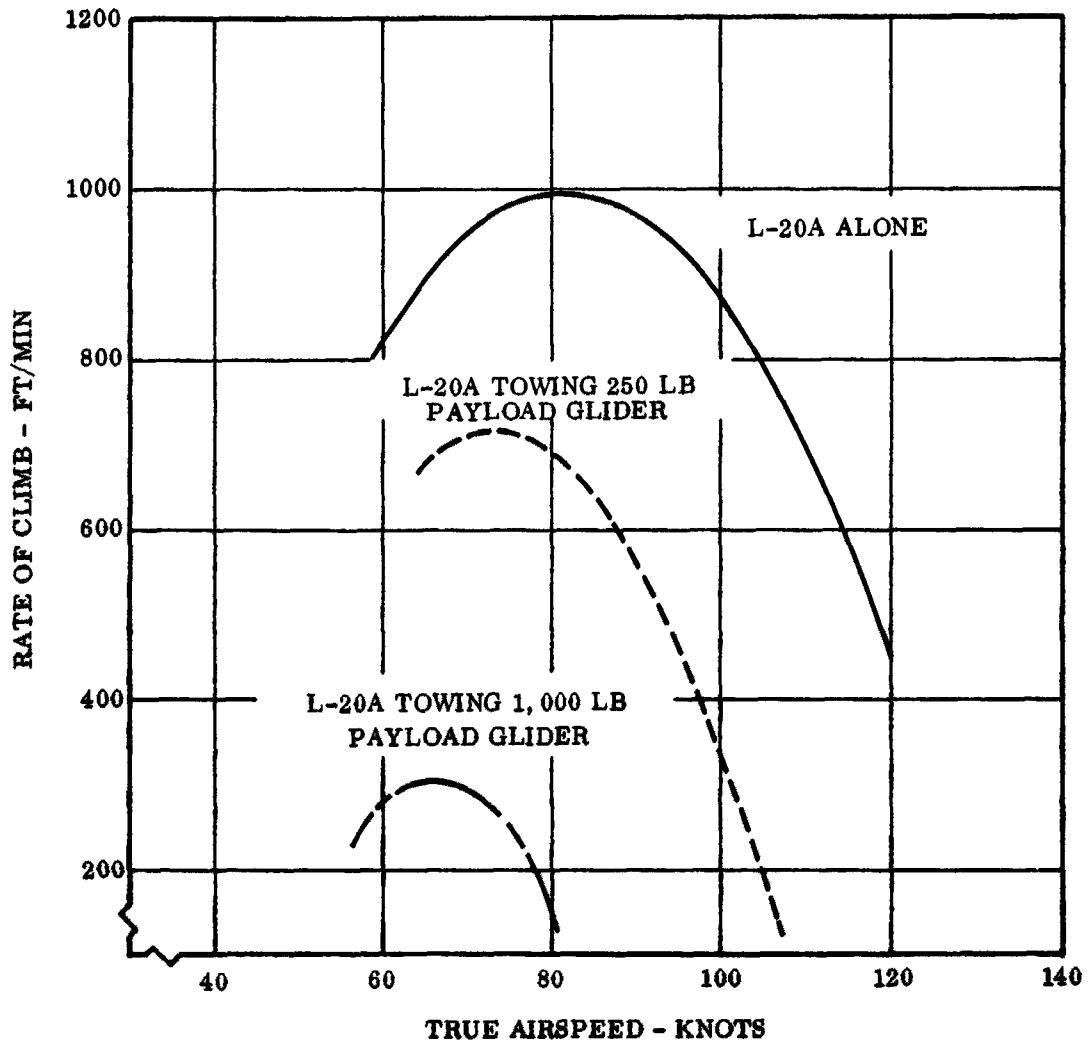


Figure 37 Rate of Climb, L-20A and Gliders

L-20A MISSION PROFILE

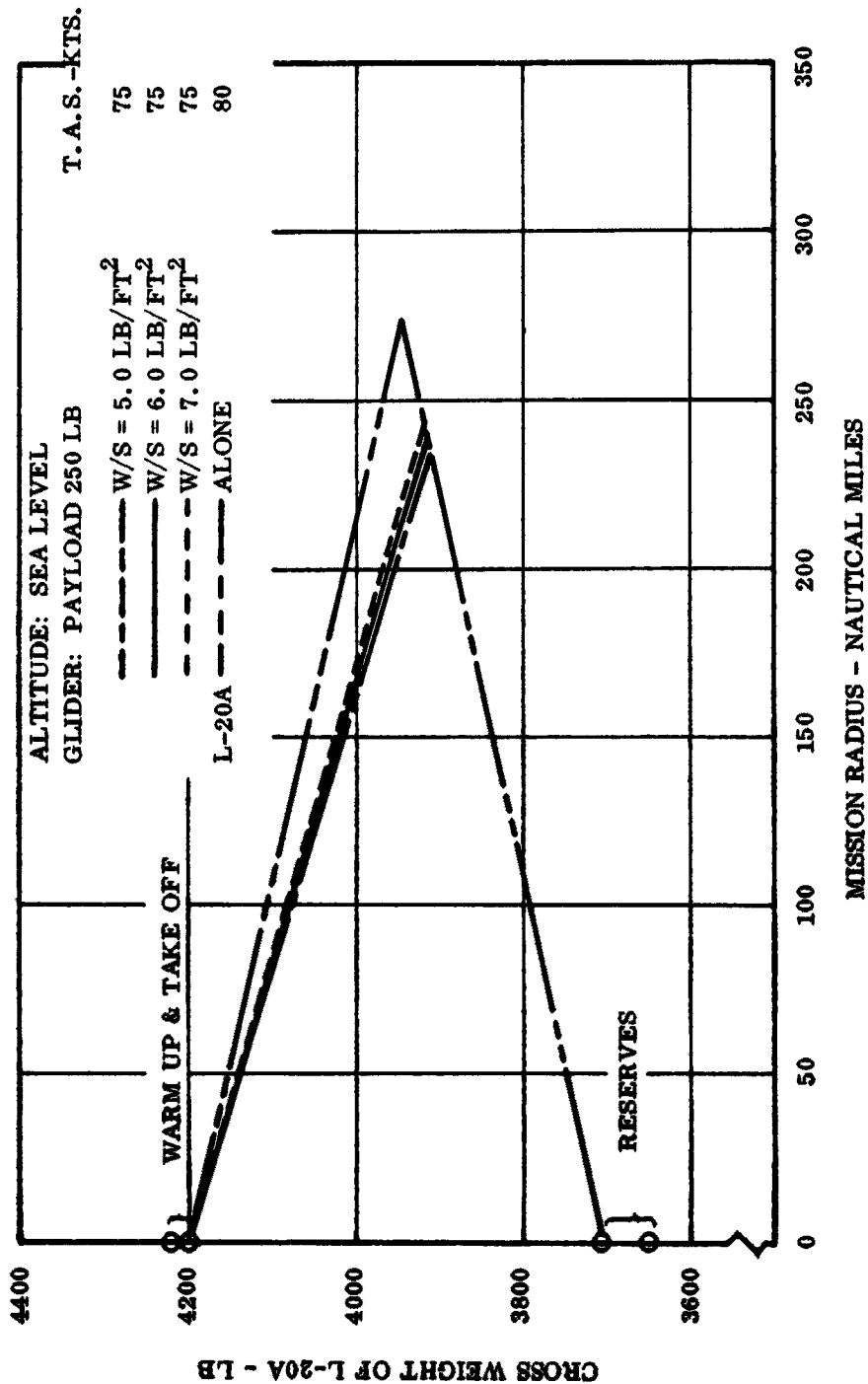


Figure 38 Mission Profiles, L-20A and Gliders

L-20A MISSION PROFILE

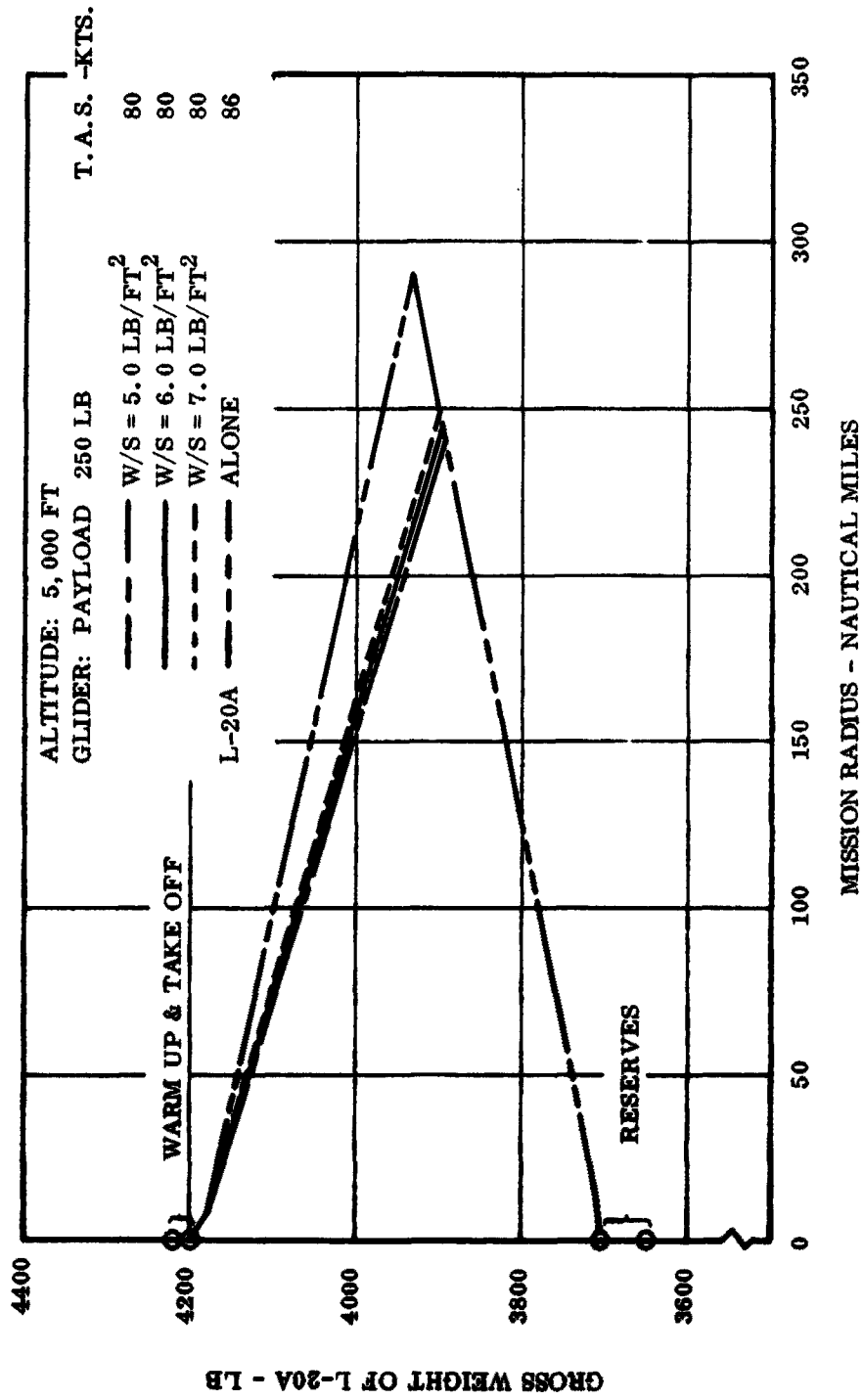


Figure 39 Mission Profiles, L-20A and Gliders

L-20A MISSION PROFILE

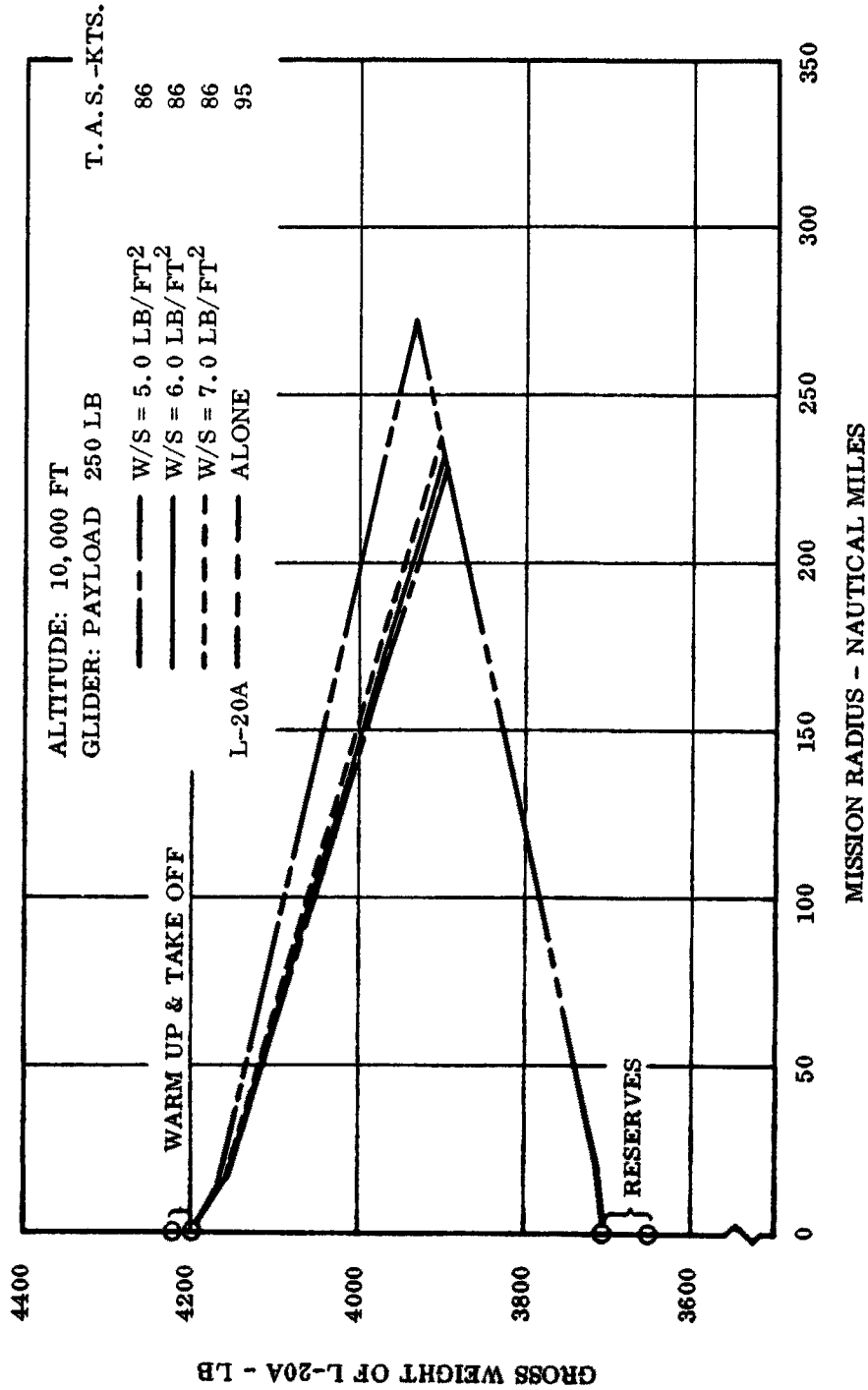


Figure 40 Mission Profiles, L-20A and Gliders

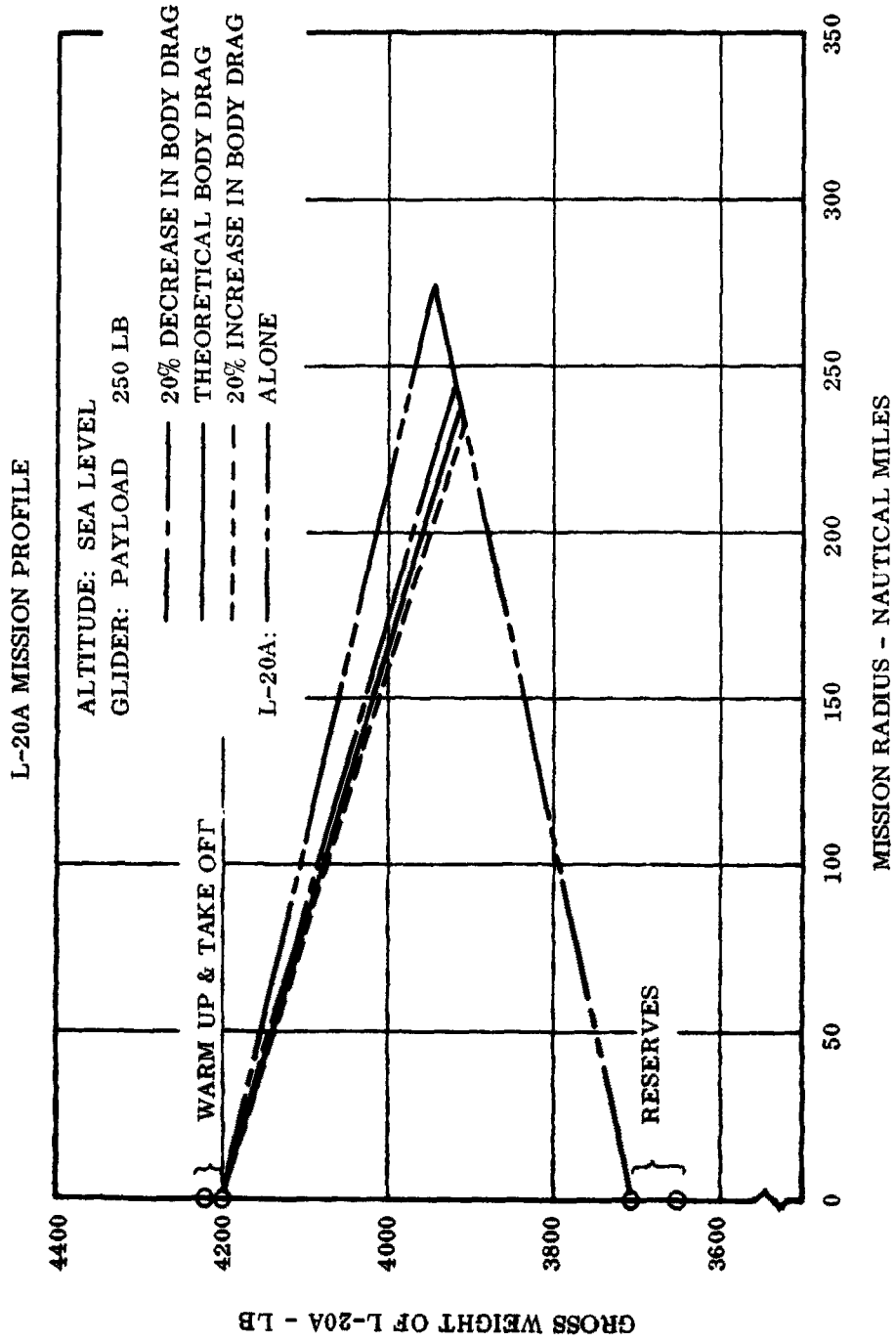


Figure 41 Mission Profiles, L-20A and Gliders

L-20A MISSION PROFILE

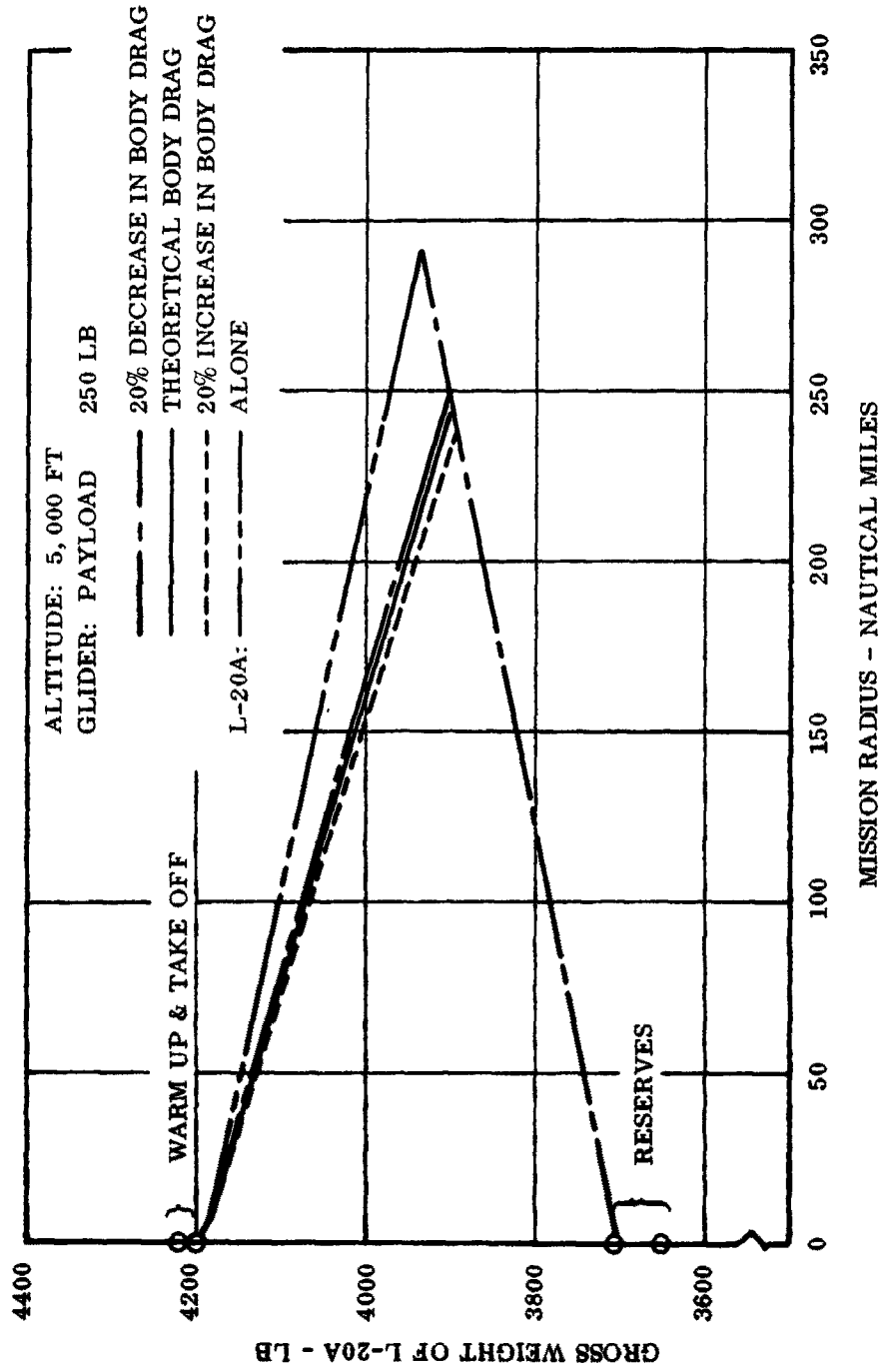


Figure 42 Mission Profiles, L-20A and Gliders

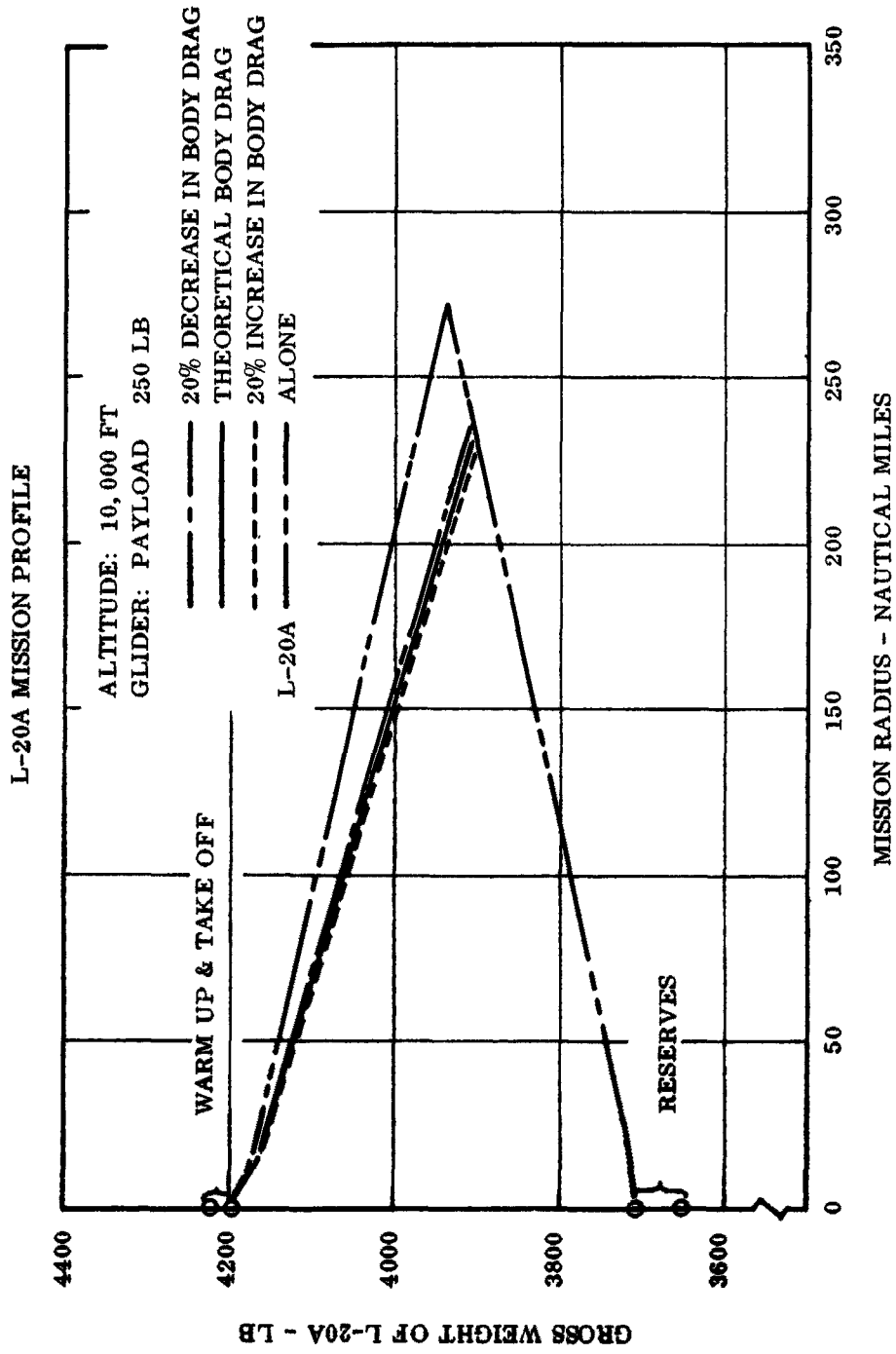


Figure 43 Mission Profiles, L-20A and Gliders

L-20A MISSION PROFILE

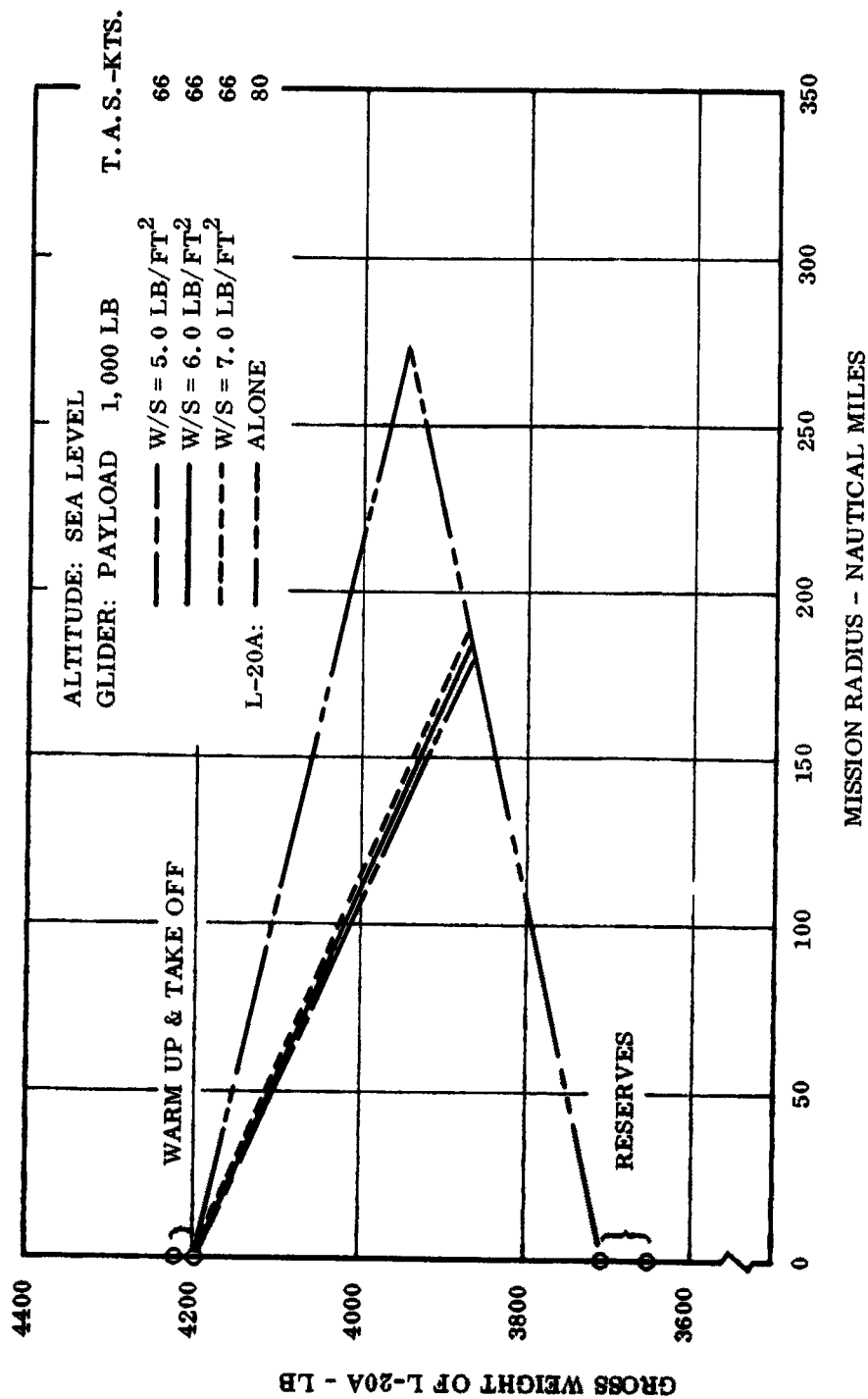


Figure 44 Mission Profiles, L-20A and Gliders

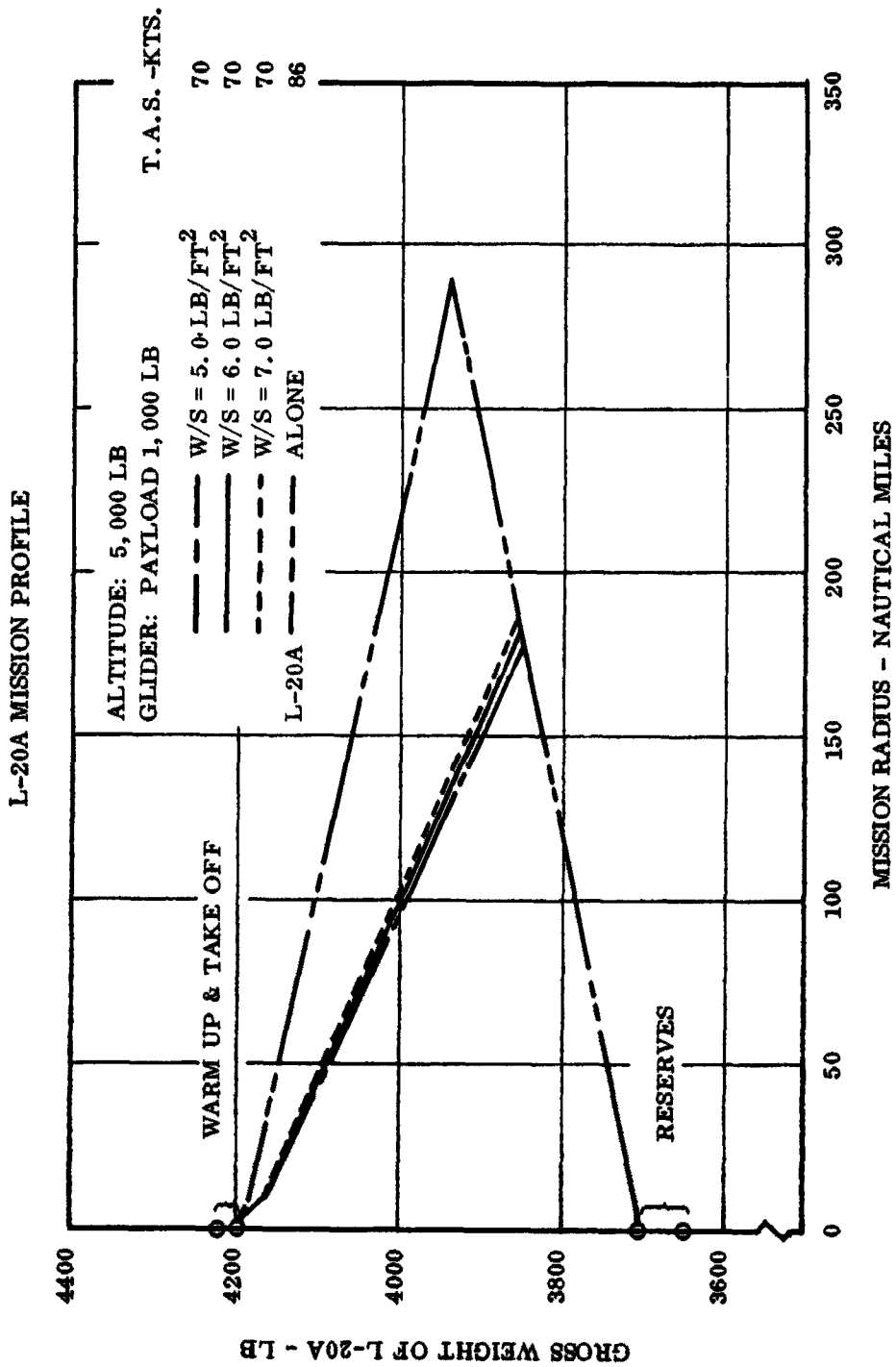


Figure 45 Mission Profiles, L-20A and Gliders

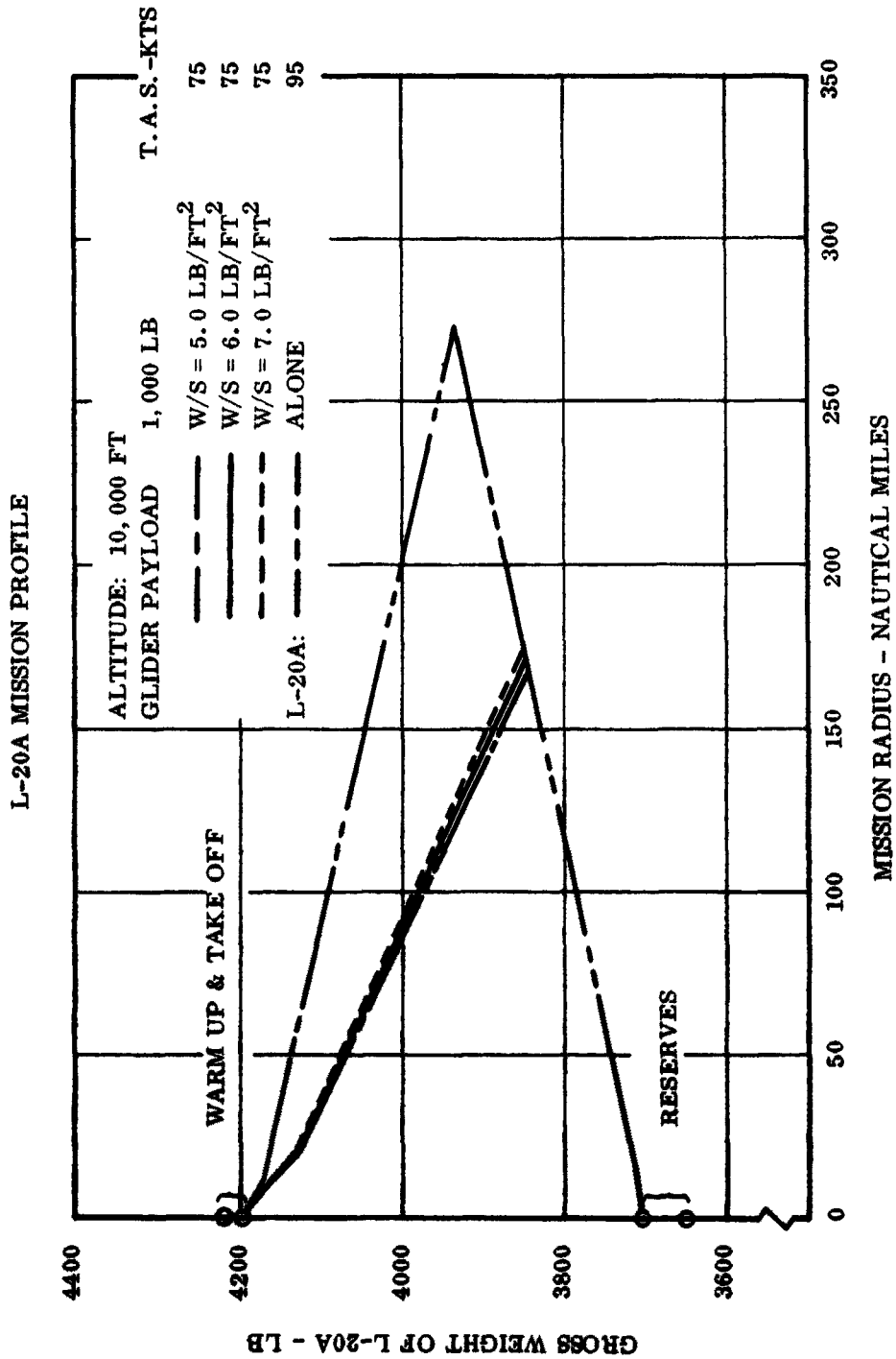


Figure 46 Mission Profiles, L-20A and Gliders

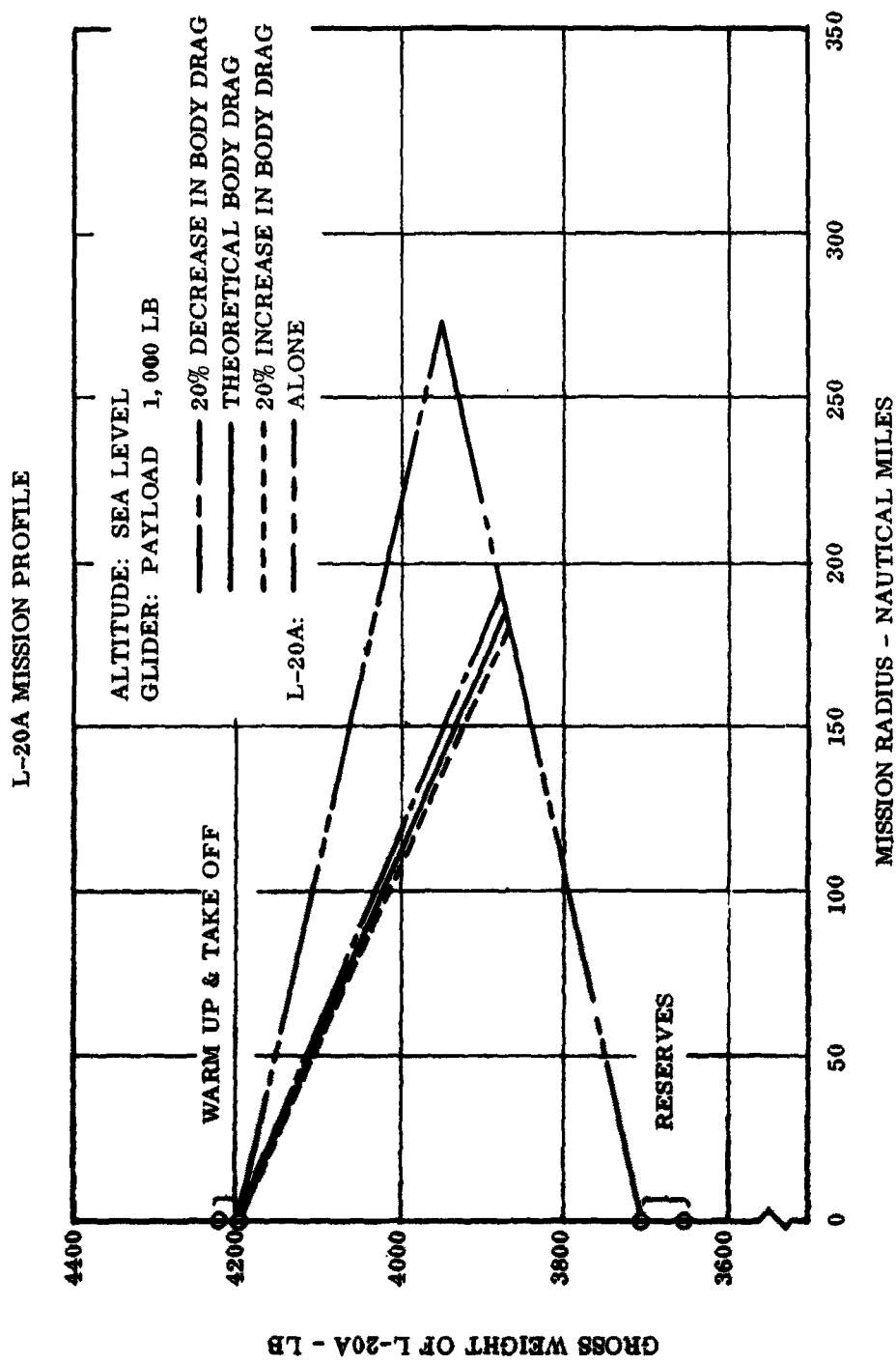


Figure 47 Mission Profiles, L-20A and Gliders

L-20A MISSION PROFILE

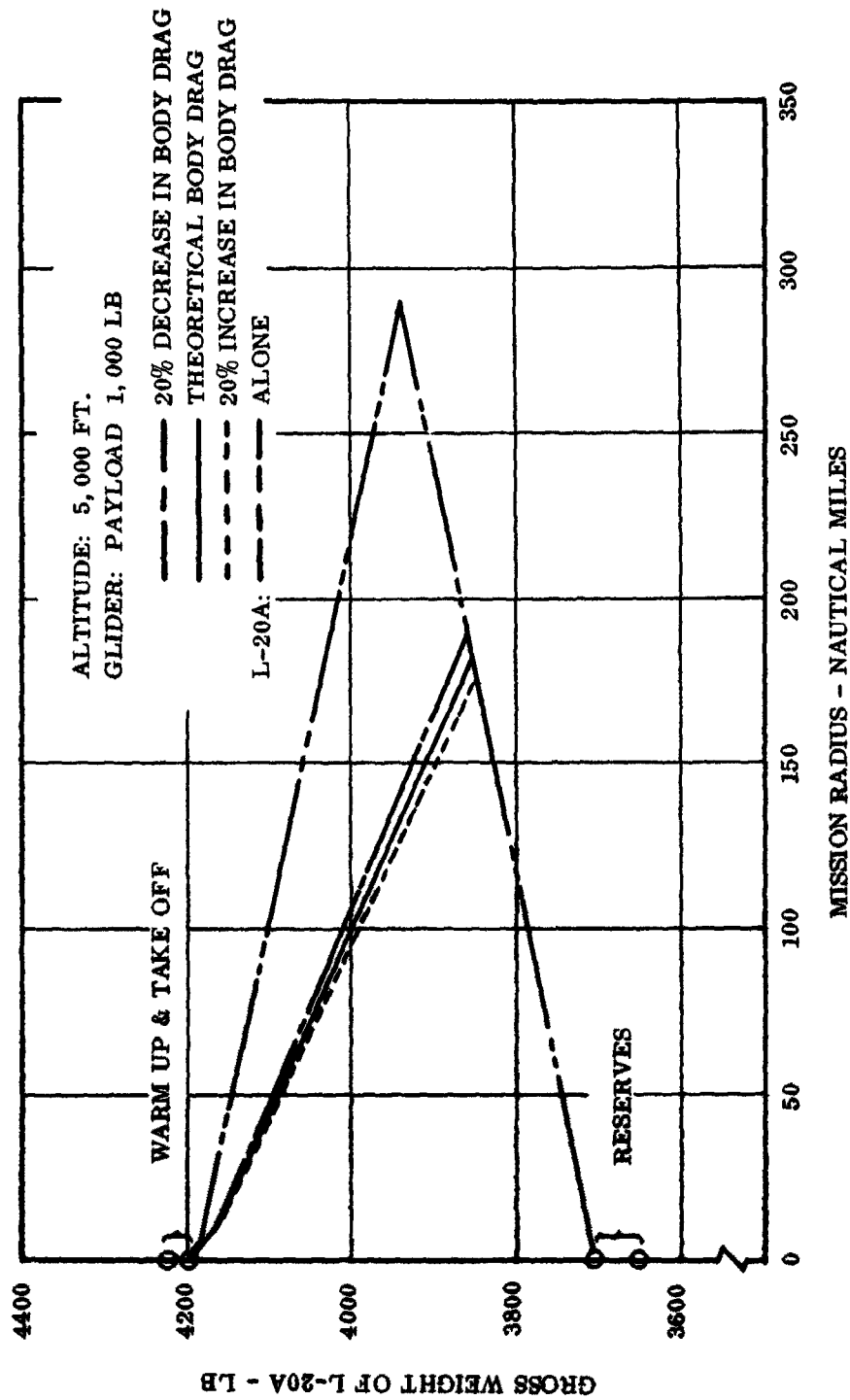


Figure 48 Mission Profiles, L-20A and Gliders

L-20A MISSION PROFILE

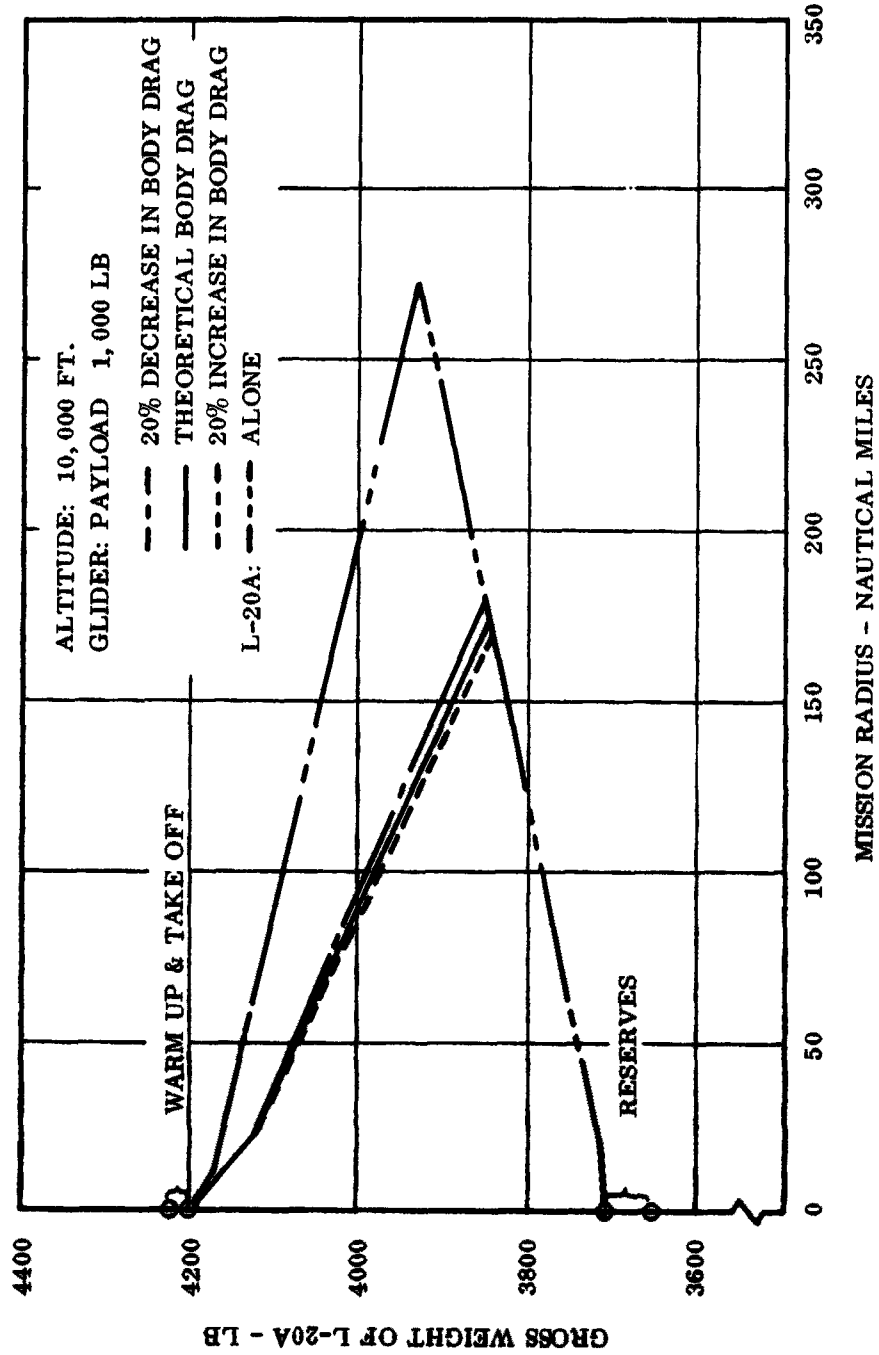


Figure 49 Mission Profiles, L-20A and Gliders

TAKE-OFF DISTANCE VS. GLIDER DESIGN PAYLOAD  
SEA LEVEL STANDARD DAY  
H-23D HELICOPTER (W - 2478 LB)

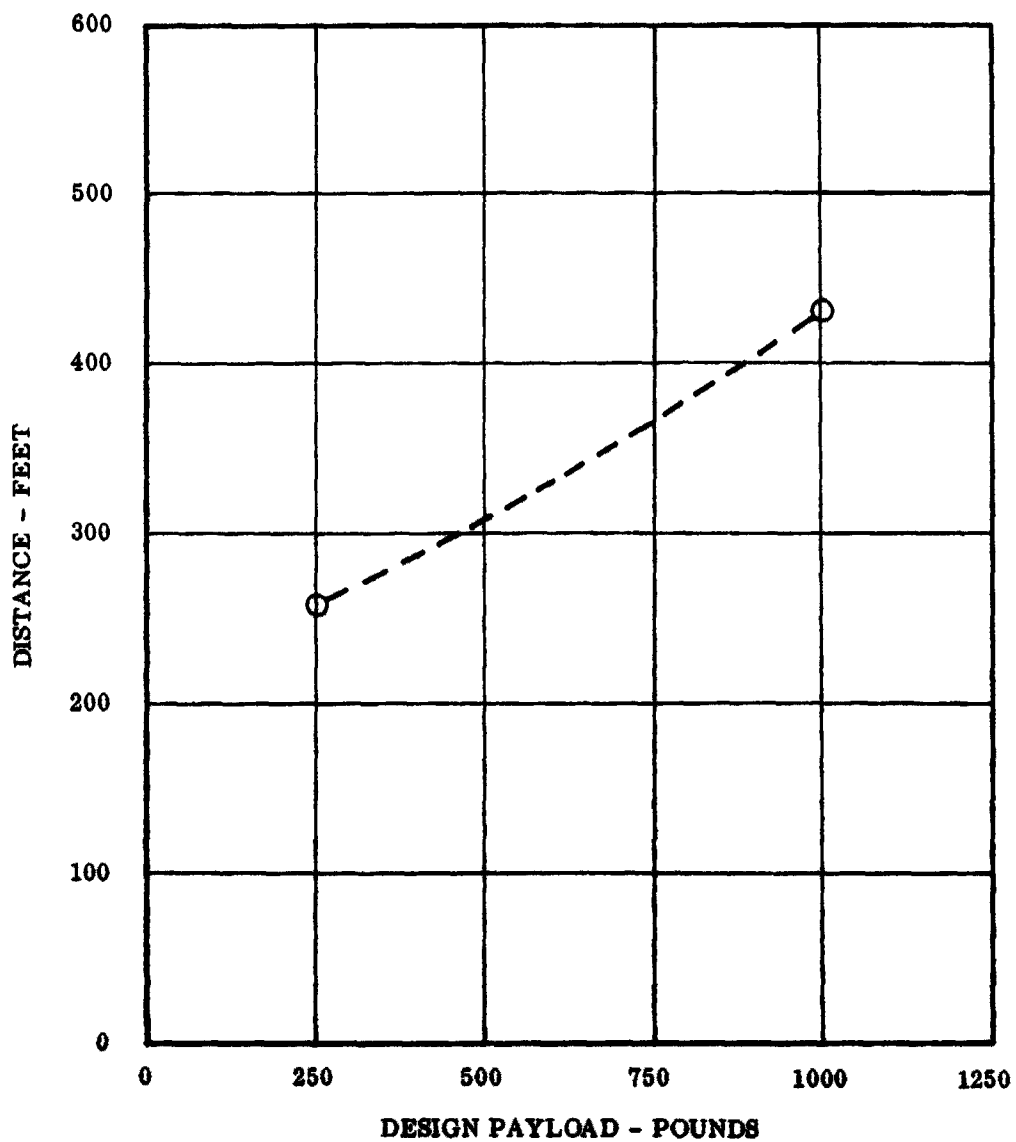


Figure 50 Take-off Distances, Helicopters with Gliders

TAKE-OFF DISTANCE VS. GLIDER DESIGN PAYLOAD  
SEA LEVEL STANDARD DAY  
HU-1B HELICOPTER (W - 5954 LB)

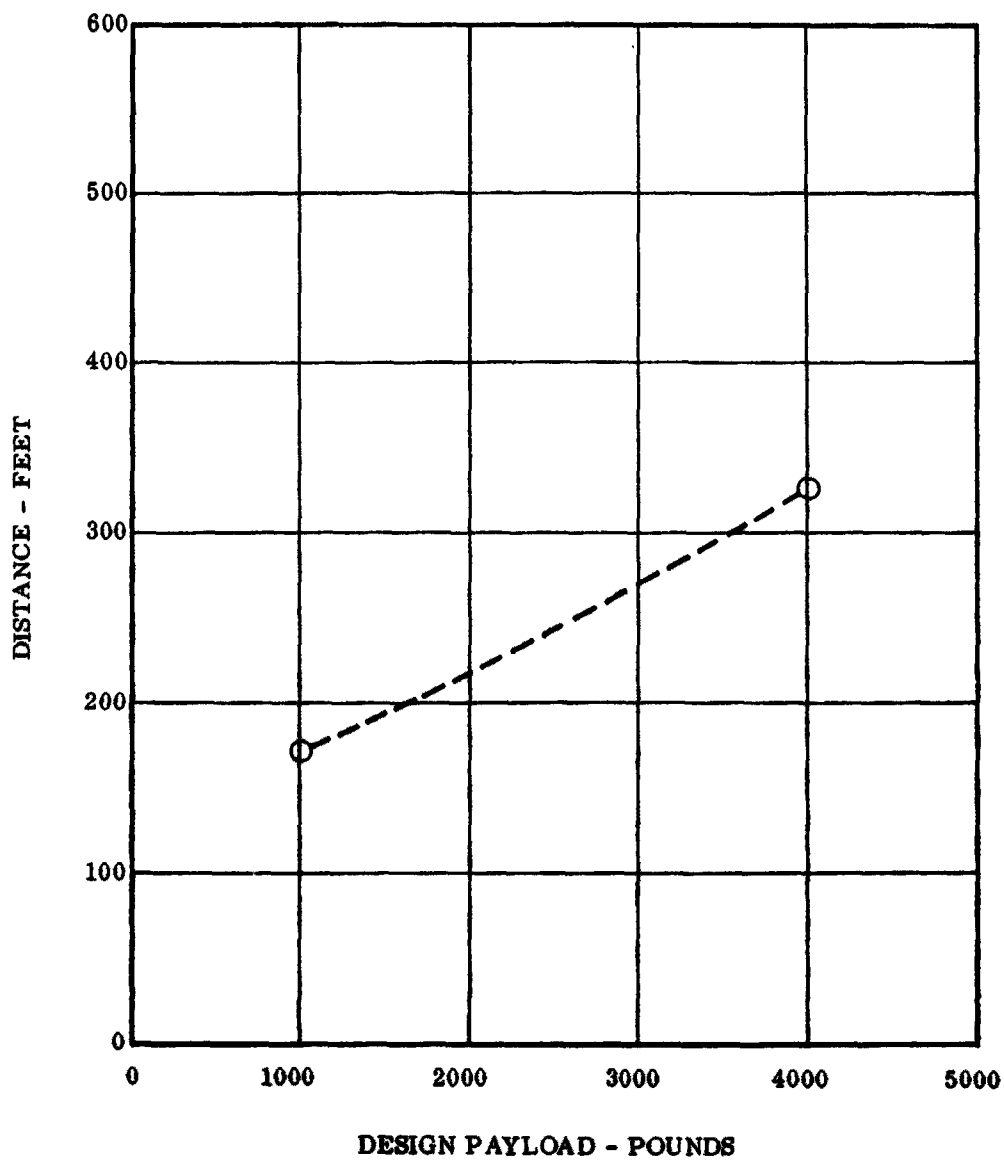


Figure 51 Take-off Distances, Helicopters with Gliders

TAKE-OFF DISTANCE VS. GLIDER DESIGN PAYLOAD  
SEA LEVEL STANDARD DAY  
H-34A HELICOPTER (W - 9789 LB)

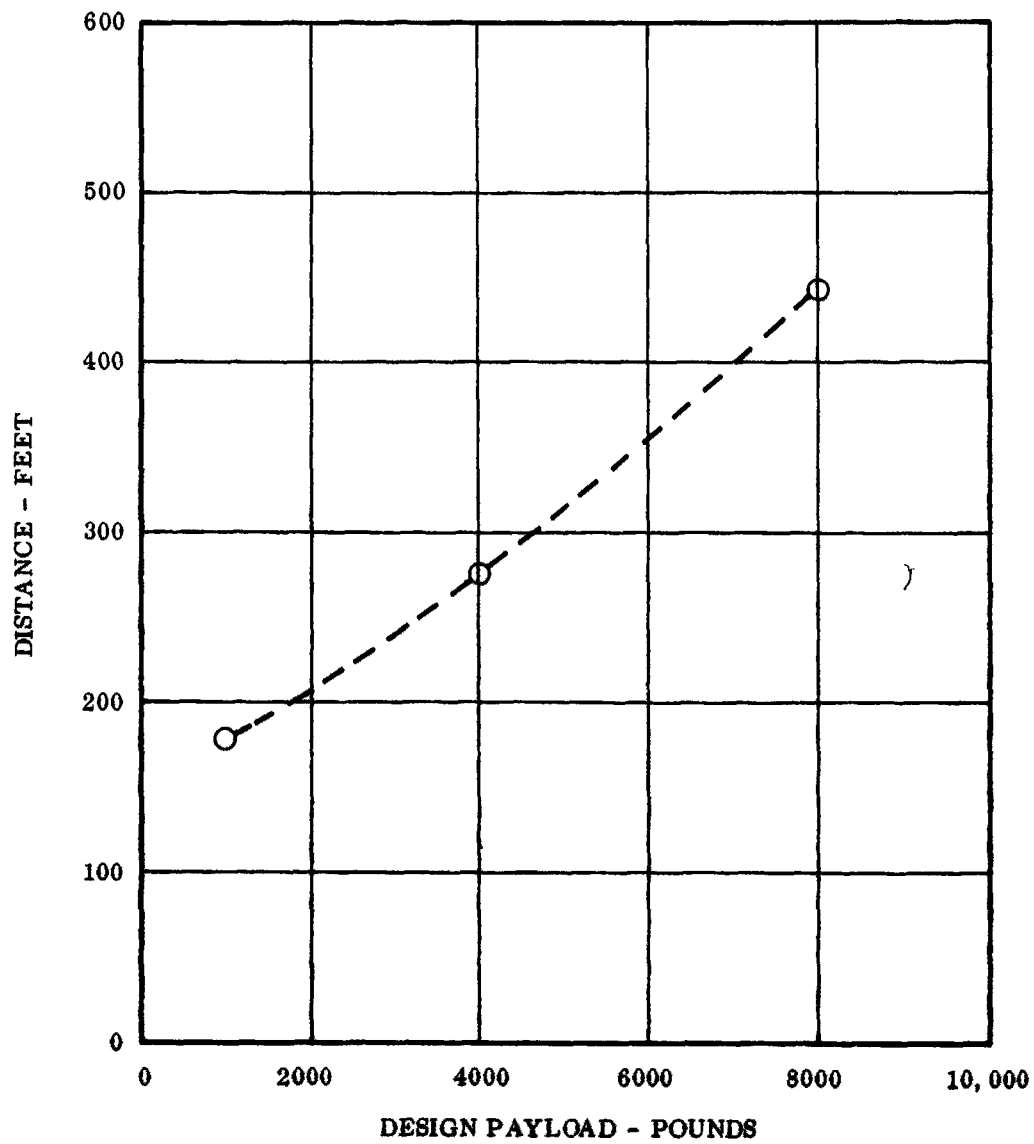


Figure 52 Take-off Distances, Helicopters with Gliders

HILLER  
H-23D  
HORSEPOWER VS. TRUE AIRSPEED

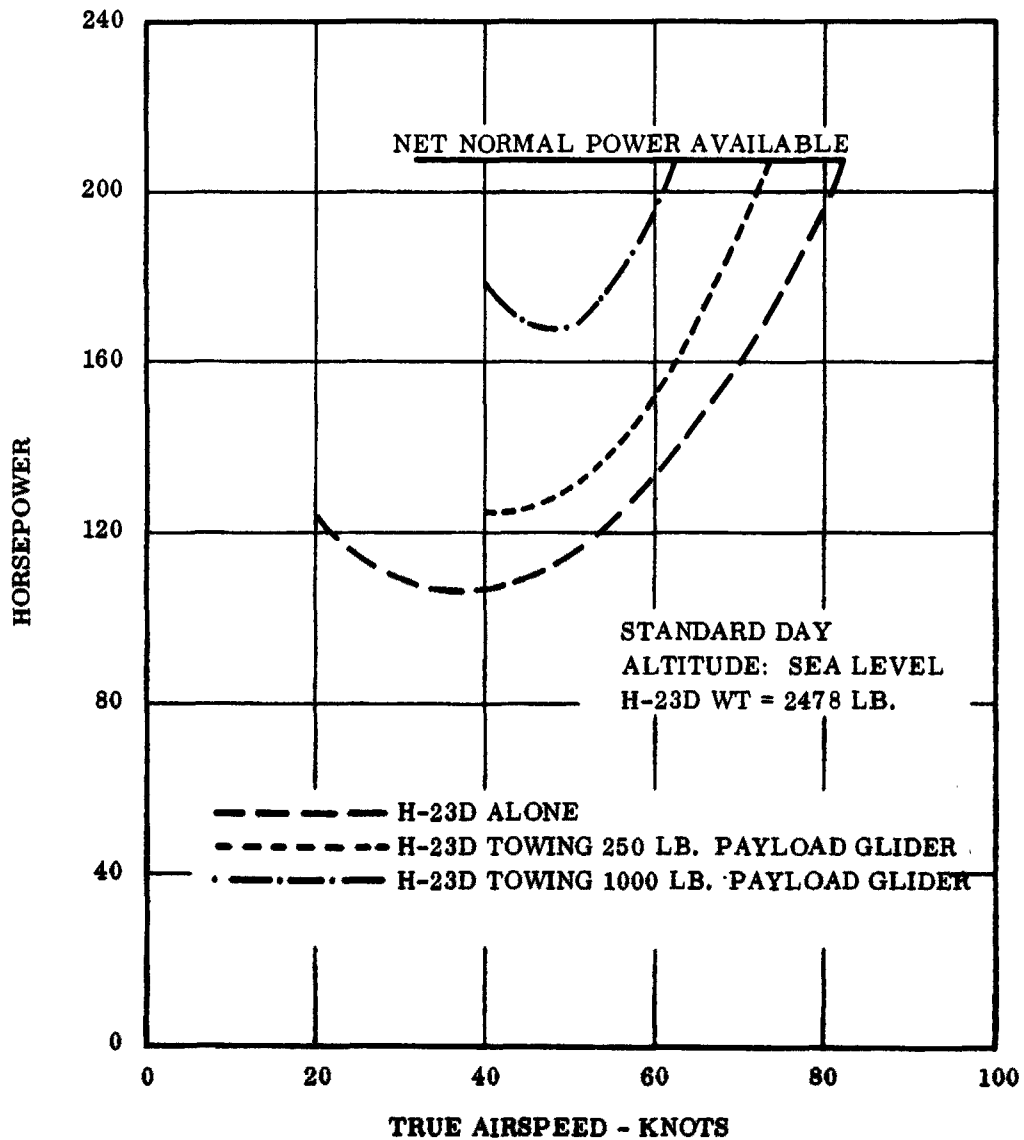


Figure 53 Power Required and Available Helicopters and Gliders

HILLER  
H-23D  
HORSEPOWER VS. TRUE AIRSPEED

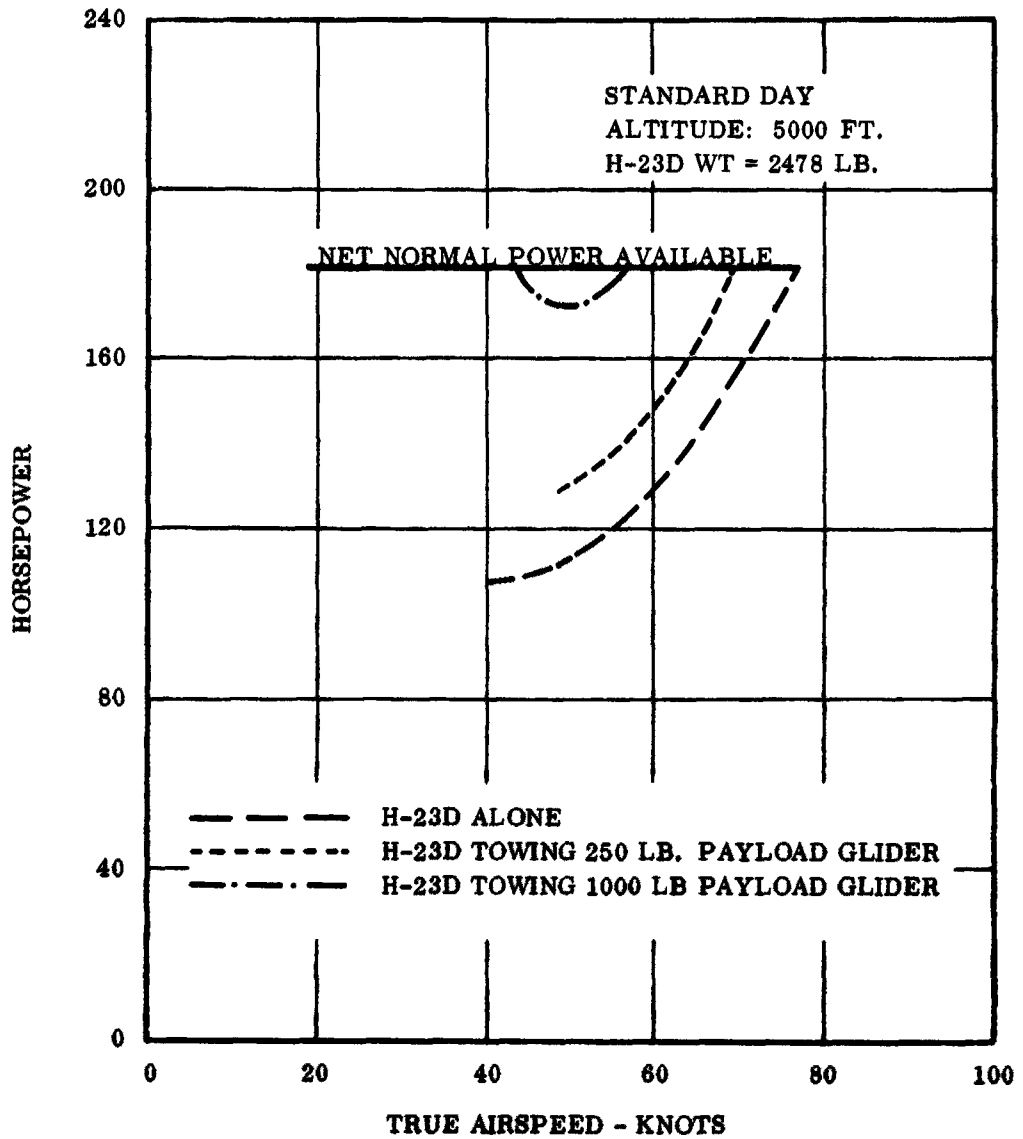


Figure 54 Power Required and Available Helicopters and Gliders

HILLER  
H-23D  
HORSEPOWER VS. TRUE AIRSPEED

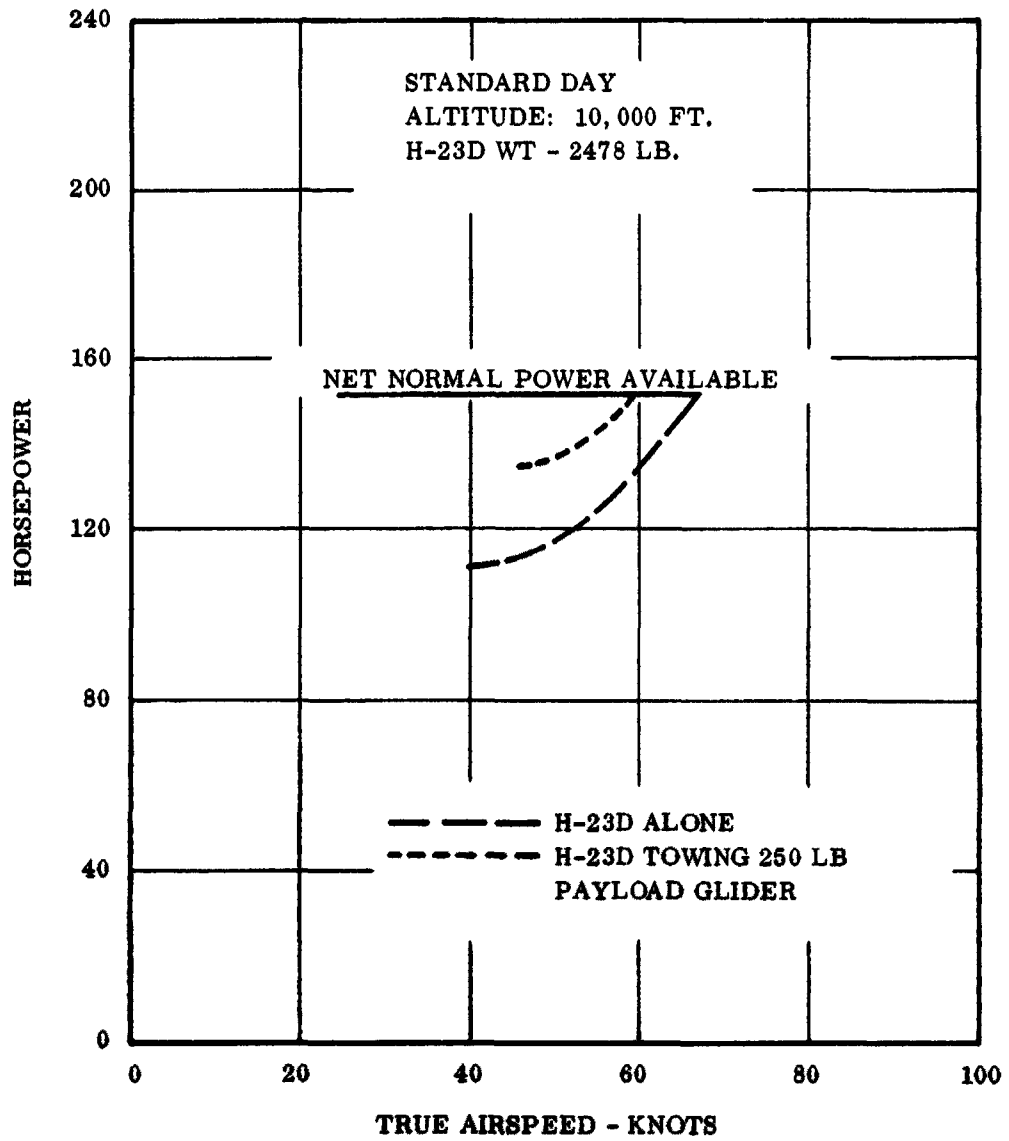


Figure 55 Power Required and Available Helicopters and Gliders

BELL  
 HU-1B  
 HORSEPOWER VS. TRUE AIRSPEED

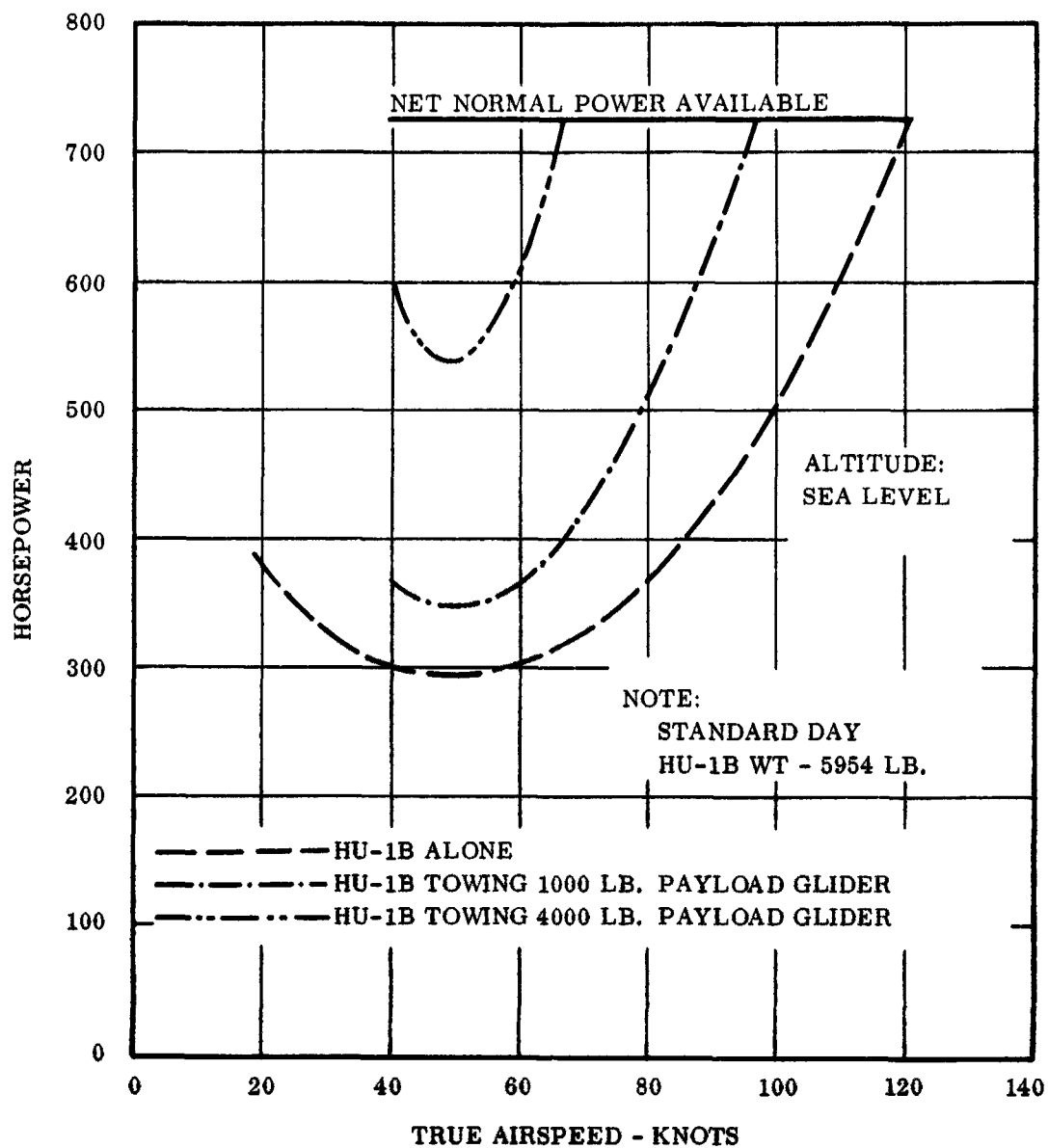


Figure 56 Power Required and Available Helicopters and Gliders

BELL  
 HU-1B  
 HORSEPOWER VS. TRUE AIRSPEED

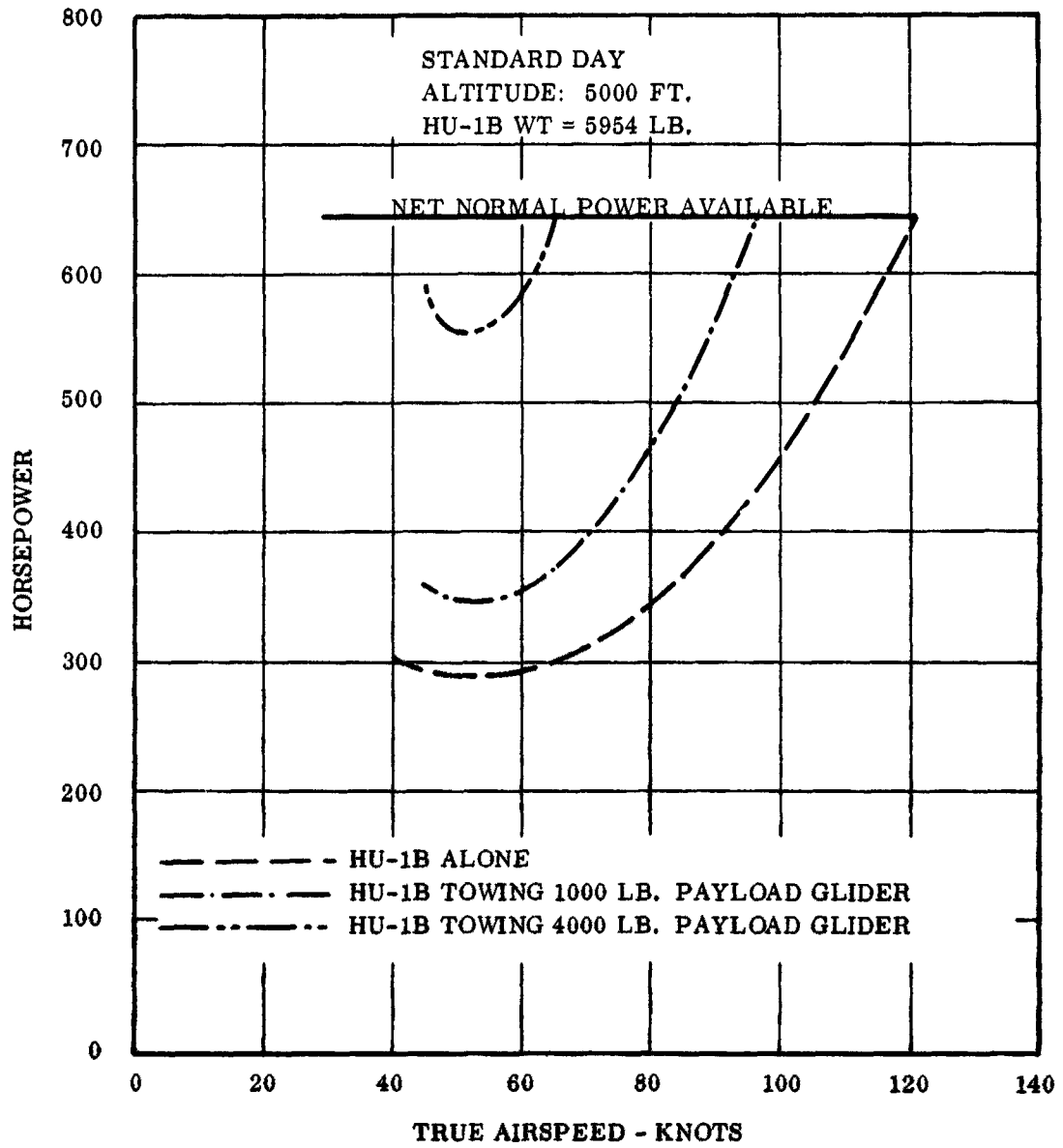


Figure 57 Power Required and Available Helicopters and Gliders

BELL  
 HU-1B  
 HORSEPOWER VS. TRUE AIRSPEED

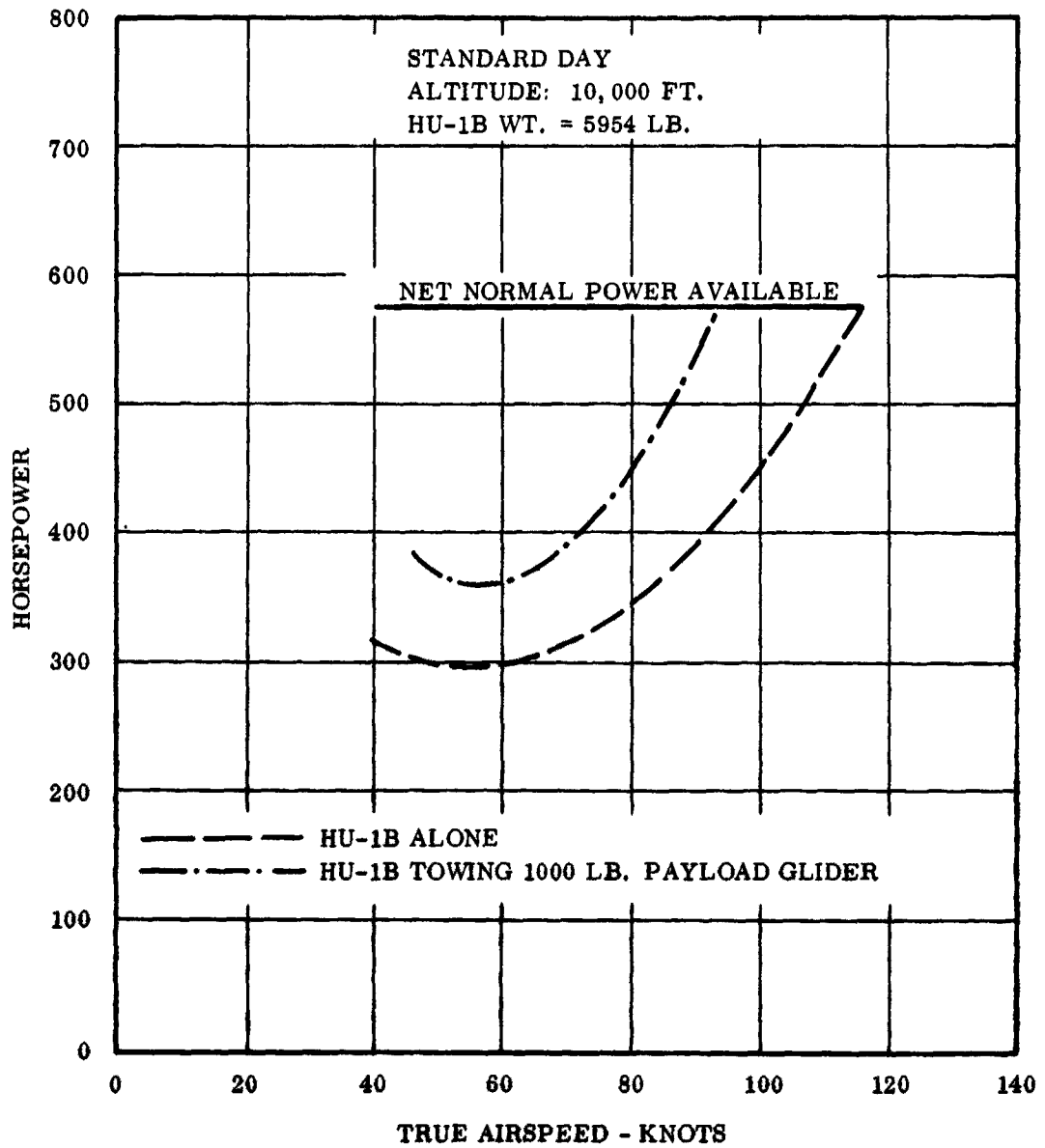


Figure 58 Power Required and Available Helicopters and Gliders

SIKORSKY  
H-34A  
HORSEPOWER VS. TRUE AIRSPEED

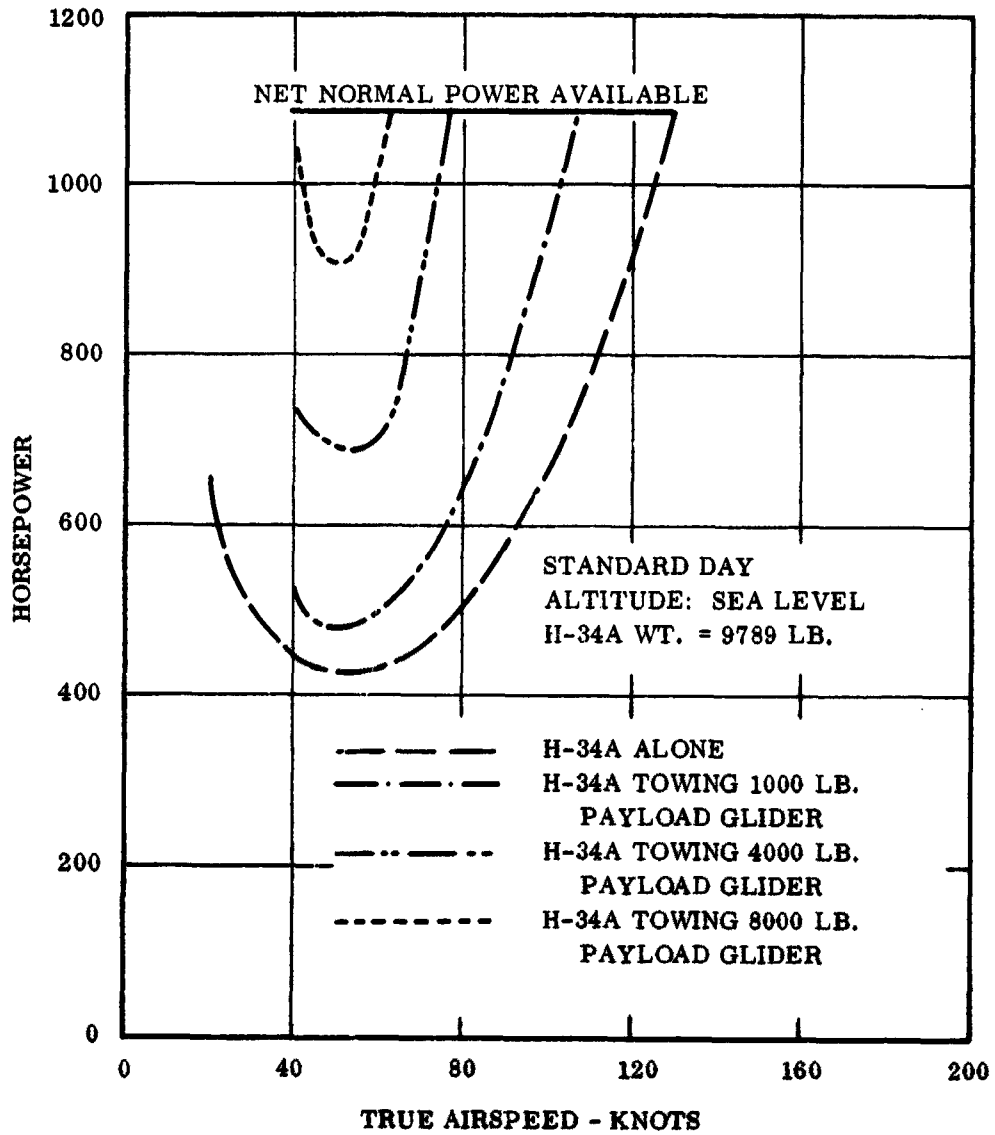


Figure 59 Power Required and Available Helicopters and Gliders

SIKORSKY  
H-34A  
HORSEPOWER VS. TRUE AIRSPEED

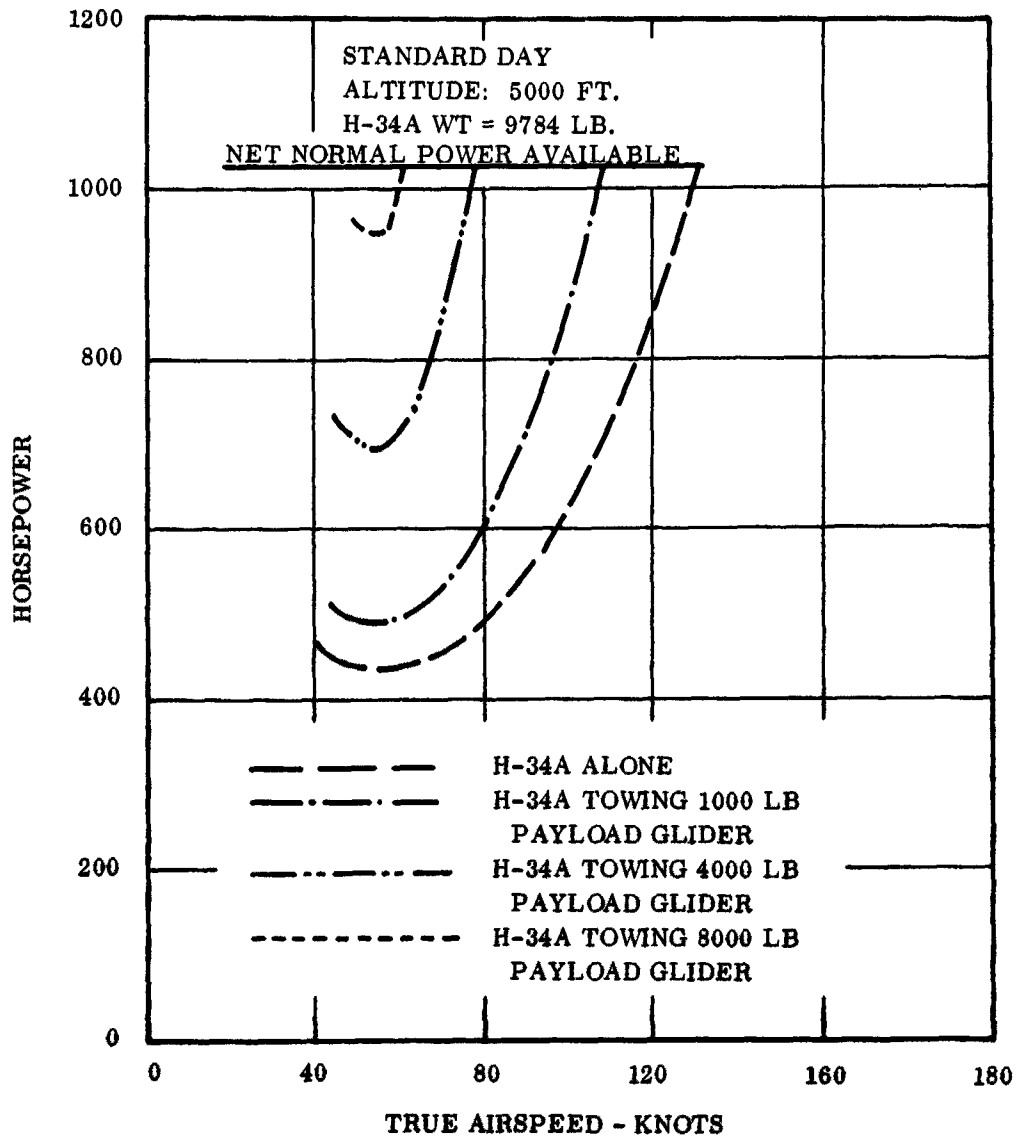


Figure 60 Power Required and Available Helicopters and Gliders

SIKORSKY  
H-34A  
HORSEPOWER VS. TRUE AIRSPEED

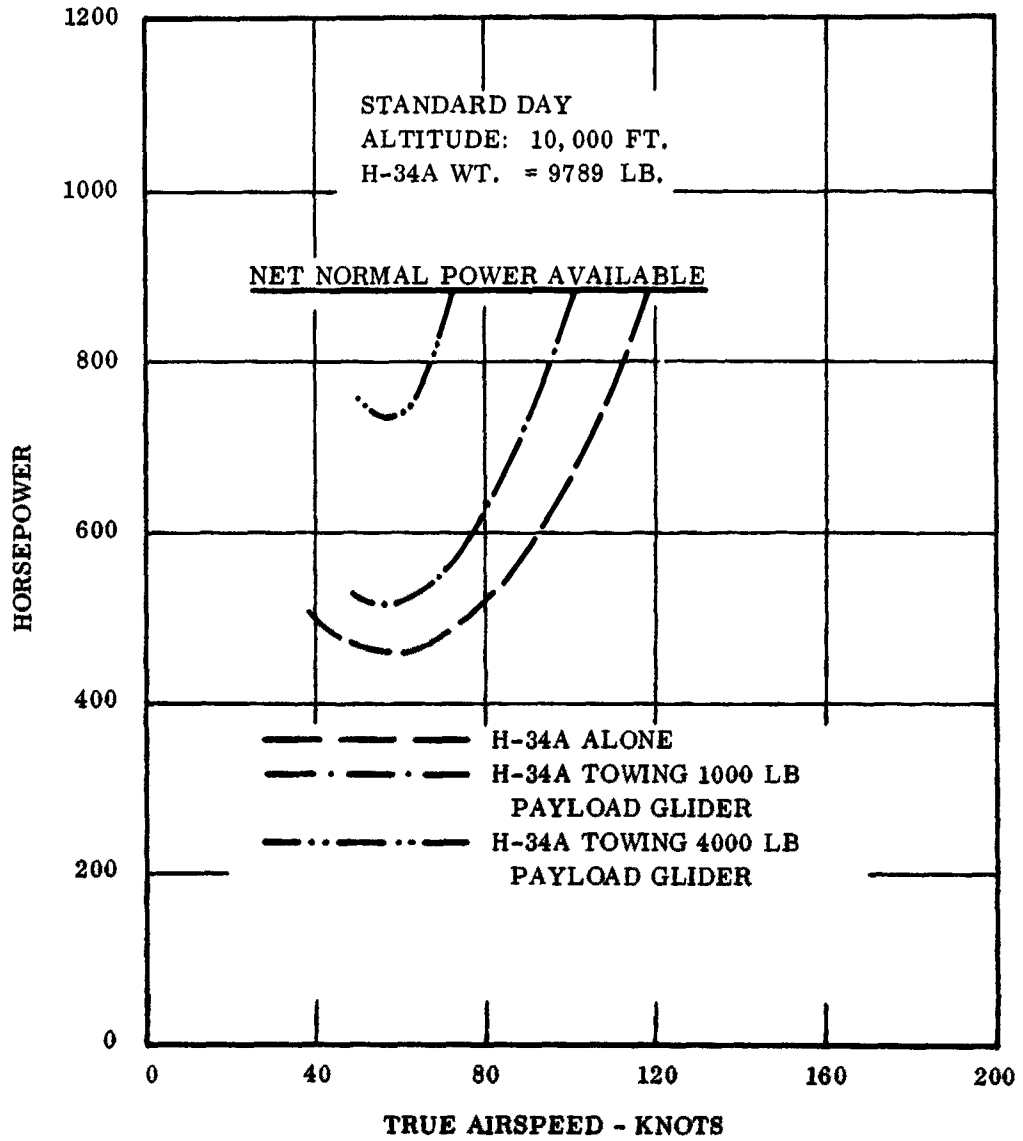


Figure 61 Power Required and Available Helicopters and Gliders

HILLER  
H-23D  
MAXIMUM RATE OF CLIMB

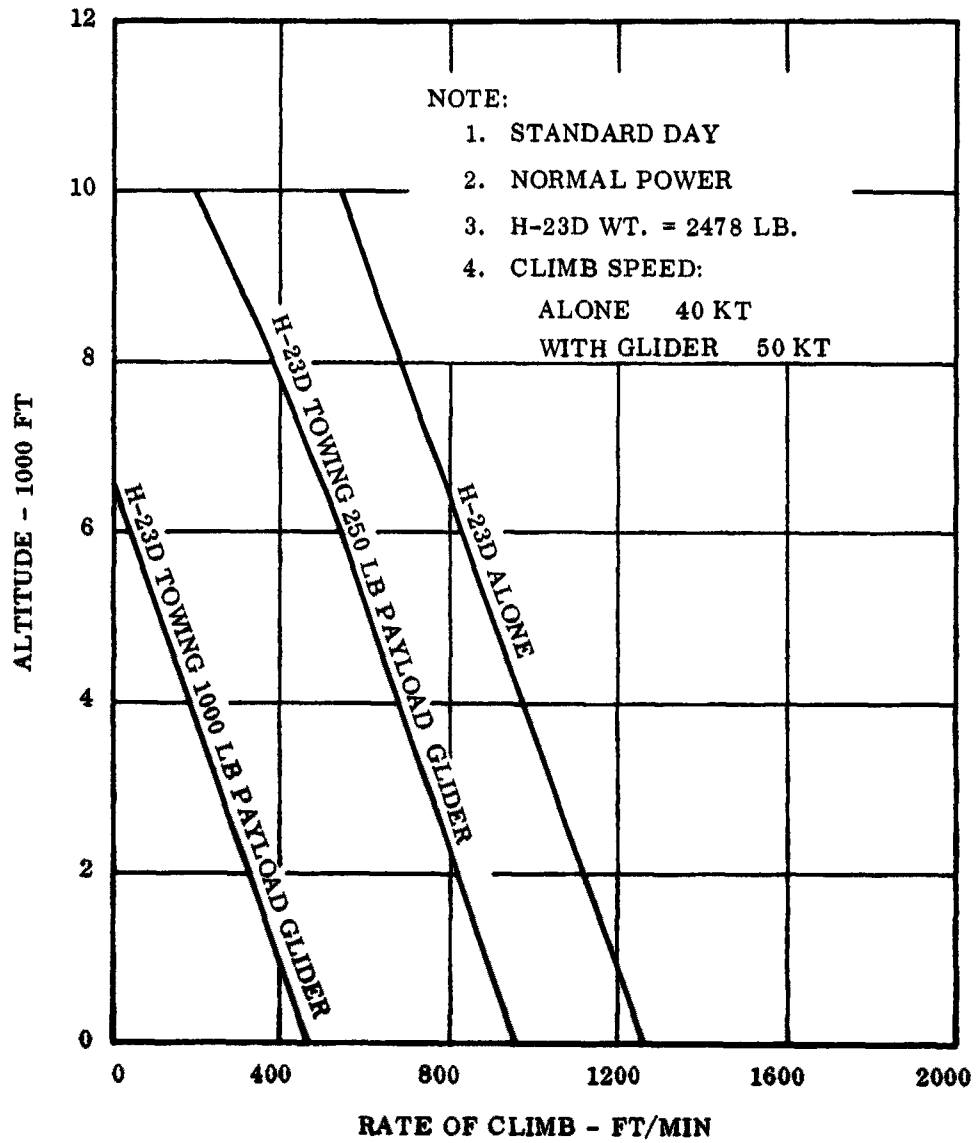


Figure 62 Rate of Climb, Helicopters and Gliders

BELL  
HU-1B  
MAXIMUM RATE OF CLIMB

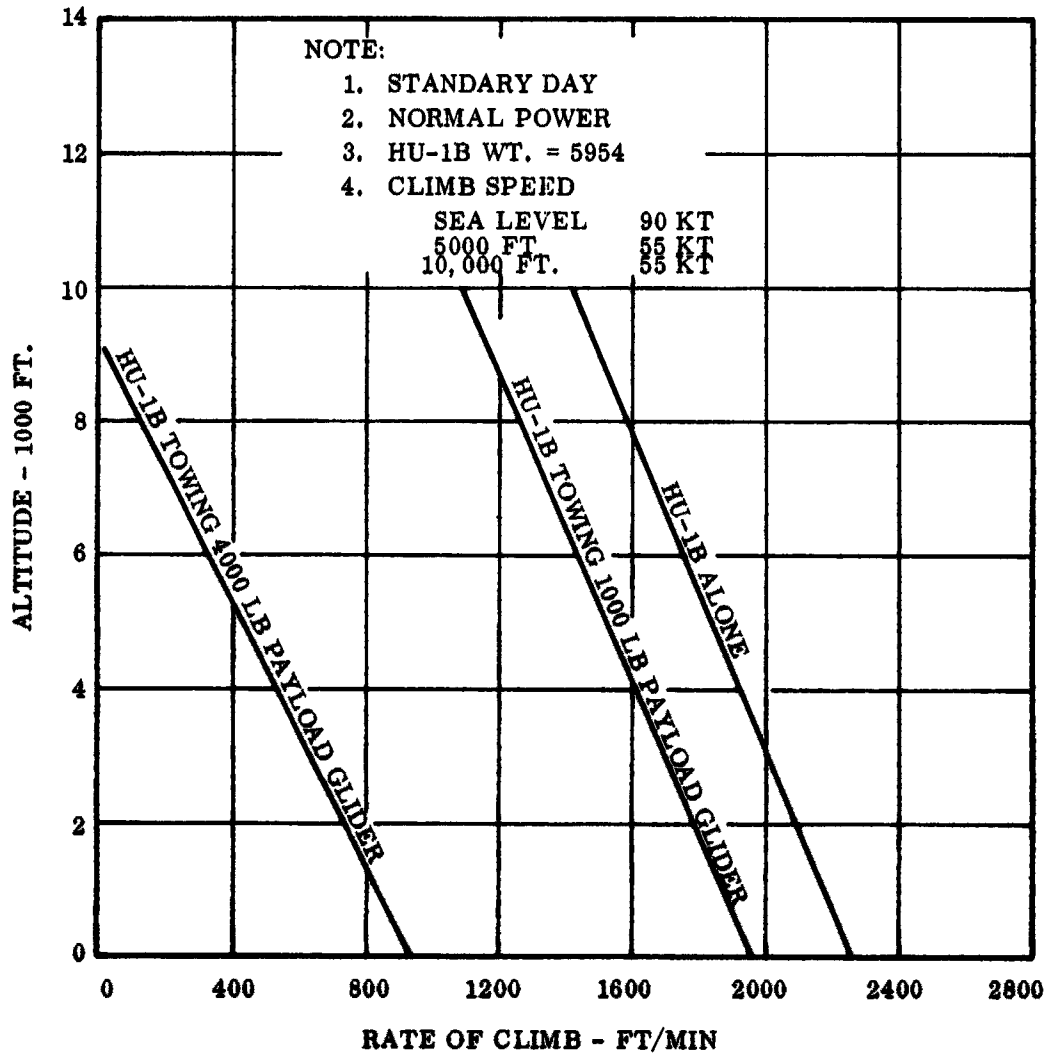


Figure 63 Rate of Climb, Helicopters and Gliders

SIKORSKY  
H-34A  
MAXIMUM RATE OF CLIMB

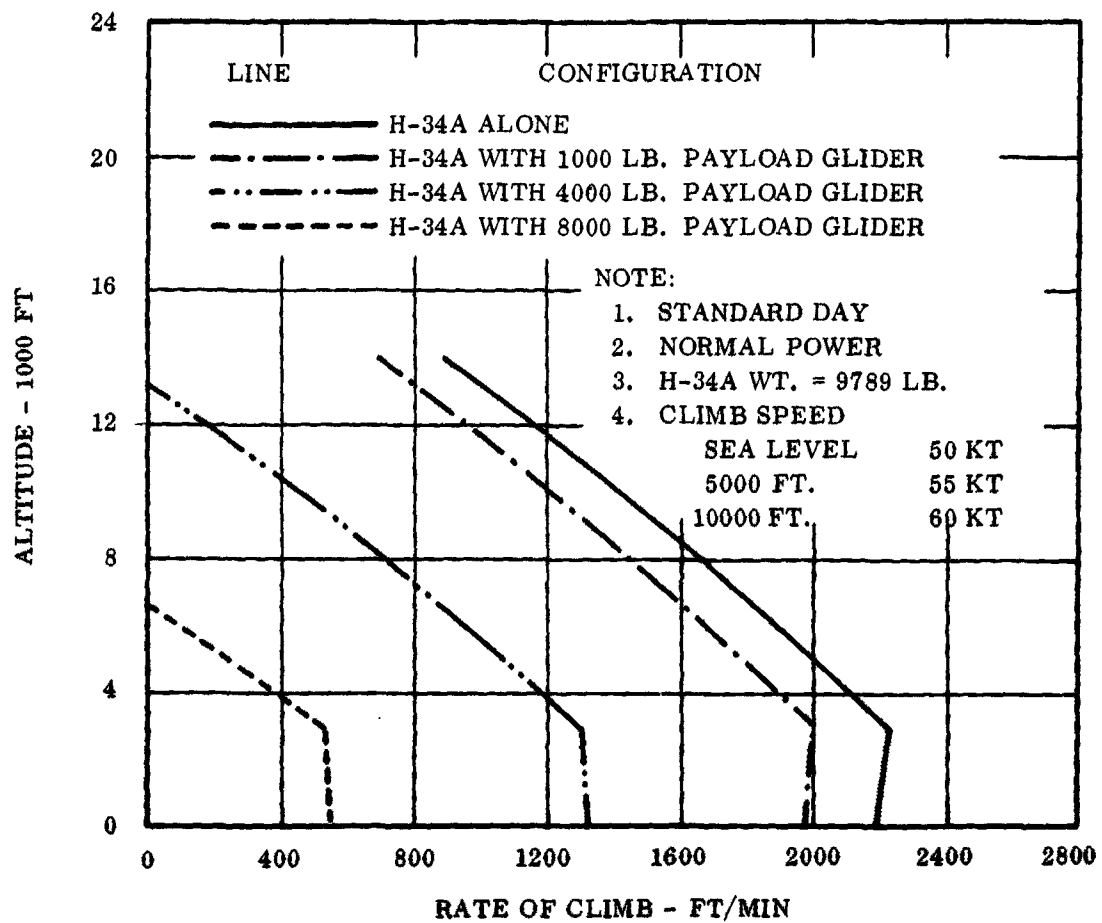


Figure 64 Rate of Climb, Helicopters and Gliders

HILLER  
H-23D  
MISSION PROFILE

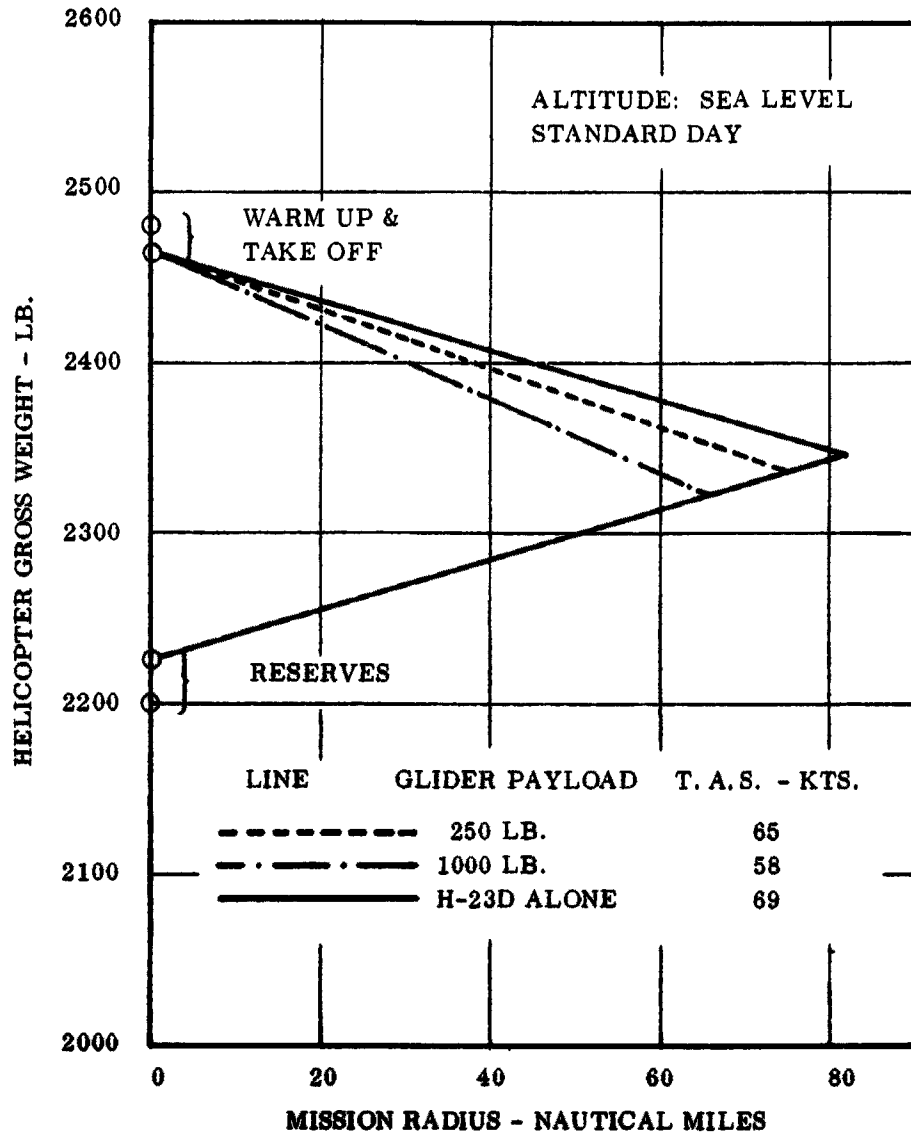


Figure 65 Mission Profiles, Helicopters and Gliders

HILLER  
H-23D  
MISSION PROFILE

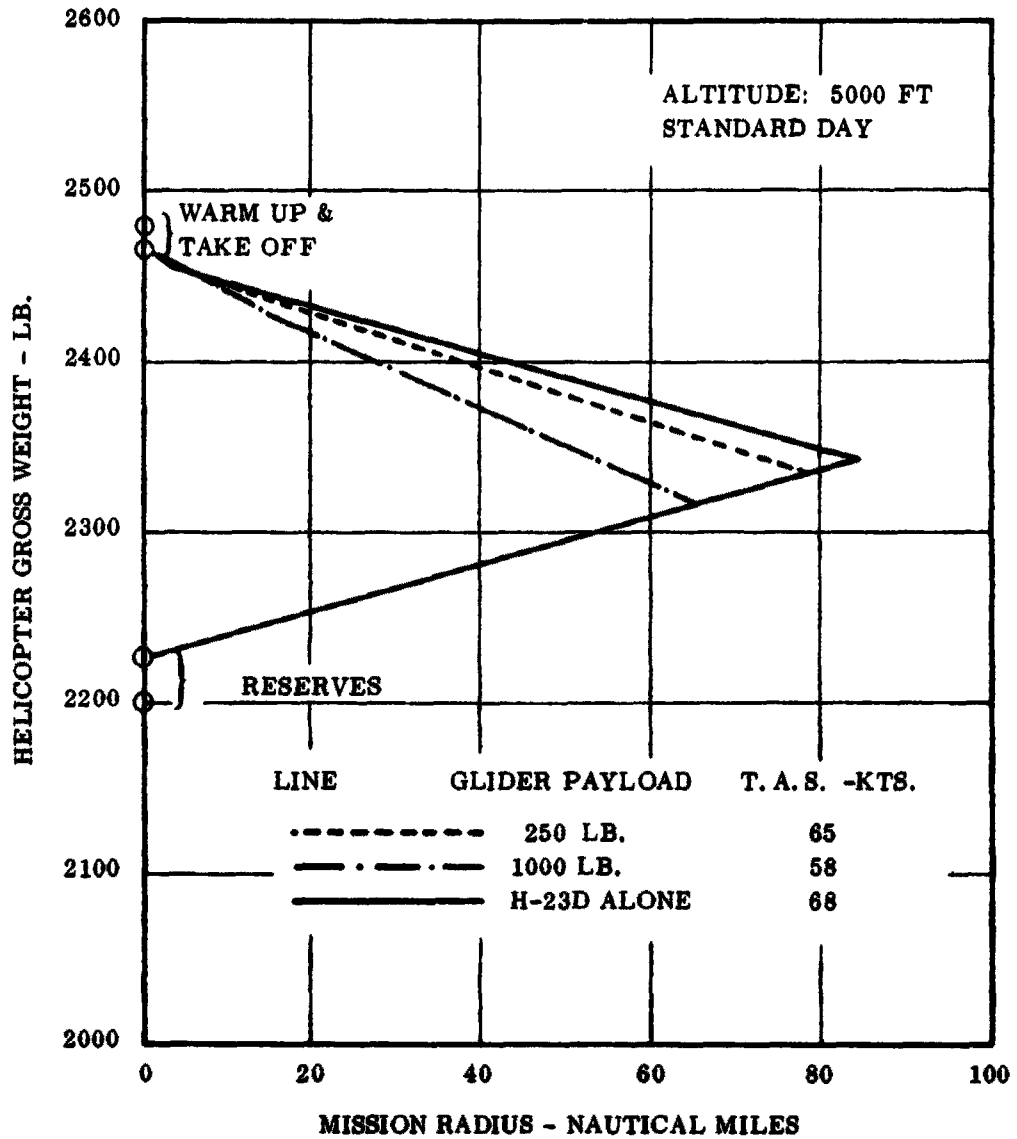


Figure 66 Mission Profiles, Helicopters and Gliders

HILLER  
H-23D  
MISSION PROFILE

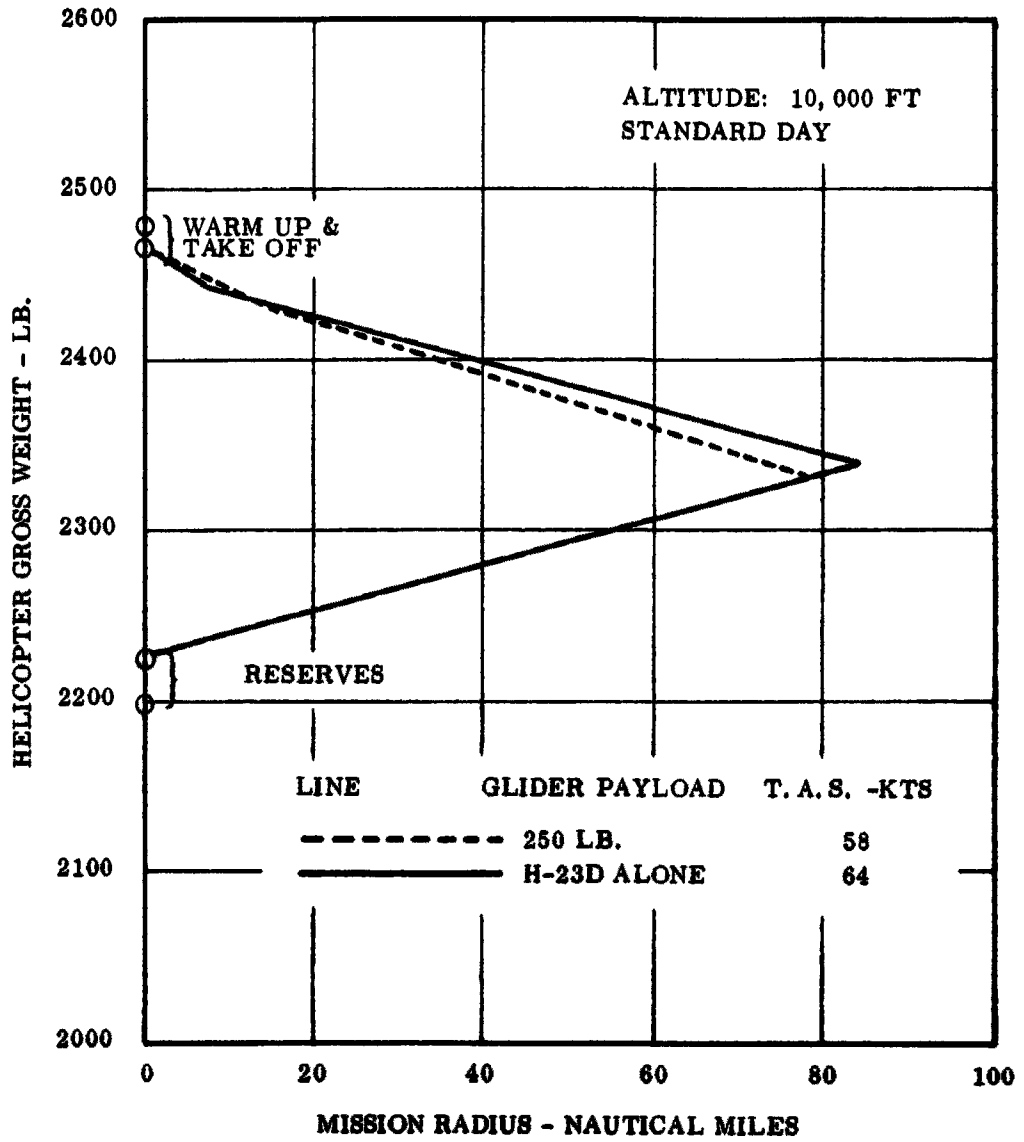


Figure 67 Mission Profiles, Helicopters and Gliders

BELL  
 HU-1B  
 MISSION PROFILE

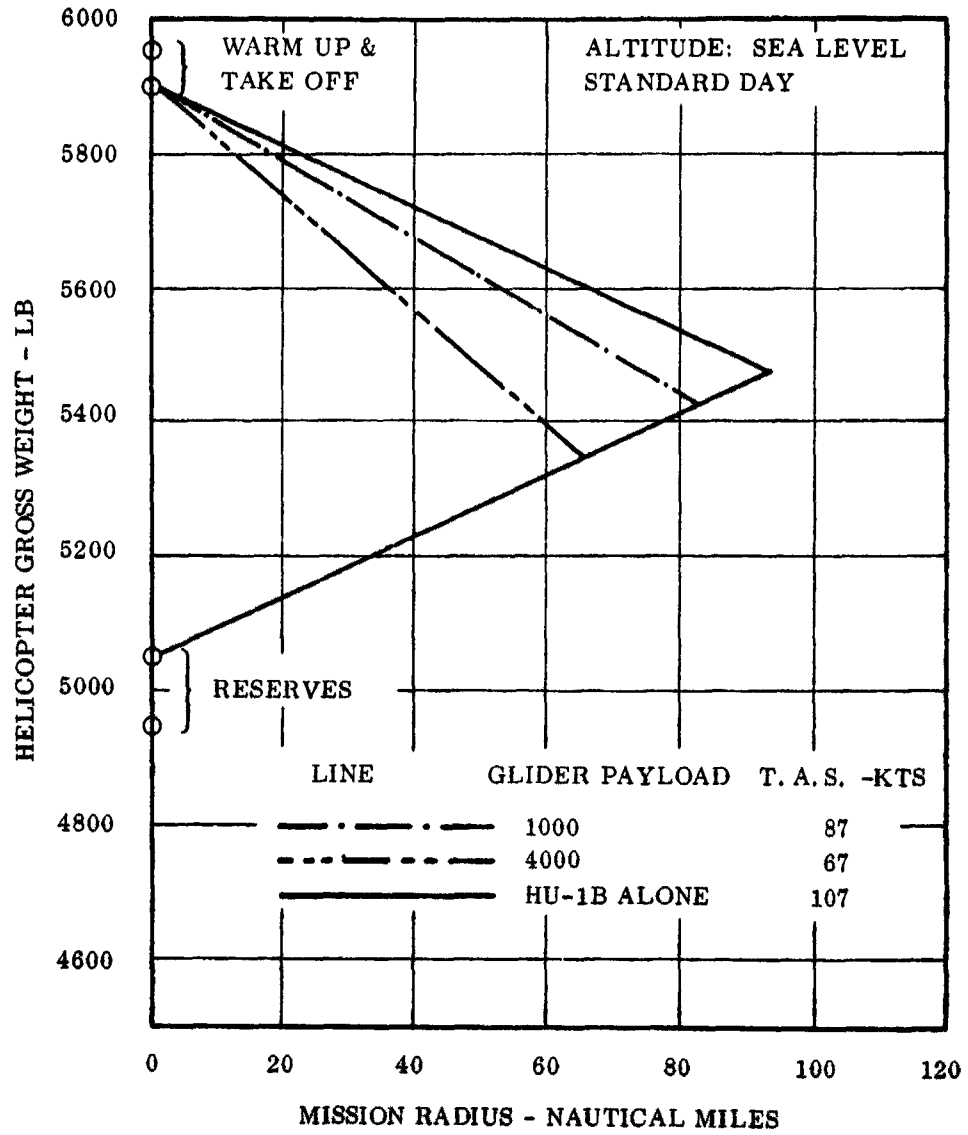


Figure 68 Mission Profiles, Helicopters and Gliders

BELL  
 HU-1B  
 MISSION PROFILE

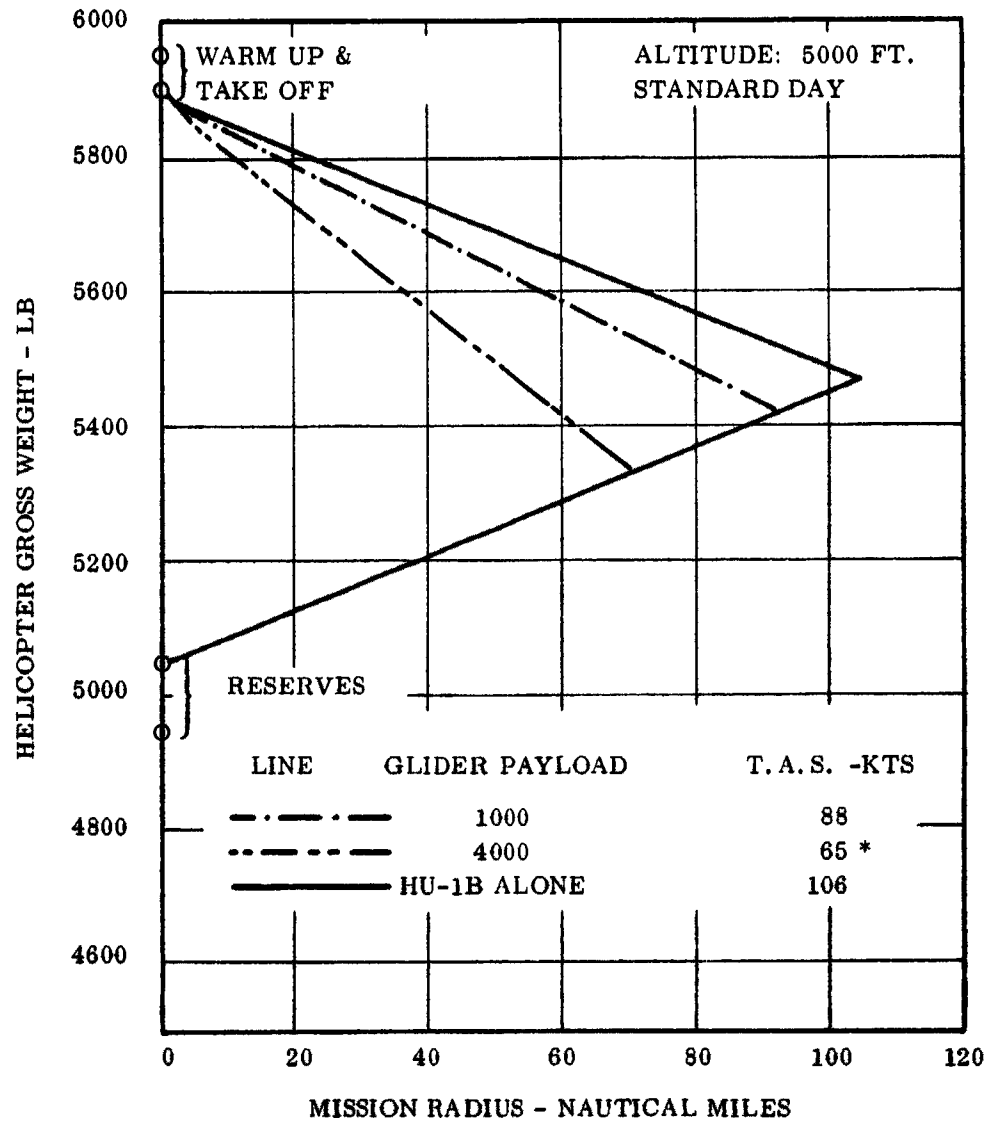


Figure 69 Mission Profiles, Helicopters and Gliders



SIKORSKY  
H-34A  
MISSION PROFILE

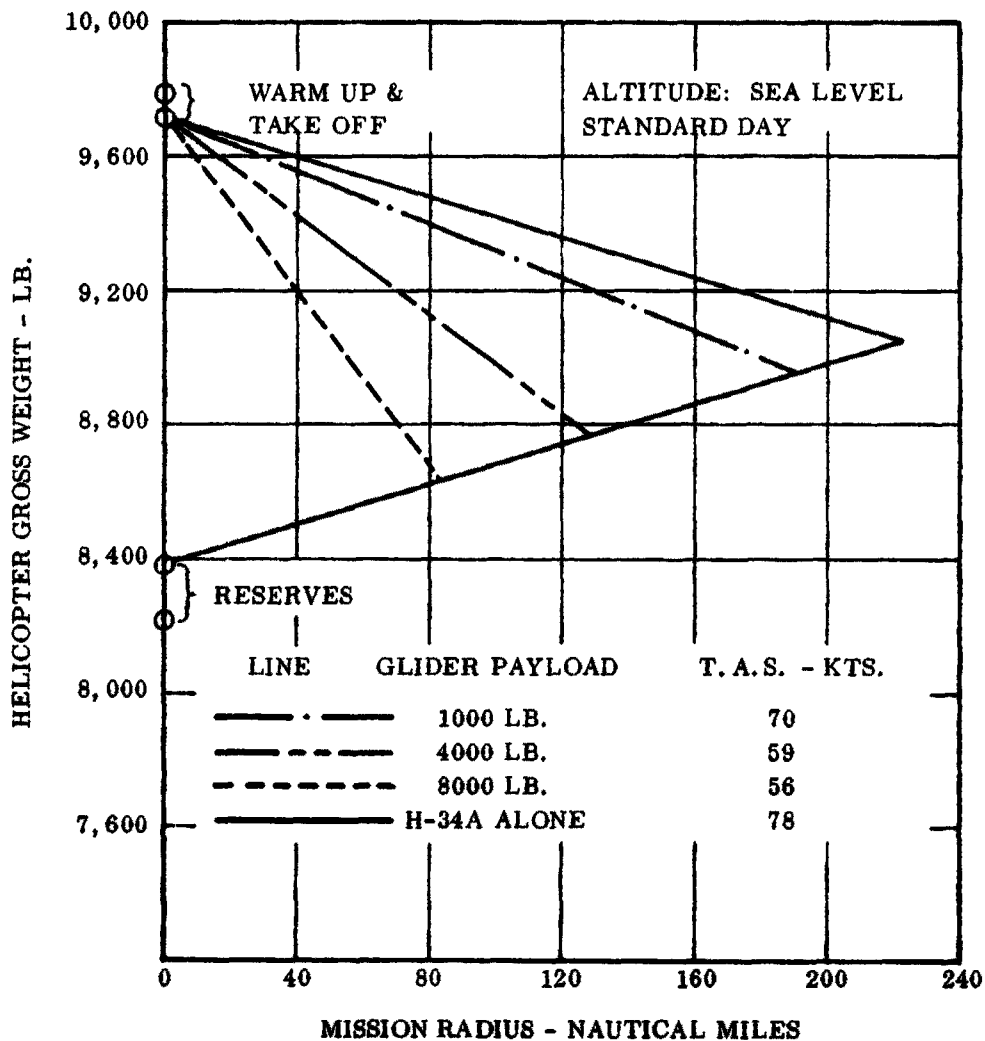


Figure 71 Mission Profiles, Helicopters and Gliders



SIKORSKY  
H-34A  
MISSION PROFILE

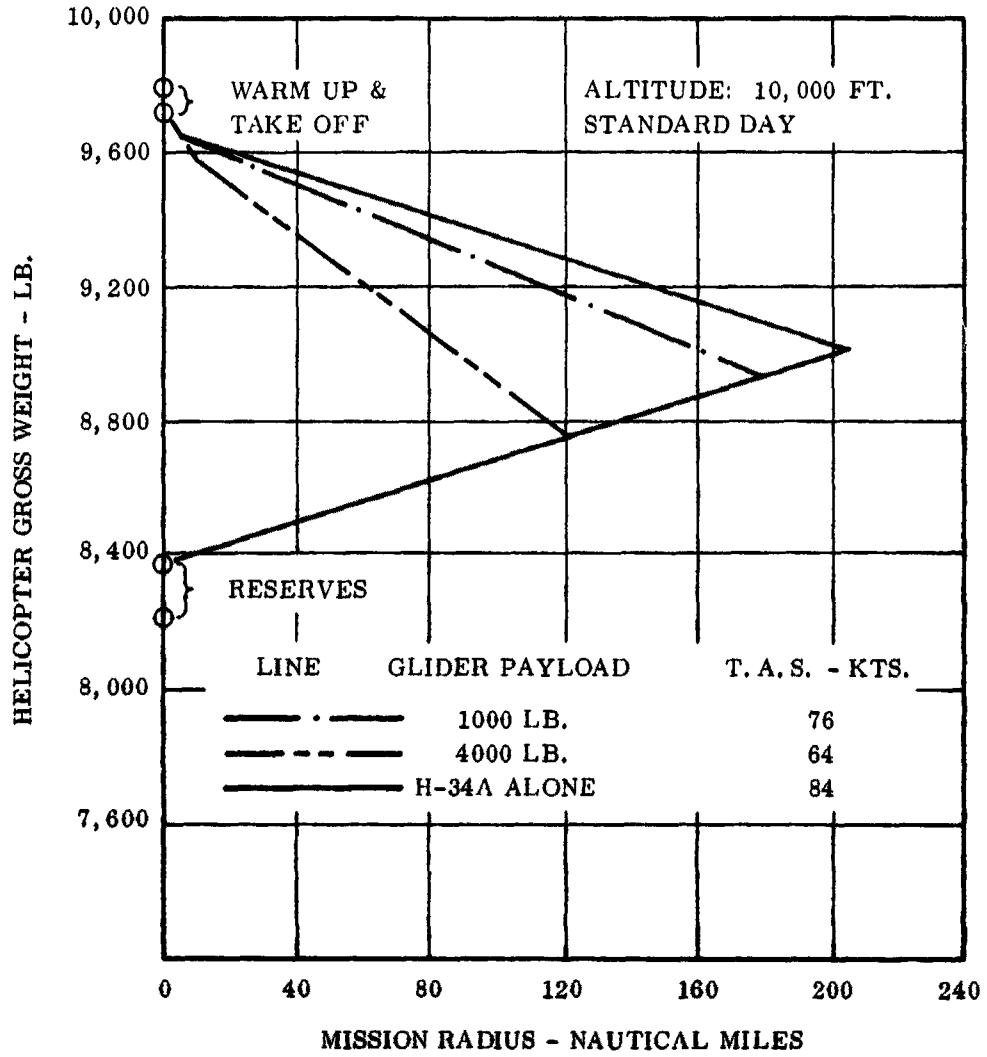


Figure 73 Mission Profiles, Helicopters and Gliders

## CONCLUSIONS

1. The performance characteristics of the towed gliders of all configurations studied show a compatibility with towing aircraft now in the Army inventory.
2. The wing loading of the towed glider may be matched with the towing aircraft's performance to achieve maximum performance of the combination.
3. Best performance for the wing loading studied occurred at true airspeeds of 50 to 60 knots with landing speeds at 40 to 50 knots.
4. The average lift/drag for the configurations studied is 3.5.
5. The drag of the towing line is in all configurations, less than 1 percent of the drag of the towed vehicle.
6. Only the 250 and 1,000 pound payload vehicles were studied for the air drop capability from the AC-1 (Caribou) aircraft and were satisfactory.

## II. STABILITY, CONTROL AND DYNAMICS

### SUMMARY

A static and dynamic stability analysis of the towed glider revealed the necessity for a wind tunnel program for final determination of longitudinal and directional static stability for static trim requirements and dynamic stability.

In the lateral-directional dynamic mode a precise ratio of directional stability to effective dihedral,  $C_{\eta\beta}/C_{l\beta}$ , must be maintained to assure convergence of both the dutch roll and the spiral mode.  $C_{\eta\beta}/C_{l\beta}$  should be designed, either through wing positioning or vertical tails, to be as large as possible for best dutch roll damping, yet not so large as to cause spiral divergence. A ratio of -.25 for  $C_{\eta\beta}/C_{l\beta}$  is about the best that is applicable to all configurations, at cruise. For climb and flare the ratio will necessarily become less. For climb and flare wing settings, products of inertia,  $I_{xz}$ , become greater. The increase in products of inertia while  $C_{\eta\beta}/C_{l\beta}$  is becoming smaller is in the direction of oscillatory divergence; consequently, the criterion of maximum possible directional stability at cruise will guard against dutch roll divergence for other lift coefficients. Furthermore, sufficient directional stability must be provided to account for adverse  $I_{xz}$  values arising from hasty cargo loading and lashing under field conditions.

Analysis of lateral-directional dynamic stability during tow specified minimum towline length of 4.7 keel lengths to ensure convergence of oscillations resulting from a disturbance. The chosen line length of 300 ft. is long enough to satisfy this requirement.

The free flight longitudinal static stability is adequate for the 4,000 and 8,000 lb. configurations; however, the 250 and 1,000 lb. gliders are statically stable if the wing is repositioned aft. This will be a relatively simple fix and will stabilize the vehicle in both modes.

Control longitudinally and directionally is through c. g. shift by wing deflections. A roll control mechanism which uses wing aerodynamic compressive loads to relieve control forces is feasible, with the optimum position of the hinge at 60.0 per cent of the span.

Preliminary studies of a longitudinal tow bridle using tow forces to trim resulted in an estimate of bridle attach points and bridle length for the cruise condition. A bridle length 92 per cent of the keel length is proposed with attach points at the body nose, and at  $\frac{X}{c_r} = .094$ ,  $\frac{Z}{c_r} = .045$  on the wing.

The dynamic stability of the H-34-A helicopter in combination with the 8000 lb. glider was studied by analyzing the frequency content of the individual configurations for possible coupling of the modes. The helicopter, at cruise, is deadbeat, while the glider frequency on tow is 7.9 rad/sec. This obviates dynamic instability due to resonance in the system.

## METHOD OF APPROACH

The stability and control analysis of the towed glider is separated into four categories - dynamics and statics, in free flight and during tow.

In the lateral-directional mode analysis concentrated on dynamic stability in free flight and during tow. Since static directional stability affects this mode critically, this particular area of statics was also scrutinized. The possibility of dynamic coupling between glider and helicopter was studied through analysis of the frequency content of the system.

In the longitudinal mode emphasis was on study of static trim conditions since the necessity of including the non-linear induced drag contribution to the static margin introduces unconventional terms and is usually ignored. Neutral points are presented graphically.

A study was made of a proposed lateral control system for optimum hinge lines. Equations for static lateral pilot control forces are developed, and hinge moment coefficients computed.

A method of mechanizing velocity dependent longitudinal tow hinge moments for trim was studied, and bridle length and attach points for tow near the cruise condition were determined.

### Dynamic Stability

Standard small perturbation equations of motion and stability derivatives were used in this analysis. The body axes are the trim stability axes. The equations are:

### Longitudinal

$$u = A_u u + A_{\alpha} \dot{\alpha} + A_{\alpha} \alpha + A_{\theta} \vartheta + A_{\delta_w} \alpha_w - \frac{g}{57.3} (\cos \gamma_0) \theta \quad 3.1.a$$

$$\dot{\alpha} = B_u u + B_{\alpha} \dot{\alpha} + B_{\alpha} \alpha + B_{\theta} \vartheta + B_{\delta_w} \delta_w - \frac{g}{U_0} (\sin \gamma_0) \theta \quad 3.1.b$$

$$\vartheta = C_u u + C_{\alpha} \dot{\alpha} + C_{\alpha} \alpha + C_{\theta} \vartheta + C_{\delta_w} \delta_w$$

Where

$A_u = X_u$	$B_u = Z_u (57.3/U_0)$	$C_u = 57.3 M_u$
$A_{\alpha} = X_w U_0 / 57.3$	$B_{\alpha} = Z_w$	$C_{\alpha} = U_0 M_w$
$A_{\alpha} = X_w U_0 / 57.3$	$B_{\alpha} = Z_w$	$C_{\alpha} = U_0 M_w$
$A_{\theta} = H_q / 57.3$	$B_{\theta} = 1 + Z_q / U_0$	$C_{\theta} = M_q$
$A_{\delta_w} = X_{\delta_w} / 57.3$	$B_{\delta_w} = Z_{\delta_w} / U_0$	$C_{\delta_w} = M_{\delta_w}$
$X_u = \frac{\rho S U}{m} (-C_D - C_{D_u}) + \frac{1}{m} \left( \frac{\partial T}{\partial u} \right) \cos (\alpha_T + \alpha_0)$	$Z_u = \frac{\rho S U}{m} (-C_L - C_{L_u}) - \frac{1}{m} \left( \frac{\partial T}{\partial u} \right) \sin (\alpha_T + \alpha_0)$	$M_u = \frac{\rho S U c}{I_y} (C_m + C_{m_u}) + \frac{z_T}{I_y} \left( \frac{\partial T}{\partial u} \right)$
$X_w = \frac{\rho S U}{m} (C_L - C_{D_{\alpha}})$	$Z_w = \frac{\rho S U}{2m} (-C_{L_{\alpha}} - C_D)$	$M_w = \frac{\rho S U c}{2I_y} (C_{m_{\alpha}})$
$X_{\delta_w} = \frac{\rho S U^2}{2m} (-C_{D_{\delta_w}})$	$Z_w = \frac{\rho S c}{4m} (-C_{L_{\alpha}})$	$M_w = \frac{\rho S c^2}{4I_y} (C_{m_{\alpha}})$
	$Z_q = \frac{\rho S U c}{4m} (-C_{L_q})$	$M_q = \frac{\rho S U c}{4I_y} (C_{m_q})$
	$Z_{\delta_w} = \frac{\rho S U^2}{2m} (-C_{L_{\delta_w}})$	$M_{\delta_w} = \frac{\rho S U^2 c}{2I_y} c_r$

## Lateral Directional Perturbation Equations

### LATERAL

$$\begin{array}{lll}
 Y_{\beta} = \frac{\rho S U}{2m} C_{y_{\beta}} & L_{\beta} = \frac{\rho S U^2 c_r}{2I_x} C_{l_{\beta}} & N_{\beta} = \frac{\rho S U^2 c_r}{2I_z} C_{n_{\beta}} \\
 Y_{\dot{\beta}} = \frac{\rho S c_r}{4m} C_{y_{\dot{\beta}}} & L_{\dot{\beta}} = \frac{\rho S U c_r^2}{4I_x} C_{l_{\dot{\beta}}} & N_{\dot{\beta}} = \frac{\rho S U c_r^2}{4I_z} C_{n_{\dot{\beta}}} \\
 Y_p = \frac{\rho S c_r}{4m} C_{y_p} & L_p = \frac{\rho S U c_r^2}{4I_x} C_{l_p} & N_p = \frac{\rho S U c_r^2}{4I_z} C_{n_p} \\
 Y_r = \frac{\rho S c_r}{4m} C_{y_r} & L_r = \frac{\rho S U c_r^2}{4I_x} C_{l_r} & N_r = \frac{\rho S U c_r^2}{4I_z} C_{n_r} \\
 Y_{\delta_a} = \frac{\rho S U}{2m} C_{y_{\delta_a}} = \frac{\rho S U}{2m} C_L & L_{\delta_a} = \frac{\rho S U^2 Z}{2I_x} c.g. C_L & N_{\delta_a} = \frac{\rho S U^2}{2I_z} (X_{a.c.} - X_{c.g.}) C_L
 \end{array}$$

### DEFINITIONS

- T            Tow, lbs.
- $\alpha_T$         Angle between tow axis and body x-axis
- $\alpha_o$         Initial angle of attack
- $z_T$         Tow moment arm, ft.

The solutions of these equations are -

### LONGITUDINAL TRANSFER FUNCTIONS

The longitudinal transfer functions have the form

$$\frac{\underline{u}}{\delta\omega} = \frac{A_u s^3 + B_u s^2 + C_u s + D_u}{D_{\text{long}}} \quad 3.3.a$$

$$\frac{\underline{w}}{\delta\omega} = \frac{A_w s^3 + B_w s^2 + C_w s + D_w}{D_{\text{long}}} \quad 3.3.b$$

$$\frac{\underline{\theta}}{\delta_w} = \frac{A_\theta s^2 + B_\theta s + C_\theta}{D_{\text{long}}} \quad 3.3.c$$

where  $D_{\text{long}}$  is the characteristic polynomial given by

$$D_{\text{long}} = A_0 + A_1 s + A_2 s^2 + A_3 s^3 + A_4 s^4 \quad 3.3.e$$

and

$$A_u = X_{\delta_w} (1 - Z_w) + Z_{\delta_w} X_{\delta}$$

$$B_u = -X_{\delta_w} \left( M_q (1 - Z_w) + Z_w + M_w (U_0 + Z_q) \right) + Z_{\delta_w} (X_w + M_w X_q - M_q X_w) \\ + M_{\delta_w} \left( X_w (U_0 + Z_q) + X_q (1 - Z_w) \right)$$

$$C_u = X_{\delta_w} \left( M_q Z_w - M_w (U_0 + Z_q) + M_w g (\sin \gamma_0) \right) + Z_{\delta_w} (M_w X_q - M_q X_w - M_w g (\cos \gamma_0)) \\ + M_{\delta_w} \left( X_w (U_0 + Z_q) - X_q Z_w - g (\cos \gamma_0) (1 - Z_w) - g X_w (\sin \gamma_0) \right)$$

$$D_u = g (\cos \gamma_0) (M_{\delta_w} Z_w - Z_{\delta_w} M_w) + g (\sin \gamma_0) (M_w X_{\delta_w} - M_{\delta_w} X_w)$$

$$A_w = Z_{\delta_w}$$

$$B_w = X_{\delta_w} Z_u + Z_{\delta_w} (-M_q - X_u) + M_{\delta_w} (U_0 + Z_q)$$

$$C_w = X_{\delta_w} (M_u (U_0 + Z_q) - M_q Z_u) + Z_{\delta_w} (M_q X_u - X_q M_u) \\ + M_{\delta_w} (X_q Z_u - X_u (U_0 + Z_q) - g (\sin \gamma_0))$$

$$D_w = g (\cos \gamma_0) (Z_{\delta_w} M_u - M_{\delta_w} Z_u) + g (\sin \gamma_0) (M_{\delta_w} X_u - X_{\delta_w} M_u)$$

$$A_\theta = Z_{\delta_w} M_w + M_{\delta_w} (1 - Z_w)$$

$$B_\theta = X_{\delta_w} (M_w Z_u + M_u - M_u Z_w) + Z_{\delta_w} (M_w + X_w M_u - M_w X_u) \\ + M_{\delta_w} (-Z_w - X_u + X_u Z_w - X_w Z_u)$$

$$C_\theta = X_{\delta_w} (M_w Z_u - M_u Z_w) + Z_{\delta_w} (M_u X_w - M_w X_u) + M_{\delta_w} (Z_w X_u - X_w Z_u)$$

$$A_{az} = A_w$$

$$B_{az} = B_w - U_0 A_\theta$$

$$C_{az} = C_w - U_0 B_\theta + g (\sin \gamma_0) A_\theta$$

$$D_{az} = D_w - U_0 C_\theta + g (\sin \gamma_0) B_\theta$$

$$E_{az} = D_w - U_0 C_\theta + g (\sin \gamma_0) C_\theta$$

$$A_h = -A_w$$

$$B_h = -B_w + U_0 A_\theta$$

$$C_h = -C_w + U_0 B_\theta$$

$$D_h = -D_w + U_0 C_\theta$$

$$A_4 = 1 - Z_w$$

$$A_3 = -(1 - Z_w) (X_u + M_q) - Z_w - M_w (U_0 + Z_q) - X_w Z_u$$

$$\begin{aligned}
A_2 &= X_u \left( M_q (1 - Z_w) + Z_w + M_w (U_o + Z_q) \right) - M_u \left( X_w (U_o + Z_q) + X_q (1 - Z_w) \right) \\
&\quad + M_q Z_w + Z_u \left( M_q X_w - X_w X_q M_w \right) + M_w g(\sin \gamma_o) - M_w (U_o + Z_q) \\
A_1 &= g(\sin \gamma_o) \left( M_u X_w + M_w - M_w (X_u) \right) + g(\cos \gamma_o) \left( Z_u M_w + M_u (1 - Z_w) \right) \\
&\quad + M_u \left( -X_w (U_o + Z_q) + Z_w X_q \right) + Z_u \left( X_w M_q - X_q M_w \right) \\
&\quad + X_u \left( M_w U_o + Z_q \right) - M_q Z_w \\
A_o &= g(\cos \gamma_o) \left( M_w Z_u - Z_w M_u \right) + g(\sin \gamma_o) \left( M_u X_w - X_u M_w \right)
\end{aligned}$$

### LATERAL TRANSFER FUNCTIONS

The lateral transfer functions have the form

$$\frac{\beta}{\delta_a} = \frac{A_\beta s^4 + B_\beta s^3 + C_\beta s^2 + D_\beta s}{D_{lat}} \quad 3.4.a$$

$$\frac{\phi}{\delta_a} = \frac{A_\phi s^3 + B_\phi s^2 + C_\phi s + D_\phi}{D_{lat}} \quad 3.4.b$$

$$\frac{\psi}{\delta_a} = \frac{A_\psi s^3 + B_\psi s^2 + C_\psi s + D_\psi}{D_{lat}} \quad 3.4.c$$

$$\frac{a_y}{\delta_a} = \frac{(A_{aya} s^4 + B_{aya} s^3 + C_{aya} s^2 + D_{aya} s + E_{aya}) s}{D_{lat}} \quad 3.4.e$$

where  $D_{lat}$  is the characteristic polynomial given by

$$D_{lat} = s(A_0 + A_1 s + A_2 s^2 + A_3 s^3 + A_4 s^4) \quad 3.4.f$$

and

$$A_\beta = Y_{\delta_a} \left( 1 - \Gamma_{xz}^2 / I_x I_z \right)$$

$$B_{\beta a} = Y_{\delta a} (-N_r - L_p - L_r I_{xz}/I_z - N_p I_{xz}/I_x) + L_{\delta a} (Y_p - I_{xz}(1 - Y_r)/I_z) + N_{\delta a} (Y_p I_{xz}/I_x - (1 - Y_r))$$

$$C_{\beta a} = Y_{\delta a} (L_p N_r - N_p L_r) + L_{\delta a} (-Y_p N_r - N_p(1 - Y_r + g(\cos \gamma_0))/U_0 + g(\sin \gamma_0) I_{xz}/I_z U_0) + N_{\delta a} (L_r Y_p + L_p(1 - Y_r) + g(\sin \gamma_0)/U_0 + g(\cos \gamma_0) I_{xz}/I_x U_0)$$

$$D_{\beta a} = g L_{\delta a} (N_p(\sin \gamma_0) - N_r(\cos \gamma_0))/U_0 + g N_{\delta a} (L_r(\cos \gamma_0) - L_p(\sin \gamma_0))/U_0$$

$$A_{\phi a} = L_{\delta a} + N_{\delta a} I_{xz}/I_x$$

$$B_{\phi a} = Y_{\delta a} (L_{\beta} + N_{\beta} I_{xz}/I_x) - L_{\delta a} (N_r + Y_{\beta}) - N_{\delta a} (Y_{\beta} I_{xz}/I_x - L_r)$$

$$C_{\phi a} = -Y_{\delta a} (L_{\beta} N_r - L_r N_{\beta}) + L_{\delta a} (N_{\beta} - N_{\beta} Y_r + Y_{\beta} N_r) - N_{\delta a} (Y_{\beta} L_r + L_{\beta} - L_{\beta} Y_r)$$

$$D_{\phi a} = -L_{\delta a} N_{\beta} g(\sin \gamma_0)/U_0 + N_{\delta a} L_{\beta} g(\sin \gamma_0)/U_0$$

$$A_{\psi a} = N_{\delta a} + L_{\delta a} I_{xz}/I_z$$

$$B_{\psi a} = Y_{\delta a} (N_{\beta} + L_{\beta} I_{xz}/I_z) + L_{\delta a} (N_p - Y_{\beta} I_{xz}/I_z) - N_{\delta a} (Y_{\beta} + L_p)$$

$$C_{\psi a} = Y_{\delta a} (L_{\beta} N_p - L_p N_{\beta}) + L_{\delta a} (N_{\beta} Y_p - N_p Y_{\beta}) + N_{\delta a} (L_p Y_{\beta} - L_{\beta} Y_p)$$

$$D_{\psi a} = g(\cos \gamma_0) (L_{\delta a} N_{\beta} - L_{\beta} N_{\delta a})/U_0$$

$$A_{aya} = U_o Y_{\delta_a} A_4$$

$$B_{aya} = U_o Y_{\delta_a} A_3 + U_o Y_{\beta} A_{\beta a}$$

$$C_{aya} = U_o Y_{\delta_a} A_2 + U_o Y_{\beta} B_{\beta a}$$

$$D_{aya} = U_o Y_{\delta_a} A_1 + U_o Y_{\beta} C_{\beta a}$$

$$E_{aya} = U_o Y_{\delta_a} A_o + U_o Y_{\beta} D_{\beta a}$$

$$A_4 = 1 - (I_{xz})^2 / I_x I_z$$

$$A_3 = -Y_{\beta} (1 - I_{xz}^2 / I_x I_z) - L_p - N_r - N_p I_{xz} / I_x - L_r I_{xz} / I_z$$

$$A_2 = N_{\beta} (1 - Y_r) + L_p (Y_{\beta} + N_r) - Y_p (N_{\beta} I_{xz} / I_x + L_{\beta}) + N_p (Y_{\beta} I_{xz} / I_x - L_r) \\ + Y_{\beta} (L_r I_{xz} / I_z + N_r) + L_{\beta} (1 - Y_r) I_{xz} / I_z$$

$$A_1 = -N_{\beta} \left( (1 - Y_r) L_p + L_r Y_p + I_{xz} g(\cos \gamma_o) / I_x U_o + g(\sin \gamma_o) / U_o \right) \\ + N_p \left( L_{\beta} (1 - Y_r) + Y_{\beta} L_r \right) - L_p N_r Y_{\beta} + L_{\beta} N_r Y_p - L_{\beta} g(\cos \gamma_o) / U_o \\ - L_{\beta} g I_{xz} (\sin \gamma_o) / I_z U_o$$

$$A_o = g(\cos \gamma_o) (L_{\beta} N_r - N_{\beta} L_r) / U_o + g(\sin \gamma_o) (N_{\beta} L_p - L_{\beta} N_p) / U_o$$

An existing small perturbation IBM 650 program was used to compute the transfer function of wing deflection response. Only the lateral-directional transfer functions were used, since the longitudinal stability margin varies greatly with wing deflection. The longitudinal characteristic equation, however, for a fixed wing setting remains valid. Either an analog computer or numerical integration is required for solution of the longitudinal transfer function. Flare transients, for instance, cannot be computed from the linear longitudinal equations.

### Dynamic Stability During Tow

The equations of Reference 9 were programmed on the IBM 650 to determine the dynamic stability of the 8,000 lb. glider during tow. The characteristic equation of the towed vehicle, including tow line static derivatives is:

$$D_{\text{tow}} = S^3(AD^6 + BD^5 + CD^4 + ED^3 + FD^2 + GD + H) \quad 3.4. a$$

where:

$$A = 32\mu^3 K_Z^2 K_X^2 - 32\mu^3 K_{XZ}^2$$

$$B = 8\mu^2 K_Z^2 C_{l_p} - 16\mu^2 K_X^2 K_Z^2 C_{Y_\beta} - 8\mu^2 K_{XZ} C_{n_p} + 16\mu^2 K_{XZ}^2 C_{Y_\beta} \\ - 8\mu^2 K_{XZ}^2 C_{l_r} - 8\mu^2 K_X^2 C_{n_r}$$

$$C = -16\mu^2 K_Z^2 T_{l_\phi} - 16\mu^2 K_X^2 T_{n_\psi} - 16\mu^2 K_X^2 K_Z^2 T_{y_{y'}} + 2\mu C_{n_r} C_{l_p} \\ - 2\mu C_{n_p} C_{l_r} + 4\mu K_Z^2 C_{Y_\beta} C_{l_p} + 4\mu K_X^2 C_{Y_\beta} C_{n_r} + 16\mu^2 K_X^2 C_{n_\beta} + 16\mu^2 K_{XZ}^2 C_{l_\beta} \\ - 16\mu^2 K_{XZ} T_{n_\phi} + 4\mu K_{XZ} C_{n_p} C_{Y_\beta} + 16\mu^2 K_{XZ}^2 T_{y_{y'}} + 4\mu K_{XZ} C_{Y_\beta} C_{l_r} - 16\mu^2 K_{XZ} T_{l_\psi}$$

$$E = 4\mu C_{n_r} T_{l_\phi} + 4\mu C_{l_p} T_{n_\psi} - 4\mu C_{n_p} T_{l_\psi} - 4\mu C_{l_r} T_{n_\phi} + 8\mu K_Z^2 C_{Y_\beta} T_{l_\phi} \\ + 8\mu K_X^2 C_{Y_\beta} T_{n_\psi} + 4\mu K_Z^2 C_{l_p} T_{y_{y'}} + 4\mu K_X^2 C_{n_r} T_{y_{y'}} - 8\mu K_X^2 C_{n_\beta} T_{y_\psi} \\ - 8\mu K_Z^2 C_{l_\beta} T_{y_\phi} - C_{Y_\beta} C_{n_r} C_{l_p} + C_{Y_\beta} C_{n_p} C_{l_r} - 4\mu C_{n_\beta} C_{l_p} + 4\mu C_{l_\beta} C_{n_p} \\ - 8\mu K_Z^2 C_{l_\beta} C_w - 8\mu K_{XZ} T_{y_\psi} C_{l_\beta} - 8\mu K_{XZ} C_w C_{n_\beta} - 8\mu K_{XZ} T_{y_\phi} C_{n_\beta} \\ + 8\mu K_{XZ} T_{n_\phi} C_{Y_\beta} + 4\mu K_{XZ} T_{y_{y'}} C_{l_r} + 8\mu K_{XZ} C_{Y_\beta} T_{l_\psi} + 4\mu K_{XZ} C_{n_p} T_{y_{y'}}$$

$$\begin{aligned}
F = & -2C_{Y\beta} C_{n_r} T_{l_\phi} + 2C_{Y\beta} C_{n_p} T_{l_\psi} - 2C_{Y\beta} C_{l_p} T_{n_\psi} + 2C_{Y\beta} C_{l_r} T_{n_\phi} \\
& - C_{n_r} C_{l_p} T_{y_{y'}} + C_{n_p} C_{l_r} T_{y_{y'}} - 8\mu C_{n_\beta} T_{l_\phi} + 8\mu C_{l_\beta} T_{n_\phi} + 2C_{n_\beta} C_{l_p} T_{y_\psi} \\
& - 2C_{n_\beta} C_{\phi_r} T_{y_\phi} + 2C_{l_\beta} C_{n_r} T_{y_\phi} - 2C_{l_\beta} C_{n_p} T_{y_\psi} + 8\mu K_X^2 C_{Y\beta} T_{n_{y'}} \\
& - 8\mu K_X^2 C_{n_\beta} T_{y_{y'}} - 8\mu K_{XZ} T_{y_{y'}} C_{l_\beta} - 8\mu K_{XZ} C_W T_{n_{y'}} + 8\mu K_{XZ} C_{Y\beta} T_{l_{y'}} \\
& - 8\mu K_Z^2 C_W T_{l_{y'}} + 2C_{l_\beta} C_{n_r} C_W - 2C_{n_\beta} C_{l_r} C_W
\end{aligned}$$

$$\begin{aligned}
G = & 4C_{l_\beta} C_W T_{n_\psi} - 4C_{n_\beta} C_W T_{l_\psi} + 2C_{n_r} C_W T_{l_{y'}} - 2C_{l_r} C_W T_{n_{y'}} - 2C_{Y\beta} C_{l_p} T_{n_{y'}} \\
& + 2C_{y_\beta} C_{n_p} T_{l_{y'}} + 2C_{n_\beta} C_{l_p} T_{y_{y'}} - 2C_{l_\beta} C_{n_p} T_{y_{y'}}
\end{aligned}$$

$$H = -4C_{n_\beta} C_W T_{l_{y'}} + 4T_{n_{y'}} C_{l_\beta} C_W$$

$$\mu = m/\rho S C_r$$

$$K_X^2 = I_{XX}/m C_r^2$$

$$K_Z^2 = I_{ZZ}/m C_r^2$$

$$K_{XZ} = I_{XZ}/m C_r^2$$

$$C_W = G. W. /qS$$

$$C_T = C_D/\cos \epsilon$$

$$l = \text{Line Length}/C_r$$

$$T_{y_{y'}} = -C_T/l$$

$$T_{y_\psi} = -C_T \frac{C_D}{C_r} \left( \frac{FS}{C_p} \text{ attach} - \frac{FS \text{ c. g.}}{C_p} \right) + \cos \epsilon$$

$$T_{y\psi} = -C_T - \frac{C_D}{C_r} \left( \frac{WL}{C_p} \text{ attach} - \frac{WL \text{ c.g.}}{C_p} \right) + \sin \epsilon$$

$$T_{n_{y'}} = -\frac{C_D}{C_r} \left( \frac{FS}{C_p} \text{ attach} - \frac{FS \text{ c.g.}}{C_p} \right) T_{y_{y'}}$$

$$T_{n_\psi} = -\frac{C_D}{C_r} \left( \frac{FS}{C_p} \text{ attach} - \frac{FS \text{ c.g.}}{C_p} \right) T_{y_\psi}$$

$$T_{n_\phi} = -\frac{C_D}{C_r} \left( \frac{FS}{C_p} \text{ attach} - \frac{FS \text{ c.g.}}{C_p} \right) T_{y_\phi}$$

$$T_{l_{y'}} = \frac{C_D}{C_r} \left( \frac{WL}{C_p} \text{ attach} - \frac{WL \text{ c.g.}}{C_p} \right) T_{y_{y'}}$$

$$T_{l_\psi} = \frac{C_D}{C_r} \left( \frac{WL}{C_p} \text{ attach} - \frac{WL \text{ c.g.}}{C_p} \right) T_{y_\psi}$$

$$T_{l_\phi} = \frac{C_D}{C_r} \left( \frac{WL}{C_p} \text{ attach} - \frac{WL \text{ c.g.}}{C_p} \right) T_{y_\phi}$$

$\epsilon$  = Angle, in the plane of symmetry, between the tow line and the relative wind.

The roots of equation 3.4. a are of the form

$$D = -r_1, -r_2, -R_1 \pm jI_1, -R_D \pm jI_D$$

Where the tow analog to the free flight dutch roll is given by -

$$\text{Damped natural frequency} = \omega_D = I_D V/C_r \quad 3.4. a$$

Inverse time to damp to half amplitude =

$$1/T_{1/2} = -R_D V/C_r \ln 1/2 \quad 3.4. b$$

To investigate the possibility of dynamic instability arising from resonance between glider and helicopter, the natural frequency of the helicopter at cruise was computed, using the data and method of reference (10).

The damped natural frequency of the helicopter is given by Equation 27 of Reference 10 as

$$\omega_{D(H)} = \left( \frac{-\bar{M}_\alpha}{I_y} - \left( \frac{\bar{M}_q}{I_y} \right) \left( \frac{q}{WV} I_\alpha \right) - \left( \frac{1}{2} \frac{M_q}{I_y} - \frac{1}{2} \frac{q I_\alpha}{WV} \right)^2 \right)^{\frac{1}{2}} \quad 3.4.c$$

where

$\bar{M}_\alpha$  is the longitudinal stability, dimensionalized

$\bar{M}_q$  is the pitch damping, dimensionalized

$\bar{L}_\alpha$  is the lift-curve slope, dimensionalized

$\omega$  = gross weight

$V$  = velocity

$I_y$  = pitching moment of inertia.

Since the rotor is symmetric, the lateral-directional rotor derivatives may be approximated by the longitudinal derivatives. Equation 3.4.c is therefore applicable to the lateral-directional dynamics.

### Static Stability

#### Longitudinal

Figure 75 explains pictorially the symbols and axis convention. The variation of c. g. with wing deflection appears in Figure 76, computed from Equations 3.5.

$$\frac{X_{c.g.}}{C_r} = \frac{X_H}{C_r} + \frac{C_p}{C_r} \left( \frac{WL_H}{C_p} - \frac{WL_{c.g.}}{C_p} \right) \sin \delta_W - \left( \frac{FS_H}{C_p} - \frac{FS_{c.g.}}{C_p} \right) \cos \delta_W \quad 3.5.a$$

$$\begin{aligned} \frac{Z_{c.g.}}{C_r} &= \frac{ZH}{C_r} - \frac{C_p}{C_r} \left( \frac{WLH}{C_p} - \frac{WL_{c.g.}}{C_p} \right) \cos \delta_W \\ &+ \left( \frac{FSH}{C_p} - \frac{FS_{c.g.}}{C_p} \right) \sin \delta_W \end{aligned} \quad 3.5.b$$

To solve for the hinge line position to produce a required static margin, Equations 3.5 become

$$\begin{aligned} \frac{C_p}{C_r} \left( \frac{FSH}{C_p} \right) &= \frac{C_p}{C_r} \left( \frac{FS_{c.g.}}{C_p} \right) + \left( \frac{XH}{C_r} - \frac{X_{c.g.}}{C_r} \right) \cos \alpha_{trim} \\ &+ \left( \frac{XH}{C_r} - \frac{Z_{c.g.}}{C_r} \right) \sin \alpha_{trim} \end{aligned} \quad 3.6.a$$

$$\begin{aligned} \frac{C_p}{C_r} \left( \frac{WLH}{C_p} \right) &= \frac{C_p}{C_r} \left( \frac{WL_{c.g.}}{C_p} \right) - \left( \frac{XH}{C_r} - \frac{X_{c.g.}}{C_r} \right) \sin \alpha_{trim} \\ &+ \left( \frac{ZH}{C_r} - \frac{Z_{c.g.}}{C_r} \right) \cos \alpha_{trim} \end{aligned} \quad 3.6.b$$

The neutral points are delineated in Figure 77, and the static margin for a specified lift coefficient is computed from the graph and equations of Figure 78. These two Figures are the graphical results of Equations 3.7.

$$a_{22} = dC_N / dC_L \quad 3.7.j$$

$$a_{11} \left( \frac{Z_{a.c.}}{C_r} - \frac{Z_{c.g.}}{C_r} \right) + a_{12} \left( \frac{X_{a.c.}}{C_r} - \frac{X_{c.g.}}{C_r} \right) =$$

$$-C_{m_0} - \Delta C_{m_\alpha} (\alpha - \delta w) \quad 3.7.k$$

$$a_{21} \left( \frac{Z_{a.c.}}{C_r} - \frac{Z_{c.g.}}{C_r} \right) + a_{22} \left( \frac{X_{a.c.}}{C_r} - \frac{X_{c.g.}}{C_r} \right) =$$

$$dC_m / dC_L - \frac{\Delta C_{m_\alpha}}{C_{L_\alpha}} \quad 3.7.l$$

$$\Delta = a_{11} a_{22} - a_{12} a_{21} \quad 3.7.m$$

$$m_X = -a_{11} / \Delta \quad 3.7.m$$

$$\frac{X_{c.g.}}{C_r} n.p. = \frac{a_{21}}{\Delta} C_{m_0} + \frac{X_{a.c.}}{C_r} \quad 3.7.n$$

$$m_Z = a_{12} / \Delta \quad 3.7.o$$

$$\frac{Z_{c.g.}}{C_r} n.p. = \frac{a_{22}}{\Delta} C_{m_0} \quad 3.7.p$$

$$\frac{X_{c.g.}}{C_r} = m_X \frac{dC_m}{dC_L} + \frac{X_{c.g.}}{C_r} n.p. \quad 3.7.q$$

$$\frac{Z_{c.g.}}{C_r} = m_Z \frac{dC_m}{dC_L} + \frac{Z_{c.g.}}{C_r} n.p. \quad 3.7.r$$

$$C_L = C_{L_\alpha} (\alpha - \alpha_{0L}) + \Delta C_L \quad 3.7.a$$

$$C_D = C_{D0} + C_{D_{C_L}} C_L + C_{D_{C_L^2}} C_L^2 \quad 3.7.b$$

$$C_N = C_L \cos \alpha + C_D \sin \alpha \quad 3.7.c$$

$$C_A = C_D \cos \alpha - C_L \sin \alpha \quad 3.7.d$$

$$C_m = - \left( \frac{Z_{a.c.}}{C_r} - \frac{Z_{c.g.}}{C_r} \right) C_A + \left( \frac{X_{a.c.}}{C_r} - \frac{X_{c.g.}}{C_r} \right) C_N \quad 3.7.e$$

$$C_N + C_{m_0} + \Delta C_{m_\alpha} (\alpha - \delta w) = 0$$

$$\frac{dC_m}{dC_L} = - \left( \frac{Z_{a.c.}}{C_r} - \frac{Z_{c.g.}}{C_r} \right) \frac{dC_A}{dC_L} + \left( \frac{X_{a.c.}}{C_r} - \frac{X_{c.g.}}{C_r} \right) \frac{dC_N}{dC_L} + \frac{\Delta C_{m_\alpha}}{C_{L_\alpha}} \quad 3.7.f$$

$$a_{11} = -C_A \quad 3.7.h$$

$$a_{12} = C_N \quad 3.7.i$$

$$a_{21} = -dC_A / dC_L \quad 3.7.g$$

The following calculations demonstrate the use of these graphs and tables.

250 lb. payload, cruise condition

$$\delta_w \doteq \alpha = 19.0^\circ$$

from Table I. A.

$$C_L = 2.7 (19/57. - .15) = .47$$

from Table I. B.

$$\Delta C_{m_\alpha} = .0795$$

from Figure 76

$$\frac{X \text{ c. g.}}{C_r} = -.55$$

$$\frac{Z \text{ c. g.}}{C_r} = -.35$$

from Figure 77

$$\frac{X \text{ c. g. n. p.}}{C_r} = -.527$$

$$\frac{Z \text{ c. g. n. p.}}{C_r} = .237$$

From Figure 78

$$m_X = 1.0$$

$$m_Z = 6.75$$

$$\frac{dC_m}{dC_L} = \frac{1}{-6.75} (.35 - .235) + .37 (.0795) = +.0121$$

The longitudinal instability may be corrected by moving the wing aft.

## Static Stability

### Directional

Unlike longitudinal static stability, the directional stability is amenable to standard aircraft calculations. For example, for the 250 lb. payload, cruise condition.

From Figure 76

$$\frac{x_{c.g.}}{c_r} = -.55$$

$$\frac{z_{c.g.}}{c_r} = .35$$

$$\sin \alpha = .326$$

$$\cos \alpha = .9455$$

$$\left( \frac{x_{c.g.}}{c_r} + .50 \right) \cos \alpha + \left( \frac{z_{c.g.}}{c_r} \right) \sin \alpha = .06683$$

$$\left( \frac{z_{c.g.}}{c_r} \right) \cos \alpha - \left( \frac{x_{c.g.}}{c_r} \right) \sin \alpha + .50 = .3472$$

From Table I. A.

$$C_{n\beta} = .0384 - .0411 (.47) = .01908$$

$$C_{y\beta} = -.158 - .173 (.47) = -.2393$$

$$C_{n\beta \text{ wing}} = .91908 - (.06683) (-.2393) = .03507$$

From Table I. B.

$$C_{n\beta} = .03507 - .0795 = -.04443$$

The directional instability may be corrected by moving the wing aft.

## Control

### Lateral

Roll control is achieved by lateral wing deflection as portrayed in Figure 81. From this roll geometry Equations 3.8 for static pilot forces are written.

$$\overline{DA} = \overline{DE} + \overline{EA} \quad 3.8.a$$

$$\overline{DE} = \frac{\eta l \cos \phi}{2} \quad 3.8.b$$

$$\begin{aligned} \overline{EA} &= \overline{(AC)} - \overline{(EC)} \\ &= \left( l(1-\eta) \right)^2 - \left( \eta l \sin \phi \right)^2 \quad 1/2 \end{aligned} \quad 3.8.c$$

$$\overline{DA} = \eta l \cos \phi + \left( l(1-\eta)^2 - (\eta l \sin \phi)^2 \right)^{1/2} \quad 3.8.d$$

$$\overline{DA} = \eta l \cos \phi + l \left( 1 - 2\eta + (\eta \cos \phi)^2 \right)^{1/2} \quad 3.8.e$$

$$\overline{CB} = \overline{DA} \cos \phi - \eta l \quad 3.8.f$$

$$\overline{CB} = \left( \eta l \cos \phi + l \right) \left( 1 - 2\eta + (\eta \cos \phi)^2 \right)^{1/2} \cos \phi - \eta l \quad 3.8.g$$

$$\cos \delta = \frac{\overline{CB}}{\overline{AC}} \quad 3.8.h$$

$$\cos \delta = \frac{\cos \phi \left( 1 - 2\eta + (\eta \cos \phi)^2 \right)^{1/2} - \eta \sin^2 \phi}{1 - \eta} \quad 3.8.i$$

Considering the static balance of the forces acting during control actuation for a roll, Equations 3.9 apply.

$$F_p \cos \delta = W_B Z \sin \phi - 2 F_H \eta l \sin \phi \quad 3.9$$

Cos  $\delta$  is defined by Equation 3.8, i in terms of  $\eta$  and the angle  $\phi$ .  
Solving for  $PF_p$  we have:

$$PF_p = \frac{(-2 F_H \eta l \sin \phi)(1 - \eta)}{\cos \phi \left(1 - 2\eta + (\eta \cos \phi)^2\right)^{1/2} - \eta \sin^2 \phi} \quad 3.10$$

if  $c_r$  = wing keel length (See Figure 81)

$$Z = z c_r \quad 3.11. a$$

$$l = y c_r = x c_r \cot \mathcal{A} \quad 3.11. b$$

where  $\mathcal{A}$  is leading edge sweepback  
prior to roll

$$F_H = C_{H_H} q S c_r / x c_r = C_{H_H} q s / x \quad 3.11. c$$

where  $s c_r$  is location, on keel, of the spreader bar.

$$\text{Define } C_{H_p} = F_p / q S c_r \quad 3.11. d$$

Substitution of Equation 3.11 into Equation 3.10 results in Equation 3.12 for the hinge moment coefficient in terms of  $\eta$  and the roll angle  $\phi$ .

$$C_{H_p} = \frac{(-2 C_{H_H} \eta \cot \mathcal{A} \sin \phi)(1 - \eta)}{\cos \phi \left(1 - 2\eta + (\eta \cos \phi)^2\right)^{1/2} - \eta \sin^2 \phi} \quad 3.12$$

The solution of Equation 3.12 requires knowledge of the geometry of a particular vehicle and of the apex hinge-moment coefficient,  $C_{HH}$ . The apex hinge-moment coefficient can be estimated from the wind tunnel force data available from NASA. These data are shown in Figure 85 as a function of angle of attack and leading edge sweepback angle. The variation of wing sweepback angle,  $\Lambda$ , with the wing deflection angle,  $\phi$ , is shown in Figure 86. These curves were found through the solution of the Equation 3.13 for an initial sweepback angle,  $\Lambda$ , of  $50^\circ$ .

$$\cot \Lambda / \cot \Lambda = \eta \cos \phi + (1 - 2\eta + (\eta \cos \phi)^2)^{1/2} \quad 3.13$$

The variation of the control hinge moment coefficient with the hinge line parameter,  $\eta$ , is shown in Figure 87 for three angles of attack at  $z = .4$ . These curves are applicable for an initial wing sweepback angle of  $50^\circ$ . Of interest is the optimum value of  $\eta$  of about 0.6. The curves of Figures 88 and 89 show the complete range of values of the control hinge moment coefficient with variations in wing deflection angle, wing lift coefficient and the parameter  $\eta$ .

## Control

### Longitudinal Tow

Figure 79 depicts the proposed bridle arrangement for imposing velocity dependent static control hinge moments. Figure 80 specifies the hinge moments required from the towing vehicle to trim the glider at a lift coefficient. The attach points and bridle length necessary to mechanize the hinge moments may be computed from Equations 3.14.

$$C_T \cos \epsilon = C_{T_\mu} \cos (\delta_\mu - \alpha) + C_{T_\ell} \cos \delta_\ell = C_{D_w} + C_{D_B} \quad 3.14.a$$

$$C_T \sin \epsilon = -C_{T_\mu} \sin (\delta_\mu - \alpha) + C_{T_\ell} \sin \delta_\ell = \frac{G.W.}{qS} - C_L \quad 3.14.b$$

$$\left(\frac{Z_u}{C_r} - \frac{Z_{\mathbb{H}}}{C_r}\right) C_{T_\mu} \cos \delta_\mu - \left(\frac{X_\mu}{C_r} - \frac{X_{\mathbb{H}}}{C_r}\right) C_{T_\mu} \sin \delta_\mu = C_{h_\mu} \quad 3.14.c$$

$$\left(\frac{F.S._\ell}{C_r} - \frac{F.S._{\mathbb{H}}}{C_r}\right) C_{T_\ell} \sin \delta_\ell + \left(\frac{W.L._\ell}{C_r} - \frac{W.L._{\mathbb{H}}}{C_r}\right) C_{T_\ell} \cos \delta_\ell = C_{h_\ell} \quad 3.14.d$$

where:

$$C_T = T/qS \quad 3.14. e$$

$$C_{T_\mu} = T_\mu / qS \quad 3.14. f$$

$$C_{T_\ell} = T_\ell / qS \quad 3.14. g$$

$$C_{h_\mu} = - \left( \frac{X_{a.c.}}{C_r} - \frac{X_{\mathbb{H}}}{C_r} \right) C_N - \left( \frac{Z_{\mathbb{H}}}{C_r} \right) C_A$$

$$\left( \frac{X_{w.c.g.}}{C_r} - \frac{X_{\mathbb{H}}}{C_r} \right) \left( \frac{W_w}{qS} \cos \alpha - \frac{Z_{\mathbb{H}}}{C_r} \right) \frac{W_w}{qS} \sin \alpha - C_{m_o} \quad 3.14. h$$

$$C_{h_\ell} = \left( \frac{FSc.g.B}{C_r} - \frac{FS_{\mathbb{H}}}{C_r} \right) \frac{W_B}{qS} \quad 3.14. i$$

The bridle line length imposes geometric constraints on the forces and moments of Equations 3.14. These constraints are from Equations 3.15.

$$\cos \delta_\mu - \frac{\lambda_\ell}{\lambda_\mu} (\cos \alpha \cos \delta_\ell + \sin \alpha \sin \delta_\ell) = A/\lambda_\mu \quad 3.15. a.$$

$$\sin \delta_\mu - \frac{\lambda_\ell}{\lambda_\mu} (\sin \alpha \cos \delta_\ell - \cos \alpha \sin \delta_\ell) = B/\lambda_\mu \quad 3.15. b.$$

$$\lambda = \lambda_\mu + \lambda_\ell = \lambda_\mu \left( 1 + \frac{\lambda_\ell}{\lambda_\mu} \right) \quad 3.15. c.$$

where:

$$\lambda_\mu = \text{length of upper bridle} \quad 3.15. d.$$

$$\lambda_\ell = \text{length of lower bridle} \quad 3.15. e.$$

$$\lambda = \text{Total bridle length} \quad 3.15. f.$$

$$A = (X_{\mu} - X_u) + (FS_{\ell} - FS_{\mu}) \cos \alpha - (WL_{\ell} - WL_{\mu}) \sin \alpha \quad 3.15.g.$$

$$B = (Z_{\mu} - Z_u) + (FS_{\ell} - FS_{\mu}) \sin \alpha + (WL_{\ell} - WL_{\mu}) \cos \alpha \quad 3.15.h.$$

The line tension components are available from Equations 4.14 by re-arranging the equations according to 3.16.

$$\begin{pmatrix} C_{T_{\mu}} \cos \delta_{\mu} \\ C_{T_{\mu}} \sin \delta_{\mu} \\ C_{T_{\ell}} \cos \delta_{\ell} \\ C_{T_{\ell}} \sin \delta_{\ell} \end{pmatrix} = \begin{bmatrix} \cos \alpha & \sin \alpha & 1.0 & 0 \\ \sin \alpha & -\cos \alpha & 0 & 1.0 \\ \left(\frac{Z_{\mu}}{Cr} - \frac{Z}{Cr}\right) - \left(\frac{X_{\mu}}{Cr} - \frac{X}{Cr}\right) & 0 & 0 & 0 \\ 0 & 0 & \left(\frac{WL_{\ell}}{Cr} - \frac{WL}{Cr}\right) \left(\frac{F\delta_{\ell}}{Cr} - \frac{FS}{Cr}\right) & 0 \end{bmatrix}^{-1} \begin{pmatrix} C_D \\ 0 \\ C_{h_{\mu}} \\ C_{h_{\ell}} \end{pmatrix} \quad | \quad 3.16$$

Perfunctory calculations of Equations 3.14 through 3.16 to determine attach points were made. Conditions near  $L/D_{\max}$  were chosen. The resulting attach points are

$$\frac{X_{\mu}}{Cr} = -.094$$

$$\frac{Z_{\mu}}{Cr} = .0445$$

$$\frac{FS_{\ell}}{Cr} = 0$$

$$\frac{WL_{\ell}}{Cr} = 0$$

The bridle length associated with these attach points is

$$\frac{\lambda}{c} = .92$$

with

$$\lambda_{\mu} = \lambda_{\ell}$$

### Stability Derivatives

The wing static stability derivatives were obtained from NASA wind tunnel data, Reference 1.

The wing dynamic stability derivatives were estimated by use of References 2 through 7.

The body stability derivatives were computed from Reference 8.

The towline derivatives are those of Reference 9.

The helicopter stability derivatives were obtained by the method of Reference 10.

## TECHNICAL DISCUSSION

### Static Stability, Longitudinal

The 250 lb. vehicle as shown here has an unstable static margin of +.0121 because of the large body destabilizing contribution. This vehicle may be made stable by repositioning the body with relation to the wing. The 1,000 lb. configuration shows an unstable static margin of +.00986; and the same fix as indicated for the 250 lb. configuration will produce the required stability margin.

Identical calculations for the other configurations show -

$$1000 \text{ lb. payload, } \frac{dC_M}{dC_L} = +.00986,$$

$$4000 \text{ lb. payload, } \frac{dC_M}{dC_L} = -.0201,$$

$$8000 \text{ lb. payload, } \frac{dC_M}{dC_L} = -.0211,$$

### Static Stability, Directional

The proximity of the wing to the body causes some weathercocking for all configurations. The 250 lb. payload suffers an additional static instability due to the large  $C_r/C_p$  ratio. Additional directional stability must be attained by repositioning the wing farther aft. The wing hinge line is moved parallel to the resultant lift-drag vector to maintain the same trim  $C_L$  by the wing drag. This movement away from the body increases the longitudinal static margin as well as enhancing the directional stability.

Equations e. 2 enable one to compute hinge line positions required for a specified  $C_L$  and stability margin, assuming that the cruise condition for zero body angle of attack is the hinge line design condition.

## Dynamics

### Lateral Directional, Free Flight

A three-degree-of-freedom small perturbation analysis for the 250 and 8,000 lb. configurations revealed the need for additional directional stability to assure dynamic stability.

Two configurations were analyzed for the 250 lb. payload. For one study all the body mass was concentrated at the c. g. and only the wing moments of inertia and stability derivatives were considered. This condition, while unrealistic, was studied for the purpose of developing a dynamic stability criterion for the flexible wing, an innovation in gliders which is believed to fly satisfactorily in the manner. In this case the dutch roll converges to half amplitude in 1.21 cycles. The spiral mode is also convergent, damping to half amplitude in 21.5 seconds. This configuration is directionally stable, with  $C_{\eta\beta} / C_{\ell\beta} = -.11$ , at cruise.

The second study of the 250 lb. glider accounted for the body mass distribution and aerodynamic influence. Because an excessively large vertical tail was required for static stability, only neutral weather-cocking,  $C_{\eta\beta} = 0$  was assumed. Both the dutch roll and spiral mode diverged. The dutch roll doubled amplitude in 5.27 cycles, the spiral mode in 5.6 seconds.

For the 8000 lb. payload configuration  $C_{\eta\beta} / C_{\ell\beta} = -.109$ , at cruise. The effects of increasing the directional stability on the free flight dynamics are documented in Figure 82. The spiral mode, which should be convergent for this vehicle in free flight since the usual pilot corrections are absent, becomes divergent at  $C_{\eta\beta} / C_{\ell\beta} = -.26$ .

This is the limit for improving dutch roll damping in free flight. Note the small margin between divergence of the spiral mode and dutch roll instability.

Three other conditions for the 8,000 lb. configuration are documented in Figure 82. We assumed that  $C_{\eta\beta}$  had been re-designed to be  $-.20 C_{\ell\beta}$  at  $C_L = .54$ . The geometry thus attained will result in -

Altitude	$C_L$	$C_{n\beta}/C_{l\beta}$
Sea level	1.0	- .146
5,000 ft.	.54	- .200
10,000 ft.	.54	- .200

In all cases the spiral mode remained convergent but the deterioration of damping at high speed resulted in divergent oscillations at 10,000 ft. Also, at sea level take-off or flare, the increase of effective dihedral at high lift coefficients, in conjunction with the more deleterious product of inertia, caused a marked reduction in the dutch roll stability.

After the 10,000 ft. condition was run it was discovered that the H-34-A helicopter was probably incapable of towing this glider to this altitude; consequently, one concludes that the resulting design is dynamically stable, although marginal, throughout the expected flight regime.

Again, the desirability of designing close to spiral divergence is emphasized, since the spiral mode is affected primarily by aerodynamic coefficients, which can be designed to be reasonable invariant with handling environment. The dutch roll stability, on the other hand, is dependent upon a small principal axis inclination with the roll axis and aerodynamic coefficients. The principal axis inclination is sensitive to cargo loading practices in the field. This cannot be predicted accurately or controlled dependably.

#### Lateral-Directional, on Tow

The equations of Reference 9 were programmed on the IBM 650 to analyze the effects of tow line length and attach points on the dynamic stability of the glider during tow. A corrected mistake on page 22 of Reference 9 resulted in good agreement between observation and theory. Figures 83 and 84 explain graphically, for the 8,000 lb. glider, the effects of variation of tow line parameters.

Tow from above ( $\epsilon = +15.0^\circ$ ), below ( $\epsilon = -15.0^\circ$ ) and at the same altitude all affected the dynamic stability about the same. The spiral and rolling modes were not appreciably changed by variation of tow line derivatives. The dutch roll responded most drastically to tow conditions; consequently, only this mode is presented in Figures 83 and 84, for

$$C_{\eta_{\beta}} / C_{\ell_{\beta}} = -.2.$$

The paramount fact indicated by Figure 83 is the danger of instituting a dutch roll divergence if too short a line length is used. For the 8,000 lb. vehicle this divergence will occur when the line is shorter than 4.7 keel lengths or 230 ft.

Figure 84 discloses that there is no danger of a dutch roll divergence arising from a badly attached line. Furthermore, at least for the 8,000 lb. configuration, moving the attach point forward and up is stabilizing over most of the range.

The damped natural frequency of the helicopter is given by Equation 3.4.c for the following parameters,

$$W = 9,700 \text{ lb.}$$

$$V = 70 \text{ knots}$$

$$\frac{g}{wV} \bar{L}_{\alpha'} = .445$$

$$\frac{\bar{M}_{\alpha}}{I_y} = .55$$

$$\frac{\bar{M}_q}{I_y} = -.98$$

$$W_{D(H)} = \left( (-.55 - (-.98)(.445) - \left( \frac{-.98}{2} - \frac{-.445}{2} \right)^2 \right)^{\frac{1}{2}} = \sqrt{-.6215}$$

Since the parameter is negative the mode is deadbeat. The frequency of the glider on tow is about 7.9 rad/sec. No coupling is indicated.

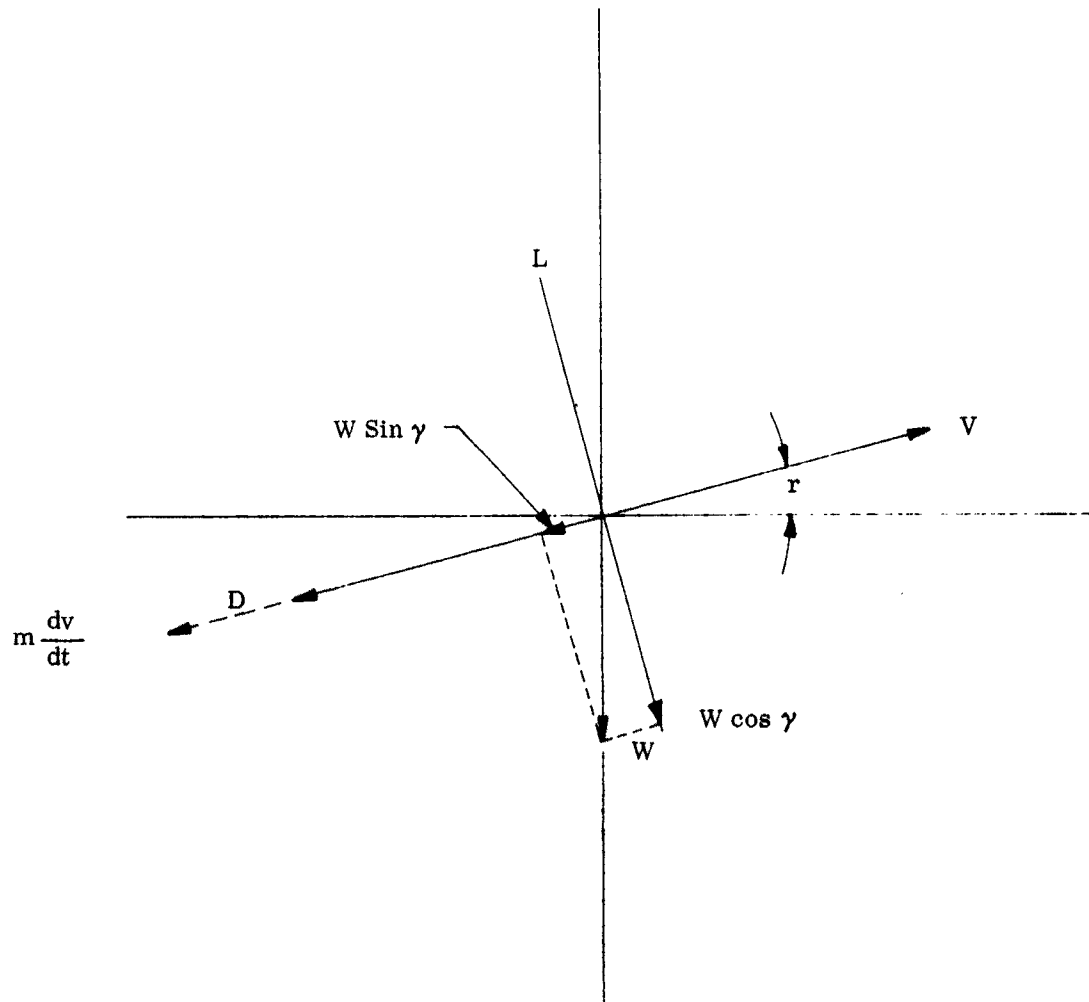


Figure 74 Axis System Convention

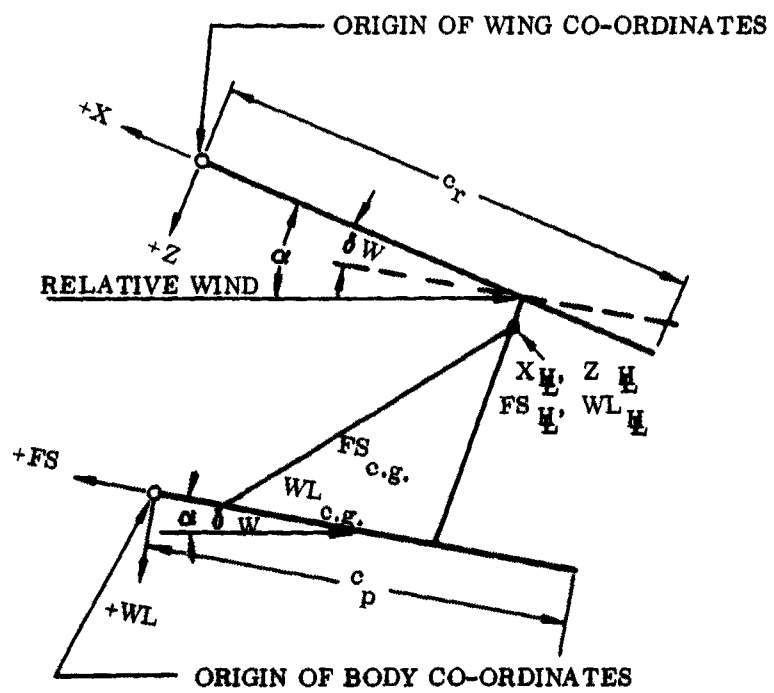


Figure 75 Longitudinal Geometry

CENTER OF GRAVITY VARIATION  
WITH  
WING ANGLE

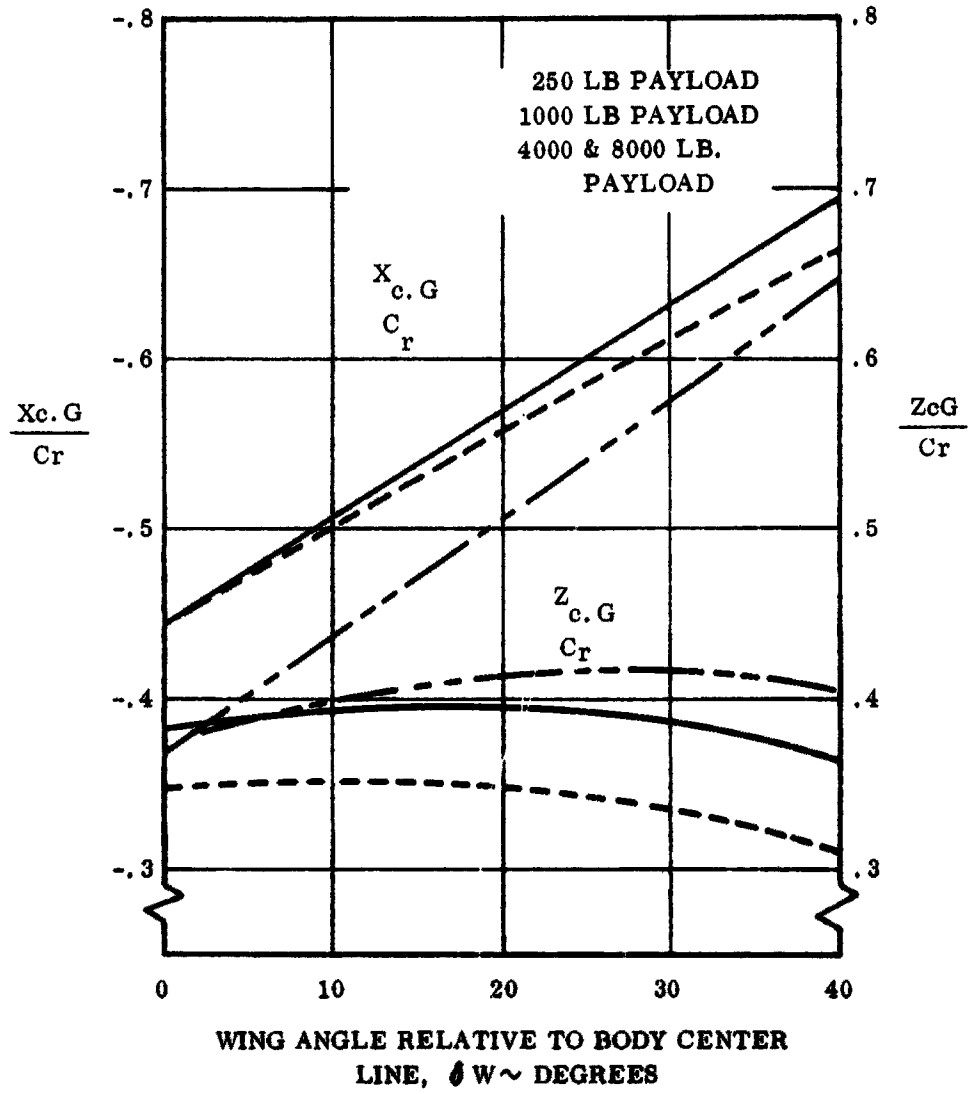


Figure 76 Center of Gravity Variation with Wing Angle

TOWED GLIDER  
 TRIM NEUTRAL POINTS  
 WING ALONE

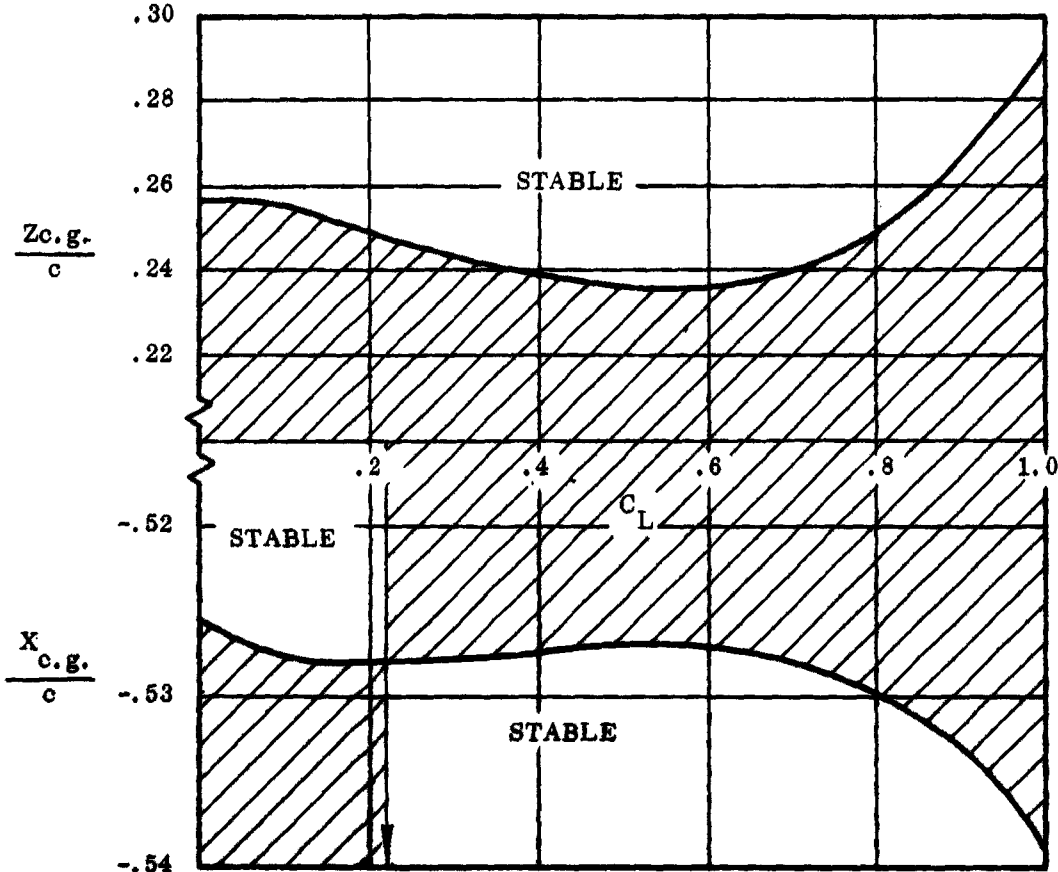


Figure 77 Towed Glider Trim Neutral Points, Wing Alone

GLIDER  
TRIM REQUIREMENTS

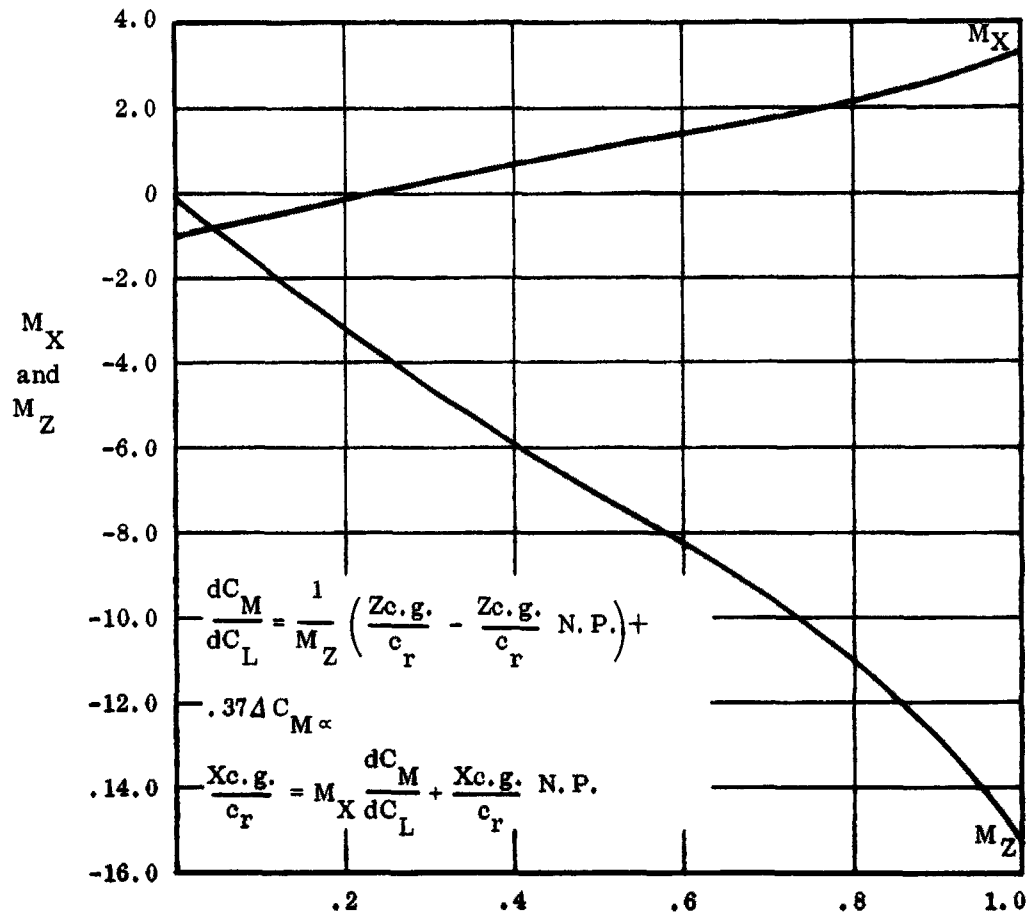


Figure 78

Glider Trim Requirements

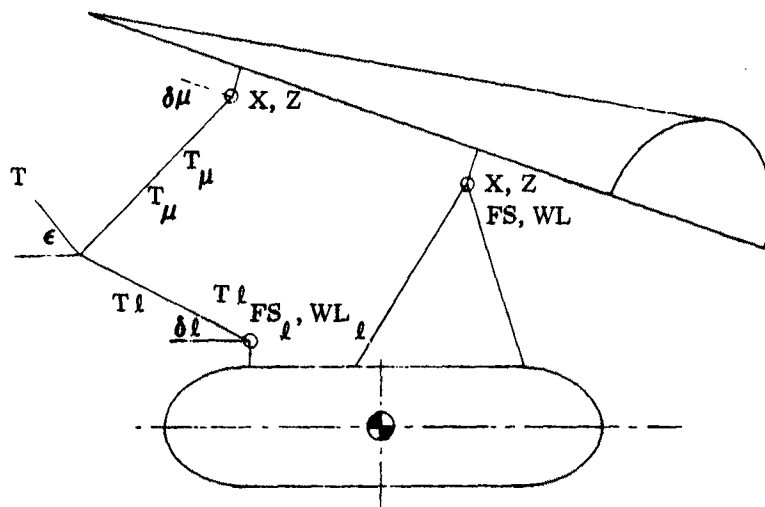


Figure 79 Longitudinal Tow Bridge

TOW CONTROL STATIC HINGE MOMENTS

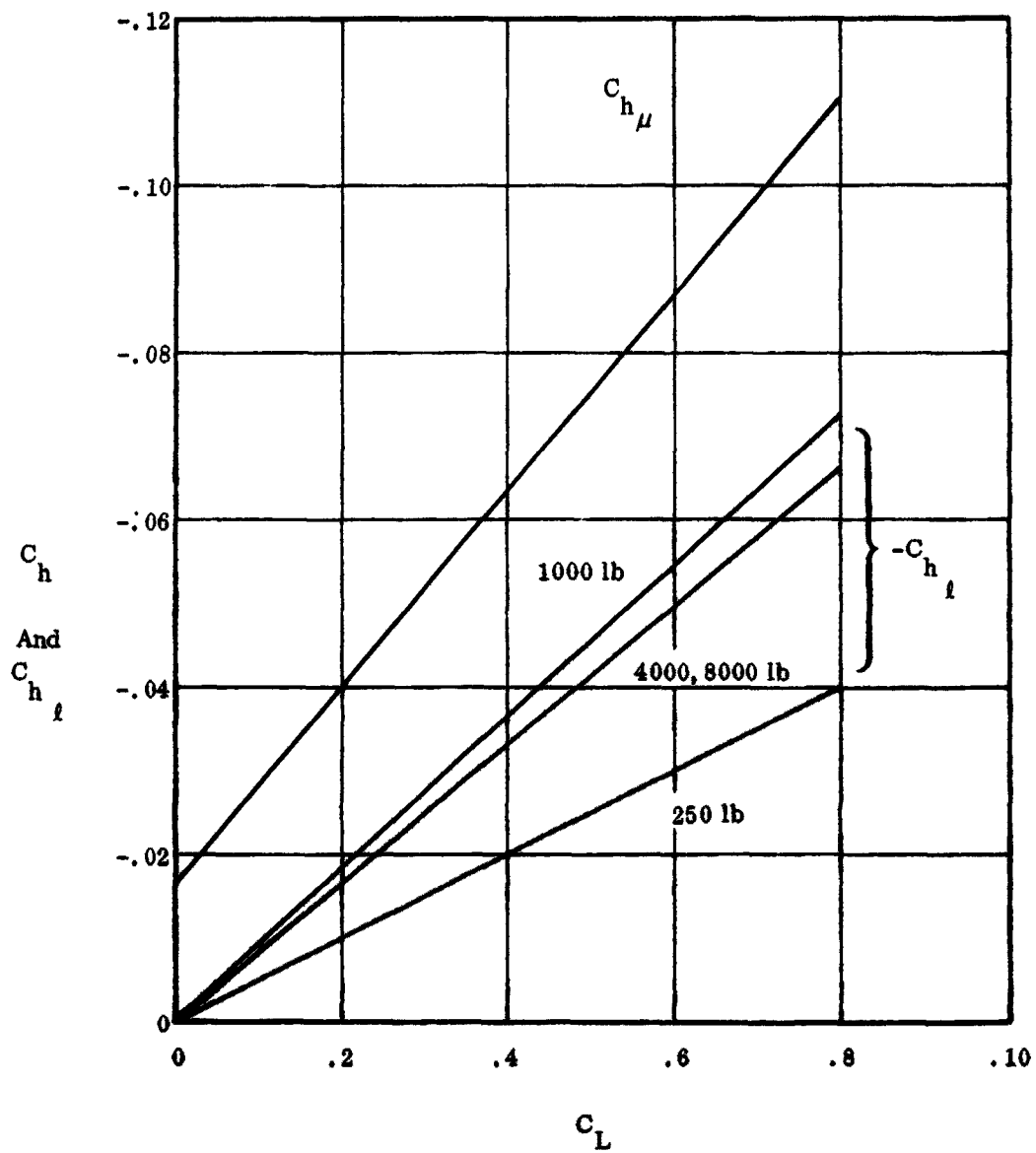


Figure 80 Tow Control Static Hinge Moments

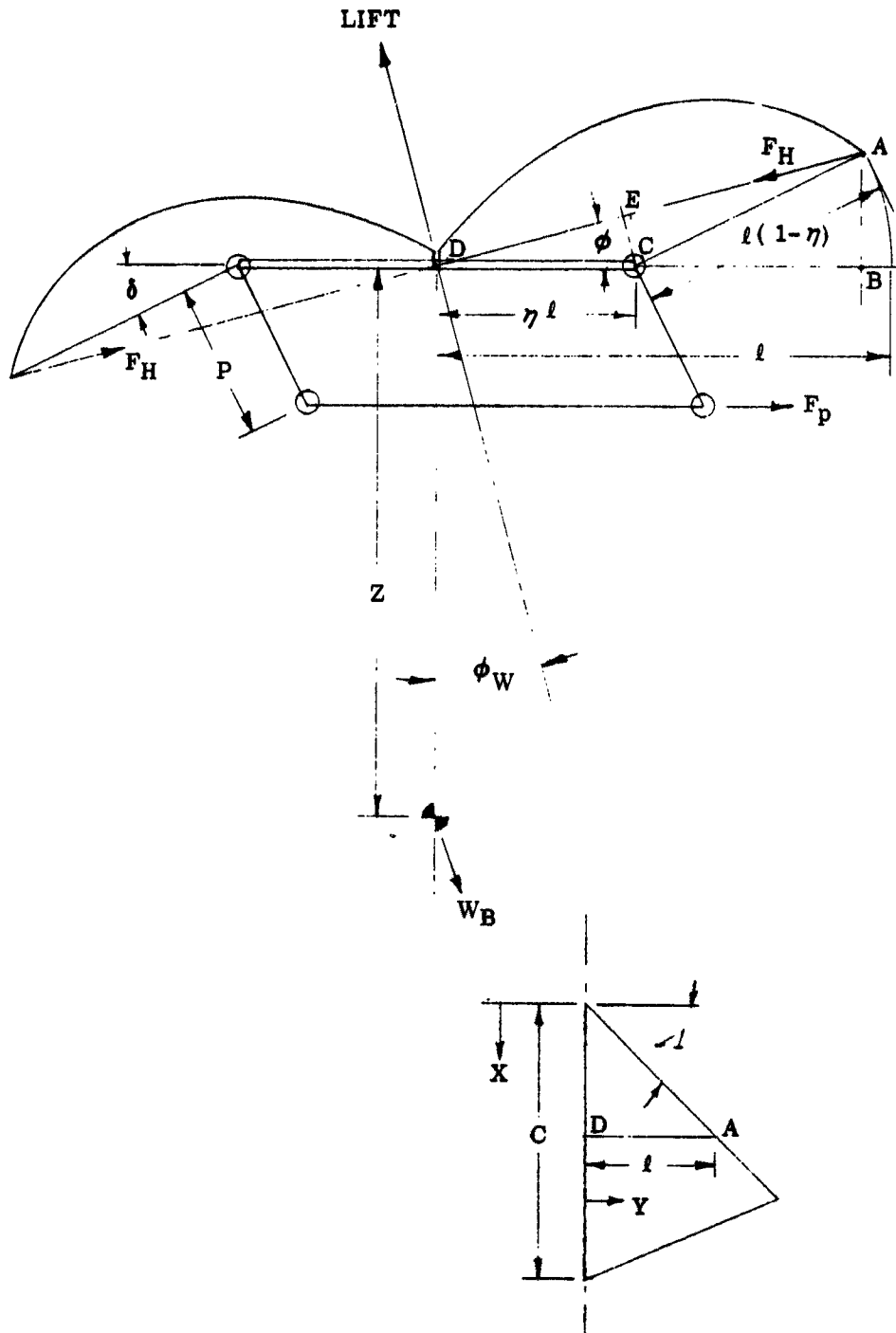


Figure 81 Roll Control Geometry

DYNAMIC STABILITY  
VARIATION WITH DIRECTIONAL STABILITY

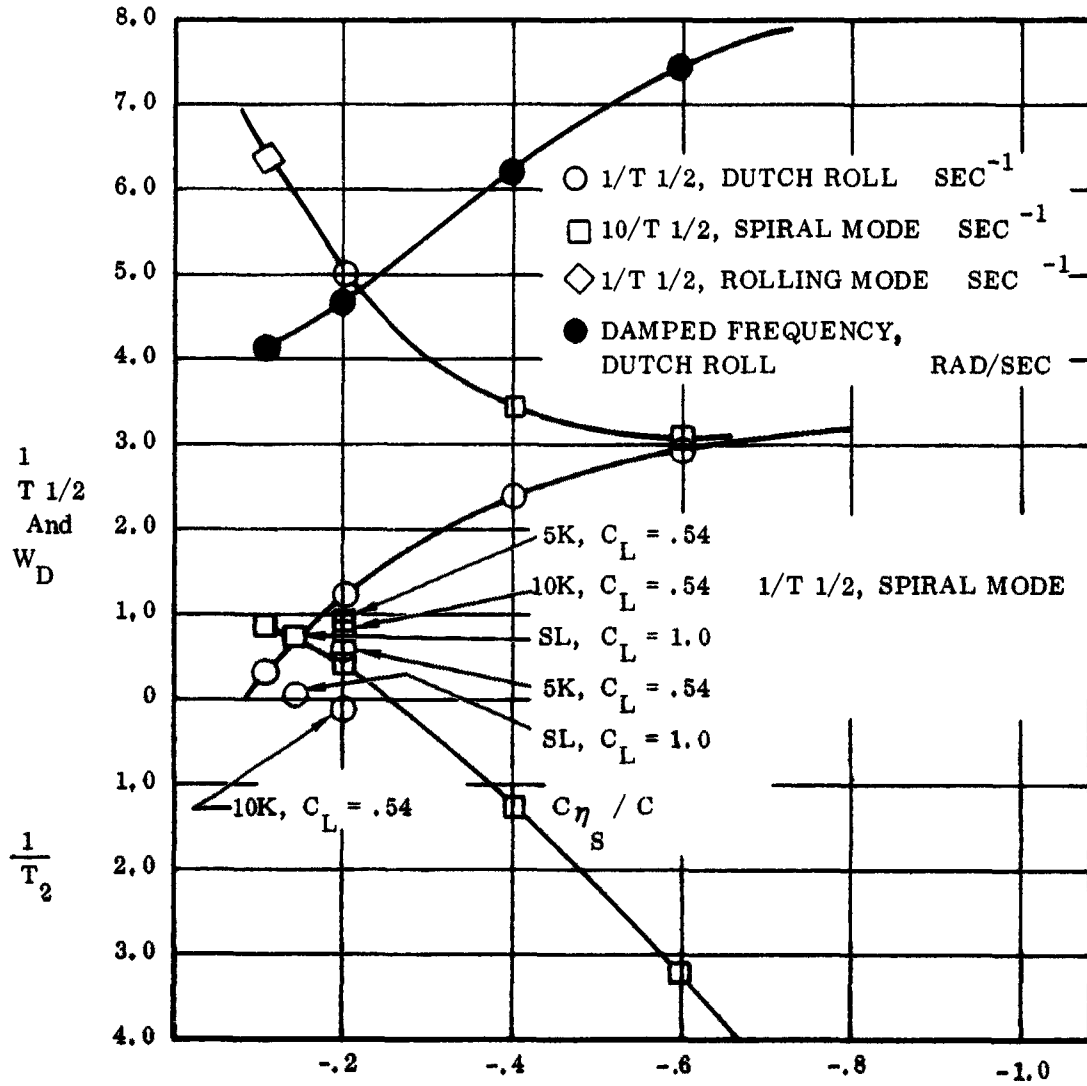


Figure 82 Dynamic Stability Variation with Directional Stability

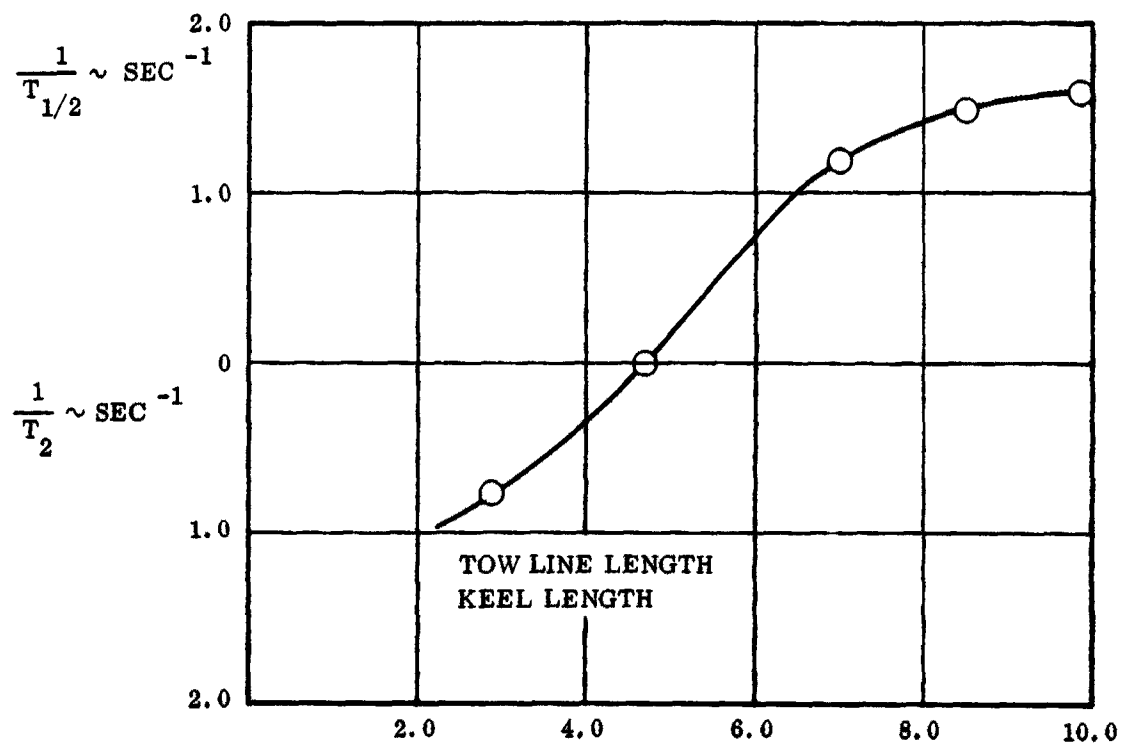


Figure 83 Dynamic Stability During Tow - Effect of Tow Line Length

DYNAMIC STABILITY DURING TOW  
EFFECTS OF ATTACH POINTS

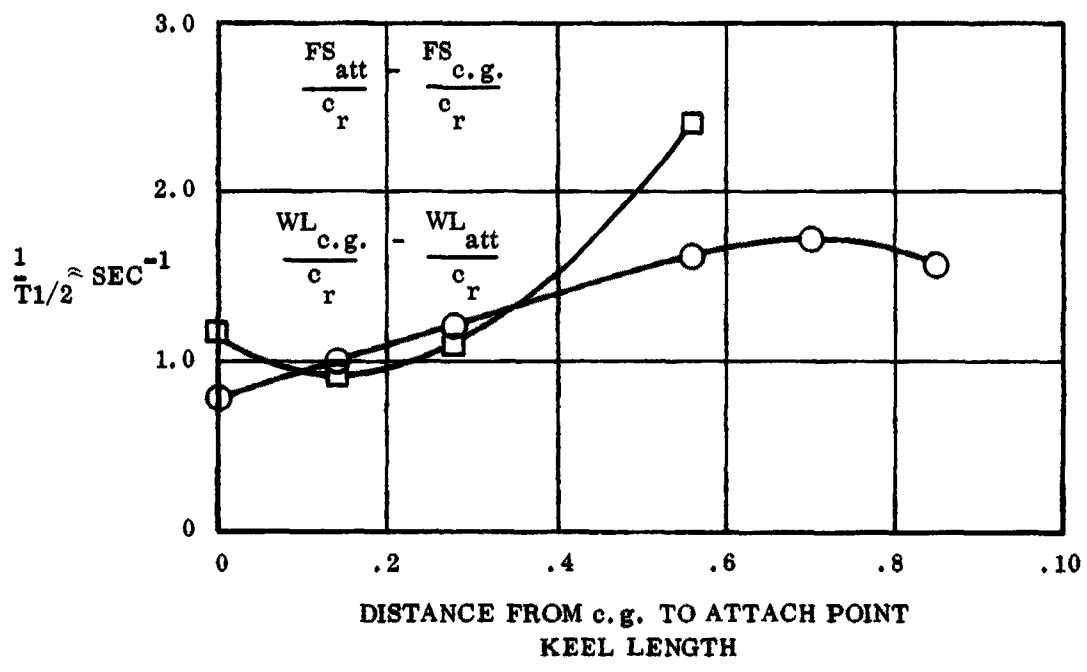


Figure 84 Dynamic Stability During Tow - Effects of Attach Points

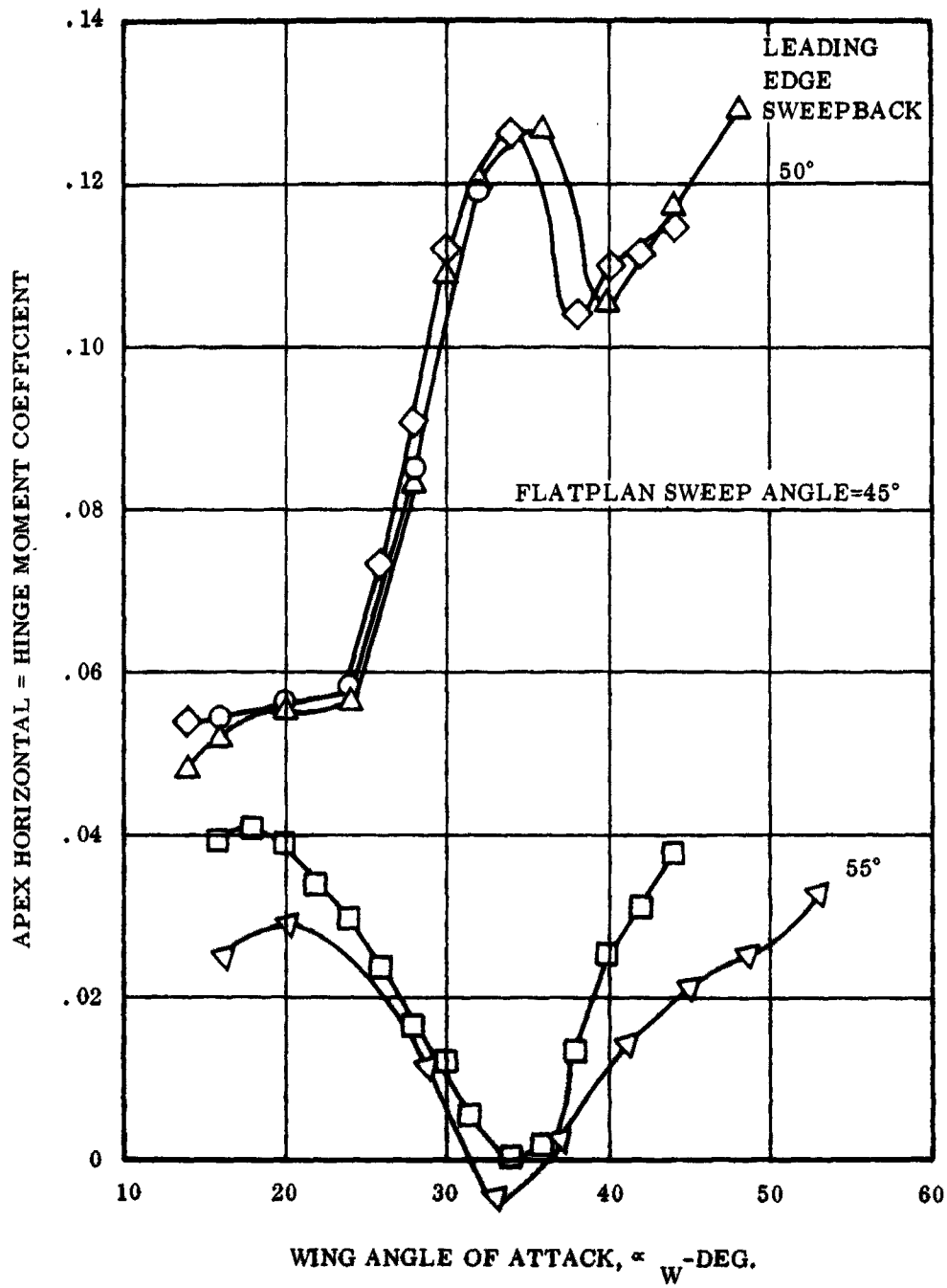


Figure 85 Apex Horizontal Hinge-Moment Coefficient vs. Wing Angle of Attack

WING SWEEPBACK ANGLE  
 VS.  
 WING LATERAL DEFLECTION

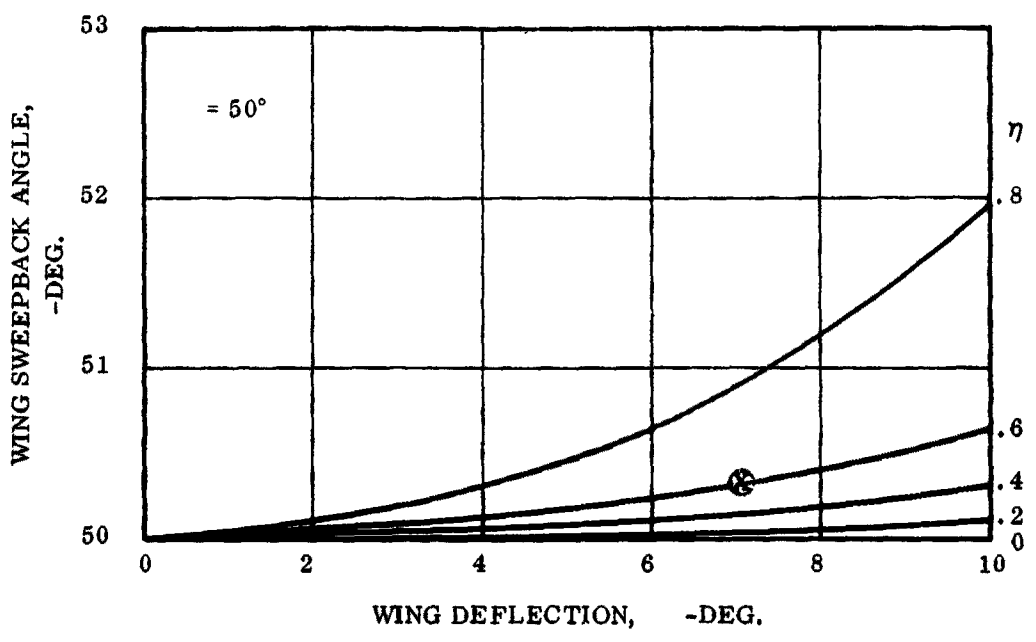


Figure 86 Wing Sweepback Angle vs. Wing Lateral Deflection

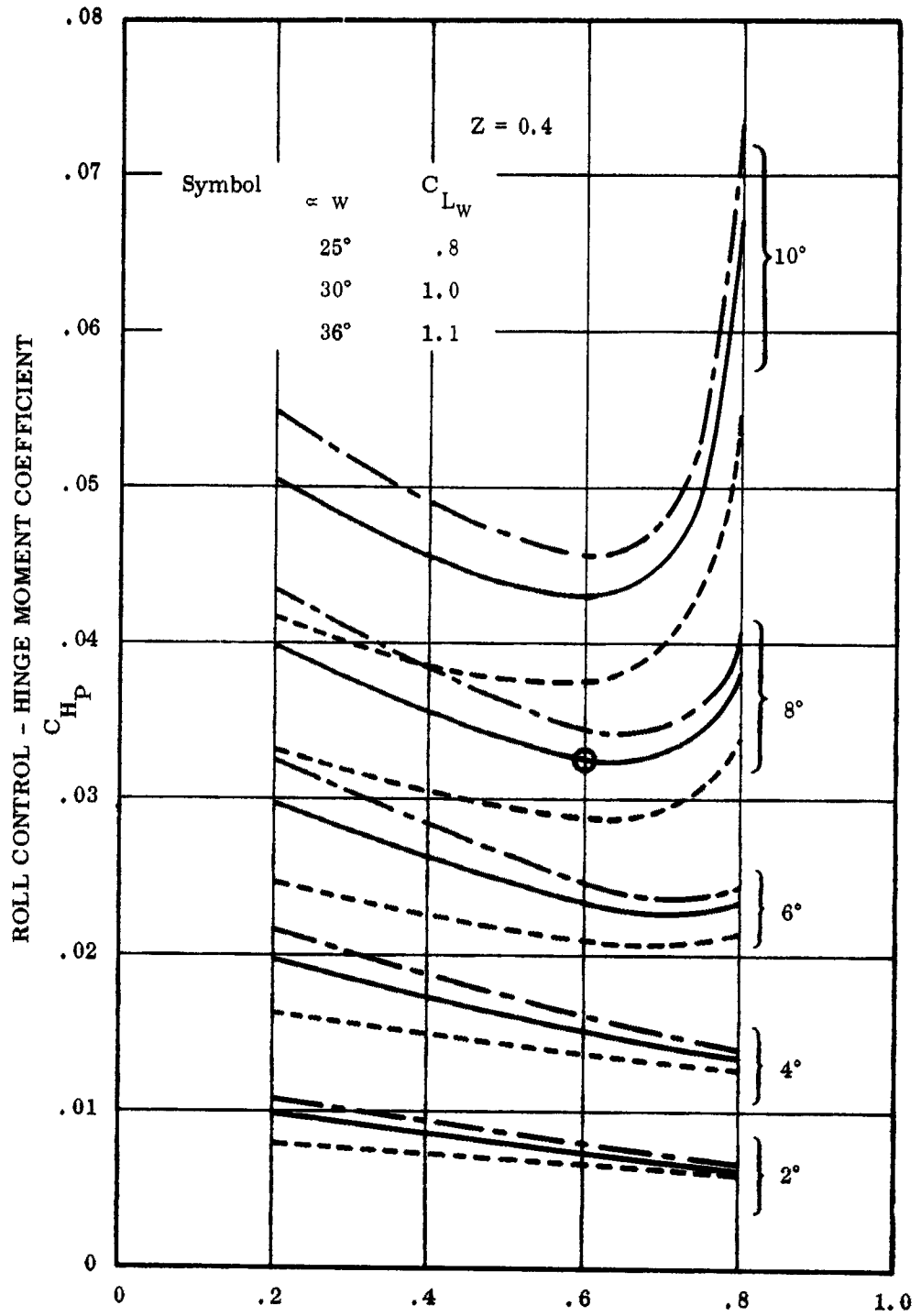


Figure 87 Control Hinge Moment Coefficient vs.  $\eta$

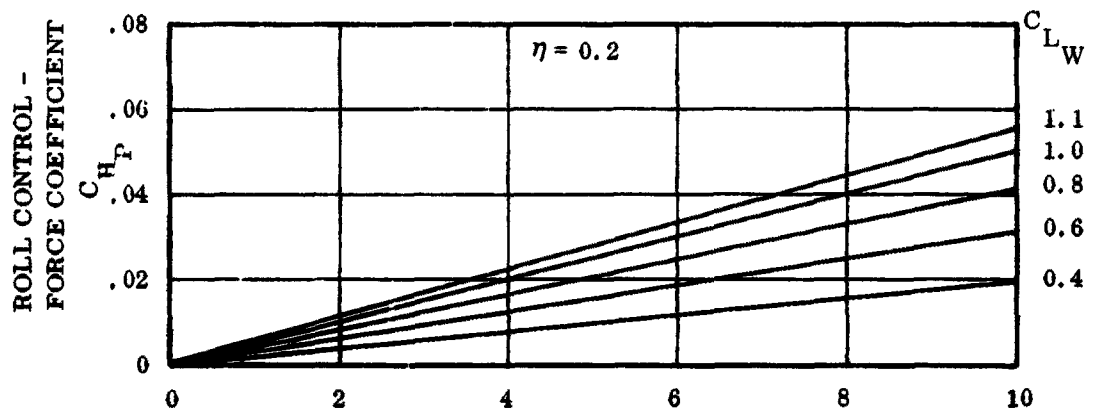
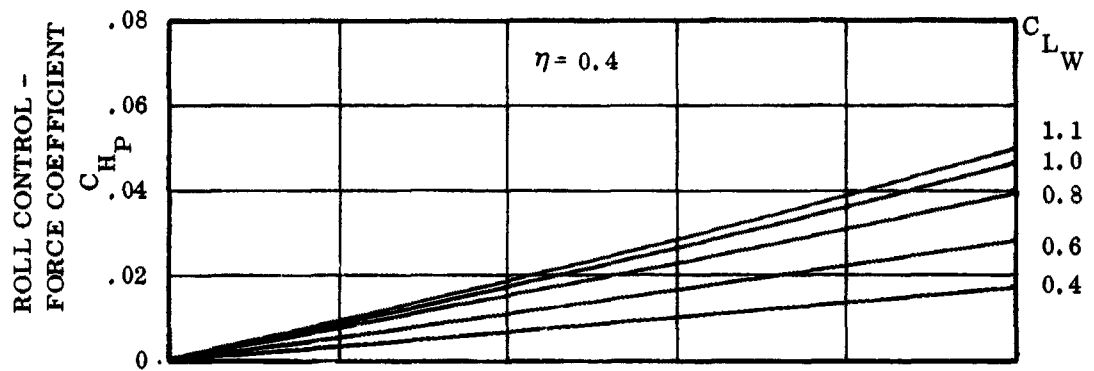


Figure 88 Roll Control Hinge Moment Coefficient vs. Wing Deflection

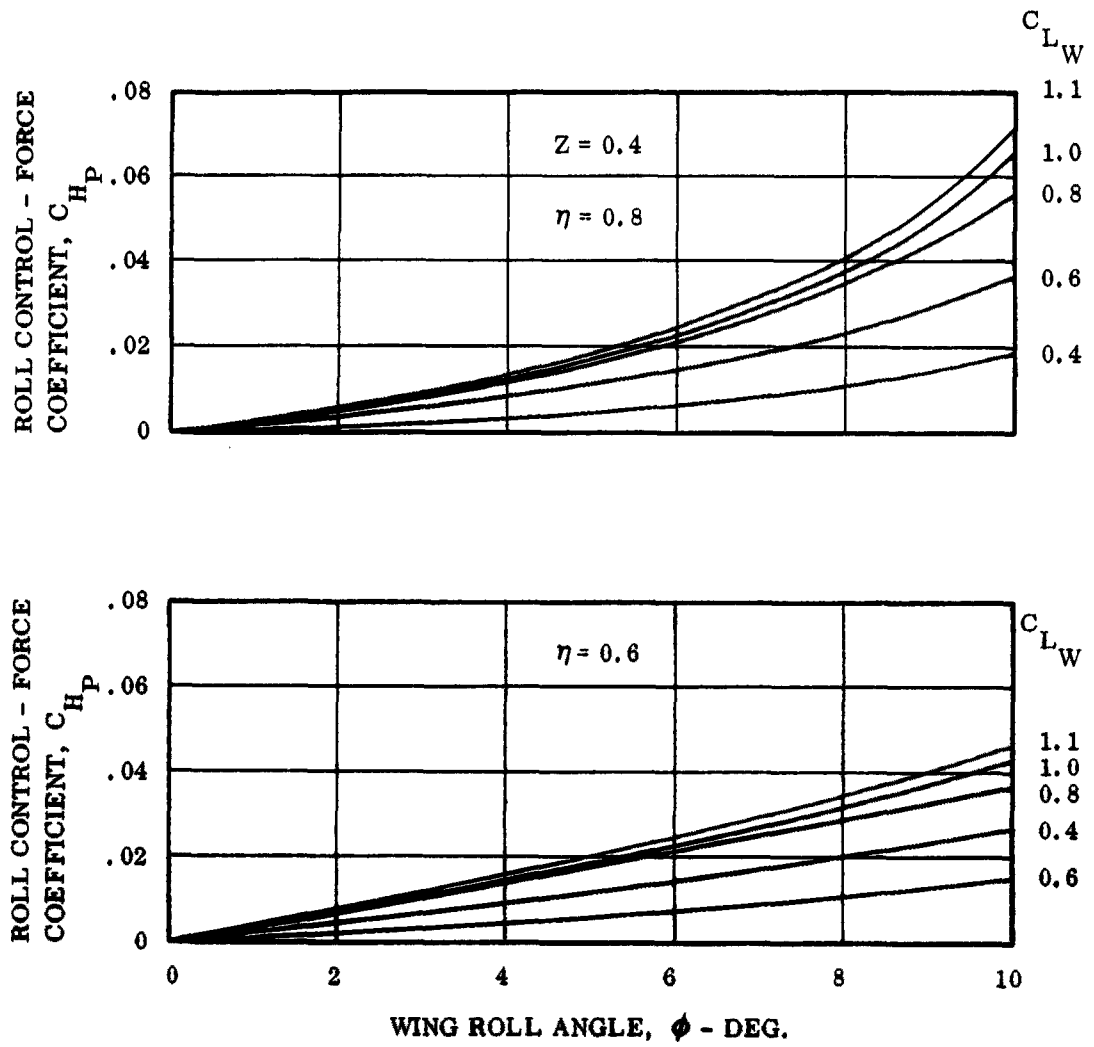


Figure 89 Roll Control Hinge Moment Coefficient vs. Wing Deflection

TABLE I.A  
 FLEXIBLE-WING STABILITY DERIVATIVES  
 LOW SPEED, WING ALONE  
 SPREADER BAR IN  
 STABILITY AXIS SYSTEM

$S_{ref}$	$S_{flat-plan}$	$b_{ref} = C_r = C_{keel}$	$C_{ref} = C_r = C_{keel}$
$\Lambda_{LE_{flat-plan}}$	= 45 deg	$\Lambda_{LE_{deployed}}$	= 50 deg
$\Lambda_{TE_{flat-plan}}$	= -20 deg	$\Lambda_{TE_{deployed}}$	= -23 deg
$AR = 4 \cos \Lambda_{IE}$		$AR_{deployed} = 2.57$	$\bar{C} = \frac{2}{3} C_r$
$X_{c.g.}/C_r$	- .50	$Z_{c.g.}/C_r = 0$	
LIFT		PITCHING MOMENTS	
$C_{L_\alpha} = 2.7 \text{ RAD}^{-1}$		$X_{a.c.}/C_r = -.46$	
$\alpha_{OL} = .157 \text{ RAD}$		$C_{m_o} = -.016$	
$C_{L_q} = .410 \text{ RAD}^{-1}$		$C_{m_q} = -.309 \text{ RAD}^{-1}$	
$C_{L_\alpha} = .694 \text{ RAD}^{-1}$		$C_{m_\alpha} = -.163 \text{ RAD}^{-1}$	
DRAG		ROLLING MOMENTS	
$C_{D_o} = .06$		$C_{l_\beta(C_L 0)} = .037 \text{ RAD}^{-1}$	
$C_{D_{C_L}} = -.10$		$C_{l_\beta}/C_L = -.226 \text{ RAD}^{-1}$	
$C_{D_{C_L}} = .3125$		$C_{l_p(C_L 0)} = -.201 \text{ RAD}^{-1}$	

TABLE I. A (Cont.)

ROLLING MOMENTS (Cont.)

$C_{l_r} / C_L = 0$	$C_{l_r} / C_L = .283 \text{ RAD}^{-1}$
SIDE FORCES	DIRECTIONAL MOMENTS
$C_{y_{\beta}(C_L = 0)} = -.158 \text{ RAD}^{-1}$	$C_{\eta_{\beta}(C_L = 0)} = .0384 \text{ RAD}^{-1}$
$C_{y_{\beta}/CL} = -.173 \text{ RAD}^{-1}$	$C_{\eta_{\beta} C_L} = -.0411 \text{ RAD}^{-1}$
$C_{Y_p} / C_L = .52 \text{ RAD}^{-1}$	$C_{\eta_r(C_L = 0)} = -.0347 \text{ RAD}^{-1}$
$C_{\eta_{\beta}(C_L = 0)} = -.0126 \text{ RAD}^{-1}$	$C_{\eta_r} / C_L^2 = -.0354 \text{ RAD}^{-1}$
$C_{y_r/C_L} = -.0138 \text{ RAD}^{-1}$	$C_{\eta_p} / C_L = -.448 \text{ RAD}^{-1}$
$C_{y_r} / C_L^2 = -.0295 \text{ RAD}^{-1}$	

TABLE I. B

BODY STABILITY DERIVATIVES  
MOMENTS ARE ABOUT SYSTEM C. G. AT CRUISE

UNITS -  $\text{RAD}^{-1}$

Configurations	$\Delta C_{L_{\alpha}}$	$\Delta C_{m_{\alpha}}$	$\Delta C_{m_q}$	$\Delta C_{y_{\beta}}$	$\Delta C_{\eta_{\beta}}$	$\Delta C_{y_r}$	$\Delta C_{\eta_r}$
250 lb. payload	.0932	.0795	.1356	-.0932	-.0795	-.1590	-.1356
1000 lb. payload	.0604	.0368	.0448	-.0604	-.0368	-.0736	-.0448
4000 lb. payload	.0410	.01948	.01835	-.0343	-.0163	-.0324	-.01537
8000 lb. payload	.0352	.01695	.01615	-.0360	-.0173	-.0345	-.01665

TABLE II

LATERAL-DIRECTIONAL

STABILITY DERIVATIVE C. G. TRANSLATION

WING

$$C_{y\beta} = -.158 - .173 C_L$$

$$C_{y_p} = .52 C_L + 2 \frac{Z_{c.g.}}{c_r} \cos \alpha - \left( \frac{x_{c.g.}}{c_r} + .50 \right) \sin \alpha C_{y\beta}$$

$$C_{y_r} = -.0126 - (.0295 C_L + .0138) C_L - 2 \left( \frac{x_{c.g.}}{c_r} + .50 \right) \cos \alpha + \left( \frac{Z_{c.g.}}{c_r} \right) \sin \alpha C_{y\beta}$$

$$C_{y\delta_a} = C_L$$

$$C_{l_\beta} = .037 - .226 C_L + \left( \frac{Z_{c.g.}}{c_r} \right) \cos \alpha - \left( \frac{x_{c.g.}}{c_r} + .50 \right) \sin \alpha C_{y\beta}$$

$$C_{l_p} = -0.201 + \left( \frac{Z_{c.g.}}{c_r} \right) \cos \alpha - \left( \frac{x_{c.g.}}{c_r} + 5.0 \right) \sin \alpha C_{y_p}$$

$$C_{l_r} = .283 C_L + \left( \frac{Z_{c.g.}}{c_r} \right) \cos \alpha - \left( \frac{x_{c.g.}}{c_r} + 5.0 \right) \sin \alpha C_{y_r}$$

$$C_{l_{\delta_a}} = \left( \frac{Z_{c.g.}}{c_r} \right) \cos \alpha - \left( \frac{x_{c.g.}}{c_r} + .46 \right) \sin \alpha C_{y_{\delta_a}}$$

$$C_{\eta_\beta} = - \left( \frac{x_{c.g.}}{c_r} + .50 \right) \cos \alpha + \frac{Z_{c.g.}}{c_r} \sin \alpha C_{y_\beta} + .0384 - .0411 C_L$$

$$C_{\eta_p} = -.448 (C_L) - \left( \frac{Xc.g.}{c_r} + .50 \right) \cos \alpha + \frac{Zc.g.}{cr} \sin \alpha \quad C_{y_p}$$

$$C_{\eta_r} = -.0347 - .0354 C_L^2 - \left( \frac{Xc.g.}{cr} + .50 \right) \cos \alpha + \left( \frac{Zc.g.}{c_r} \right) \sin \alpha \quad C_{y_r}$$

$$C_{\eta_{\delta_a}} = - \left( \frac{Xc.g.}{C_r} + .46 \right) \cos \alpha + \frac{Zc.g.}{cr} \sin \alpha \quad C_{y_{\delta_a}}$$

## CONCLUSIONS

1. All configurations studied will meet the longitudinal and directional static stability requirements by repositioning of the wing.
2. Flight test will determine the final stability margins.
3. Acceptable c. g. travel ranges may be established for all configurations.
4. The minimum tow line length is 4.7 keel lengths.
5. The lateral control hinge line must be located at 60 percent of the span.
6. It appears that dynamic coupling between the glider and the towing vehicle will cause no objectional characteristics.

### III. DESIGN CRITERIA AND STRUCTURAL DESCRIPTION

#### SUMMARY

In compliance with the statement of work of the contract, four basic configurations of the towed air logistics glider were established. Structurally, each of the configurations is of the same design family, varying only in size to accommodate the design payloads of 250, 1,000, 4,000 and 8,000 lbs. each. Exceptions were made in certain features of the 250 and 1,000 lb. payload configurations to facilitate air drop requirements. One version of the 1,000 lb. payload vehicle was examined to determine the feasibility of a flexible, or cable attachment of wing to body rather than a standard rigid truss support.

The basic design criteria were formulated from MIL-A-8860 (ASG) and the applicable specifications. A thorough search of current specifications revealed none relating directly to towed gliders. Specifications MIL-A-8861 and 8862 were used as a guide for design criteria for each of the configurations. To the extent practicable, the high standards for safety of flight were maintained in the referenced specifications for manned flight vehicles. Recommended model specifications applicable to the Flexible Wing Towed Air Logistic Gliders are included in Appendix.

Analysis of the loads based on wind tunnel data obtained from NASA and from Ryan experience with the Flexible Wing test bed shows that gust conditions, rather than the maneuvering loads, will dictate the critical design points.

The following table establishes the maximum structural design conditions for each of the four basic configurations:

Nominal Payload	Stalling Speed $V_s$ (knots)	Speed for Max. Gust Intensity $V_G$ (knots)	Gust Load Factor $G$
250	40	100	4.70
1000	40	100	3.90
4000	40	100	3.05
8000	40	100	2.65

All the above values for  $\frac{W}{S} = 6$  psf

A study of the design requirements for the air drop configurations revealed that the practical approach was erection delay of the wing until the vehicle had decelerated to a velocity of 147 fps and 134 fps, which would be compatible with the gust load factor noted in the above table for the respective 250 and 1,000 lb. payload configurations.

Major effort in the study was toward structural requirements, wing design, and the supporting structure. Only cursory investigation was made of the body sections of each of the configurations, since items of manufacturing cost, sizing for cargo accommodations, and expected attrition rate will have significant influence on final design.

Preliminary studies and past experience in the development of flexible wings showed that the rigid concept would be applicable for the basic requirements. The wing should be comprised of two rigid beam leading edge members, a rigid keel member, and the flexible membrane. Considering control and trim requirements (a function of establishing a predetermined relation between the center of gravity of the body and the center of pressure of the wing), it is noted that a tubular truss structure would be ideally suited for the function of joining the wing to the body. The requirement to fold or collapse the wing also led to simplifying the folding joints of the truss structure. This minimized the number of attaching points to the body.

The leading edge members of the 250 and 1000 lb. configurations are standard streamline tubes, oriented in the direction of the membrane outflow. The leading edge members of the other configurations are built-up beams of streamline section employing standard aircraft type construction. The material used is aluminum. The keel members of

configurations are built-up rectangular sections capable of transmitting bending loads in two planes. The structure is standard aircraft type and the material is aluminum. The wing membrane material may be chosen from several suitable types of fabrics and coating. As a result of tests conducted during previous applications of the Flexible Wing, a polyester impregnated Dacron is suited for this application. The weight of the material required varies according to the load. Sections of the wing membrane are joined by a cold bonding process. The elongation characteristics of the membrane fabric minimize transverse stretching and a tendency of the material to fold. The three rigid members of the wing are joined at the apex to permit folding of the complete assembly.

The supporting structure joining the wing and body of each of the configurations - basically two "A" frames - is of welded steel tubing. The frames are orientated so that the base picks up two attaching points of the body (laterally each) at the forward and aft ends; then converge to a single attachment connecting to the keel of the wing. The wing spreader bar is a structural member used to spread the wing and to insure prescribed sweep angle. It also serves in the directional control function. A single steel tube is used in the 250 and 1,000 lb. payload configurations, but to accommodate the higher loads a truss work of steel tubing is required for the 4,000 and 8,000 lb. configurations.

The bodies of the 1,000, 4,000 and 8,000 lb. payload are similar in shape and type of construction, the shape being basically a rectangular box with faired ends to minimize drag. Construction concepts may range from use of crude welded tubular trusses to the standard type of present cargo aircraft. Using the former would greatly reduce cost, but would disregard weight. Loads would be carried by the basic truss members and no use made of the covering for structural purposes other than dynamic pressure loads. Using standard aircraft material, however, would require a field tension type of construction. This would be a combination of frame, longitudinal stringers and skin.

The landing gear presented are of the quadricycle type to insure adequate ground stability. An alternate concept using landing skids and a ground dolly for takeoff represents a low cost version. Except in the 250 lb. version, the landing gear is located on the corner extremities of the cargo box. The load absorbing mechanism of the gear is of two basic types - an air/oil shock strut for the forward components and

torsion bar suspension for the rear components. Since requirements for floatation characteristics are yet to be finalized, sizing of the rolling components has been held to a minimum. The landing gear of the 250 lb. configuration is cantilevered spring type, with the attachment direct to the wing and body attachment saddle.

TABLE  
TOWED AIR LOGISTICS GLIDER GENERAL  
DIMENSIONAL DATA

	250#	Payload Version			
		1000# Folding Pylon Air Drop	1000# Cable Air Drop	Rigid Tow	8000#
Over-all Length (159) Flight Configuration (in)	108	197	248	197	387
Over-all Length (159) Folded Configuration (in)	122	233.50	242	207(0°)	412(0°)
Over-all Width (190) Flight Configuration (in)	133	266	170	266	530
Over-all Width (190) Folded Configuration (in)	42.50	71	71	71	125
Over-all Height (190) Flight Configuration (in)	73.25	148	275	148	276
Over-all Height (190) Folded Configuration (in)	67.50	71.75	66.50	115.50(0°)	213(0°)
Keel Length (in)	103	207	242.40	207	412
Wing Area (Flat Plan ft <sup>2</sup> )	53	208	234	208	833
Body Length ) Less (in)	105	162	162	162	231
Body Width ) Handling (in)	24	54	54	54	81
Body Height ) Gear (in)	24	53.50	53.50	53.50	72
Cargo Compartment Length (in)	48	96	96	96	168
Cargo Compartment Width (in)	23	48	48	48	72
Cargo Compartment Height (in)	23	36	36	36	60
Cargo Volume (ft <sup>3</sup> )	12.50	96	96	96	400
Wheel Base (in)	41.50	86	86	86	140
Wheel Tread - Front (in)	40	67	67	67	113
Wheel Tread - Rear (in)	40	67	67	67	80
Static Ground Clearance (in)	4.00	4.00	4.00	4.00	4.50
Empty Weight (lb)	118	499	422	479	1642
Gross Weight (lb)	368	1499	1422	1479	5642

## METHOD OF APPROACH

Design criteria of the towed air logistic gliders were established from applicable specifications referenced in MIL-A-8860 (ASG). Investigations showed that there were no specifications relating to unmanned towed gliders. Review therefore of specifications was made, and, where conflict with design objectives indicated, modifications, deletions or additions were introduced. The following basic design philosophy was formulated.

Payload capabilities of 250, 1000, 4000 and 8,000 lbs. will be adhered to for establishment of the dimension parameters.

Wing loadings (W/S) will be finalized to the parameters between 5 and 7 pounds per square foot of Wing Area.

Cargo Compartments will be sized for a Cargo density of ten pounds per cubic foot.

Rigid standards of design practices compatible with man carrying air vehicles will be adhered to.

Each vehicle will contain the inherent ruggedness and have the strength capabilities compatible with the requirements of normal ground and air combat operations.

Design must insure lift/drag ratios for thrust requirements of the towed vehicle to be compatible with the thrust outputs of fixed wing aircraft and helicopters common to the inventory of the U. S. Army.

Each vehicle must be inherently stable while under tow, and each vehicle must be provided with a simplified self-contained control system for the free flight modes.

Wings and supporting structure of each vehicle will be foldable to present the smallest package possible when not in operation.

Vehicles having payloads of 250 and 1,000 lbs. will have the capability of being carried aboard the AC-1 (Caribou) airplane externally or internally, and of being successfully jettisoned on command, with the wing erecting automatically. The vehicle, under remote or automatic control, glides to a satisfactory landing.

With the above objectives in mind, the design staff, with direct support of the loads, stress and weights, configured each of the vehicles.

Detail loads and strength characteristics and requirements were developed by stress personnel. Results are incorporated in a proposed version of the specification MIL-A-8861 and MIL-A-8862, copies of which appear in the Appendix. A detail stress analysis was completed of each of the configurations except the 4,000 lb. payload configuration. It was felt that since structurally the vehicles are of a family, the strength requirements could safely be extrapolated from an analysis of the 1,000 and 8,000 lb. payload configurations. The extrapolated data is found in this volume.

## TECHNICAL DISCUSSION

Design criteria for the towed air logistics gliders using the flexible wing concept have been established in accordance with requirements of the recommended two specifications - for Vehicle Strength and Rigidity for Flight Loads, and for Vehicle Strength and Rigidity for Landing and Ground Handling Load. These are presented in model form herein, based on the requirements and applicable specifications of MIL-A-8861 and 8862.

Structural design was based upon the maximum flight loads with a gust occurring in towed flight. Gust load factors, evaluated for each of the configurations in accordance with standard procedures, are listed below:

Configuration by payload size	250	1,000	4,000	8,000
Gust factor	4.7	3.9	3.05	2.65

Speeds for maximum gust intensity and resultant load factors were computed from the equation:

$$n = 1 \pm \rho_o \frac{V_e U_{de} m K_W}{2 W/S}$$

Where:

$V_e$       airspeed, FPS, EAS

$U_{de}$      gust velocity, FPS, EAS

$m$         slope of curve  $C_{NA}$  vs

$K_W$       gust factor       $\mu \frac{2 W/S}{gcmp}$

W Weight, pounds  
S Wing Area, sq. ft.  
g  $32.2 \text{FPS}^2$   
c average chord, ft. (area/span)

Selection of the material for the wing membrane was made after reviewing the results of previously conducted tests at Ryan laboratories. Prime consideration was given to availability or off the shelf materials. The requirements for properties of the membrane material were established as:

Flexibility  
Crease resistance  
Effect of folds on other properties  
Strength, tensile and yield  
Density  
Strength-to-weight ratio  
Elastic and plastic deformation properties  
Fatigue strength  
Tear resistance  
Notch strength  
Resistance to abrasion (Rain, dust, material)  
High temperature properties  
Low temperature properties  
Gas permeability  
Resistance to humidity, fungus, etc.  
Emissivity and reflectivity properties  
Cost

In addition to the engineering properties, the fabrication properties are considered in material selection. Other things equal, cost becomes the primary consideration in fabrication, but other factors include:

Resistance to damage by handling  
Ease of joining  
Joint efficiency and reliability  
Fabrication time  
Amount of specialized technique necessary  
Need for special equipment and other facilities  
Methods and reliability of repair

Tests at Ryan Aerospace narrowed the material evaluation to Nylon, Dacron, and Fortisan fiber materials as most promising for overall efficiency. Tests of these materials include weathering tests, wear tests, and mechanical tests, as well as fabrication evaluations.

Tests have shown serious disadvantages of continuous films. Notch tear strength of Mylar films is extremely low, the stress necessary to propagate a tear being measured in ounces as against pounds for cloth of the same tensile strength. Based on tensile strength, the strength weight ratio of Mylar film is somewhat less than that of a coated Dacron cloth when cloth is tested in the thread direction. Mylar film shows a lower yield strength than the cloth and also shows up to 100% elongation. Heavy Mylar film, .0075", exhibits stiffness and a tendency to kink on double folding.

The tables and curves presented in the following pages demonstrate the properties and characteristics of the candidate materials.

## LOADS AND STRESS ANALYSIS

Stress and loads analyses conducted on the towed glider configurations are presented to fulfill the requirements of Contract Number DA 44-177-TC-779.

The analyses indicate the structural feasibility of the proposed vehicles. Conventional methods of analyses were employed throughout the investigation.

In the stress and loads analyses of the towed glider vehicles, conventional methods of analysis were employed. No attempt was made to present a complete detailed analysis. Only major structural areas were investigated. Simplified static and dynamic studies were conducted to determine the critical loading conditions.

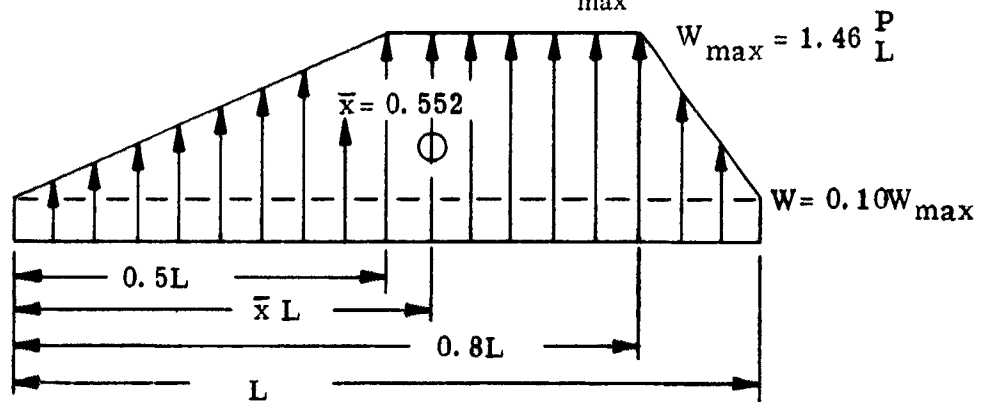
Load distribution on the wing membrane and beams was calculated to define shear and moment curves for the keel and leading edges of the wing. Simplified bending and shear analyses were made on the wing elements to substantiate the structural integrity of the design.

The wing-to-body strut members were analyzed as columns for loads induced by the aerodynamic loads imposed on the wing.

Landing loads were calculated on the basis of a sink speed of 10 fps. An arbitrary load factor of 3 g's was assumed. The required landing gear designs do not impose impractical requirements structurally and mechanically.

### Loads Analysis

The following loads are based on an idealized load distribution along the keel and leading edges for the  $C_{L_{max}}$  condition.



Three main loading cases are considered.

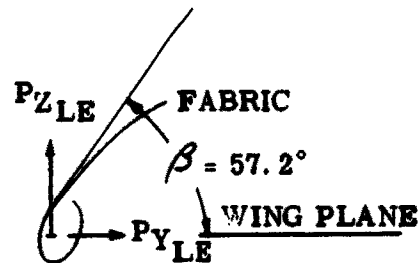
- Case I Maximum load on the leading edge
- Case II Maximum load on the keel
- Case III Asymmetrical keel loading condition

#### Case I - Maximum Load On the Leading Edge

Leading Edge Load

$$P_{Z_{LE}} = 0.35 nW$$

$$P_{Y_{LE}} = 0.223 nW$$

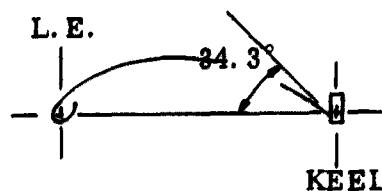


**Case II - Maximum Load On the Keel**

Keel Load

$$P_{Z_K} = 0.42 \text{ nW}$$

$$P_{Y_K} = 0 \text{ (By reason of symmetry)}$$



**Case III - Asymmetrical Flight Condition**

$$P_{Y_K} = 0.073 \text{ nW}$$

(Ref: CAR-3 Paragraph 3.191)

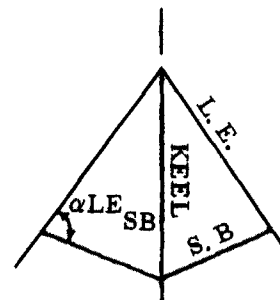
Two other necessary loads are derived from one of the three cases.

- (a) Fabric Load (All cases)
- (b) Spreader Bar Load (Case I)

$$P_{SB_{Comp}} = \frac{P_{Y_{LE_{SB}}}}{\sin \alpha_{LE_{SB}}}$$

$$P_{Y_{LE_{SB}}} = 0.22 \text{ nW}$$

$$\bar{X}_{LE_{SB}} = \frac{X_{LE_{SB}}}{L}$$

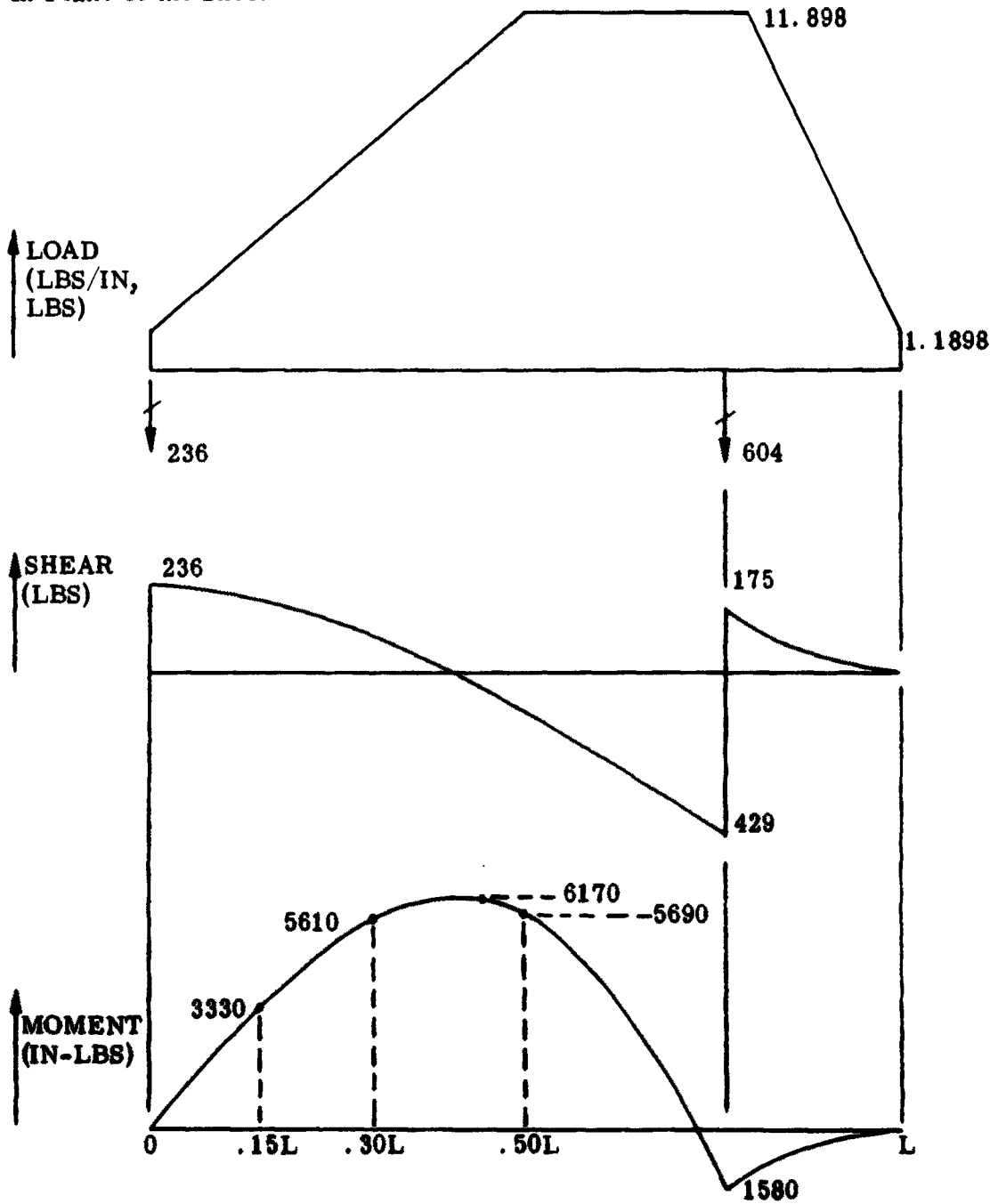


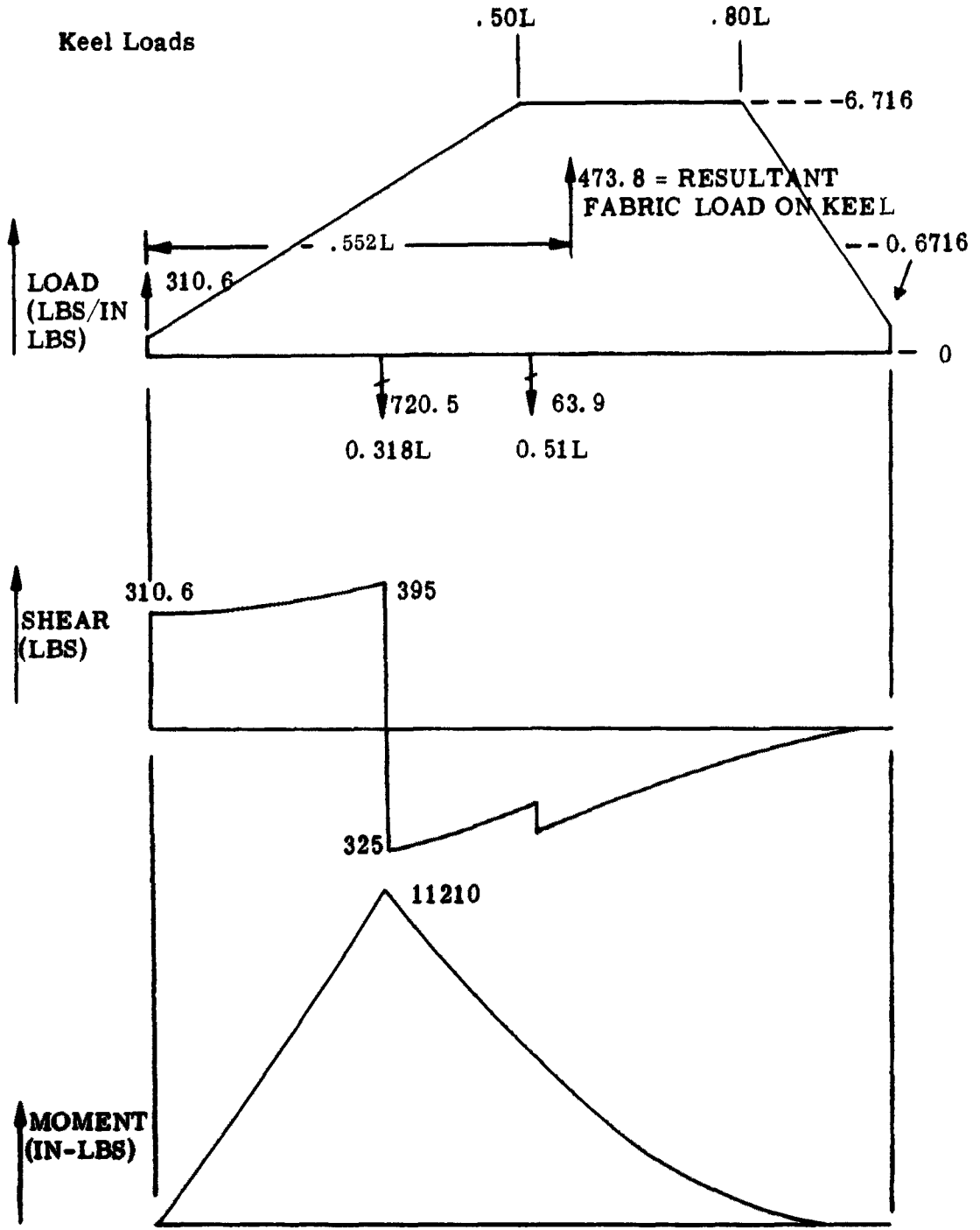
Axial and shear loads for the spreader bar for each vehicle are given in the following table.

Vehicle Payload	250 LB	1000 LB	4000 LB	8000 LB
S. B. Axial Load	593 C.	1965 C.	*	10350 C
S. B. Shear Load	397 ↑	1184 ↑	*	9680 ↑

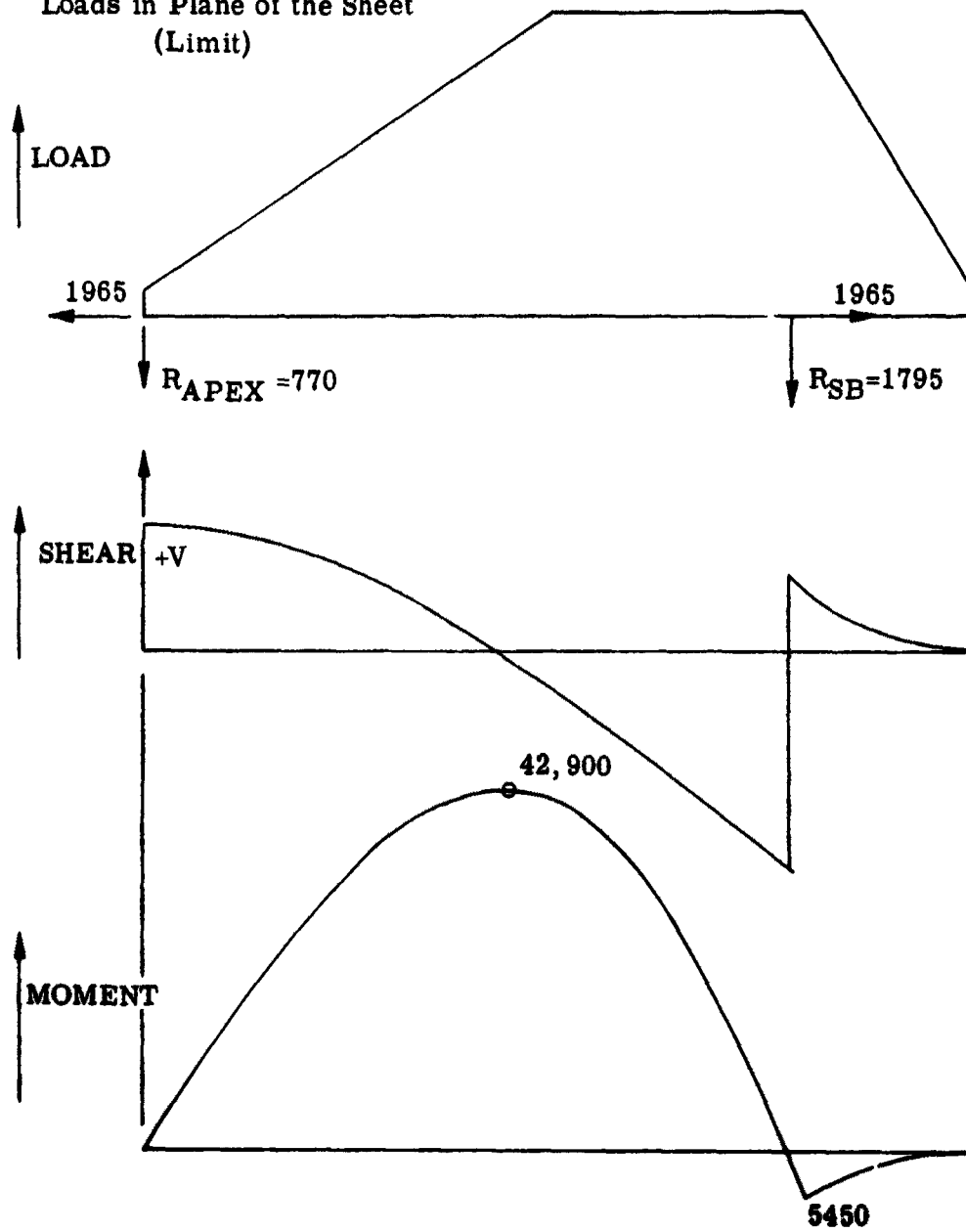
250 Lb. Payload Tow Glider

Loads in Wing Elements  
 Leading Edge Loads  
 In Plane of the Sheet

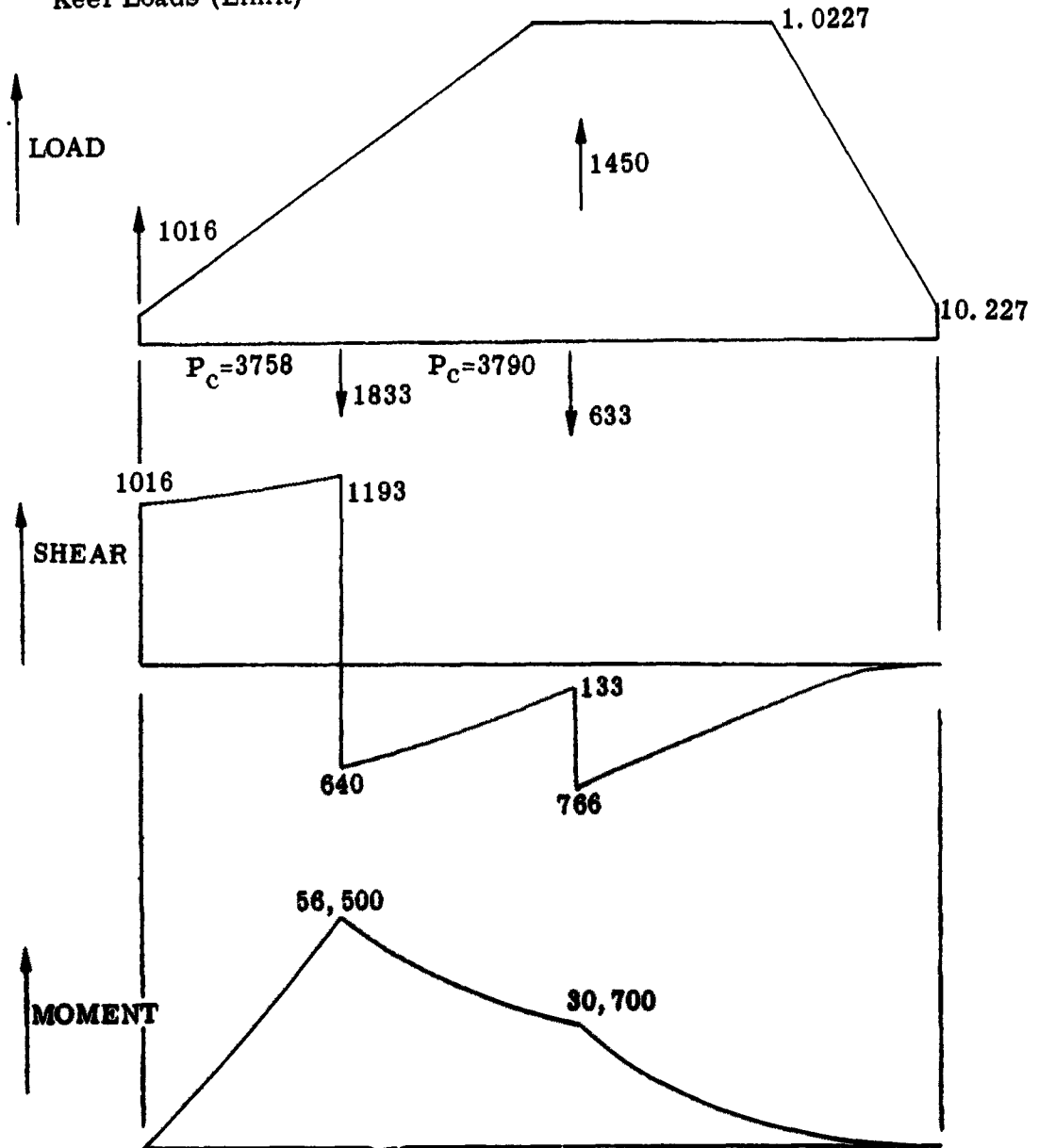




1,000 Lb Payload Tow Glider  
 Loads in Wing Elements  
 Leading Edge Loads (Cont.)  
 Loads in Plane of the Sheet  
 (Limit)

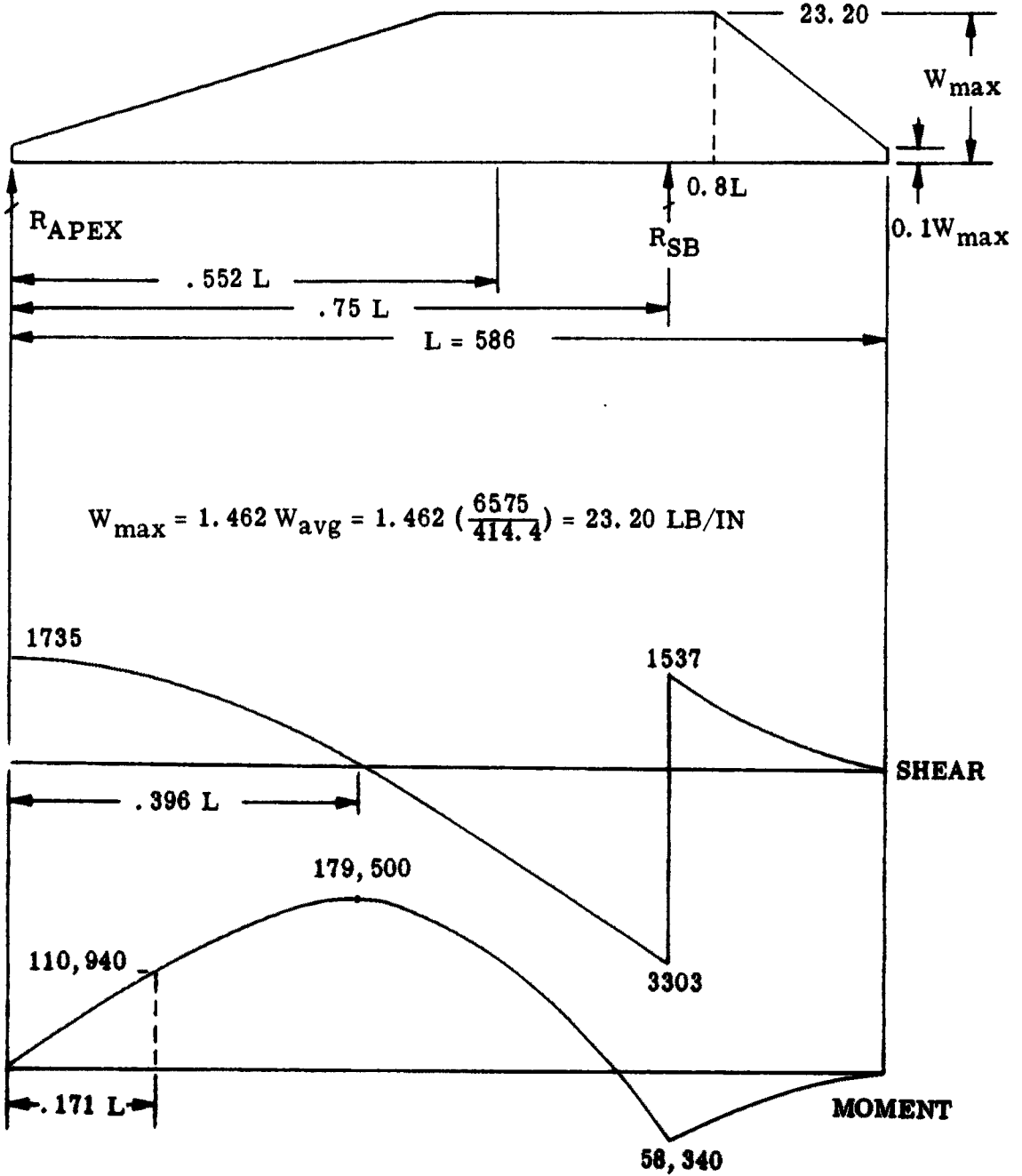


1,000 Lb Payload Tow Glider  
 Loads in Wing Elements  
 Keel Loads (Limit)

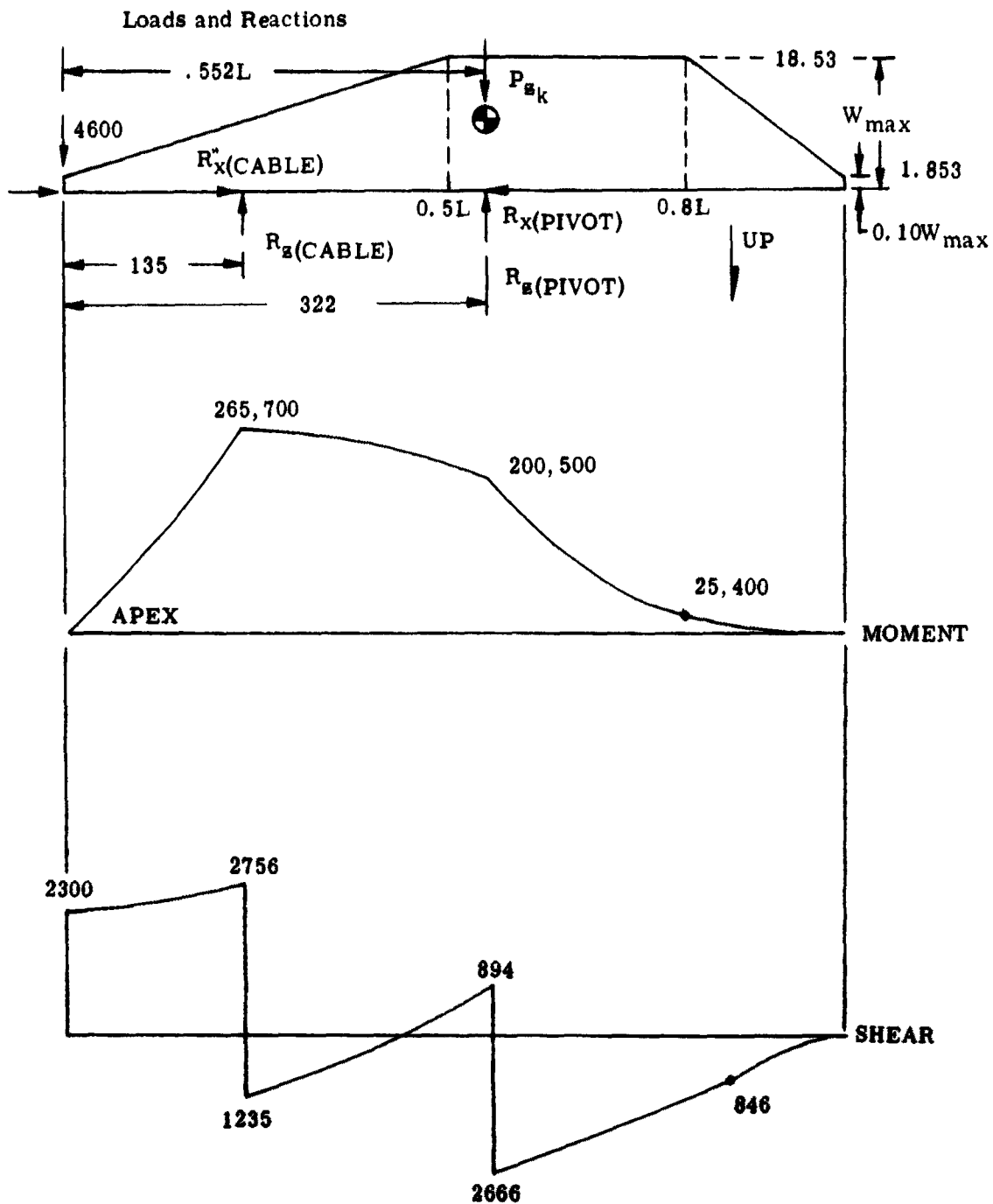


# 4000 Lb Payload Tow Glider

## Shear and Bending Moment

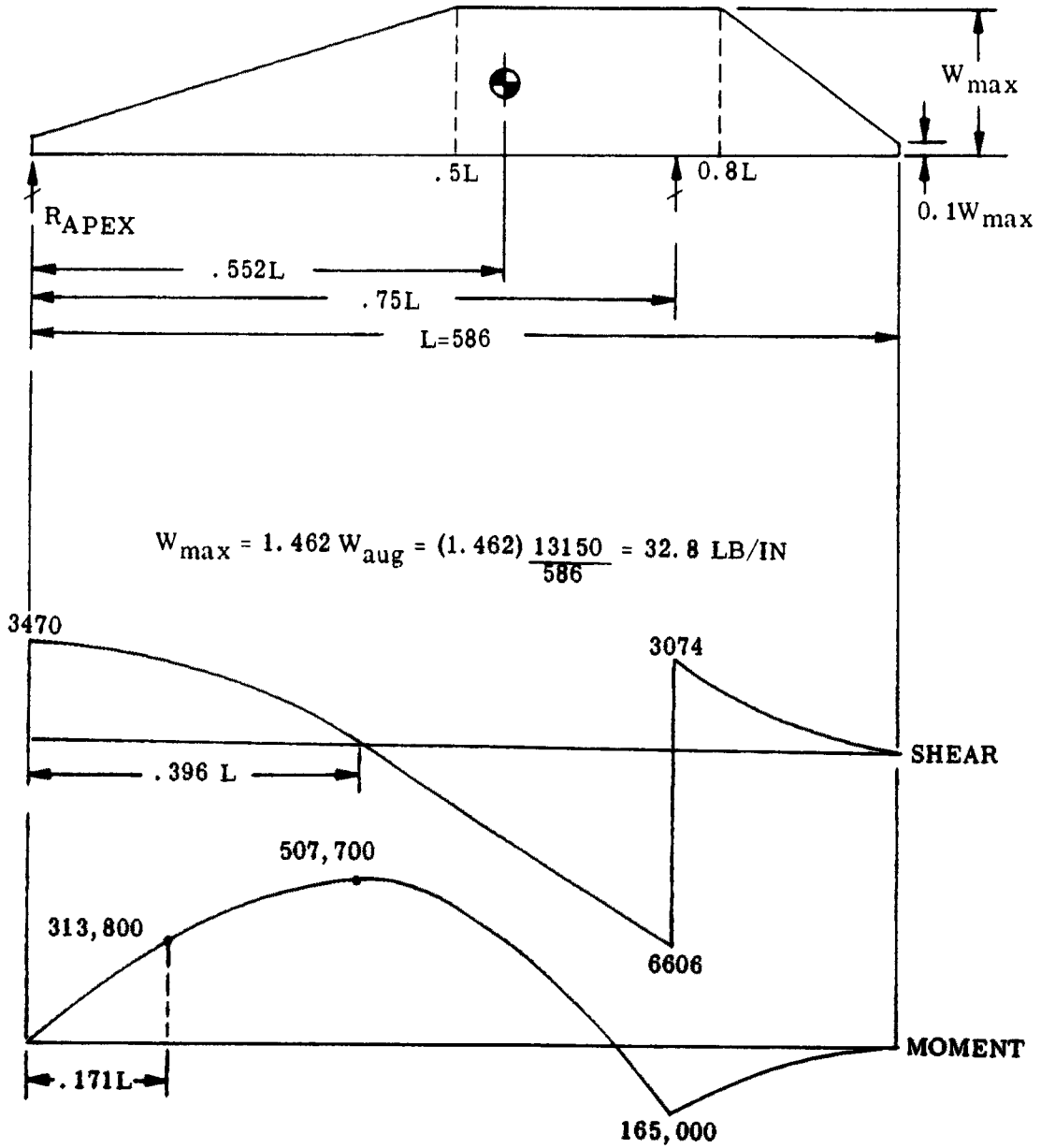


4000 Lb Payload Tow Glider

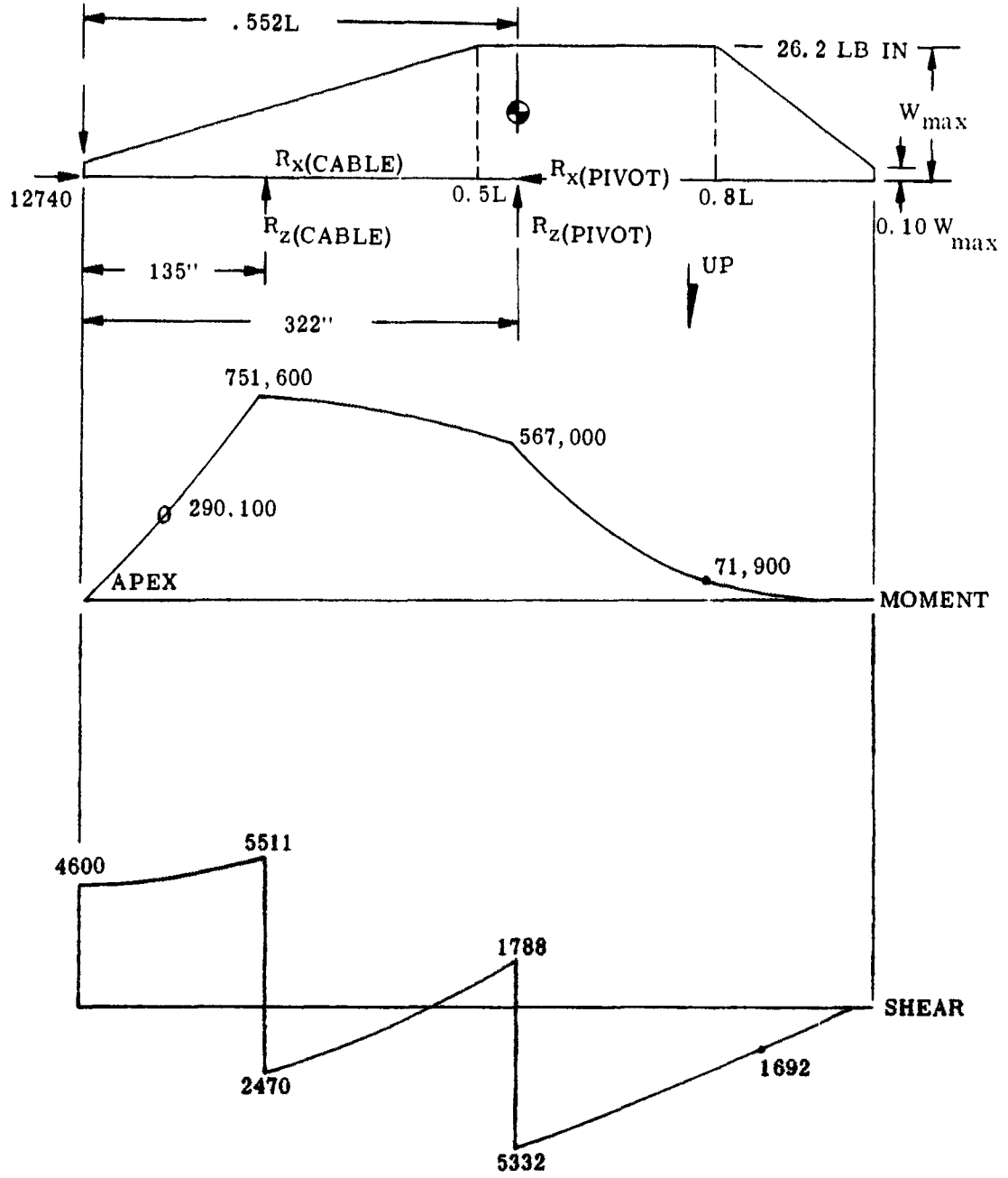


8000 Lb Payload Tow Glider

Shear and Bending Moment



Loads and Reactions



### Landing Loads

$V_s$  = Vertical velocity = 7 fps (optimum)

Design  $V_s$  = 10 fps

$$(I) \quad a = \frac{V_s^2}{S} \quad (\text{Leaf spring and torsion bar type gears})$$

$$(II) \quad a = \frac{V_s^2}{2 S (.85)} \quad (\text{Hydraulic landing gears})$$

$$n = \frac{a}{32.2} \quad (\text{Landing load factor})$$

The landing load factor has arbitrarily been established at  $n_z = 3$ .

$$\therefore a = (3) (32.2) = 96.6 \text{ fps}^2$$

$$(I) \quad s = \frac{(10)^2}{96.6} = 1.035' = 12.4''$$

$$(II) \quad s = \frac{(10)^2 (12)}{(2) (96.6) (.85)} = 7.3''$$

The preceding analysis indicates that the landing gear designs established are adequate to meet the loads expected. Ground clearance of the skids does not allow the full deflections required as indicated in the analysis. However, the skids incorporated in all of the configurations are designed to absorb the remaining energy in conjunction with the landing gears.

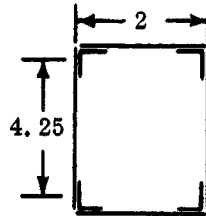
### Stress Analysis

Conventional methods of analysis have been employed to substantiate the structural integrity of these paraglider vehicles. Although a detailed preliminary analysis has been made, this report covers only bending and column analyses. Skin panel shear analyses have been omitted for brevity.

250 Lb. Payload Vehicle

Wing

Keel at Station .52L



$$\text{Total cap area} = (.75 - .75) \times .10 \times 2 = .300 \text{ in}^2$$

Mat'l: 2014-T6 Alclad  
 $F_{cy} = 55,000 \text{ psi}$

Max. Bending Moment = 16815 in-lb ultimate

$$\text{Cap Load} = \frac{16815}{4.25} = 3955 \text{ lbs.}$$

$$f_e = \frac{3955}{.30} = 13183 \text{ psi}$$

$$F_{cr} = F_{cy} = 55,000 \text{ psi} \quad \text{M. S.} = \frac{55,000}{13,183} - 1 = \text{HIGH}$$

Leading Edge at Sta. .42L

The leading edge is formed in the shape of a streamlined tube. For ease of analysis, an effective round tube is analyzed.

Diameter = 2.00 inches

$t = 0.035 \text{ inches}$

$Z = 0.1043 \text{ inches}^3$

$M_{\text{max}} = 9,255 \text{ in-lb net}$

Mat'l: steel H. T. = 125,000 psi

Let  $F_b = F_{tu}$

$$f_b = \frac{9255}{0.1043} = 88,700 \text{ psi}$$

$$\text{M. S.} = \frac{125,000}{88,700} - 1 = \underline{\underline{0.41}}$$

Spreader Bar

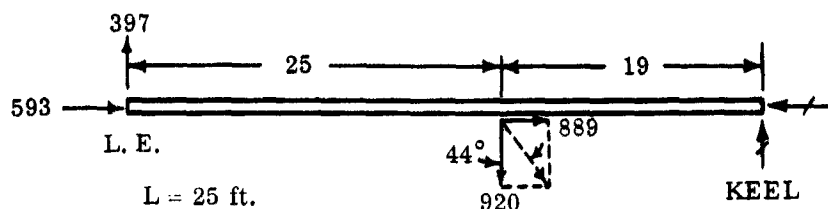
Material: Steel Tube 3.0 x .120 H. T. = 125,000 psi

$$A = 1.0857 \text{ in.}^2$$

$$Z = 0.7517 \text{ in.}^3$$

$$= 0.1043 \text{ in.}$$

$$F_{tu} = F_b$$



$L = 25 \text{ ft.}$

$L = 50 \text{ ft.}$

$$L/\lambda = \frac{50}{1.0191} = 49.1 \quad F_{cr} = 100,000 - 8.74 (49.1)^2 = 78,950 \text{ psi}$$

$$f_c = \frac{P_c}{A} = \frac{593 \times 1.5}{1,0857} = 820 \text{ psi}$$

$$\frac{f_c}{F_{cr}} = \frac{820}{78950} = 0.011 \quad 1 - \frac{f_c}{F_{cr}} = 0.989$$

$$f_b = \frac{M}{D \cdot 0.989} = \frac{593 \times 25 \times 1.5}{0.989} = 22,500 \text{ psi}$$

NOT CRITICAL

Membrane

Material: Dacron cloth, polyester coating

Maximum radius of curvature of membrane = .484L

$$R = .484(103) = 49.8 \text{ inches}$$

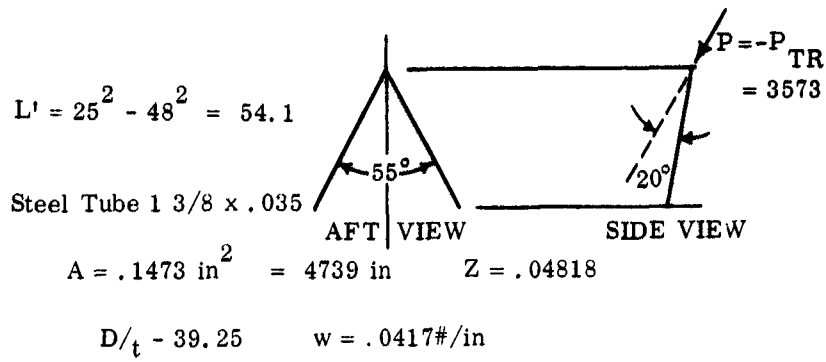
$$\text{Hoop Load} = P^R = \frac{6.73}{144} \times 49.8 = 2.33 \text{ lb/in}$$

NOT CRITICAL

Center Inerted "V" Struts

Load induced in struts

$$P_c = \frac{1.5 (3573)}{2 (\cos 20^\circ) \cos (55^\circ)} = \frac{5360}{2 (.940)(.887)} = 3214\# \text{ Ult.}$$



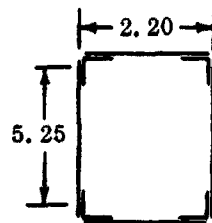
$$\frac{L'}{A} = \frac{54.1}{.4739} = 114.3 \quad F_c = 24.5$$

$$P_c = A F_c = .1473 (24.5) = 3.609^k \quad \text{M.S.} = \frac{3.609}{3.214} - 1 = \underline{-.12}$$

1,000 Lb. Payload Vehicle

Wing

Keel at Station 52.2



$$\text{Total cap area} = (675 - .75) \times .125 \times 2 = .375 \text{ in}^2$$

Material: 2014-T6 Alclad  
 $F_{cy} = 55,000 \text{ psi}$

Maximum Bending Moment - 84,800 psi Ult.

$$\text{Cap Load} = \frac{84800}{5.25} = 16170 \text{ lbs.}$$

$$f_c = \frac{16170}{.375} = 43120 \text{ psi} \quad \text{M.S.} = \frac{55,000}{43,120} - 1 = \underline{.27}$$

### Leading Edges

Material: Steel Streamline Tube H. T. = 125,000 psi

Equiv. Round Tube = 3" Dia.,  $t = 0.083$

$$z = .5599$$

$$F_b = 125,000 \text{ psi}$$

$$M_{\max} = 42.9 \times 1.5 = 64350 \text{ in-lb ult.}$$

$$f_b = \frac{64350}{.5599} = 114,931 \text{ psi}$$

$$M. S. = \frac{125,000}{114,931} - 1 = \underline{\underline{0.09}}$$

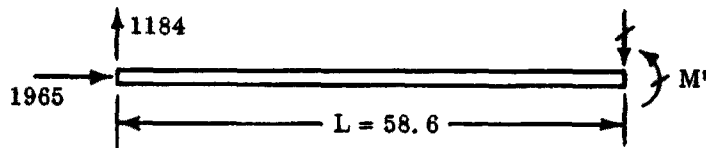
### Spreader Bar

Material: Steel Tube 3 1/2 x .120 -- 125,000 psi H. T.

$$A = 1.2742 \text{ in}^2, \quad e = 1.1958 \text{ in.}, \quad I = 1.822 \text{ in}^4$$

$$Z = 1.0411 \text{ in}^3, \quad D/t = 29.15$$

$$F_b = 125,000 \text{ psi}$$



$$L' = (2) (58.6) = 117.2''$$

$$\frac{L'}{e} = \frac{117.2}{1.1958} = 98 \quad F_{cr} = 29,500 \text{ psi}$$

$$f_c = \frac{P}{A} = \frac{1965 (1.5)}{1.2742} = 2313 \text{ psi}$$

$$1 - P/P_{cr} = 1 - \frac{2313}{29,500} = .9216$$

$$f_6 = \frac{1184 \times 1.5 \times 58.6}{.9216} = 113,000 \text{ psi}$$

$$\text{M. S.} = \frac{125}{113} - 1 = \underline{\underline{.10}}$$

### Membrane

Material: Dacron cloth, polyester coating

R = .484L (radius of curvature of membrane)

$$= .484 (207) = 100''$$

$$N = p \frac{R}{144} = \frac{6}{144} \times 100 = 4.17 \text{ lb/in}$$

NOT CRITICAL

### Center Inerted "V" Struts

Load induced in struts

$$P_c = \frac{1.5 (3573)}{2 (\cos 20^\circ) \cos (55^\circ)} = \frac{5360}{2 (.940) (.887)} = 3214 \# \text{ Ult.}$$

$$L' = 25^2 - 48^2 = 54.1$$

Steel Tube 1 3/8 x .035

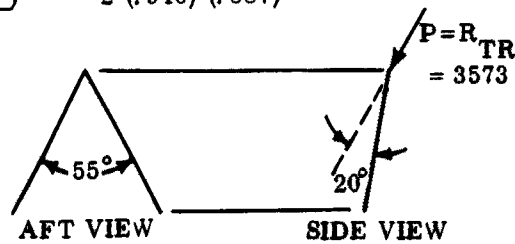
$$A = .1473 \text{ in}^2 = .4739 \text{ in.} \quad Z = .04818$$

$$D/t = 39.25 \quad w = .0417 \#/\text{in}$$

$$\frac{L'}{Z} = \frac{54.1}{.4739} = 114.3 \quad F_c = 24.5$$

$$P_c = A F_c = .1473 (24.5) = 3.609 \text{ k}$$

$$\text{M. S.} = \frac{3.609}{3,214} - 1 = \underline{\underline{.12}}$$



### 4,000 Lb. Payload Vehicle

Since this vehicle configuration is a scaled down version of the 8,000 lb. payload vehicle, no analysis is presented. Reference, however, should be made to the method of analysis of the 8,000 lb. vehicle, which is similar. The strength of this 4,000 lb. vehicle is also proportional to that of the 8,000 lb. vehicle.

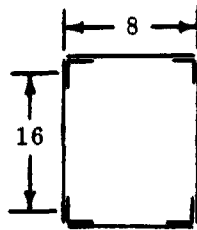
### 8,000 Lb. Payload Vehicle

#### Wing

#### Keel at Sta. 135

#### Vertical Bending

The basic keel section is shown in sketch below. The bending moment diagram for critical flight is given on page 157. The design of each cross section to resist bending and axial compression load will emphasize heavy upper cap members in order to balance extreme fiber stresses or minimize the neutral axis shift on the "effective bending section."



Mat'l: 7075-T6 ALCLAD

$$\begin{aligned} \text{Total Area} &= 2.716 \text{ in}^2 \\ I &= 135.4 \text{ in}^4 \end{aligned}$$

$$f_c = \frac{P}{A} + \frac{Mc}{I}$$

$$P_c = 23985 \text{ lbs. Ult.}$$

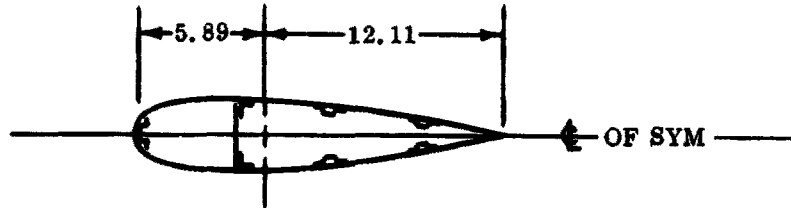
$$M = 1,130,000 \text{ in. lbs Ult.}$$

$$f_c = \frac{23985}{2.05} + \frac{1,130,000}{135.4} = 68320 \text{ psi}$$

$$F_{cc} = KF (t/b)^2 = 70,000 \text{ psi}$$

$$M. S. = \frac{70.00}{68.32} - 1 = \underline{\underline{0.02}}$$

#### Leading Edge at Sta. 232



$$I = 180.48 \text{ in}^4 \quad A = 5.06$$

$$P_t = 7330 \times 1.5 = 10990 \text{ Lbs. Ult. (spreader bar component)}$$

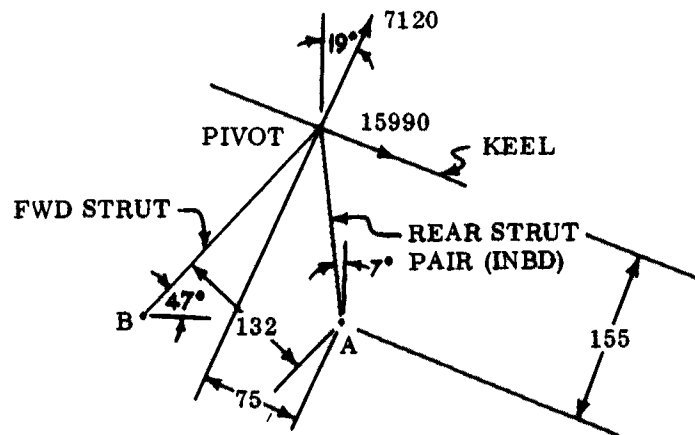
$$M = 507,700 \times 1.5 = 761,550 \text{ in-lb ult.}$$

$$f_b = \frac{761550 \times 5.89}{180.48} - \frac{10990}{5.06} = 22,680 \text{ psi C.}$$

$$F_{cc} = 23202 \text{ psi (considering flat and curve plate theory)}$$

$$M. S. = \frac{23202}{22680} - 1 = \underline{\underline{0.02}}$$

Supt. Structure Loads From Keel



Combined Supt. Struct. Loads Per Strut

$$B = B_T - B_C = 22800 - 14100 = \underline{\underline{8700}} \text{ lb (Limit-tension)}$$

$$A = A_c - A_c = 15300 - 6130 = \underline{\underline{21430}} \text{ lb (Limit-compression)}$$

Rear Strut

Assume the strut is of an effective 5" dia. round tubing.

$$D = 5.0'' \quad t = .120 \quad = 1.7259 \text{ in} \quad A = 1.8397 \text{ in}^2$$

$$L' = 180'' \quad \text{Mat'l: steel H. T.} = 125,000 \text{ psi}$$

$$\frac{L'}{e} = \frac{180}{1.7259} = 104 \quad F_{cc} = \frac{286,000,000}{104^2} = 26450 \text{ psi}$$

$$f_c = \frac{21430 \times 1.5}{1.8397} = 17500 \quad M. S. = \frac{26450}{17500} - 1 = \underline{\underline{0.51}}$$

Only this strut is analyzed as it is most critical by observation.

### CONCLUSIONS

Loads and stress analyses indicate the feasibility of the design concepts presented, and reveal no serious problems in design of the vehicles. Every effort was made to use structural design and analysis methods developed at Ryan for optimum lightweight structure.

## WEIGHTS AND BALANCE

As the payload capacity of Flexible Wing gliders increases, the trend in component groups of the glider is toward greater weight efficiency. This is shown in the following Figures 90 through 94 which are graphic summaries expressed as percent of gross weight.

The five configurations which comprise this study have two types of wing construction and two types of suspension system, as described in the following chart. (This identification is consistent in Figures 90 through 94.)

Figure Identification	Payload	Wing Construction	Suspension Type	Spreader
A	250	Tube (Constant Sect)	Rigid	Yes
B	1000	Tube (Constant Sect)	Rigid	Yes
C	1000	Tube (Constant Sect)	Cable	No
D	4000	Fabricated	Rigid	Yes
E	8000	Fabricated	Rigid	Yes

The slope of Line A-B (Fig. 90) shows that the tube wing-rigid suspension system rapidly approaches the limit of practicality as payload increases. However, the tube wing-cable suspension system, point C, with its multiple support points, allows the use of lighter tubular structure. This, with the absence of spreader bar, produces a lighter configuration which is practical and attractive beyond the one thousand pound payload class (difference in points B and C).

The fabricated wing-rigid suspension configurations, points D and E, show increased weight efficiency as payload becomes greater. This is shown by the negative slope of the curve D - E (Fig. 90).

Three types of body construction were studied for the five configurations.

Figure Identification	Payload	Construction
A	250	Drum
B	1000	Box, corrugated
C	1000	Box, corrugated
D	4000	Aircraft fuselage type
E	8000	Aircraft fuselage type

An examination of Figure 91 shows that the drum, point A, and box, points B and C, are very efficient. These simple body types, however, are structurally limited in maximum payload. This payload size restriction is not critical for aircraft type bodies, points D and E. Curve D - E (Fig. II) shows decided increase in efficiency (weightwise) with increasing payload size.

As seen in Figure 92, the alighting gear group becomes more weight efficient as the payload increases. Part of this increase in efficiency is due to better use of the potential load bearing capabilities of the wheels, tires, and tubes.

Again, weight efficiency of the controls group increases as the payload becomes greater. The slope of the curve is a reflection of areas of the electronics group which remain relatively constant in weight, regardless of vehicle gross weight. Examples of these items are receiver, decoder, and controller weights.

As seen in Figure 94, the summation of component groups, each of which shows a tendency to increase weight efficiency with increasing payload, yields a curve which also shows weight efficiency rising with increased payload. The difference in weight efficiency between the two 1000 lb. payload configurations, points B and C, is due to wing group weight, and has been described in Figure 90.

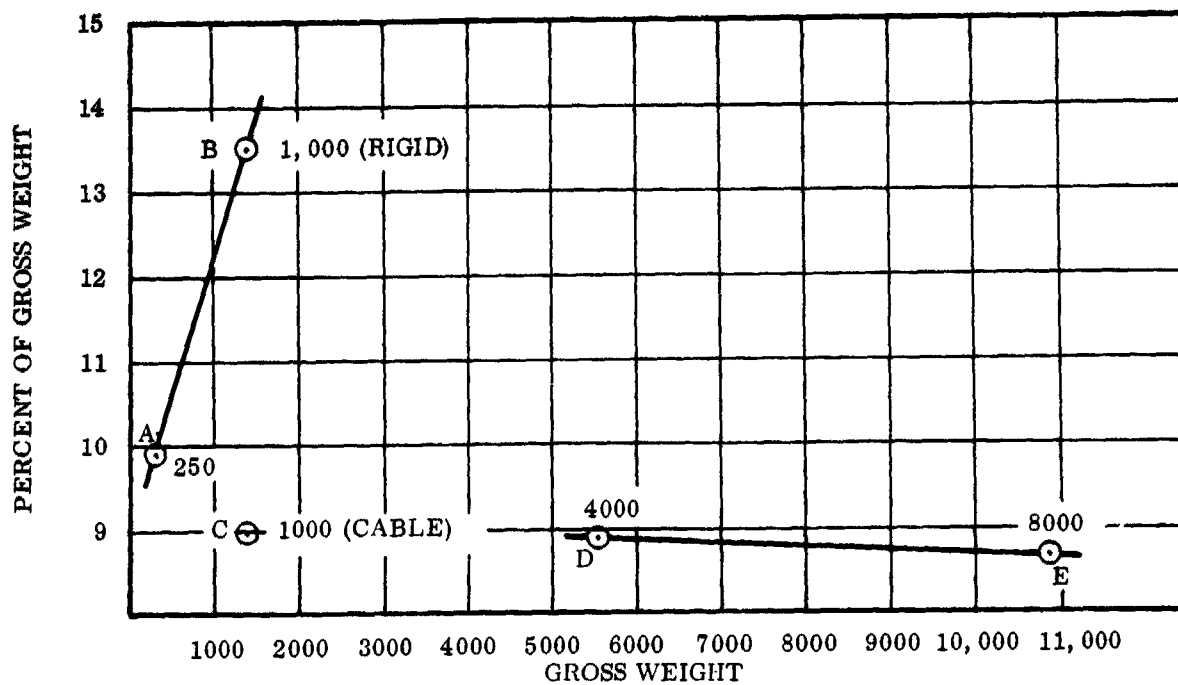


Figure 90 Body Group Expressed as Percent of Gross Weight for Five Glider Configurations

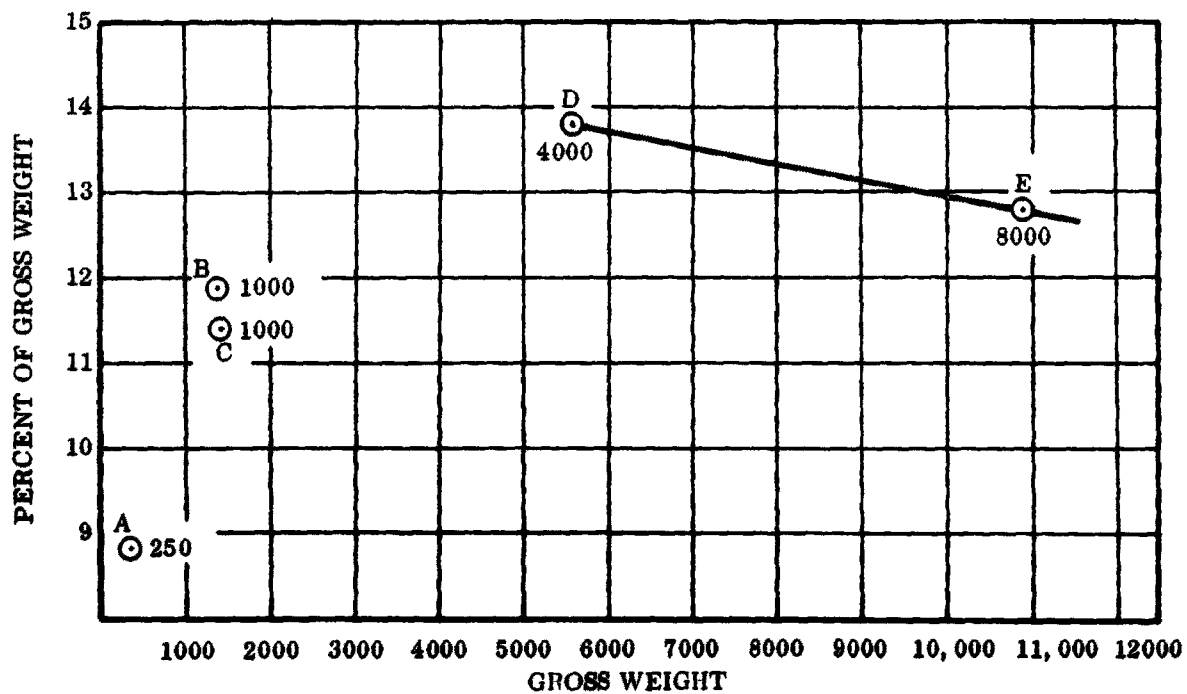


Figure 91 Body Group Expressed as Percent of Gross Weight for Five Glider Configurations

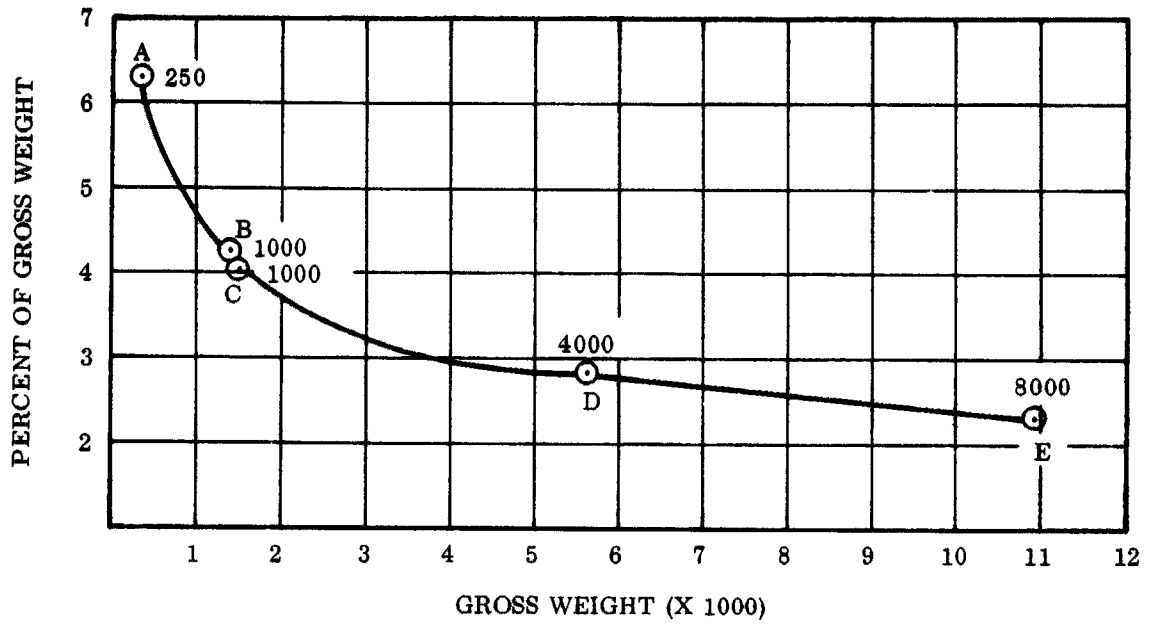


Figure 92 Alighting Gear Expressed as Percent of Gross Weight for Five Glider Configurations

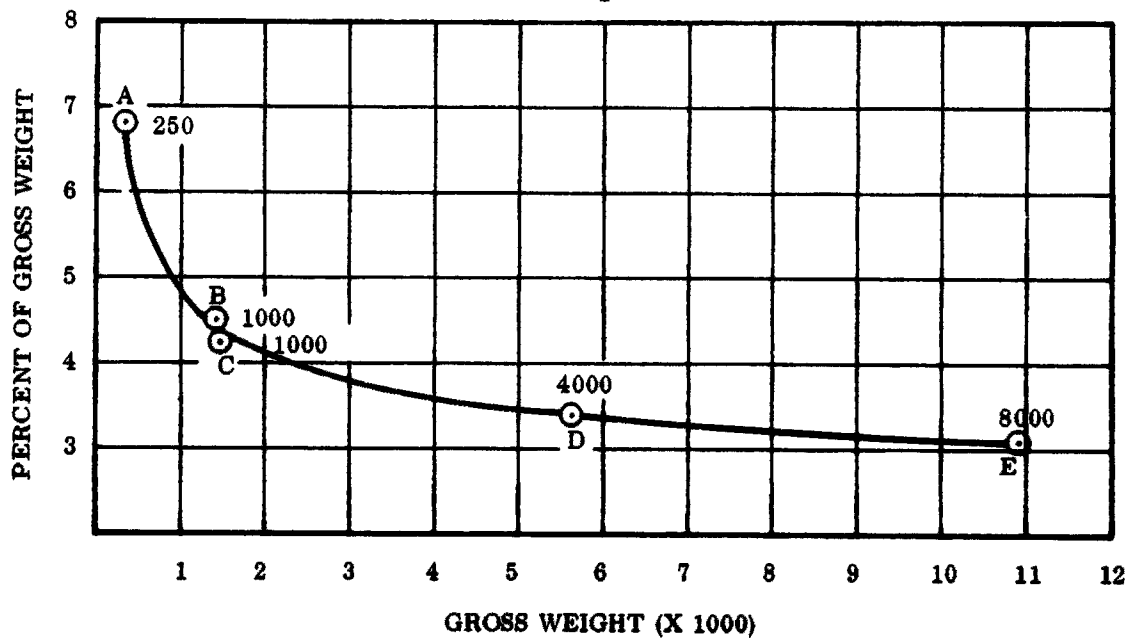


Figure 93 Controls Group Expressed as Percent of Gross Weight for Five Glider Configurations

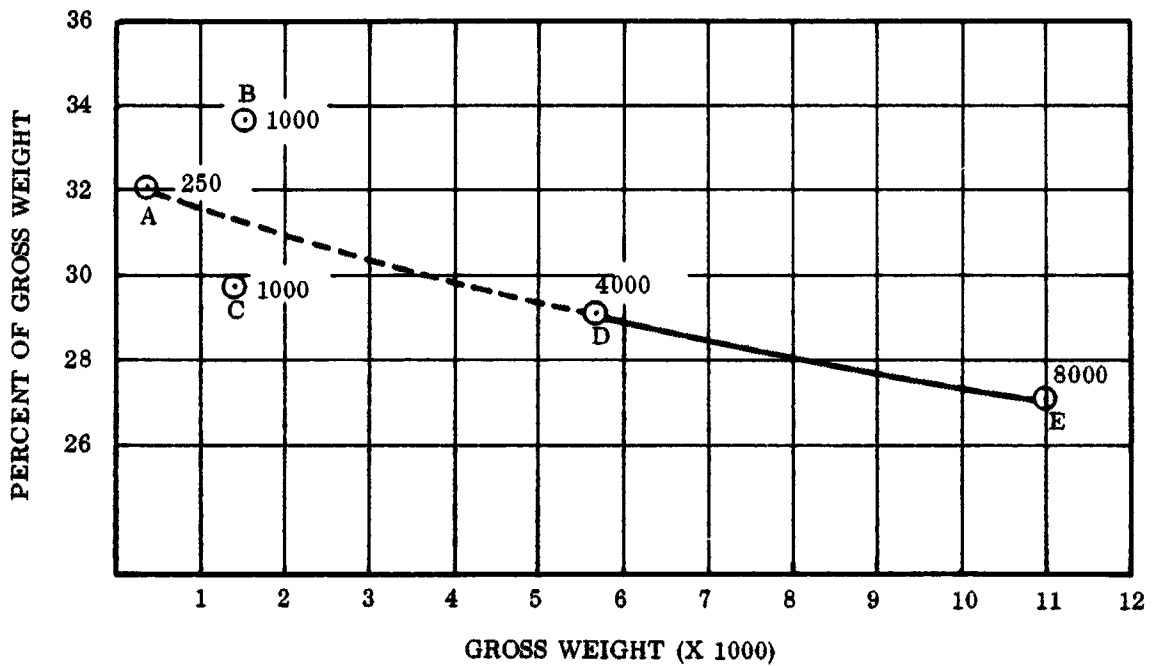


Figure 94 Weight Empty Expressed as Percent of Gross Weight for Five Glider Configurations

In the interest of increased accuracy, detail calculations, wherever possible, were made of weight, balance, and inertia. Calculations were facilitated because of extreme simplicity of the Flexible Wing configurations and ready availability of detailed drawings.

Data in this report were derived from detail weight calculations. Vendor quoted weights were used for stock procurable items. In the few instances where estimates were necessary, standard empirical equations were used.

Data are presented for each configuration as:

Group Weight Statement

Balance and Moment of Inertia Data

Aircraft weight estimate parameters normally used for preliminary weight estimation were not relevant for all areas of the Flexible Wing configuration. The parameters by Cranfield, however, in the 4,000 and 8,000 lb. configurations, were considered applicable by the Flight Controls Group. These parameters are:

Flight Controls:

Weight = 35 lb. + 0.8% gross weight

Hydraulics:

Weight = (3% ± 1%) gross weight

Wing membrane weight was calculated at either seven or eight ounces per yard.

Continued structural investigation with respect to optimum shapes and the use of magnesium, where permissible, may reduce weight in all areas.

Wheel weights for the landing gear were vendor quoted for wheel, tire, and tubes of the necessary diameter. The load bearing capabilities of these units far exceeded the anticipated load. If special wheel units were used, an estimated weight savings of the following amount could be realized:

250 payload	3.0 lb.
1000 payload	8.7 lb.
4000 payload	20.8 lb.
8000 payload	34.7 lb.

Weight estimates of the five configurations show that:

The Flexible Wing towed glider becomes more weight efficient as the configuration becomes larger.

A glider of this type has a payload weight in the range of 67% to 73% of gross weight.

GROUP WEIGHT STATEMENT  
 250 POUND TOWED LOGISTIC GLIDER  
 WEIGHT EMPTY

Wing Group		36.7
Center Section - Basic Structure	27.4	
Secondary Structure - Including Wingfold Mechanism	9.3	
Body Group		32.5
Fuselage or Hull - Basic Structure	17.1	
Secondary Structure - Fuselage or Hull	15.4	
Alighting Gear Group - Land-Type		23.4
Surface Controls Group		25.1
Automatic Pilot	16.0	
System Controls - Including Power and Feel Controls	9.1	
Total		117.7
Total Weight Empty		117.7
USEFUL LOAD AND GROSS WEIGHT		
Cargo		250.0
Gross Weights		367.7

MOMENT OF INERTIA DATA  
FOR THE  
250 POUND PAYLOAD TOWED GLIDER

WEIGHT EMPTY		LB.	117.7
PAYLOAD		LB.	250.0
GROSS WEIGHT		LB.	367.7
PITCH	$I_{y_0}$	SLUG - FT <sup>2</sup>	37.8
ROLL	$I_{x_0}$	SLUG - FT <sup>2</sup>	19.2
YAW	$I_{z_0}$	SLUG - FT <sup>2</sup>	23.5
PRODUCT	$I_{xz_0}$	SLUG - FT <sup>2</sup>	1.35
PRINCIPAL AXIS			+ 16° 5'
CENTER OF GRAVITY (% Keel Length At <u>19°</u> Incidence )			42.8%

GROUP WEIGHT STATEMENT  
 THE 1000 POUND PAYLOAD TOWED GLIDER  
 WEIGHT EMPTY

Wing Group		202.9
Center Section - Basic Structure	181.7	
Secondary Structure - Including Wingfold Mechanism	21.2	
Body Group		171.7
Fuselage or Hull - Basic Structure	108.6	
Secondary Structure - Fuselage or Hull	29.3	
- Doors, Panels and Miscellaneous	33.2	
Alighting Gear Group - Land-Type		60.7
Surface Controls Group		64.0
Automatic Pilot	33.3	
System Controls - Including Power and Feel Controls	30.7	
Total		498.7
Total Weight Empty		498.7
USEFUL LOAD AND GROSS WEIGHT		
Cargo		1000.0
Gross Weights		1498.7

MOMENT OF INERTIA DATA  
FOR THE  
1000 POUND PAYLOAD TOWED GLIDER

WEIGHT EMPTY		LB.	498.7
PAYLOAD		LB.	1000.0
GROSS WEIGHT		LB.	1498.7
PITCH	$I_{y_0}$	SLUG- FT <sup>2</sup>	477.9
ROLL	$I_{x_0}$	SLUG- FT <sup>2</sup>	357.0
YAW	$I_{z_0}$	SLUG-FT <sup>2</sup>	182.8
PRODUCT	$I_{xz_0}$	SLUG- FT <sup>2</sup>	9.36
PRINCIPAL AXIS			- 3° 4'
CENTER OF GRAVITY			43.0%
(% Keel Length At			
<u>19°</u> Incidence)			

**GROUP WEIGHT STATEMENT**  
**THE 1000 POUND PAYLOAD TOWED GLIDER**  
**(FLEXIBLE SUSPENSION)**

**WEIGHT EMPTY**

Wing Group		128.2
Center Section - Basic Structure	98.6	
Secondary Structure - Including Wingfold Mechanism	29.6	
Body Group		169.2
Fuselage or Hull - Basic Structure	108.6	
Secondary Structure - Fuselage or Hull	27.5	
- Doors, Panels and Miscellaneous	33.1	
Alighting Gear Group - Water		60.7
Surface Controls Group		64.0
Automatic Pilot	33.3	
System Controls - Including Power and Feel Controls	30.7	
Total		422.1
Total Weight Empty		422.1

**USEFUL LOAD AND GROSS WEIGHT**

Cargo		1000.0
Gross Weights		1422.1

MOMENT OF INERTIA DATA  
FOR THE  
CABLE SUSPENSION CONFIGURATION  
OF THE TOWED GLIDER

WEIGHT EMPTY		LB.	422.1
PAYLOAD		LB.	1000.0
GROSS WEIGHT		LB.	1422.1
PITCH	$I_{y_0}$	SLUG - FT <sup>2</sup>	950.0
ROLL	$I_{x_0}$	SLUG - FT <sup>2</sup>	744.0
YAW	$I_{z_0}$	SLUG - FT <sup>2</sup>	267.0
PRODUCT	$I_{xz_0}$	SLUG - FT <sup>2</sup>	182.0
PRINCIPAL AXIS			19°41'
CENTER OF GRAVITY (% Keel Length at <u>32°</u> Incidence )			28.9%

**GROUP WEIGHT STATEMENT**  
**4000 POUND PAYLOAD TOWED GLIDER**  
**WEIGHT EMPTY**

Wing Group		504.4
Center Section - Basic Structure	424.8	
Secondary Structure - Including Wingfold Mechanism	79.6	
Body Group		782.5
Fuselage or Hull - Basic Structure	521.6	
Secondary Structure - Fuselage or Hull	114.2	
- Doors, Panels and Miscellaneous	146.7	
Alighting Gear Group - Land-Type		162.3
Surface Controls Group		193.0
Automatic Pilot	61.0	
System Controls - Including Power and Feel Controls	132.0	
Total		1642.2
Total Weight Empty		1642.2
<b>USEFUL LOAD AND GROSS WEIGHT</b>		
Cargo		4000.0
Gross Weights		5642.2

MOMENT OF INERTIA DATA  
FOR THE  
4000 POUND PAYLOAD TOWED GLIDER

WEIGHT EMPTY		LB.	1642.2
PAYLOAD		LB.	4000.0
GROSS WEIGHT		LB.	5642.2
PITCH	$I_{y_0}$	SLUG - FT <sup>2</sup>	5989
ROLL	$I_{x_0}$	SLUG - FT <sup>2</sup>	4074
YAW	$I_{z_0}$	SLUG - FT <sup>2</sup>	2614
PRODUCT	$I_{xz_0}$	SLUG - FT <sup>2</sup>	215
PRINCIPAL AXIS			-8° 12'
CENTER OF GRAVITY			42.7%
(% Keel Length At			
<u>19°</u> Incidence )			

GROUP WEIGHT STATEMENT  
8000 POUND PAYLOAD TOWED GLIDER  
WEIGHT EMPTY

Wing Group		964.1
Center Section - Basic Structure	836.6	
Secondary Structure - Including Wingfold Mechanism	127.5	
Body Group		1,408.7
Fuselage or Hull - Basic Structure	1,017.9	
Secondary Structure - Fuselage or Hull	160.8	
- Doors, Panels and Miscellaneous	230.0	
Alighting Gear Group - Land-Type		257.5
Surface Controls Group		342.2
Automatic Pilot	97.0	
System Controls - Including Power and Feel Controls	245.2	
<b>Total</b>		<b>2,972.5</b>
<b>Total Weight Empty</b>		<b>2,972.5</b>

USEFUL LOAD AND GROSS WEIGHT

<b>Cargo</b>		<b>8,000.0</b>
<b>Gross Weights</b>		<b>10,972.5</b>

MOMENT OF INERTIA DATA  
FOR THE  
8000 POUND PAYLOAD TOWED GLIDER

WEIGHT EMPTY		LB.	2972.5
PAYLOAD		LB.	8000.0
GROSS WEIGHT		LB.	10972.0
PITCH	$I_{y_0}$	SLUG - FT <sup>2</sup>	20910
ROLL	$I_{x_0}$	SLUG - FT <sup>2</sup>	15356
YAW	$I_{z_0}$	SLUG - FT <sup>2</sup>	10457
PRODUCT	$I_{xz_0}$	SLUG - FT <sup>2</sup>	244
PRINCIPAL AXIS			-2° 51'
CENTER OF GRAVITY (% Keel Length At <u>19</u> ° Incidence)			43.5%

Weight and Balance Data for the 250 Pound Payload Configuration

The horizontal reference plane is 40.65 inches forward of the most forward point of the nose. The centerline reference is Buttock Line 100.0 inches. The vertical reference plane is 20.0 inches below the centerline of the body.

	<u>WEIGHT</u>	<u>X</u>	<u>Z</u>	<u>WX</u>	<u>WZ</u>
TOTAL GROSS	(367.7)	(93)	(24)	(34,124)	(8630)
TOTAL WEIGHT EMPTY	(117.7)	(92)	(35)	(10,774)	(4130)
TOTAL WING GROUP	(36.7)	(95)	(59)	(3,486)	(2161)
MEMBRANE	3.6	110	62	396	223
SPREADER	5.9	101	59	597	347
LEADING EDGE	10.3	88	64	905	659
KEEL	7.5	97	60	731	451
WING FOLD	3.7	93	61	343	226
CABANE	5.6	91	45	514	255
TOTAL BODY GROUP	(32.5)	(93)	(25)	(3029)	(804)
SADDLE ASSY	5.3	94	33	498	174
CARGO DRUM	11.8	93	20	1100	236
DRUM ATTACHMENT	2.8	92	27	257	76
TAIL CONE	4.0	128	20	510	81
NOSE CONE	4.0	59	20	236	81
EQUIPMENT FAIR.	4.6	93	34	428	156
TOTAL ALIGHTING GEAR	(23.4)	(88)	(13)	(2057)	(295)
WHEELS	10.0	89	5	888	54
SKIDS	1.6	93	8	149	12
FORK	2.0	67	9	133	18
TORQUE ARMS	8.8	90	21	794	181
FITTINGS	1.0	93	30	93	30
TOTAL SURFACE CONTROLS	(25.1)	(88)	(35)	(2202)	(870)
TOTAL PAYLOAD	(250.0)	(93)	(18)	(23350)	(4,500)

**Weight and Balance Data for the 1,000 Pound Payload Configuration**

The horizontal reference plane (Station 0.0) is 4.0 inches forward of the most forward point of the nose fairing. The centerline reference is Buttock Line 200.0 inches. The vertical reference plane (Waterline 0.0) is 50.0 inches below the horizontal centerline of the body.

	<u>WEIGHT</u>	<u>X</u>	<u>Z</u>	<u>WX</u>	<u>WZ</u>
TOTAL GROSS WEIGHT	(1498.7)	(78)	(44)	(117,317)	(87,931)
TOTAL WEIGHT EMPTY	( 498.7)	(82)	(84)	( 40,817)	(41,931)
TOTAL WING GROUP	( 202.9)	(86)	(130)	( 17,497)	(26,432)
MEMBRANE	10.2	117	134	1198	1372
SPREADER	60.3	100	123	6028	7416
LEADING EDGF	74.1	69	141	5113	10448
KEEL	37.1	92	133	3409	4928
WING FOLD	9.5	100	115	950	1089
CABANE	11.7	69	101	799	1179
TOTAL BODY GROUP	( 171.1)	(76)	(51)	( 13,020)	( 8,660)
BULGHEADS AND FRAMES	33.9	77	51	2602	1717
COVER	23.0	77	55	1757	1261
LONGERONS UPPER	10.0	77	69	763	693
LONGERONS LOWER	8.0	77	39	614	313
FLOORING	33.5	77	40	2562	1341
TAIL CONE	12.0	140	50	1680	600
NOSE CONE	9.2	16	50	142	460
FITTINGS	8.1	46	72	373	580
DOORS	33.4	77	65	2527	1695
TOTAL ALIGHTING GEAR	( 60.7)	(75)	(24)	(4539)	(1440)
WHEELS	26.0	77	20	2002	507
BRACES	6.0	120	20	720	117
SKIDS	7.5	56	34	568	256
TORQUE ARMS	7.8	77	28	597	218
YOKE	8.8	33	23	288	199
FITTINGS	4.6	81	31	364	143
TOTAL CONTROLS GROUP	( 64.0)	(90)	(84)	(5761)	(5399)
TOTAL PAYLOAD	(1000.0)	(77)	(46)	(76500)	(46000)

Weight and Balance Data for the 1,000 Cable Configuration

The horizontal reference plane (Station 0.0) is 4.0 inches forward of the most forward point of the nose fairing. The centerline is Buttock Line 200.0 inches. The vertical reference plane (Waterline 0.0) is 50.0 inches below the horizontal centerline of the body.

	<u>WEIGHT</u>	<u>X</u>	<u>Z</u>	<u>WX</u>	<u>WZ</u>
TOTAL GROSS WEIGHT	(1422.1)	(81)	(61)	(114,753)	(86,401)
TOTAL WEIGHT EMPTY	( 422.1)	(91)	(96)	( 38,253)	(40,403)
TOTAL WING GROUP	( 128.2)	(120)	(202)	( 15,348)	(25,851)
MEMBRANE	12.0	191	219	2292	2628
LEADING EDGE	56.1	120	232	6709	12978
KEFFL	30.5	116	227	3534	6914
TRIANGLE	29.6	95	112	2813	3331
TOTAL BODY GROUP	( 169.2)	(78)	(50)	( 13,152)	( 8,508)
BULKHEADS AND FRAMES	33.9	77	51	2602	1717
COVER	23.2	77	55	1763	1261
LONGERON UPPER	10.0	77	69	768	693
LONGERON LOWER	8.0	77	39	613	313
FLOORING	33.5	77	40	2564	1341
TAIL CONE	12.0	140	50	1680	600
NOSE CONE	9.2	160	50	147	460
FITTINGS	6.3	77.0	68	485	428
DOORS	33.1	77.0	65	2536	1695
TOTAL ALIGHTING GEAR	(60.7)	(75)	(24)	(4539)	(1440)
WHEELS	26.0	77	20	2002	507
BRAKES	6.0	120	20	720	117
SKIDS	7.5	56	34	568	256
TORQUE ARMS	7.8	77	28	597	218
YOKE	8.8	33	23	288	199
FITTINGS	4.6	81	31	364	143
TOTAL CONTROLS GROUP	(64.0)	(81)	(72)	(5208)	(4602)
TOTAL PAYLOAD	(1000.0)	(77)	(46)	(76500)	(46000)

**Weight and Balance Data for the 4,000 Pound Payload Configuration**

The horizontal reference plane (Station 0.0) is 135.0 inches forward of the most forward point of the nose fairing. The centerline is Buttock Line 300.0 inches. The vertical reference plane (Waterline 0.0) is 50.0 inches below the centerline of the body.

	<u>WEIGHT</u>	<u>X</u>	<u>Z</u>	<u>WX</u>	<u>WZ</u>
TOTAL GROSS WEIGHT	(5,642.2)	(248)	(61)	(1,400,488)	(341,769)
TOTAL WEIGHT EMPTY	(1,642.2)	(243)	(93)	(398,718)	(152,244)
TOTAL WING GROUP	(504.4)	(269)	(209)	(135,696)	(105,663)
MEMBRANE	71.8	313	217	22,473	15,581
SPREAD	71.7	305	211	21,870	15,149
LEADING EDGE	177.2	243	227	43,130	40,281
KEEL	104.1	284	215	29,514	22,335
WING FOLD	13.2	300	203	3,954	2,681
CABANE	66.4	222	145	14,755	9,636
TOTAL BODY GROUP	(782.5)	(245)	(43)	(191,651)	(33,292)
BULKHEADS & FRAMES	142.8	146	41	20,865	5,897
COVER	119.4	252	50	30,089	5,970
LONGERONS UPPER	65.2	252	50	16,430	3,260
LONGERON LOWER	43.0	252	50	10,836	2,150
FLOORING	151.2	252	19	38,102	2,933
TAILCONE	57.4	345	50	19,803	2,870
NOSE CONE	46.8	160	50	7,488	2,340
FITTINGS	10.0	279	70	2,789	698
DOORS & RAMPS	105.5	330	49	34,867	5,172
ACCESS	41.2	252	49	10,382	2,002
TOTAL ALIGHTING GEAR	(162.3)	(249)	(22)	(40,491)	(3,639)
WHEELS	62.4	252	21	15,756	1,310
SKIDS	45.3	252	16	11,416	725
FORK	12.6	177	32	2,230	403
TORQUE ARMS	33.6	250	31	8,384	1,025
BRAKES	8.4	322	21	2,705	176
TOTAL SURFACE CONTROLS	(193.0)	(160)	(50)	(30,880)	(9,650)
TOTAL PAYLOAD	(4000.0)	(250)	(47)	(1,001,770)	(189,525)

Weight and Balance Data for the 8,000 Pound Payload Configuration

The horizontal reference plane (Station 0.0) is 162.5 inches forward of the most forward point of the nose fairing. The centerline is Buttock Line 400.0 inches. The vertical reference plane (Waterline 0.0) is 100.0 inches below the centerline of the body.

	<u>WEIGHT</u>	<u>X</u>	<u>Z</u>	<u>WX</u>	<u>WZ</u>
TOTAL GROSS WEIGHT	(10,972.5)	(331)	(114)	(3,632,206)	(1,249,494)
TOTAL WEIGHT EMPTY	(2,972.5)	(330)	(169)	(981,725)	(501,082)
TOTAL WING GROUP	(964.1)	(356)	(339)	(343,239)	(326,930)
MEMBRANE	101.6	423	367	42,977	37,287
SPREADER	160.9	402	328	64,669	52,703
LEADING EDGE	386.8	306	367	118,540	142,048
KEEL	187.3	372	339	69,633	63,475
WING FOLD	17.2	358	336	6,158	5,786
CABANE	110.3	374	232	41,262	25,631
TOTAL BODY GROUP	(1403.7)	(347)	(91)	(488,276)	(127,572)
BUCKHEAD & FRAMES	263.2	334	91	87,909	23,940
COVER	236.0	334	100	78,824	23,600
LONGERONS	216.3	334	100	72,244	21,630
FLOORING	302.4	334	63	101,002	19,020
TAILCONE	82.0	478	100	39,196	8,200
NOSECONE	66.8	183	100	12,257	6,680
FITTINGS	12.0	380	126	4,556	1,515
DOORS	230.0	401	100	92,288	22,987
TOTAL ALIGHTING GEAR	(257.5)	(331)	(61)	(85,192)	(15,782)
TOTAL SURFACE CONTROLS	(342.2)	(190)	(90)	(65,018)	(30,798)
TOTAL PAYLOAD	(8000.0)	(331)	(94)	(2,650,481)	(748,412)

**Balance Data for the 250 Pound Payload Configuration**

The horizontal reference plane is 40.65 inches forward of the most forward point of the nose. The centerline reference is Buttock Line 100.0 inches. The vertical reference plane is 20.0 inches below the centerline of the body.

	<u>WEIGHT</u>	<u>X</u>	<u>Z</u>	<u>WX</u>	<u>WZ</u>
TOTAL GROSS	(367.7)	(93)	(24)	(34,124)	(8630)
TOTAL WEIGHT EMPTY	(117.7)	(92)	(35)	(10,774)	(4130)
TOTAL WING GROUP	(36.7)	(95)	(59)	(3,486)	(2161)
MEMBRANE	3.6	110	62	396	223
SPREADER	5.9	101	59	597	347
LEADING EDGE	10.3	88	64	905	659
KEEL	7.5	97	60	731	451
WING FOLD	3.7	93	61	343	226
CABANE	5.6	91	45	514	255
TOTAL BODY GROUP	(32.5)	(93)	(25)	(3029)	(804)
SADDLE ASSY	5.3	94	33	498	174
CARGO DRUM	11.8	93	20	1100	236
DRUM ATTACHMENT	2.8	92	27	257	76
TAIL CONE	4.0	128	20	510	81
NOSE CONE	4.0	59	20	236	81
EQUIPMENT FAIR.	4.6	93	34	428	156
TOTAL ALIGHTING GEAR	(23.4)	(88)	(13)	(2057)	(295)
WHEELS	10.0	89	5	888	54
SKIIS	1.6	93	8	149	12
FORK	2.0	67	9	133	18
TORQUE ARMS	8.8	90	21	794	181
FITTINGS	1.0	93	30	93	30
TOTAL SURFACE CONTROLS	(25.1)	(88)	(35)	(2202)	(870)
TOTAL PAYLOAD	(250.0)	(93)	(18)	(23350)	(4,500)

Balance Data for the 1000 Pound Payload Configuration

The horizontal reference plane (Station 0.0) is 4.0 inches forward of the most forward point of the nose fairing. The centerline reference is Buttock Line 200.0 inches. The vertical reference plane (Waterline 0.0) is 50.0 inches below the horizontal centerline of the body.

	<u>WEIGHT</u>	<u>X</u>	<u>Z</u>	<u>WX</u>	<u>WZ</u>
TOTAL GROSS WEIGHT	(1498.7)	(78)	(44)	(117,317)	(87,931)
TOTAL WEIGHT EMPTY	( 498.7)	(82)	(84)	( 40,817)	(41,931)
TOTAL WING GROUP	( 202.9)	(86)	(130)	( 17,497)	(26,432)
MEMBRANE	10.2	117	134	1198	1372
SPREADER	60.3	100	123	6028	7416
LEADING EDGE	74.1	69	141	5113	10448
KEEL	37.1	92	133	3409	4928
WING FOLD	9.5	100	115	950	1089
CABANE	11.7	69	101	799	1179
TOTAL BODY GROUP	( 171.1)	(76)	(51)	( 13,020)	( 8,660)
BULGHEADS AND FRAMES	33.9	77	51	2602	1717
COVER	23.0	77	55	1757	1261
LONGERONS UPPER	10.0	77	69	763	693
LONGERONS LOWER	8.0	77	39	614	313
FLOORING	33.5	77	40	2562	1341
TAIL CONE	12.0	140	50	1680	600
NOSE COWE	9.2	16	50	142	460
FITTINGS	8.1	46	72	373	580
DOORS	33.4	77	65	2527	1695
TOTAL ALIGHTING GEAR	( 60.7)	(75)	(24)	(4539)	(1440)
WHEELS	26.0	77	20	2002	507
BRAKES	6.0	120	20	720	117
SKIDS	7.5	56	34	568	256
TORQUE ARMS	7.8	77	28	597	218
YOKE	8.8	33	23	288	199
FITTINGS	4.6	81	31	364	143
TOTAL CONTROLS GROUP	( 64.0)	(90)	(84)	(5761)	(5399)
TOTAL PAYLOAD	(1000.0)	(77)	(46)	(76500)	(46000)

**Balance Data for the 250 Pound Payload Configuration**

The horizontal reference plane is 40.65 inches forward of the most forward point of the nose. The centerline reference is Buttock Line 100.0 inches. The vertical reference plane is 20.0 inches below the centerline of the body.

	<u>WEIGHT</u>	<u>X</u>	<u>Z</u>	<u>WX</u>	<u>WZ</u>
TOTAL GROSS	(367.7)	(93)	(24)	(34,124)	(8630)
TOTAL WEIGHT EMPTY	(117.7)	(92)	(35)	(10,774)	(4130)
TOTAL WING GROUP	(36.7)	(95)	(59)	(3,486)	(2161)
MEMBRANE	3.6	110	62	396	223
SPREADER	5.9	101	59	597	347
LEADING EDGE	10.3	88	64	905	659
KEEL	7.5	97	60	731	451
WING FOLD	3.7	93	61	343	226
CABANE	5.6	91	45	514	255
TOTAL BODY GROUP	(32.5)	(93)	(25)	(3029)	(804)
SADDLE ASSY	5.3	94	33	498	174
CARGO DRUM	11.8	93	20	1100	236
DRUM ATTACHMENT	2.8	92	27	257	76
TAIL CONE	4.0	128	20	510	81
NOSE CONE	4.0	59	20	236	81
EQUIPMENT FAIR.	4.6	93	34	428	156
TOTAL ALIGHTING GEAR	(23.4)	(88)	(13)	(2057)	(295)
WHEELS	10.0	89	5	888	54
SKIDS	1.6	93	8	149	12
FORK	2.0	67	9	133	18
TORQUE ARMS	8.8	90	21	794	181
FITTINGS	1.0	93	30	93	30
TOTAL SURFACE CONTROLS	(25.1)	(88)	(35)	(2202)	(870)
TOTAL PAYLOAD	(250.0)	(93)	(18)	(23350)	(4,500)

**Balance Data for the 1000 Cable Configuration**

The horizontal reference plane (Station 0.0) is 4.0 inches forward of the most forward point of the nose fairing. The centerline is Buttock Line 200.0 inches. The vertical reference plane (Waterline 0.0) is 50.0 inches below the horizontal centerline of the body.

	<u>WEIGHT</u>	<u>X</u>	<u>Z</u>	<u>WX</u>	<u>WZ</u>
TOTAL GROSS WEIGHT	(1422.1)	(81)	(61)	(114,753)	(86,401)
TOTAL WEIGHT EMPTY	( 422.1)	(91)	(96)	( 38,253)	(40,403)
TOTAL WING GROUP	( 128.2)	(120)	(202)	( 15,348)	(25,851)
MEMBRANE	12.0	191	219	2292	2628
LEADING EDGE	56.1	120	232	6709	12978
KEEL	30.5	116	227	3534	6914
TRIANGLE	29.6	95	112	2813	3331
TOTAL BODY GROUP	( 169.2)	(78)	(50)	( 13,158)	( 8,508)
BULKHEADS AND FRAMES	33.9	77	51	2602	1717
COVER	23.2	77	55	1763	1261
LONGERON UPPER	10.0	77	69	768	693
LONGERON LOWER	8.0	77	39	613	313
FLOORING	33.5	77	40	2564	1341
TAIL CONE	12.0	140	50	1680	600
NOSE CONE	9.2	160	50	147	460
FITTINGS	6.3	77.0	68	485	428
DOORS	33.1	77.0	65	2536	1695
TOTAL ALIGHTING GEAR	(60.7)	(75)	(24)	(4539)	(1440)
WHEELS	26.0	77	20	2002	507
BRAKES	6.0	120	20	720	117
SKIDS	7.5	56	34	568	256
TORQUE ARMS	7.8	77	28	597	218
YOKE	8.8	33	23	288	199
FITTINGS	4.6	81	31	364	143
TOTAL CONTROLS GROUP	(64.0)	(81)	(72)	(5208)	(4602)
TOTAL PAYLOAD	(1000.0)	(77)	(46)	(76500)	(46000)

Balance Data for the 4000 Pound Payload Configuration

The horizontal reference plane (Station 0.0) is 135.0 inches forward of the most forward point of the nose fairing. The centerline is Buttock Line 300.0 inches. The vertical reference plane (Waterline 0.0) is 50.0 inches below the centerline of the body.

	<u>WEIGHT</u>	<u>X</u>	<u>Z</u>	<u>WX</u>	<u>WZ</u>
TOTAL GROSS WEIGHT	(5,642.2)	(248)	(61)	(1,400,488)	(341,769)
TOTAL WEIGHT EMPTY	(1,642.2)	(243)	(93)	(398,718)	(152,244)
TOTAL WING GROUP	(504.4)	(269)	(209)	(135,696)	(105,663)
MEMBRANE	71.8	313	217	22,473	15,581
SPREAD	71.7	305	211	21,870	15,149
LEADING EDGE	177.2	243	227	43,130	40,281
KEEL	104.1	284	215	29,514	22,335
WING FOLD	13.2	300	203	3,954	2,681
CABANE	66.4	222	145	14,755	9,636
TOTAL BODY GROUP	(782.5)	(245)	(43)	(191,651)	(33,292)
BULKHEADS & FRAMES	142.8	146	41	20,865	5,897
COVER	119.4	252	50	30,089	5,970
LONGERONS UPPER	65.2	252	50	16,430	3,260
LONGERON LOWER	43.0	252	50	10,836	2,150
FLOORING	151.2	252	19	38,102	2,933
TAILCONE	57.4	345	50	19,803	2,870
NOSE CONE	46.8	160	50	7,488	2,340
FITTINGS	10.0	279	70	2,789	698
DOORS & RAMPS	105.5	330	49	34,867	5,172
ACCESS	41.2	252	49	10,382	2,002
TOTAL ALIGHTING GEAR	(162.3)	(249)	(22)	(40,491)	(3,639)
WHEELS	62.4	252	21	15,756	1,310
SKIDS	45.3	252	16	11,416	725
FORK	12.6	177	32	2,230	403
TORQUE ARMS	33.6	250	31	8,384	1,025
BRACES	8.4	322	21	2,705	176
TOTAL SURFACE CONTROLS	(193.0)	(160)	(50)	(30,880)	(9,650)
TOTAL PAYLOAD	(4000.0)	(250)	(47)	(1,001,770)	(189,525)

Balance Data for the 8000 Pound Payload Configuration

The horizontal reference plane (Station 0.0) is 162.5 inches forward of the most forward point of the nose fairing. The centerline is Buttock Line 400.0 inches. The vertical reference plane (Waterline 0.0) is 100.0 inches below the centerline of the body.

	<u>WEIGHT</u>	<u>X</u>	<u>Z</u>	<u>WX</u>	<u>WZ</u>
TOTAL GROSS WEIGHT	(10,972.5)	(331)	(114)	(3,632,206)	(1,249,494)
TOTAL WEIGHT EMPTY	(2,972.5)	(330)	(169)	(981,725)	(501,082)
TOTAL WING GROUP	(964.1)	(356)	(339)	(343,239)	(326,930)
MEMBRANE	101.6	423	367	42,977	37,287
SPREADER	160.9	402	328	64,669	52,703
LEADING EDGE	386.8	306	367	118,540	142,048
KEEL	187.3	372	339	69,633	63,475
WING FOLD	17.2	358	336	6,158	5,786
CABANE	110.3	374	232	41,262	25,631
TOTAL BODY GROUP	(1408.7)	(347)	(91)	(488,276)	(127,572)
BUCKHEAD & FRAMES	263.2	334	91	87,909	23,940
COVER	236.0	334	100	78,824	23,600
LONGERONS	216.3	334	100	72,244	21,630
FLOORING	302.4	334	63	101,002	19,020
TAILCONE	82.0	478	100	39,196	8,200
NOSECONE	66.8	183	100	12,257	6,680
FITTINGS	12.0	380	126	4,556	1,515
DOORS	230.0	401	100	92,288	22,987
TOTAL ALIGHTING GEAR	(257.5)	(331)	(61)	(85,192)	(15,782)
TOTAL SURFACE CONTROLS	(342.2)	(190)	(90)	(65,018)	(30,798)
TOTAL PAYLOAD	(8000.0)	(331)	(94)	(2,650,481)	(748,412)

#### IV. CONTROL AND TOWING SYSTEM DATA

##### SUMMARY

Control and guidance of the Flexible Wing Cargo Gliders are achieved through three basic means. (1) While under tow, the towed vehicle receives proportional control inputs directly from the towing vehicle by vector forces of the towing bridle. (2) During free flight, due to the inherent stability of the vehicle the prescribed glide path is achieved through predetermined and preselected longitudinal trim settings. No directional control is maintained for free flight. A trailing pendant type switch contacting the ground signals the control system which changes the incidence of the wing from an angle of  $19^\circ$  to  $34^\circ$ , and thereby executes the landing flare. (3) The third system accomplishes one or two axis control of the glider in free flight by remote radio command guidance. The system employs an ARW-55 transmitter and KY-51 coder that may be located in the towing vehicle or at a ground station. The transmitter operates in the standard military radio control band of 406 to 420 mc and has a normal output of 35 watts providing a line-of-sight control over a distance in excess of ten miles. The transmitter, a conventional frequency modulated type, in conjunction with the coder provides for the transmission of twenty channels of On-Off commands. For the 250 lb. glider and the L-20 or H-23 combinations, the transmitter would be a transistorized type of similar function but with a power output limited to 5 watts. The airborne receiver/decoder on the towed glider is a transistorized UHF FM Model 2621/1805 developed by RS Electronics Corporation of Palo Alto, California. Detail specifications are shown in Figure 95 following.

The power requirements for roll control of the 250 and 1,000 lb. towed gliders are compatible with electric actuators. Requirements of the 4,000 and 8,000 lb. versions are compatible with hydraulic system capabilities.

Change of pitch wing incidence in flight is not required in any of the four vehicles (other than is provided by the tow bridle geometry) and a step function change of pitch wing incidence at the proper height provides a satisfactory flare with acceptable vertical and horizontal velocity at touchdown. A trailing wire with ground contact switch is released from the fuselage when the glider is released from the towing vehicle. When the switch contacts the ground, the wing automatically pitches up in approximately .2 sec. The two larger vehicles employ a hydraulic cylinder-piston and solenoid-operated valve assembly to limit the terminal velocity of the wing in pitch. The 1,000 lb. glider contains a solenoid operated, speed governed clutch-brake assembly, which releases the wing and limits the wing angular velocity. The 250 lb. glider contains an electric motor actuator for trim changes in flight to provide a manned capability in this vehicle. Since the trim velocities are so much lower than the flare velocities, a solenoid operated clutched gear changer should be incorporated to use the same actuator for flare as for trimming. This will limit the wing terminal angular velocity during flare to an acceptable level.

Batteries provide power for the 250 and 1,000 lb. payload vehicles, and no in-flight recharging is provided. A ram air driven turbine provides in-flight recharging for the batteries and accumulators of the 4,000 and 8,000 lb. payload vehicles.

Analysis shows that all configurations of the Towed Air Logistics gliders can be towed satisfactorily. The following aircraft may be assigned as the towing vehicle for the towed glider as follows:

Towing Aircraft	Glider Configuration by Payload Size
L-20A	250 lbs.
H-23D	250 and 1,000 lbs.
HU-1A	1,000 and 4,000 lbs.
H-34	1,000, 4,000 and 8,000 lbs.

The towing line for helicopter tow is a bridle attached to each side of the fuselage of the helicopter. This directs the towing loads through the c. g. The bridle continues as a two-line member to a point aft of the

tail rotor, and converges to a single point for the tow-line attachment. The tow-line is Nylon cable and encases the wiring of the electrical circuitry for the release mechanisms. The minimum length of all tow-lines is 4.7 times the keel length of the towed vehicle. The tow-line extends to the bridle of the towed vehicle and is connected by a remotely controlled, electrically actuated attaching hook of standard design. The bridle of the towed vehicle is attached to the proper point on the wing keel and on the body of the vehicle. The lengths of the segments and the confluence points of the bridle of the towed vehicle are critical and will be in accordance with specified towing regimes. The geometry of the towing bridle for the 8,000 lb. glider has been established for the H-34 helicopter and is presented herein.

## METHOD OF APPROACH

The control and towing systems were developed through analytical design after investigation of the loads and control forces, based on requirements established from the performance and stability analysis.

Standard methods and equations determined the power requirements and size for the components of the control systems. The power sources were selected for each of the vehicle configurations considering operational compatibility and cost. Selection of components, where possible, was based on their availability in order to limit costs for future applications.

The towing mechanisms were designed to achieve the following objectives:

Safety in flight for the towing and towed vehicles.

Minimum modification to the towing vehicle.

Compatibility of function and strength for all towed configurations assigned to the specified towing vehicle.

## TECHNICAL DISCUSSION

### Direct Control

Release is accomplished by direct command from the remote controller on the tow vehicle. Emergency release is provided for the pilot of the towing vehicle. Both these functions are accomplished by means of separate electrical wires integrated into the tow cable. The release function releases the tow hook at the bridle of the glider and ejects the trailing pendant switch from the towed vehicle.

Direct control during free flight, by means of electrical signals to the actuators, trims roll and pitch in the 250 lb. glider. This permits a manned capability in this vehicle.

### Remote Control

The vehicles may be remotely controlled by radio command guidance operating in the standard 406 to 420 band. Roll trim only, with straight and level centering on command, is provided in all four vehicles. Pitch trim can be provided in the 250 lb. payload version by the use of two additional command channels. The transmitter is a conventional frequency modulated transmitter having a capability of transmitting 20 channels of On-Off information. Only four channels will be used for control functions. These functions are: (1) release, (both cable hook and ground contact trailing wire switch are released simultaneously), (2) right and (3) left roll and (4) straight and level or neutral roll. Remote release is provided for the drop point ground based remote controller, since the controller is better able to judge the proper release point.

The transmitter is a standard ARW-55/KY-51 transmitter/coder, except in the H-23D helicopter where the transmitter and coder will be a specially designed lightweight unit. The power output of the QRW 55 is normally 35 watts, which is more than adequate for a 10 mile line of sight range. It is expected that the lightweight unit will have a maximum power output of 5 watts.

The receiver-decoder on all vehicles is a special receiver proposed by R-S Electronics. Specifications are shown in Figure 95. This receiver is completely transistorized and will function identically to the larger, more conventional vacuum tube units weighing up to 10 or 12 lbs., except that only four channels will be provided instead of ten.

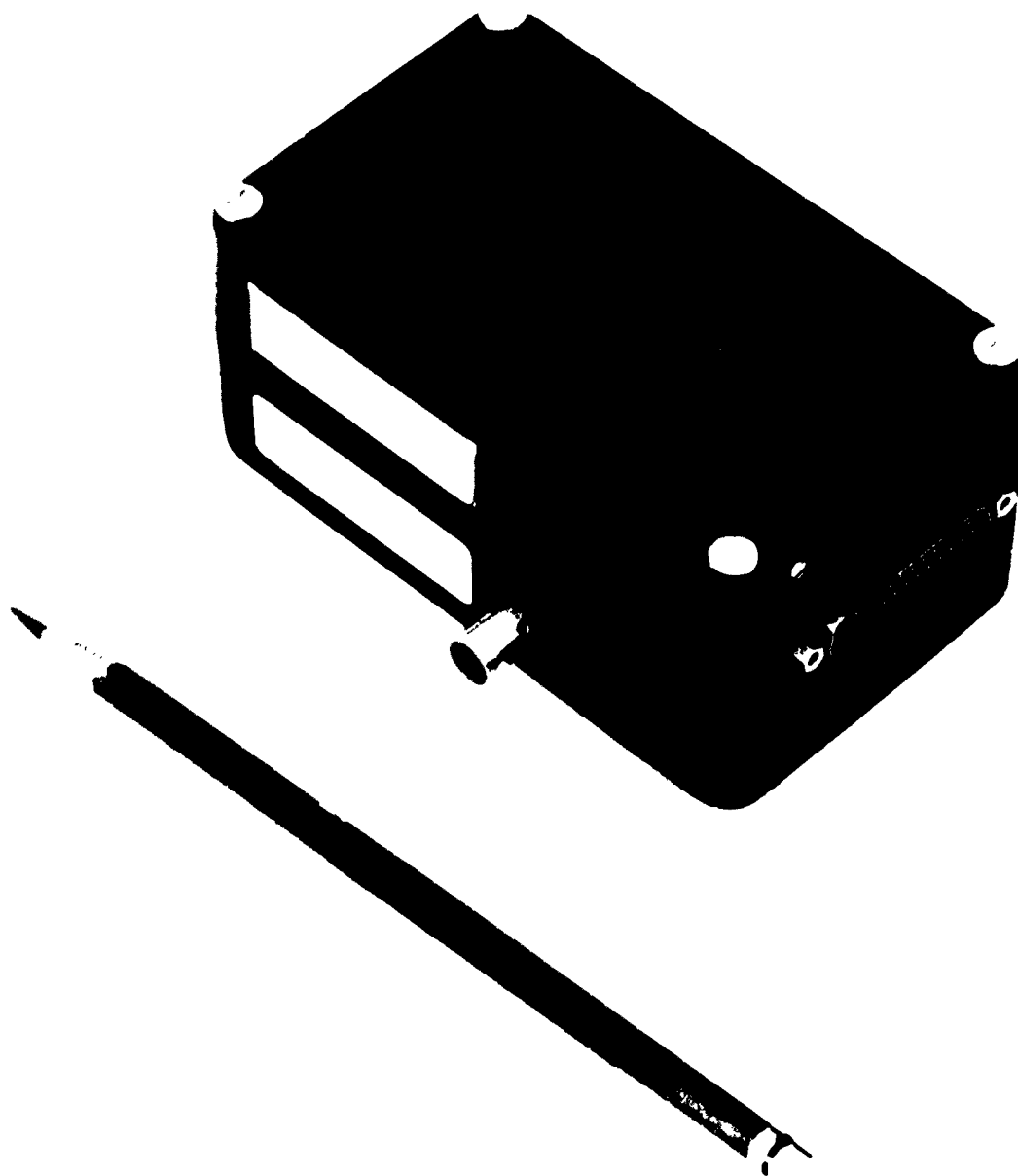
#### Electrical System

The actuators are electric in the two smaller vehicles. The electrical system for the small vehicles are powered by a 28 V storage battery with no in-flight recharging capability. These vehicles often will be expendable and the additional weight for in-flight recharging is unwarranted. The 4,000 and 8,000 lb. payload units have a ram air-driven turbine generator for battery recharging a portion of the flight. The battery sizing provides essentially all the power necessary during the 10 minute free flight portion. A small amount of power may be available from the RAT driven generator during the free flight portion of the flight. DC motor trim actuators will be used for roll trim on both of the smaller vehicles. The gear trains are designed for the required torque and speed of actuation. The motors are sized to provide the necessary power. Integral limit switches are incorporated in the actuators. A centering switch for rapid and accurate command return-to-center are provided. An integral brake holds the position achieved at the time power is removed. An electric motor actuator, similar to the roll trim actuator, is used for pitch control and flare on the 250 lb. payload unit. Flare on the 1,000 lb. payload is by a solenoid operated clutch, providing a controlled rate of change of incidence.

#### Hydraulic System

Hydraulic controls are provided in the 4,000 and 8,000 lb. payload vehicles since the power requirements dictate excessively large electrical actuators and batteries.

The hydraulic system consists of a ram air-driven turbine operating a constant displacement hydraulic pump which charges a hydraulic accumulator to 3,000 psi during the towed portion of the flight. Provisions are incorporated for unloading the pump while the turbine is coming up to speed. At this time the turbine blades are aerodynamically stalled and the torque capability is limited. The system uses a combination check valve and unloading valve to allow the speed of the RAT to build up before full pump load is applied. This prevents stalling of the fan. Power for directional control by means of roll trim is obtained from the hydraulic

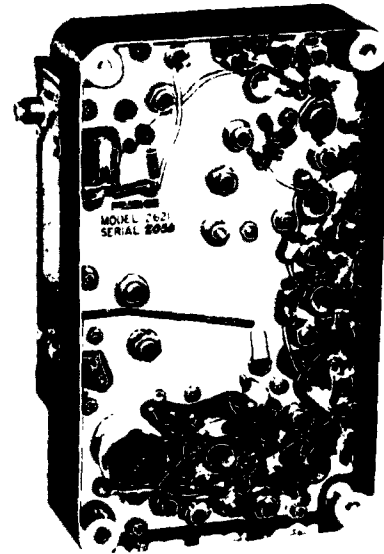


**RSE Model 2621/1805 Receiver/Decoder Combination**

## Transistorized UHF FM Receiver Model 2621

### DESCRIPTION

The RSE Model 2621 UHF Receiver is a transistorized sub-miniature fixed frequency FM receiver for missile flight guidance and safety operations. A cast aluminum case is used to provide a rigid support for an etched circuit board upon which all components are mounted. This receiver complies with the military requirements on radio interference. Complementary RSE decoders for use with this receiver include a three channel model (RSE 1803), a five channel model (RSE 1802), and a 10 channel model (RSE 1801), each of which can be mated with the receiver to form a watertight package.



### SPECIFICATIONS

Frequency	Tunable to any frequency between 406 and 549 megacycles
Frequency modulation	$\pm 150$ kc deviation; can also be supplied for $\pm 350$ kc deviation
Sensitivity	Five microvolts maximum for 6 db $\frac{S+N}{N}$ ratio with 50 kc audio bandwidth
Radio interference	Conforms to Specification MIL-I-26600 (Class I)
Limiting level	90% of maximum output at input levels of 14 microvolts or less
Selectivity	More than 60 db down at $\pm 2$ mc from carrier frequency
Image rejection	60 db
Discriminator p-p separation	400 kc minimum
I-F bandwidth (3 db points)	400 kc minimum
Power input	1.2 watts (40 milliamperes at $29 \pm 2$ volts d-c)
Operating temperature range	$-55^{\circ}$ C to $+72^{\circ}$ C
Vibration	20G from 5 to 2000 cps
Shock	100G for 11 milliseconds
Acceleration	100G
Connectors	1—Winchester Type M4P-LRN (Power and audio output) 1—Microdot Type 31-59 (RF input)
Size (excluding connectors)	$3\text{-}5/32'' \times 5'' \times 1\text{-}1/4''$ , receiver only $3\text{-}5/32'' \times 5'' \times 2\text{-}7/16''$ , with three and five channel decoders* $3\text{-}5/32'' \times 5'' \times 3\text{-}1/8''$ , with ten channel decoder*
Weight	16 ounces

Figure 95 Specifications of Transistorized UHF FM Receiver

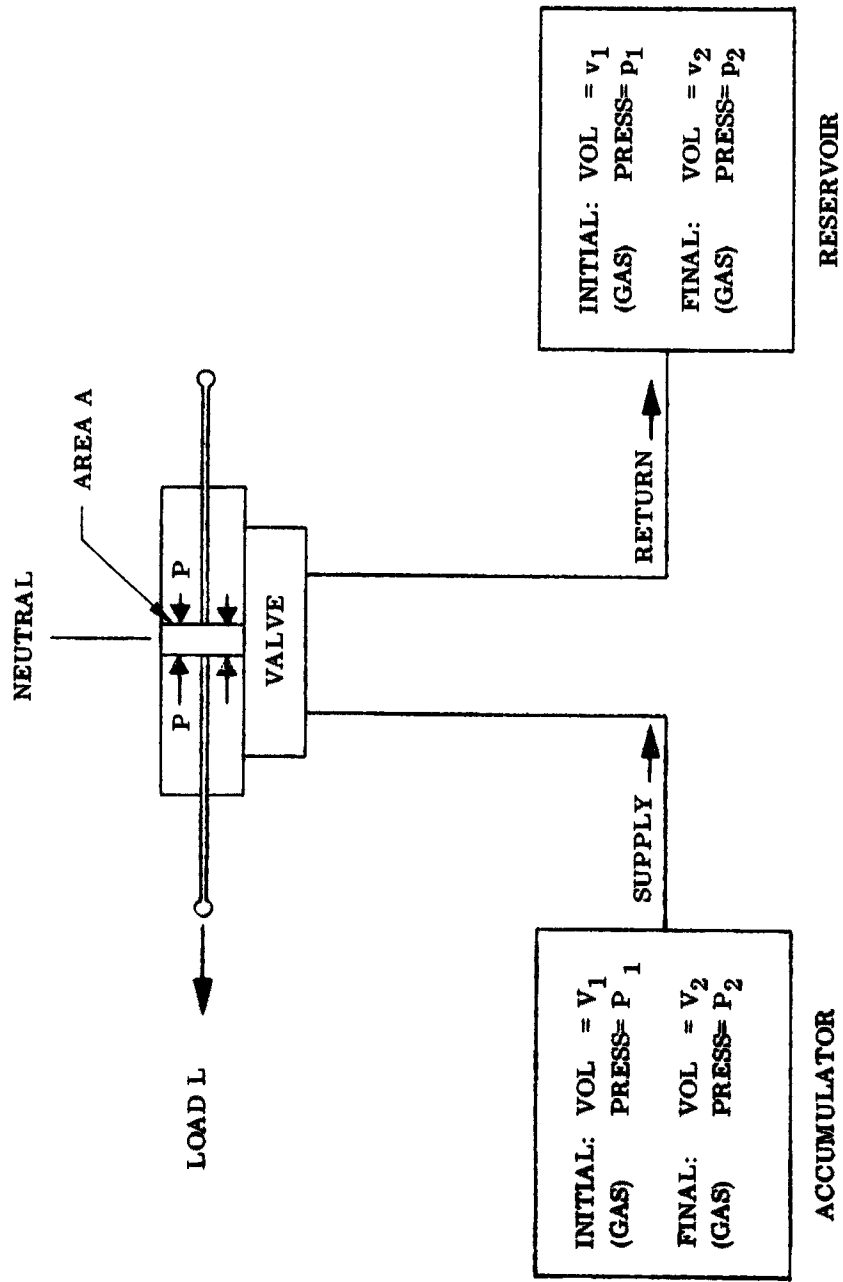


Figure 96 Roll Control Power System

accumulator during the free flight regimes. The RAT driven pump may provide a small amount of the power needed during the free flight mode. Due to the lower speed during glide, the power capability of the turbine will be somewhat limited. An advantage to the flow control unloading valve for this application (in contrast to a simple relief valve regulated, constant displacement pump or even a variable displacement pump), is that the system can utilize lower power levels that may be available from the turbine.

Roll control is accomplished by a single centrally located cylinder and piston assembly providing differential incidence control of the two wings as shown in the Figures. The actuator is controlled by a solenoid operated four-way valve which, in turn, is operated by the decoder of the command receiver. A centering switch is provided to recenter the piston in case it should drift away from the neutral position due to leakage or unbalanced forces.

The roll actuator of each vehicle is able to control all flight loads at maximum expected load factor, and minimum hydraulic supply pressure. In the 4,000 lb. vehicle (with a maximum actuator load of 4,000 lbs, and an effective actuator piston area of 3.2 in<sup>2</sup>), two rolls to maximum bank angle and eight rolls to 1/2 maximum bank angle are possible. For the 8,000 lb. vehicle (with a maximum actuator load of 8,000 lbs., and an effective actuator piston area of 6.0 in<sup>2</sup>) the same roll capability exists as for the 4,000 lb. vehicle.

A wing deflection of  $\pm 7^\circ$  is provided both vehicles with an actuator stroke of  $\pm 5.3$  in. and  $\pm 7.5$  in. from center for the 4,000 and 8,000 lb. payload vehicles respectively.

Control of the actuator is through the four-way solenoid valve, remotely controlled by radio command. Action of the valve is fully open or fully closed. The actuator stroke is limited by the length of the cylinder but the midpoint or neutral position is not. For this reason a centering switch is used to provide accurate midpoint positioning of the actuator. A centering command from the remote control station to the four-way valve will cause the actuator to move toward, and remain at center until a roll command is received. When the actuator reaches center, the centering switch will be mechanically tripped, removing the centering command signal.

Flare is accomplished by by-passing hydraulic fluid around the pitch actuator piston using a solenoid operated by-pass valve. The

solenoid is operated by the trailing wire ground contact switch. During tow and up to the initiation of flare, wing incidence is maintained by pressure on the pitch actuator piston. This pressure is ported to the high pressure line by means of a high pressure valve combined with the by-pass valve. This will prevent drift of the actuator due to leakage. It should be noted that no hydraulic power is required for flare. Because of the rigging geometry, when the pitch cable is released, the movement due to the wing lift resultant force will rotate the wing to a higher angle of attack. The hydraulic actuator, in this case, merely provides a convenient means for providing a controlled rate of change of incidence during flare. At the initiation of flare, the supply and pump lines to the actuator are closed off simultaneously with the opening of the by-pass valve, and flare operation continues independently of the remainder of the system. For re-use of the vehicle, manual retraction of the actuator piston, with the by-pass valve open and then closed, will restore the wing geometry to the normal flight configuration.

The pitch cable release cylinder will allow the wing angle of attack to change from  $19^\circ$  to  $34^\circ$  in approximately .2 sec. for the 4,000 and 8,000 lb. vehicles. Terminal angular velocities at  $-34^\circ$  for each vehicle are 2.0 rad/sec. and 1.7 rad/sec. respectively. Kinetic energies and diameters of pitch cables are respectively, 1200 ft. lbs and 3,000 ft. lbs and  $3/4$ " and  $7/8$ " for high strength steel cables. The pitch cable release cylinders effective-piston-areas and strokes are respectively,  $.7 \text{ in}^2$  and  $.86 \text{ in}^2$ , and 26 in. and 48 in. The by-pass valve orifice diameters for each are .22 and .25 inches.

The 4,000 lb. vehicle carries a standard 4 gallon accumulator with a gas precharge of 1740 psi. To bring the system pressure to 3000 psi, the pump must deliver a fluid charge of 1.7 gal. to the accumulator. The ram air-driven generator, a standard model normally used on light planes, can deliver approximately 1/6 H. P. This produces an accumulator charge time of about 18 minutes.

Similarly, the 8,000 lb. vehicle (with a standard accumulator having a total gas and fluid charge of 10 gallons, a gas pre-charge of 1660 psi, and a required fluid charge of 4.5 gal. using the same wind driven generator) would have an accumulator charge time of about 48 minutes. Charge time may be decreased, if desired, by increasing the blade diameter of the air-driven generator.

In each system an accumulator is used as a reservoir. Pump return line pressure is maintained at 50 psi for the 4,000 and 8,000

lb. vehicles respectively. Required reservoir total gas and fluid volumes are 432 in.<sup>3</sup> and 1220 in.<sup>3</sup> with a fluid charge of 1.7 gal. and 4.5 gal. respectively.

The reservoir after initial charge with fluid, reclaims its charge through the duration of the flight and additional flights can be made without recharge. Only fluid lost through leakage need be replaced. The state of gas charge may be determined from inspection of the accumulator and reservoir gas pressure gages. If these pressures are correct, both fluid volume and gas charges are satisfactory. If these pressures are incorrect, the accumulator fluid must be discharged to the reservoir, and the fluid level determined. The reservoir incorporates a device for visually ascertaining the fluid level. Inspection of the accumulator and reservoir gas pressure gages establishes deficient gas charges, which can then be restored.

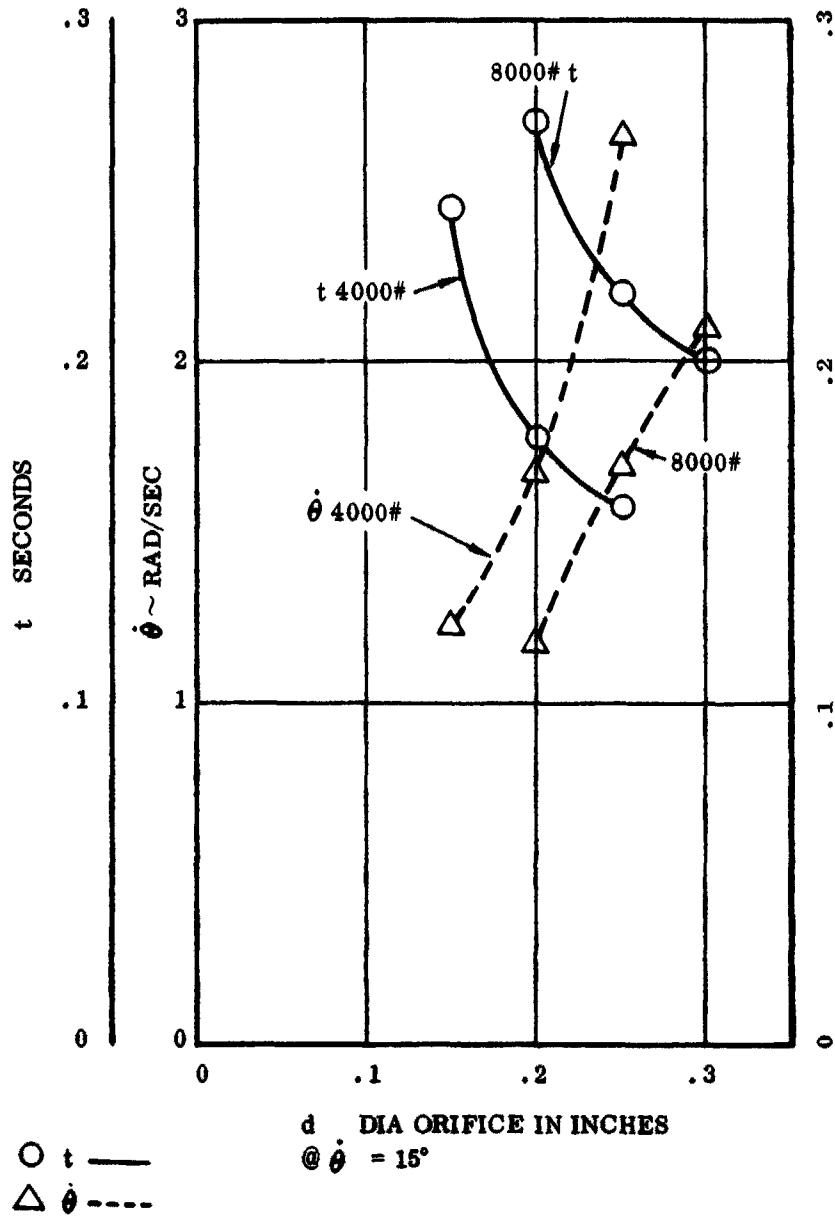


Figure 97 Flare Characteristics - 4,000 and 8,000 Lb. Payload Towed Gliders

## HYDRAULIC ACTUATOR, VALVE, AND ACCUMULATOR SIZE

### Pitch System

The flare actuator piston area and valve or orifice size will be determined for quickly accomplishing a step-function-flare (without requiring an exceptionally large flare control cable).

See Figure 97 for notation.

Neglecting line drop in the by-pass run-around line, and assuming  $R$ ,  $b$  and  $B$  as constant (these actually vary with  $O$  but, for convenience of analysis, they will be assumed constant), the equation of motion of the system can be obtained from  $M$  about the hinge, and  $F_x$  for cylinder.

$$1) \quad I O = R b - T B$$

all terms in ft. - lb. - sec. units

$$m x = T - p A$$

$$\text{The drop } p = \frac{1.65 Q^2}{(10d)^4} \quad \text{for sharp edged orifice, where } Q \text{ is}$$

flow in in<sup>3</sup>/sec.,  $d$  is orifice dia. in inches, and  $p$  is drop in psi. Noting that  $Q = A x$ , is velocity in in/sec., the product  $p A = \frac{238 A^3 x^2}{(10d)^4}$  with  $x$

in ft/sec. Eliminating  $T$  in (1) and putting  $x$  in terms of  $O$  ( $x = BO$ , etc.),

$$2) \quad O = \frac{1}{k} (C - K O^2) \quad \text{where } K = \frac{238 A^3 B^3}{(10d)^4}$$

$$C = Rb \text{ and } k = (I m B^2)$$

Integrating 2) gives,

$$3) \quad \ln \frac{\frac{C}{K} + O}{\frac{C}{K} - O} = 2 \frac{CK}{k} t \quad \text{for the velocity time}$$

relation. Integrating (3) gives,

$$4) \quad \ln \cosh \frac{CK}{k} t = \frac{KO}{k} \quad \text{for the position time relation.}$$

For angle of attack changes encountered in the flare maneuver,  $\alpha = 0 = 34^\circ - 19^\circ = 15^\circ$ . The terminal velocity  $O_t$  and the elapsed time  $t_t$  may be found from equations 3 and 4 for various values of orifice diameter  $d$ . These results are for  $O = 15^\circ$  and are shown graphically in Figure 98 for both 4,000 and 8,000 pound vehicles.  $\theta_t$  and  $t_t$  pairs can be found for  $d$  values in the ranges shown. These  $\theta_t$  values are compatible with simple, light structure and  $t_t$  values sufficiently short to insure a successful flare.

The assumed values for the characteristic parameters of the two vehicles used in the calculations are listed below.

	Unit	4000#	8000#
I	ft # sec. <sup>2</sup>	600	21000
m		neglig.	neglig.
$\theta$	radians	1/4	1/4
A	in. <sup>2</sup>	.7	.86
R	#	5750	10,400
b	ft.	2.4	3.0
B	ft.	8.4	13.5

Pitch cable size may be found from the relation  $a = \frac{2(E)M}{s^2 \ell}$

where  $a$  is cable area,  $E$  is kinetic energy ( $1/2 I \theta^2$ ),  $M$  is Youngs Modulus,  $s$  is the stress, and  $\ell$  is cable length. The solution of this equation indicates a requirement for 3/4" and 7/8" cable for the 4,000 and 8,000 lb. payload vehicles respectively to accomplish the flare pitching of the wing in approximately .2 seconds. If a longer time for accomplishing the incidence change can be allowed, the cable size can be reduced.

### Roll System

For the arrangement of components, it is desired to determine the minimum accumulator total volume and the corresponding roll actuator piston area for which the maximum load  $L$  can be overcome after an arbitrary number of actuator strokes have been made. At this time, the cylinder supply and back pressures are  $P_1$  &  $P_2$  respectively.

$$1) \quad F_x = P_2 A - L = 0$$

The total volume of fluid passing through the actuator is  $SA$ , where  $S$  is the sum of the lengths of all actuating strokes. The change in fluid volume in passing from the accumulator to the reservoir is the change in gas charge volume in both the accumulator and the reservoir. Using the gas laws, the pressure will be determined as a function of the change in gas volume.

$$V = SA = V_2 - V_1 = 1 - 2$$

and since  $P_2 = \frac{P_1 V_1}{V_2}$  and  $P_2 = \frac{P_1}{1 - 2}$  where all pressures and volumes

refer to accumulator gas charge pressure and volumes,

1) becomes

$$2) \quad P_1 \frac{(V_2 - SA)}{V_2} A - P_2 A - L = 0$$

Collecting terms and differentiating  $V_2$  with respect to  $A$ , simplifying the derivative and equating to zero in order to arrive at the minimum accumulator volume capable of supplying the requirements, we have

$$\frac{dV}{dV_2} = \frac{P_1 SA (P_1 - P_2^2) A - 2L}{(P_1 - P_2) A - L^2} = 0$$

$$A = \frac{2L}{P_1 - P_2} \quad \text{and } V_2 \text{ is a minimum and has the value } V_2 = \frac{4P_1 SL}{(P_1 - P_2)^2}$$

$$\text{In addition } P_2 = P_1 - \frac{P_1 SA}{V_2}$$

$$\text{and } 1 = \frac{P_2 SA}{P_2 - P_1}$$

In computing values (the following constants were assumed) for the 4,000 pound vehicle:

L = 4,000 pounds (see Figure 5)

$P_1$  = 3,000 psi

S = 122 in.

$V_2$  = 925 in<sup>3</sup> (4 gal) std. size

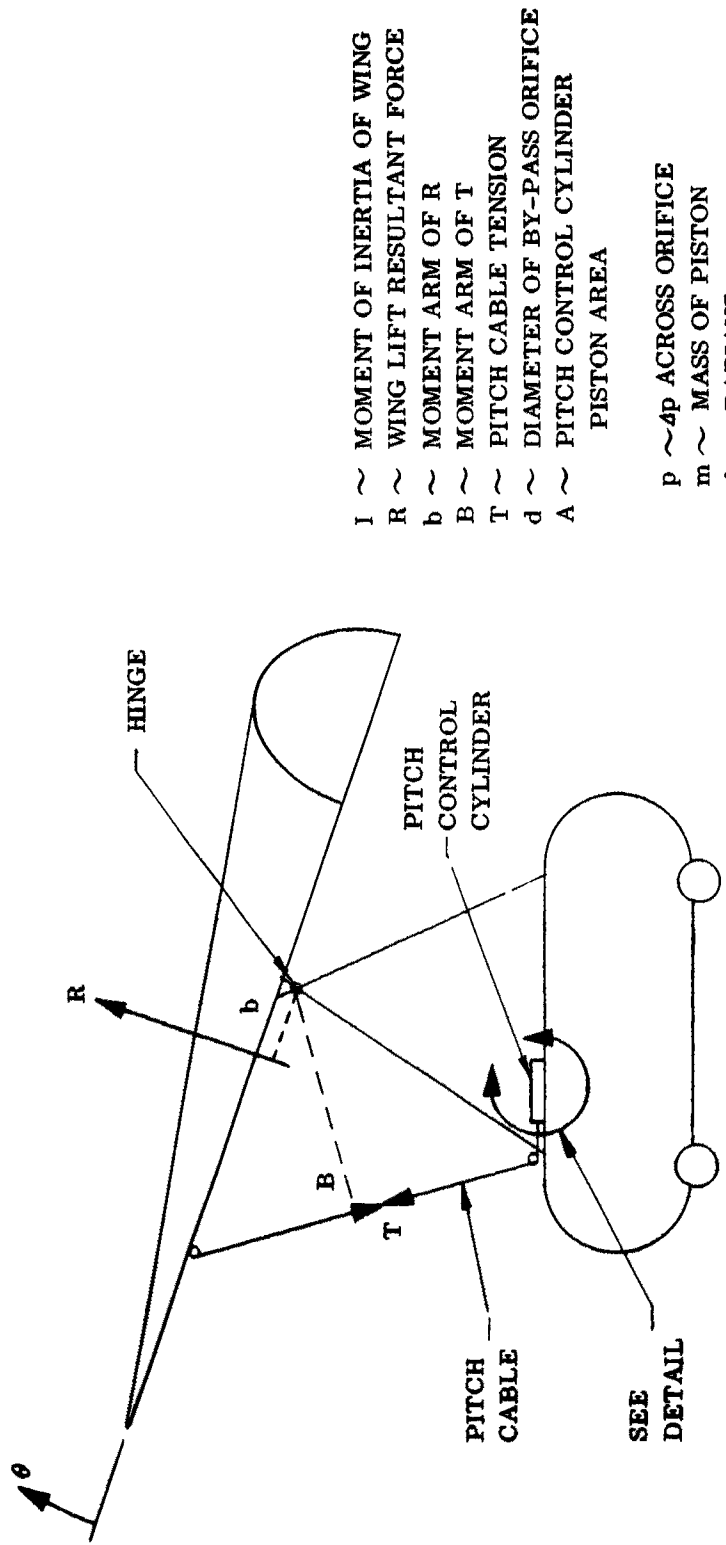
for the 8,000 pound vehicle

L = 8,000 pounds (see Figure )

$P_1$  = 3,000 psi

S = 172 in.

$V_2$  = 2310 in. (10 gal) std. size



- I ~ MOMENT OF INERTIA OF WING
- R ~ WING LIFT RESULTANT FORCE
- b ~ MOMENT ARM OF R
- B ~ MOMENT ARM OF T
- T ~ PITCH CABLE TENSION
- d ~ DIAMETER OF BY-PASS ORIFICE
- A ~ PITCH CONTROL CYLINDER
- PISTON AREA

- p ~  $\phi$ p ACROSS ORIFICE
- m ~ MASS OF PISTON
- $\theta$  ~ RADIANS
- x ~ FEET

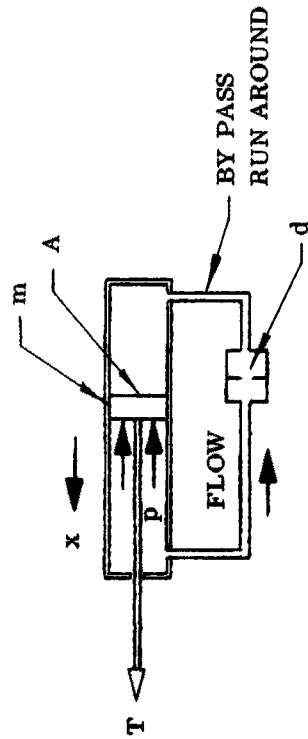


Figure 98 Pitch Change Diagram

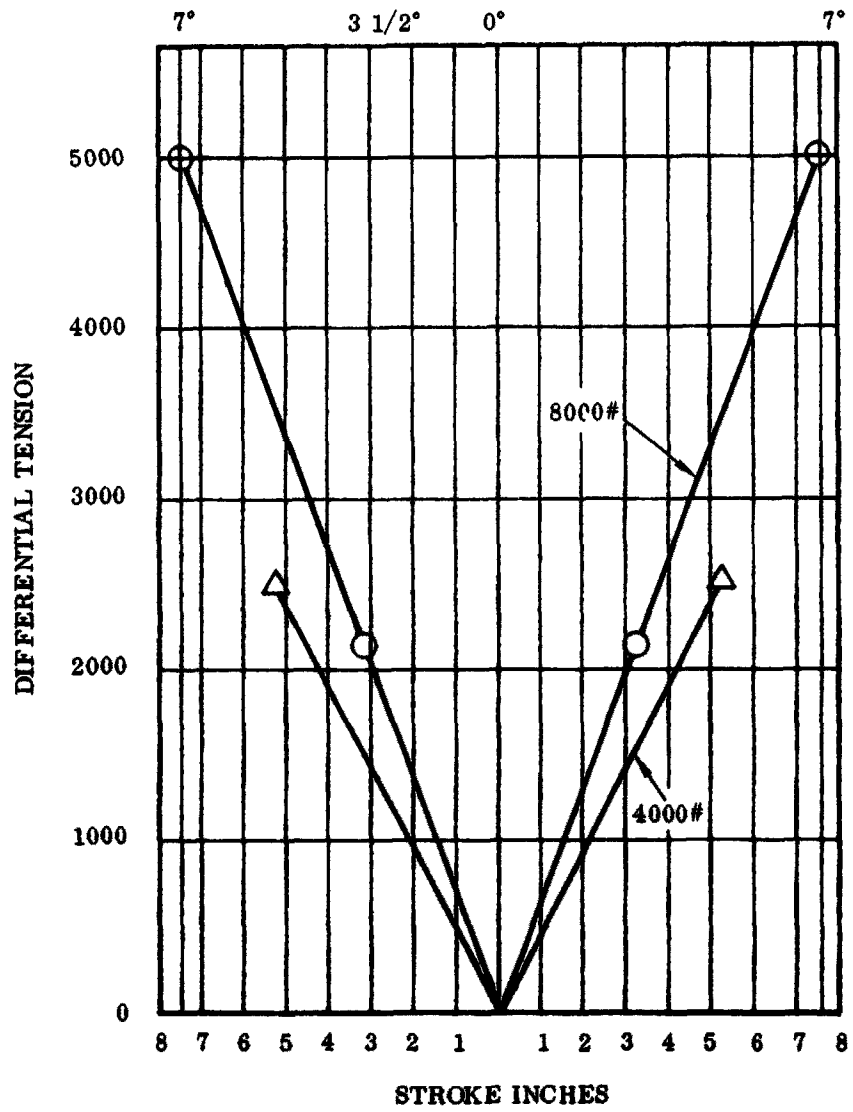


Figure 99 Cylinder Loading - 4,000 and 8,000 Lb. Towed Glider

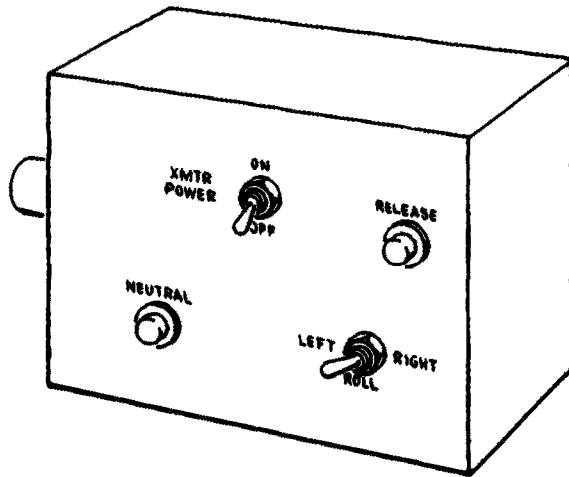
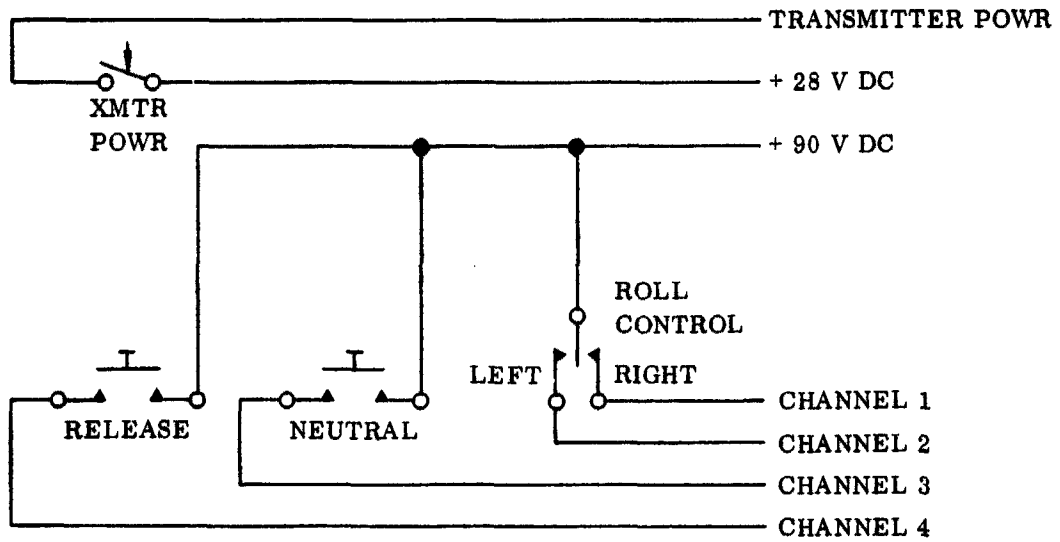


Figure 100 Remote Control Box Schematic and Layout Towed Glider

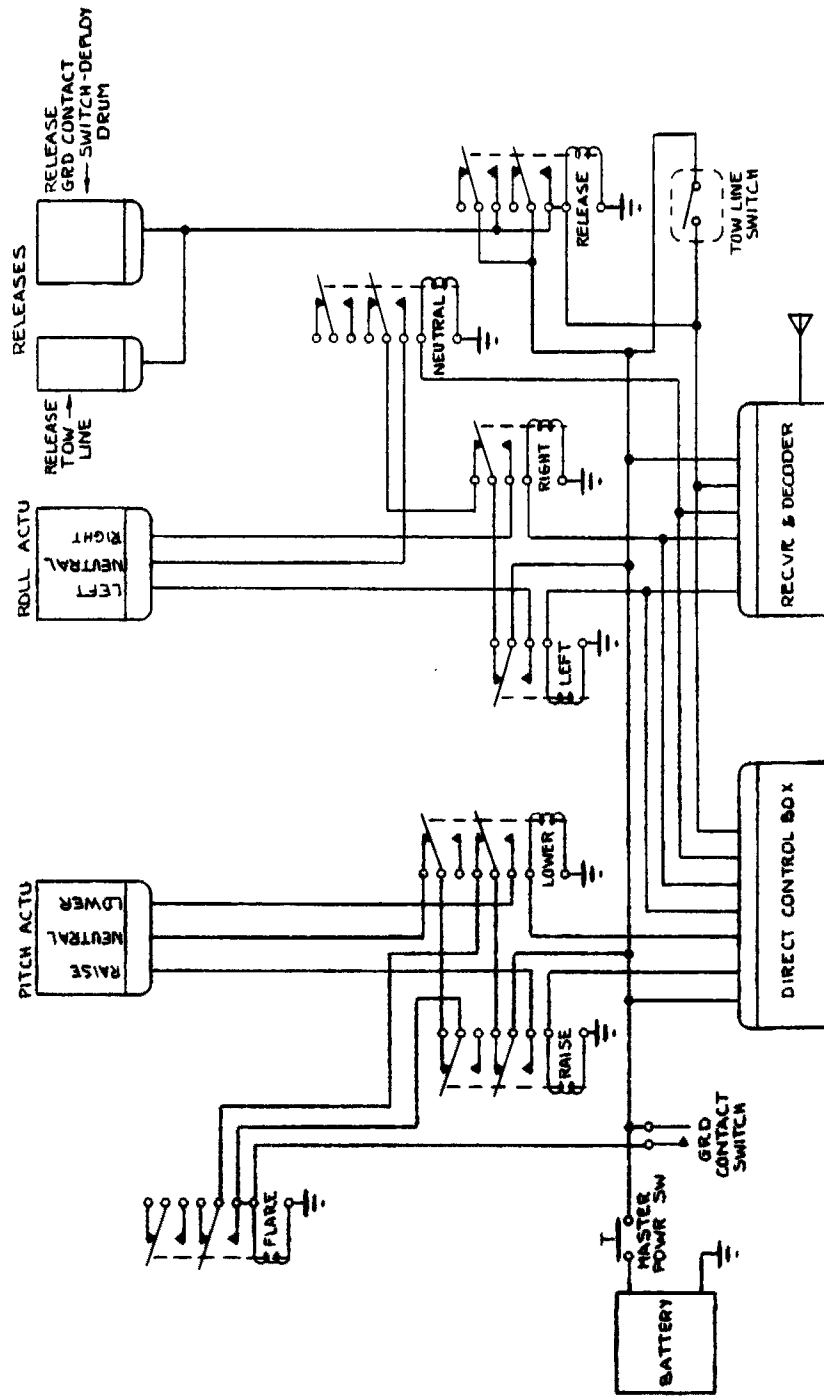


Figure 101 Electrical Schematic 250 Lb. Towed Glider

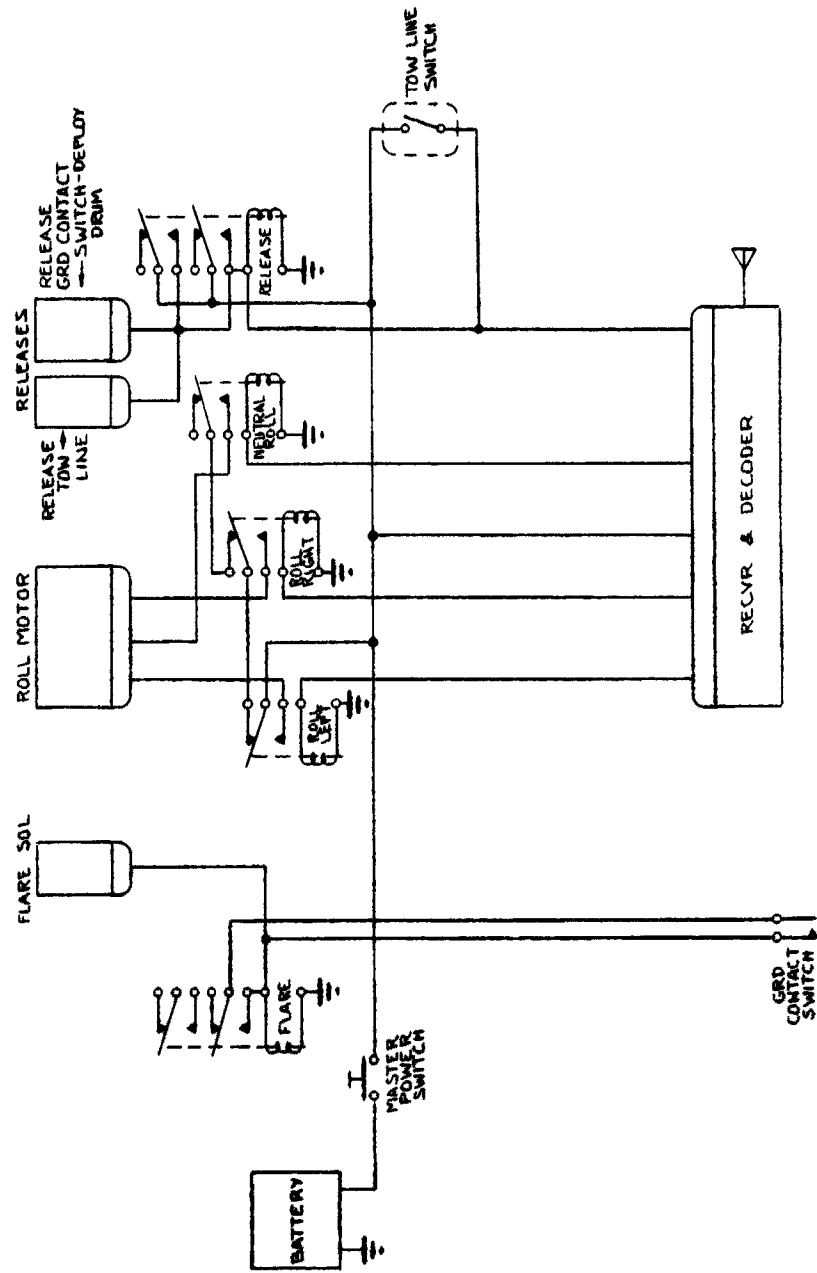


Figure 102 Electrical Schematic 1000 Lb. Towed Glider

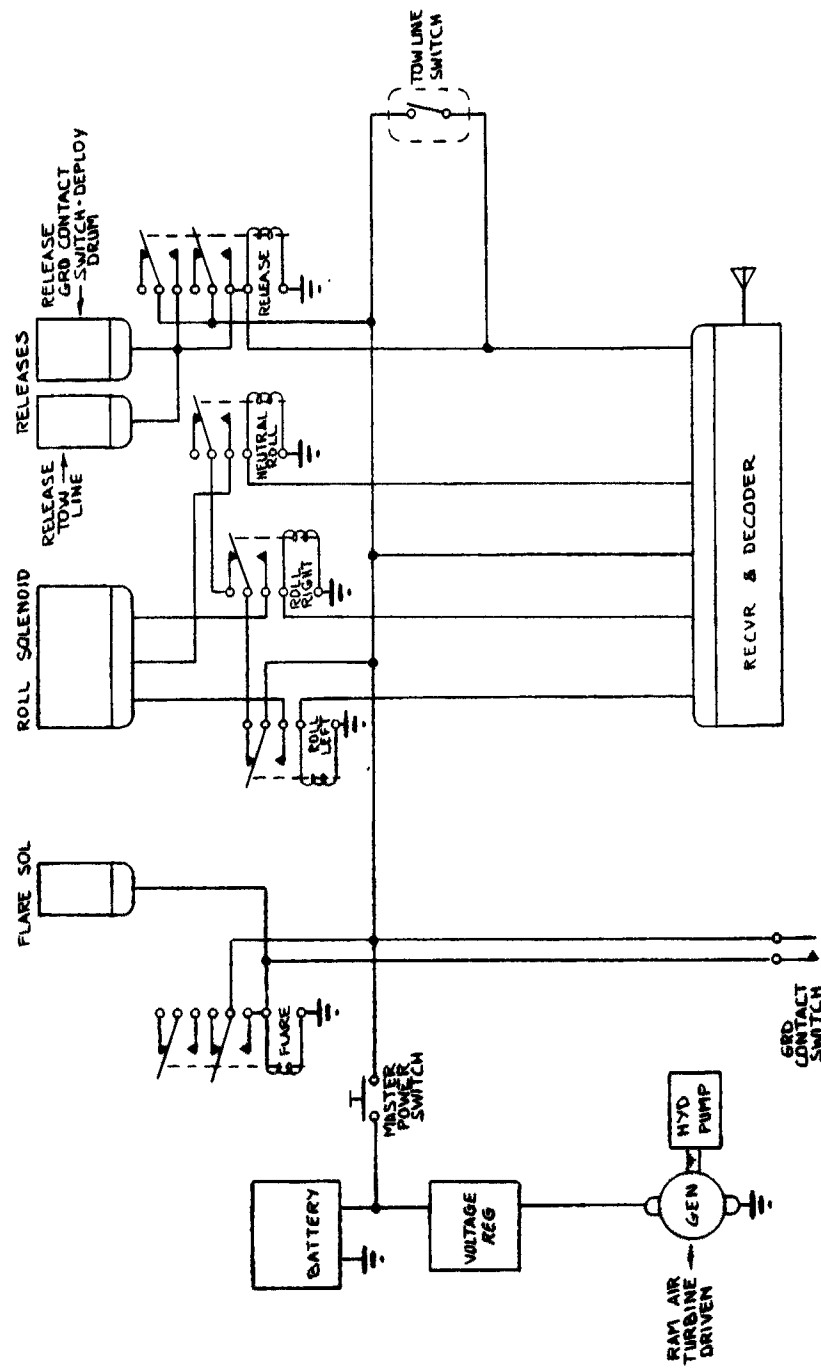


Figure 103 Electrical Schematic 4,000 and 8,000 Lb. Towed Gliders

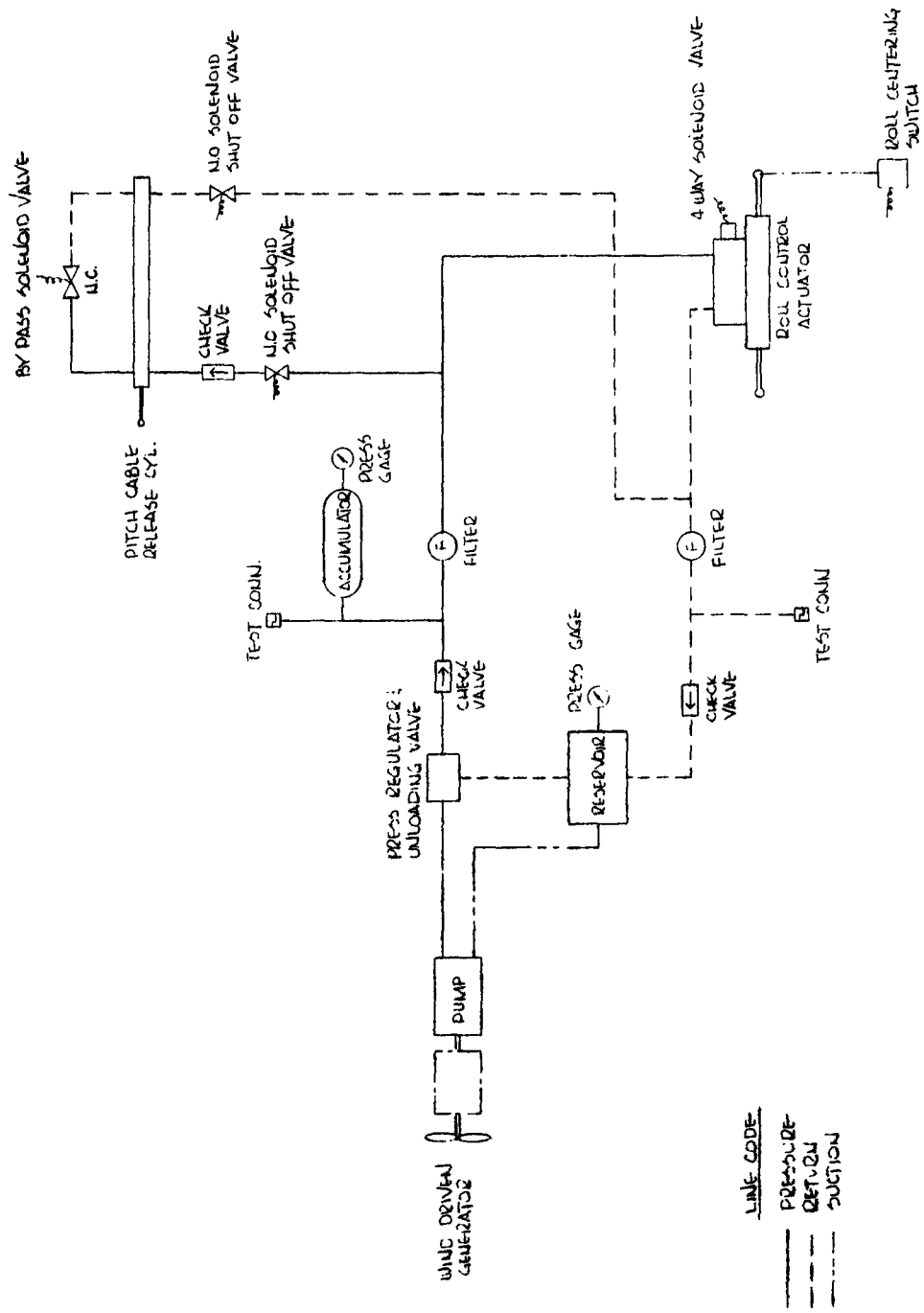


Figure 104 3000 PSI Hydraulic Control System - 8,000 and 4,000 Lb. Air Cargo Gliders

### Towing Systems and Tow Aircraft Modifications

Four different models of aircraft common to the inventory of the U. S. Army were considered adaptable for the towing of Flexible Wing towed logistic gliders. Performance studies showed that the L-20A (Beaver) and the H-23D (Raven) are suitable for towing the 250 and the 1,000 lb. gliders; the HU-1A (Iroquois) for the 1,000 and 4,000 lb. configurations; and the H-34 (Choctaw) for the 4,000 and 8,000 lb. payload vehicles.

Dynamics studies shown herein revealed that no serious effects from dynamic couple would occur between the towing and towed vehicles.

The study was limited to the design of the towing bridles and to mechanisms for attaching the bridle to the towing aircraft. Since detailed structural drawings of the towing aircraft were unavailable for the purpose of this study, hardpoints of the basic structure of the towing aircraft were estimated. The following numbered drawings show the design of the towing bridles and the modifications required for the towing aircraft. The size of the tow lines and the cable release mechanisms are also shown on the drawings.

- B063-0025 L-20 Aircraft Modifications
- B063-0010 Tow Bridle Arrangement on H-23D
- B063-0022 H-23D Helicopter modifications
- B063-0008 Tow Bridle Arrangement on the HU-1A
- B063-0026 HU-1A Helicopter Modifications
- B063-0005 Tow Bridle Arrangement on the H-34
- B063-0028 H-34 Helicopter Modifications

The study showed that the tow line length in all of the configurations must be at a minimum of 4.7 times the keel length of the towed vehicle. The geometry of the bridle of the towed vehicle must receive careful consideration for exact dimensions. The bridle arrangement for the 8,000 lb. payload vehicle is shown on Drawing B063-0032 following.

**1**

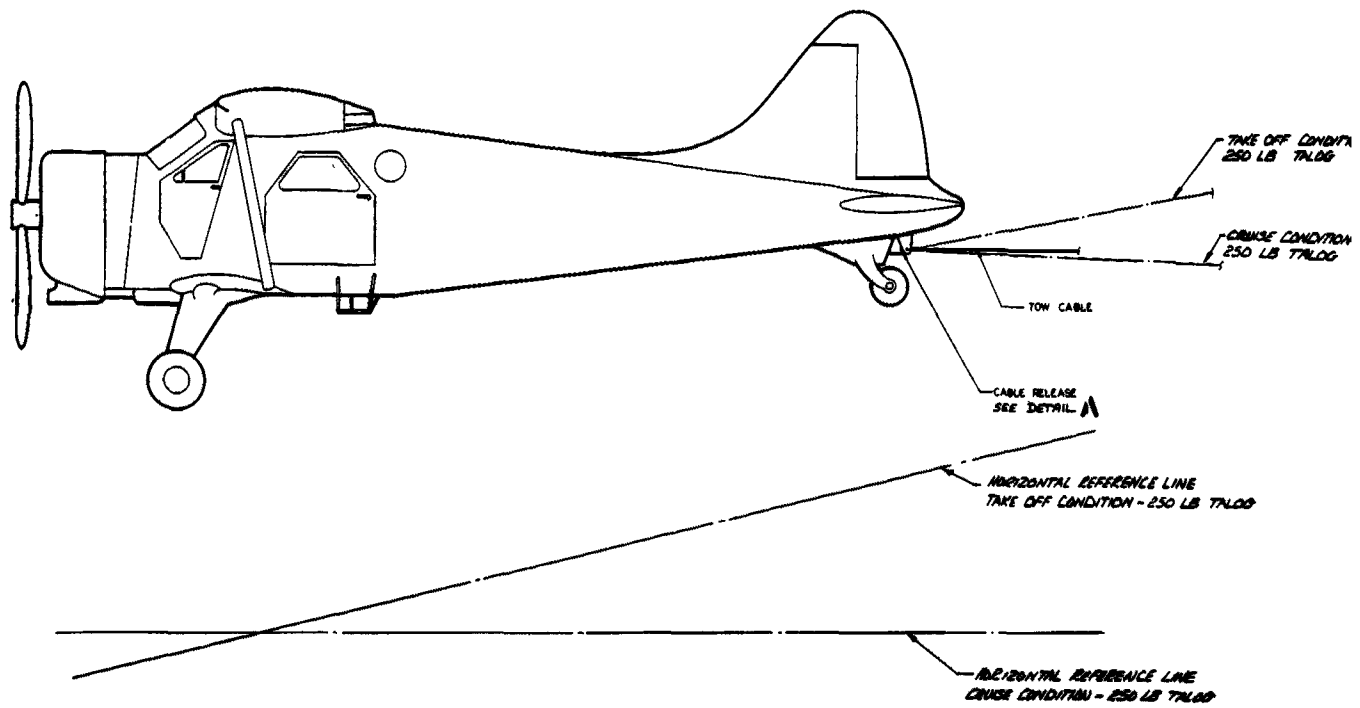
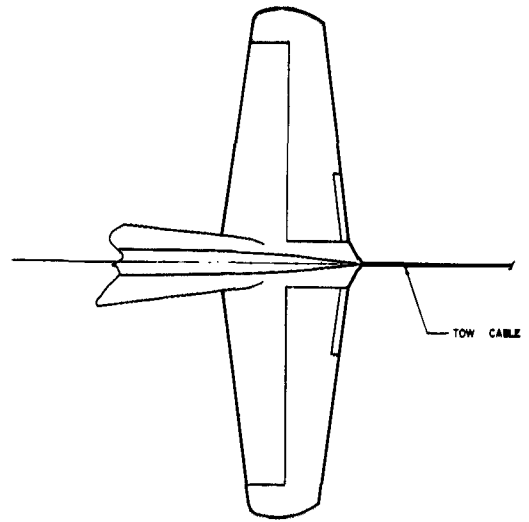
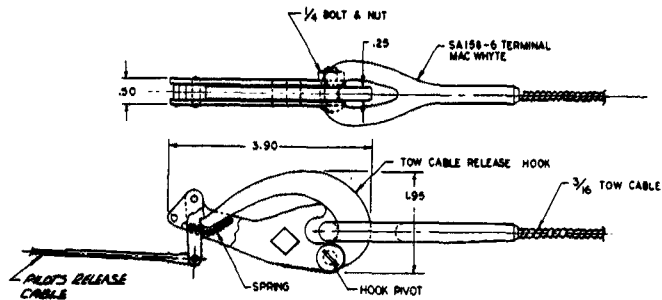
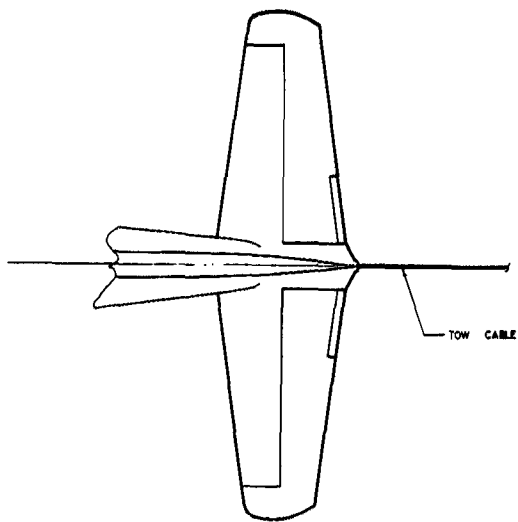


Figure 105 Stu

2



DETAIL A  
SCALE 1/1

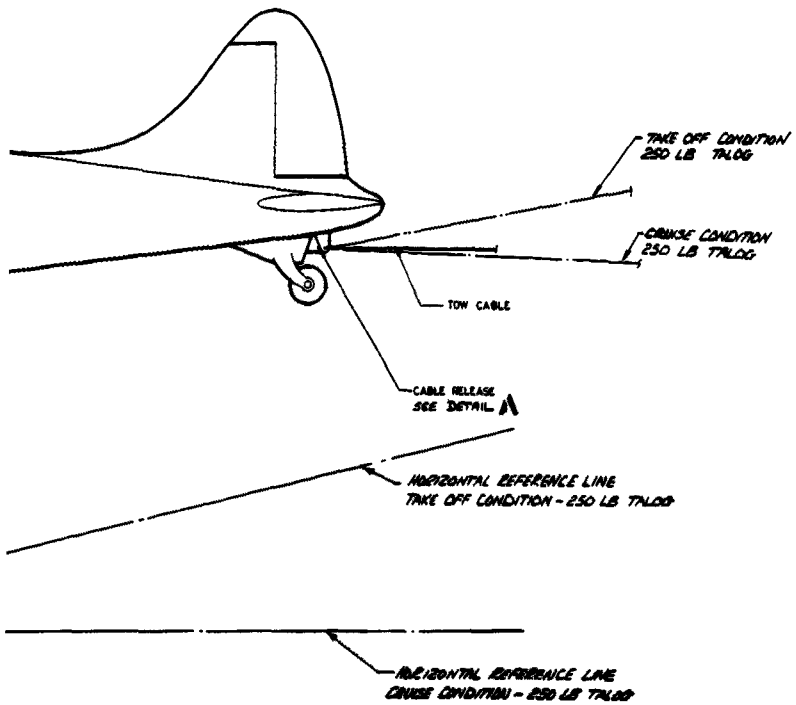


Figure 105 Study - L-20 Aircraft Modification (B063-0025)

1

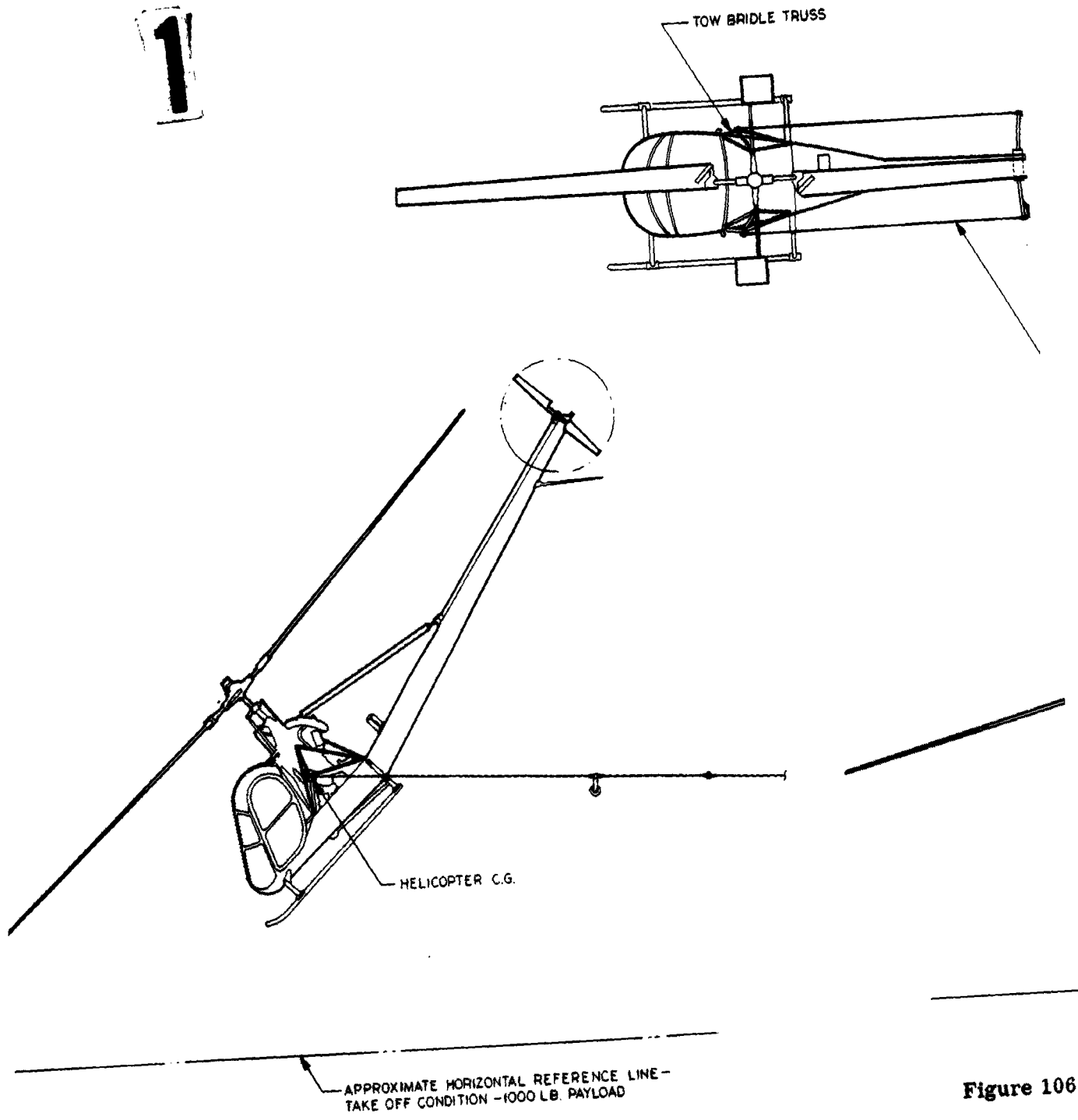


Figure 106

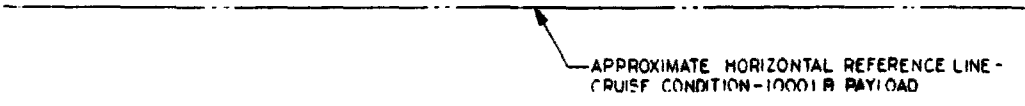
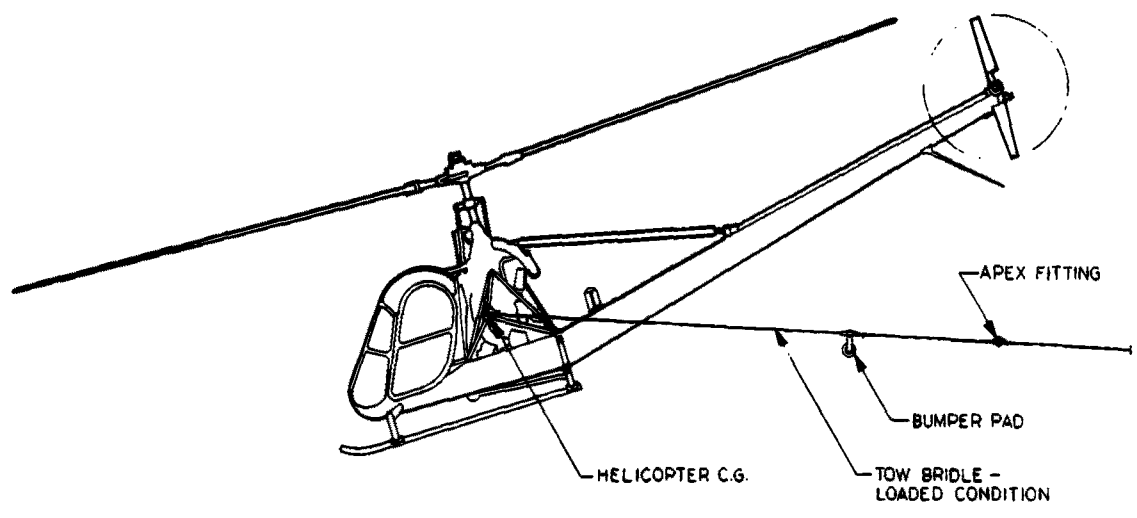
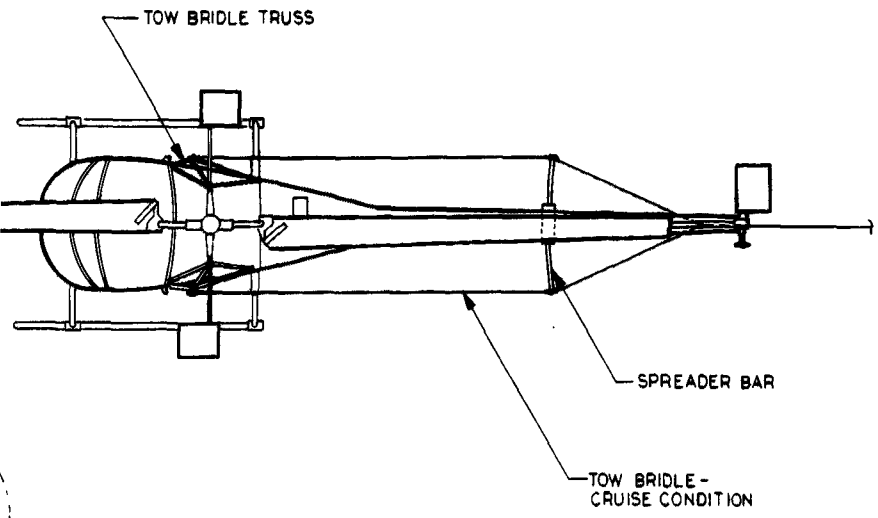
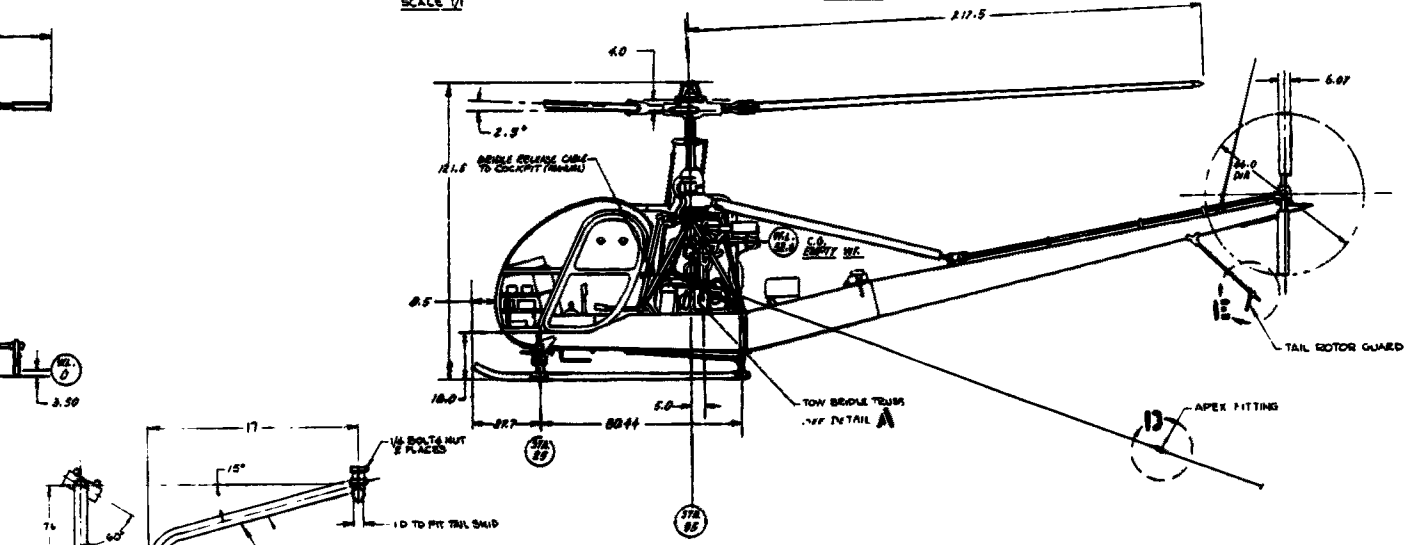
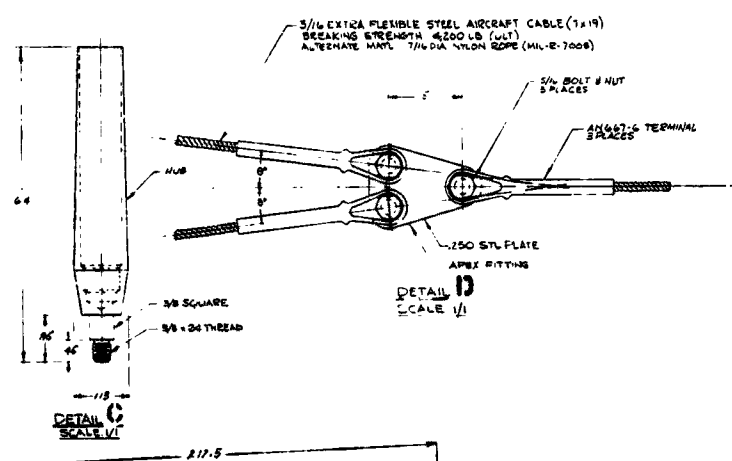
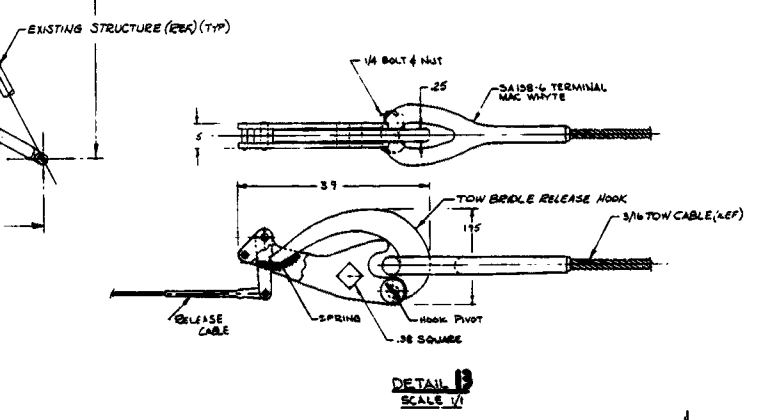
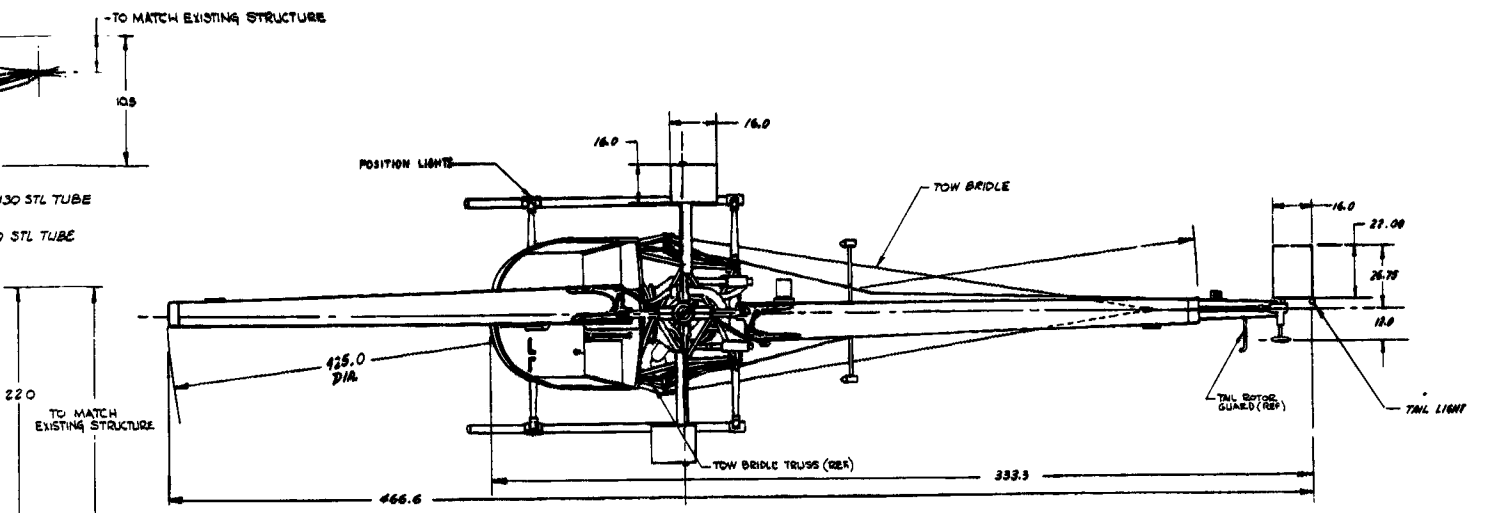


Figure 106 Tow Bridle Arrangement on H-23D Helicopter (B063-0010)  
225

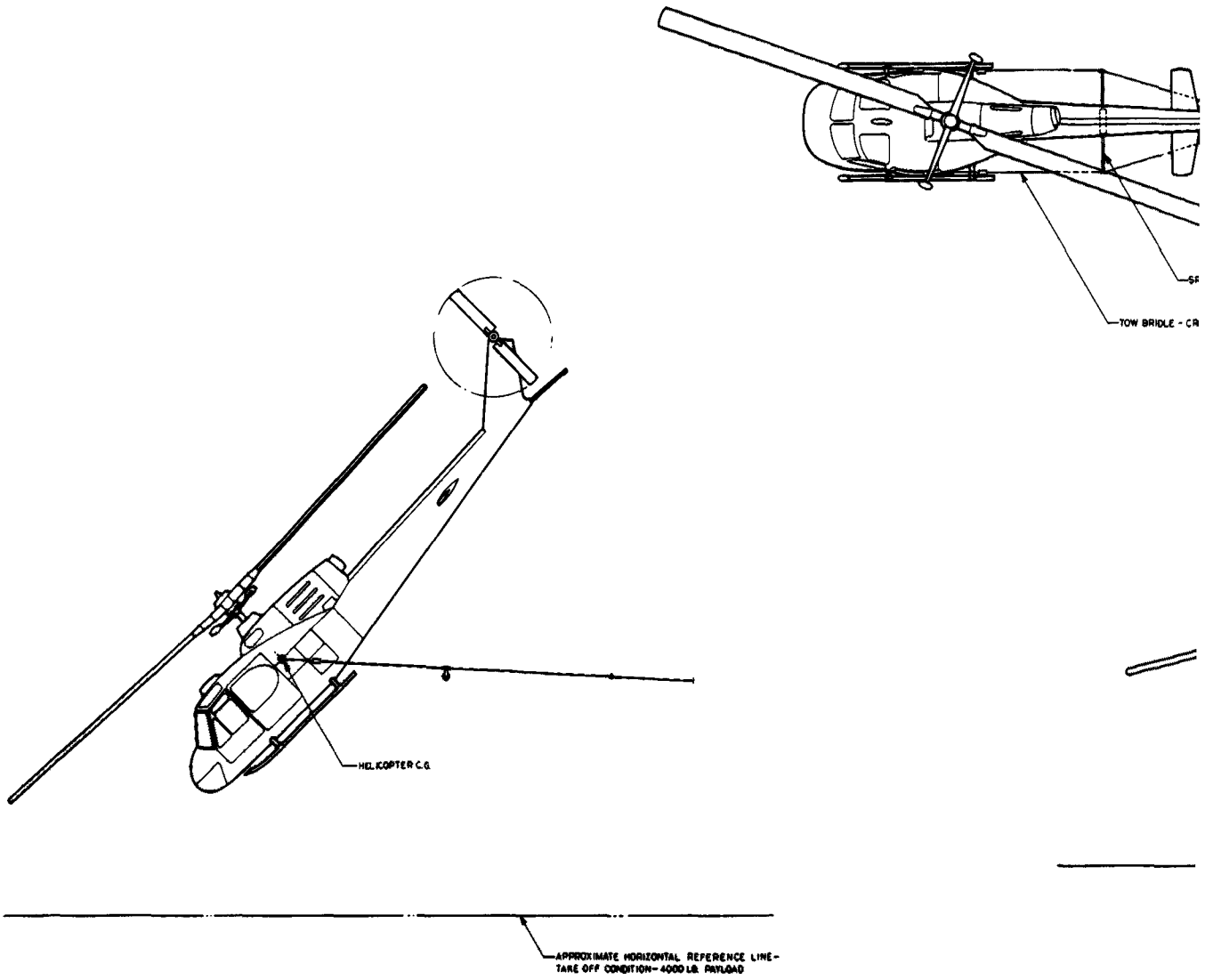
INE -





Note: Max. Load 1000 Lb. Payload Glider

Figure 107 Study - H-23D Helicopter Modifications (B063-0022)



2

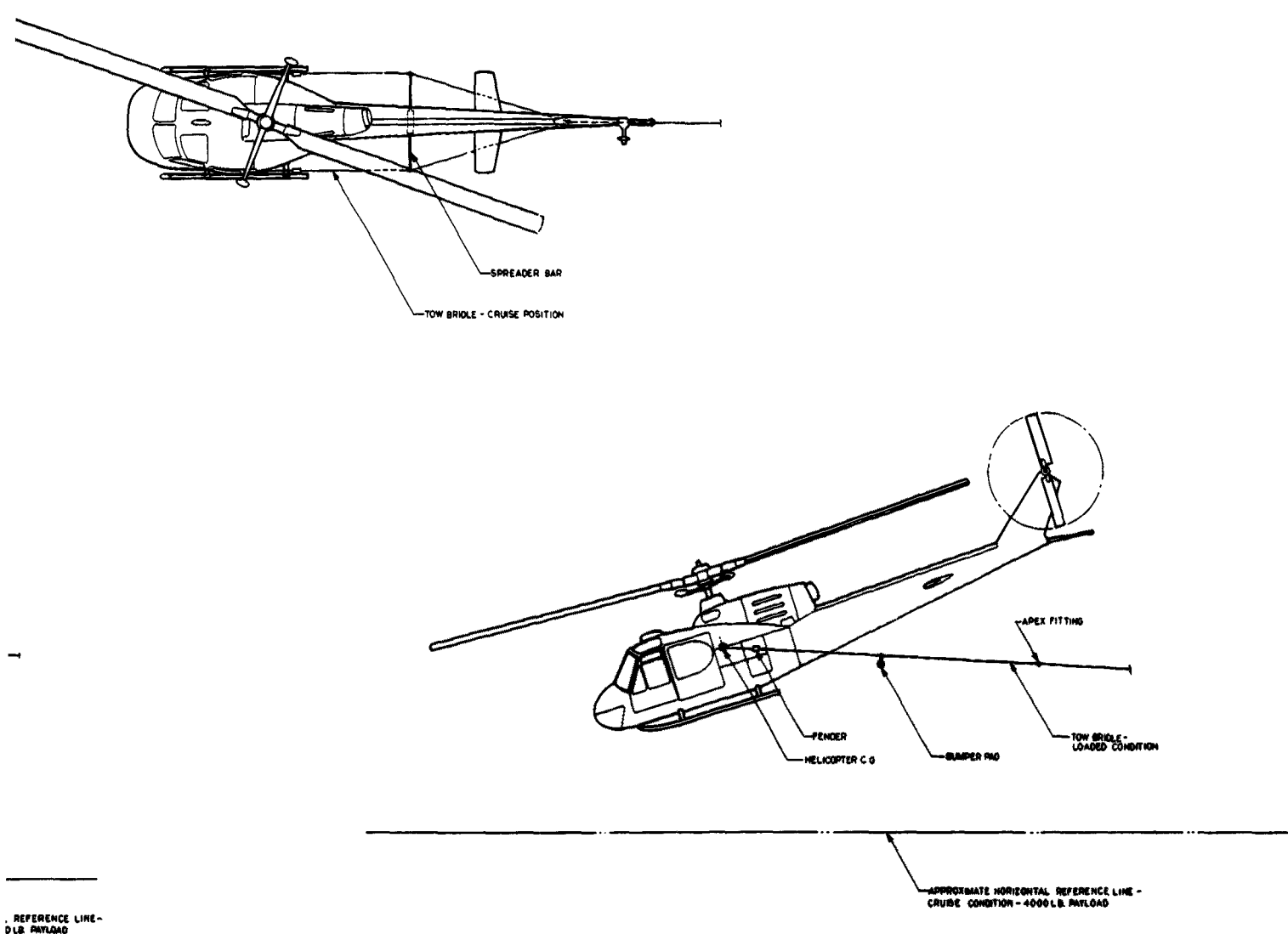
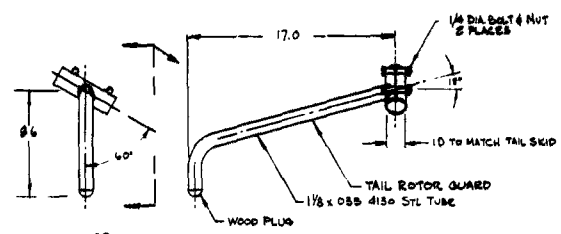
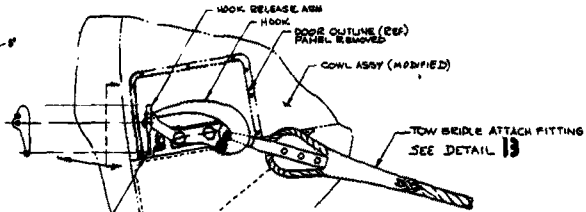
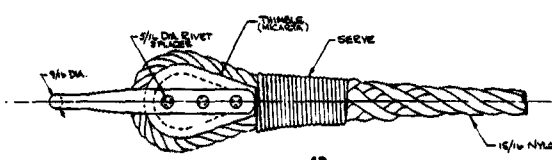
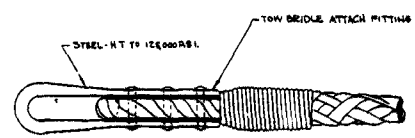
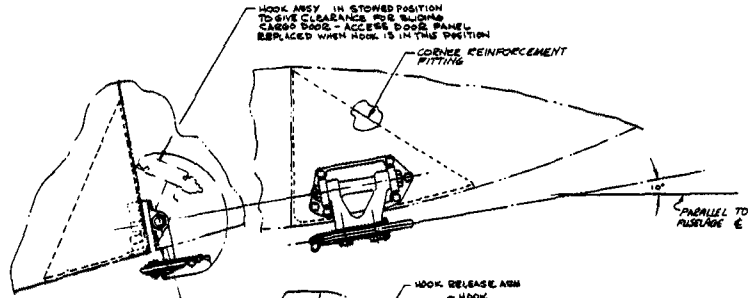
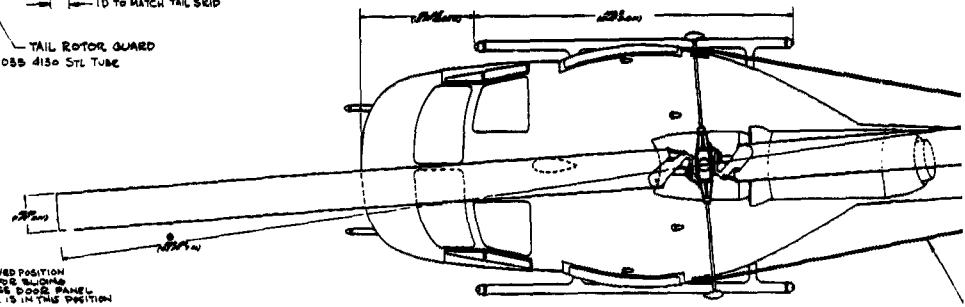


Figure 108 Tow Bridle Arrangement on HU-1A Helicopter (B063-0008)  
229

1



DETAIL 13  
SCALE 1/4



BRIDLE RELEASE CABLE  
(FROM COCKPIT) ATTACH  
POINT

DETAIL A  
SCALE 1/2

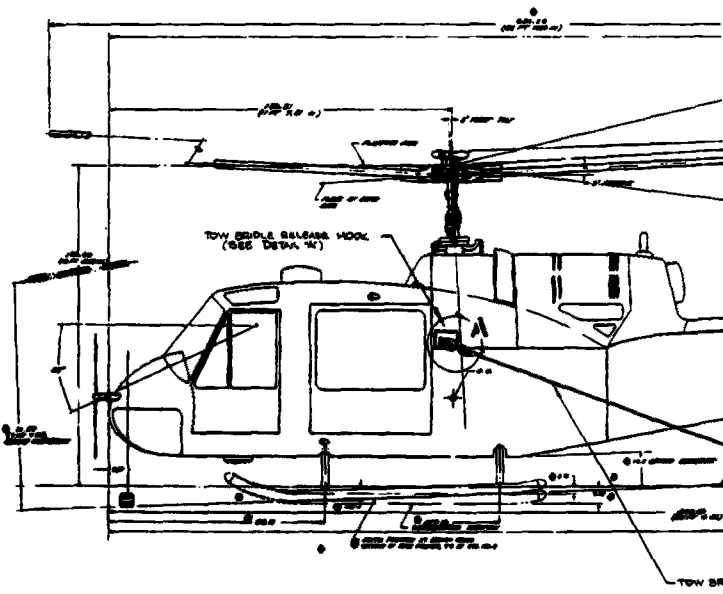
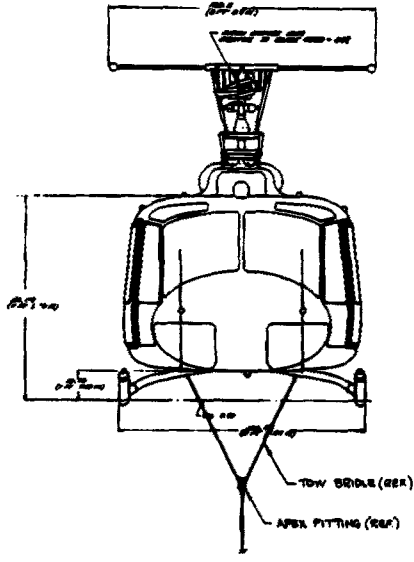
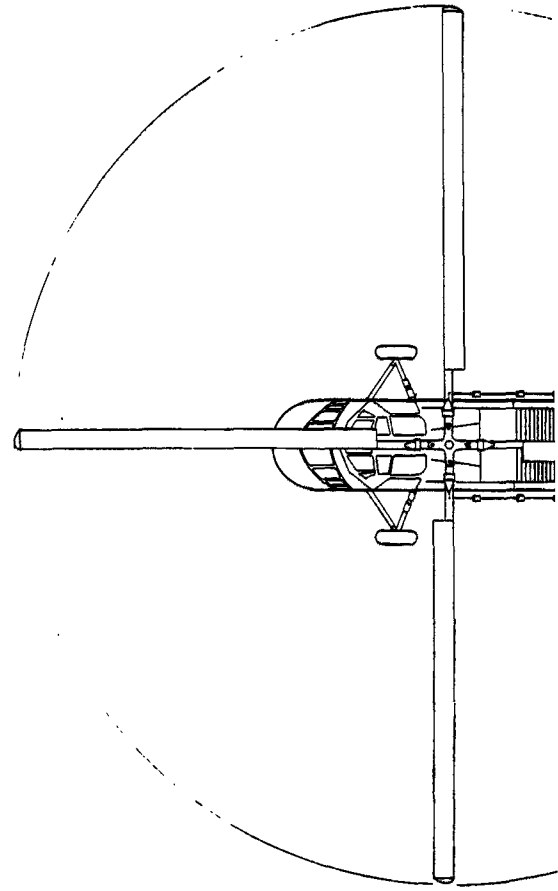


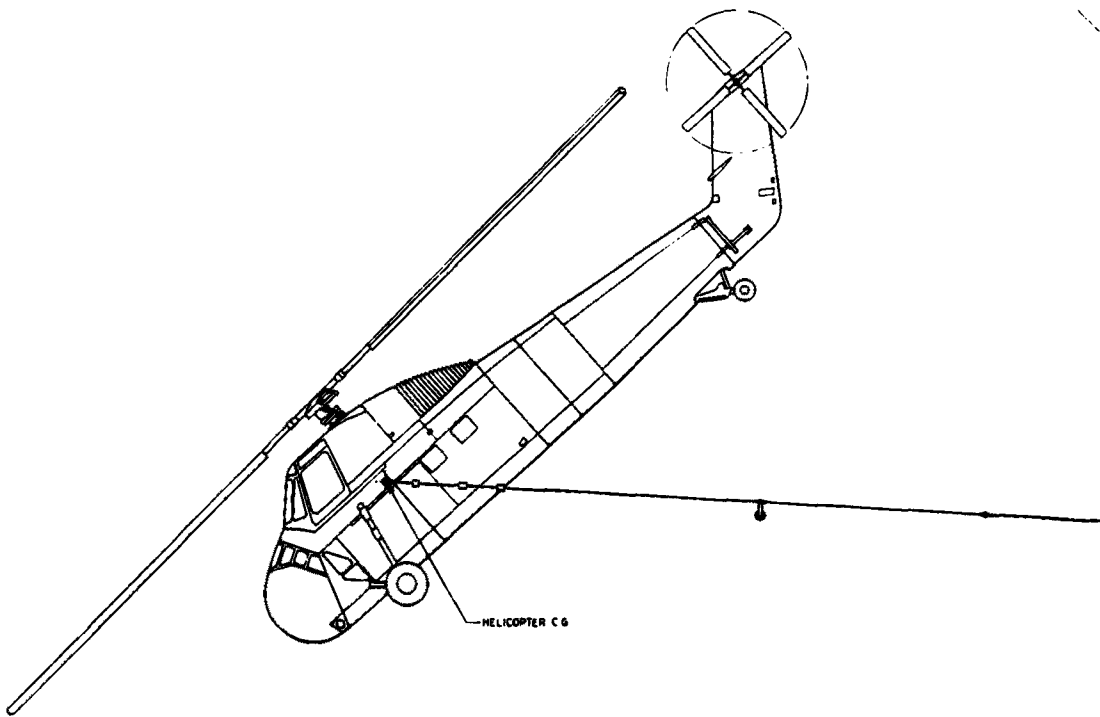
Figure 1



1

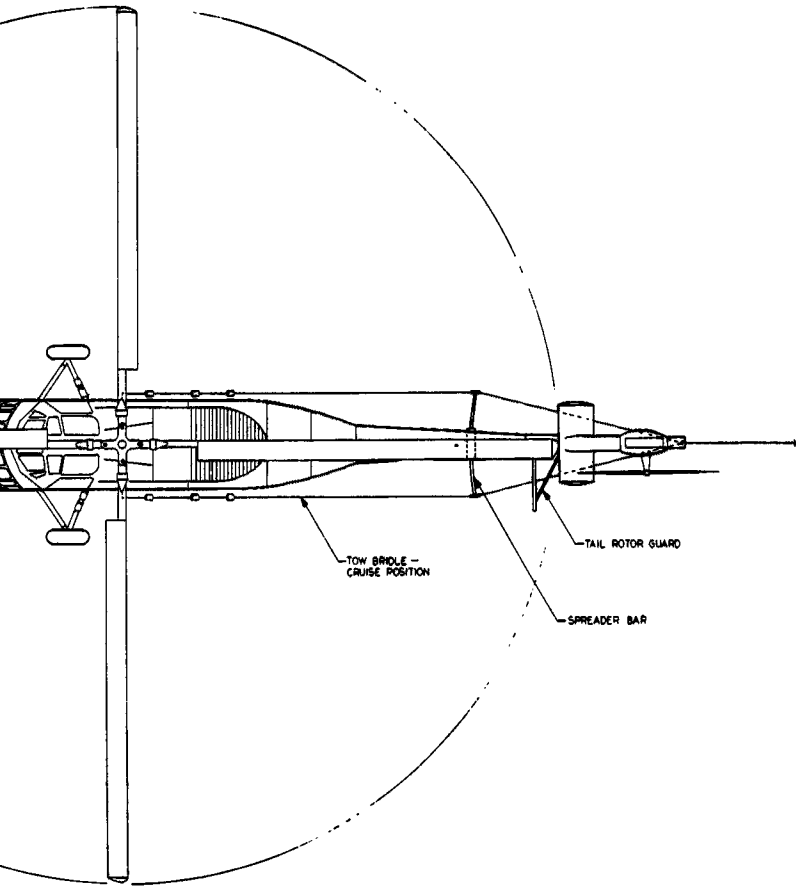


PLAN VIEW



HELICOPTER C.G.

APPROXIMATE HORIZONTAL REFERENCE LINE -  
TAKE OFF CONDITION - 8,000 LB. PAYLOAD



PLAN VIEW

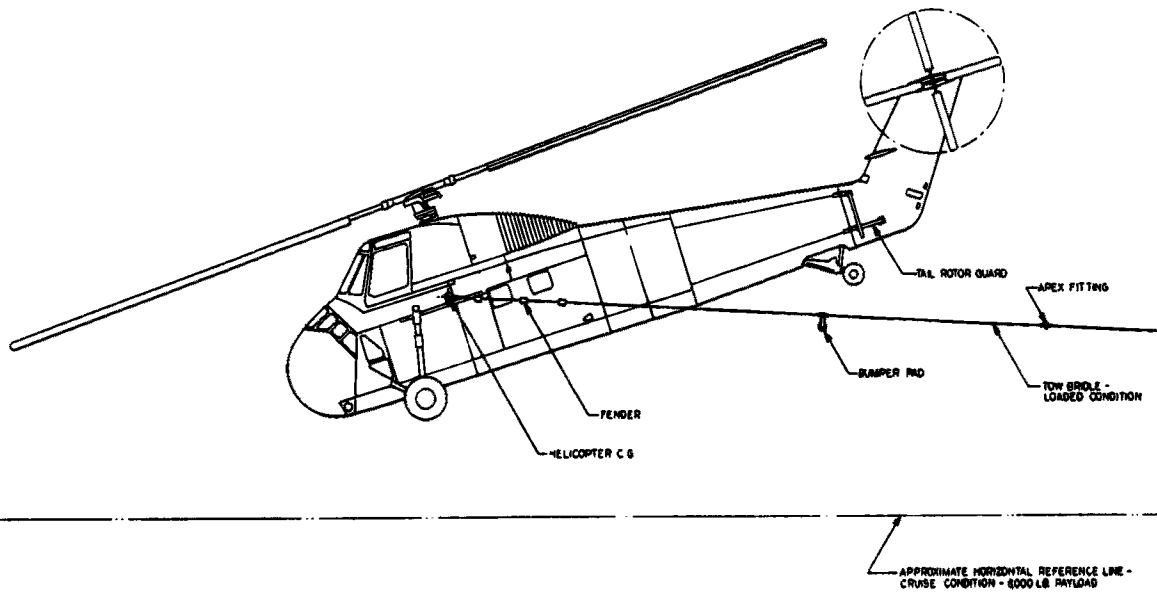


Figure 110 Tow Bridle Arrangement on H34 Helicopter (B063-0005)

## Conclusions

### Towing and Control Systems

Control and guidance may be obtained through the towing bridle arrangement while the vehicle is under tow.

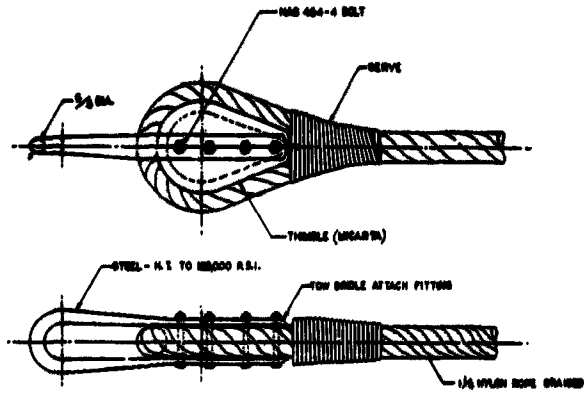
In the free flight mode, control without guidance may be achieved through preselected setting of the system. Landing flares and touchdown are controlled through an automatically initiated signal from a trailing pendant switch.

Release from the towing vehicle and directional control and guidance, with a controlled landing flare may be obtained through a remote radio link.

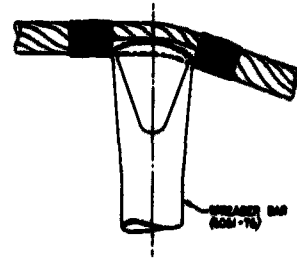
Serious effects from the dynamic couple between the towing and the towed vehicles will minimize with the specified length of the towing cable.

Modification of the towing aircraft will not be extensive.

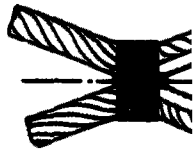
1



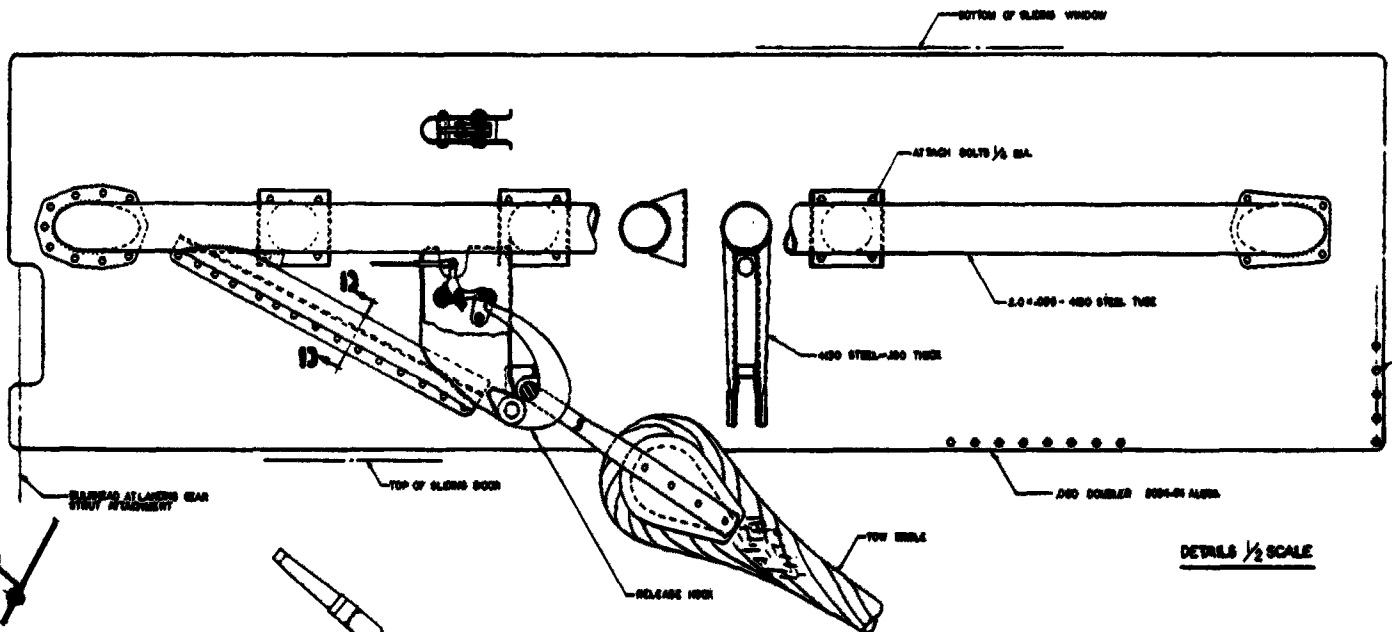
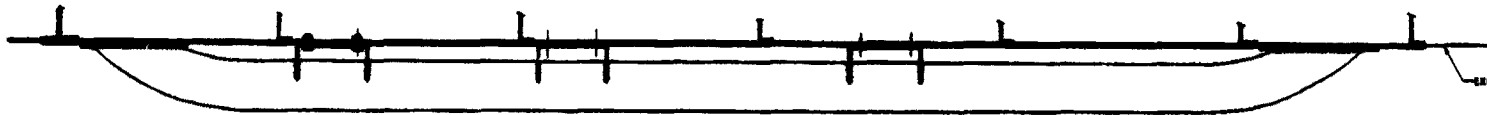
DETAIL A



DETAIL B



DETAIL C

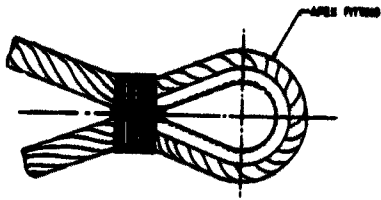


DETAILS 1/2 SCALE

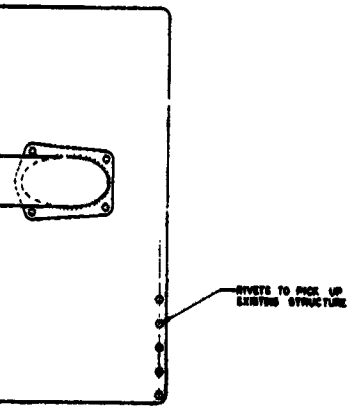
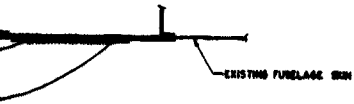
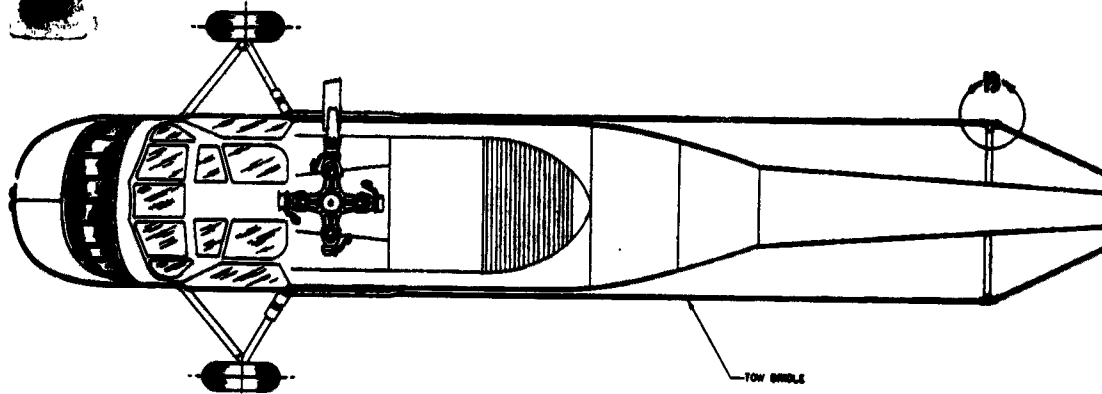


RELEASE DETAILS

2



DETAIL C



LS 1/2 SCALE

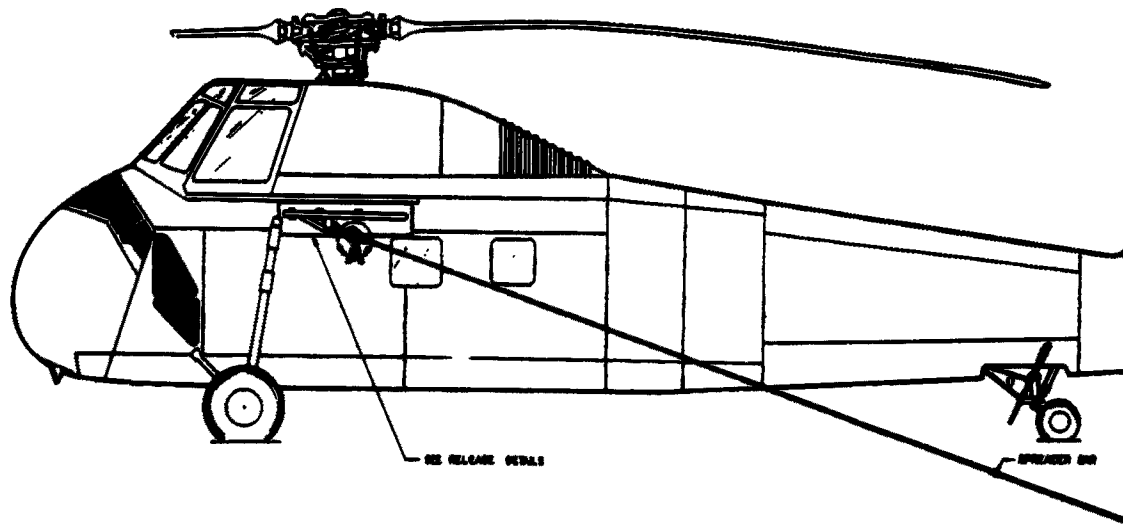


Figure 111 Study - H34 Helicopter Modificat  
237

3

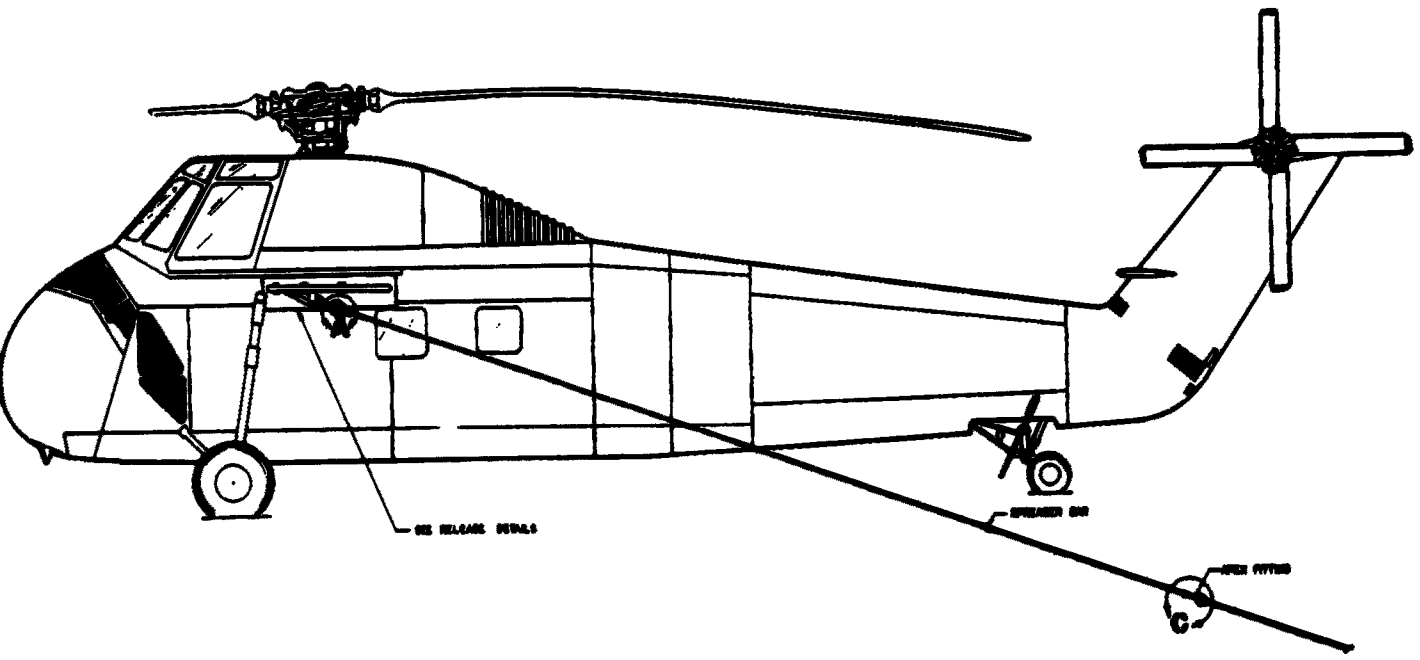
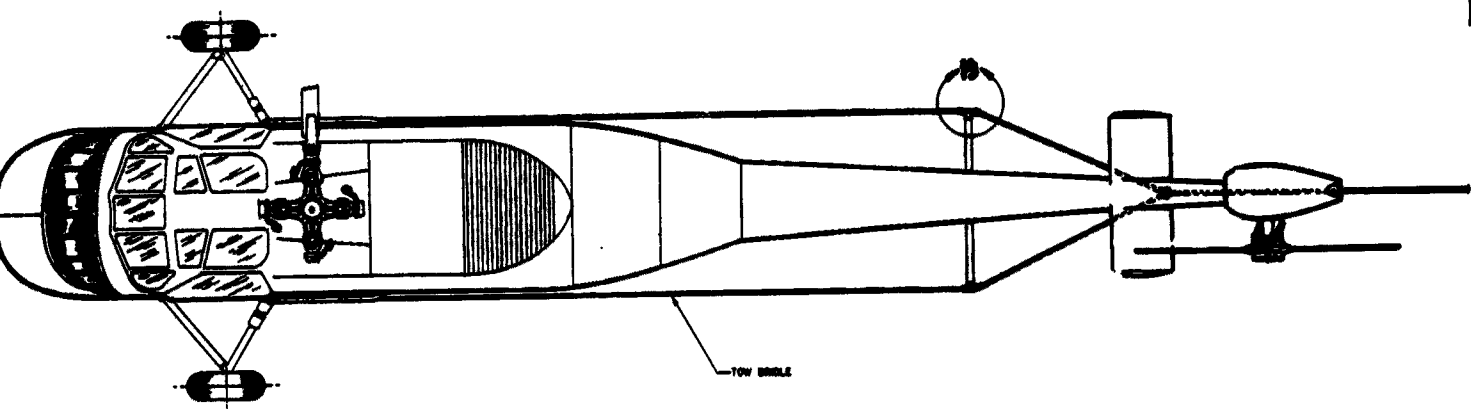
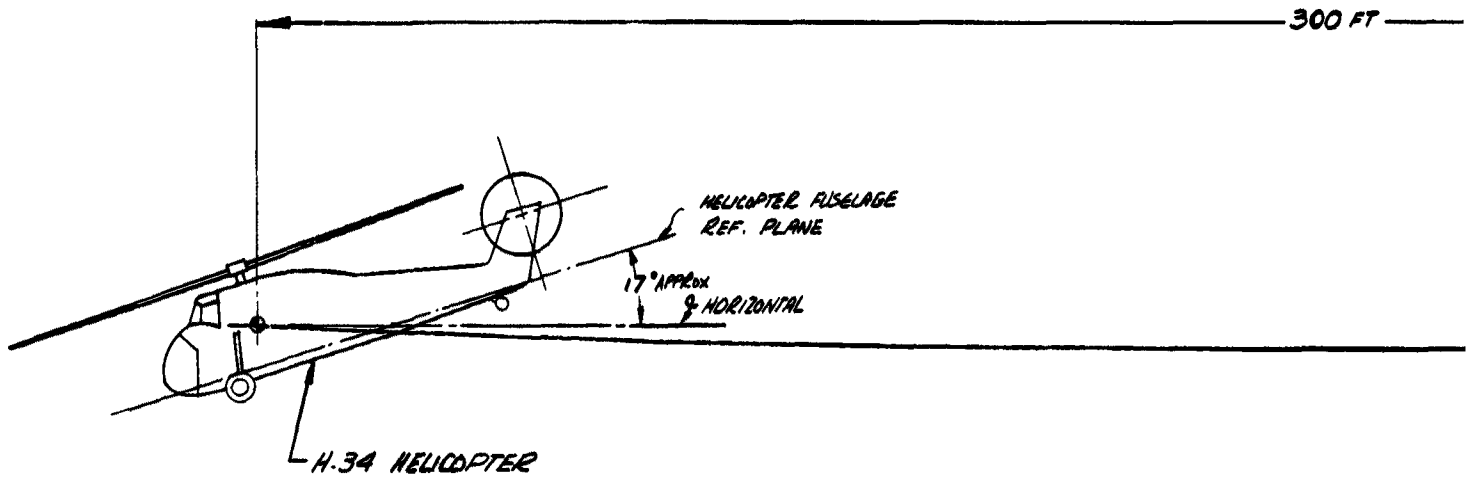


Figure 111 Study - H34 Helicopter Modification (B069-0026)  
237

1



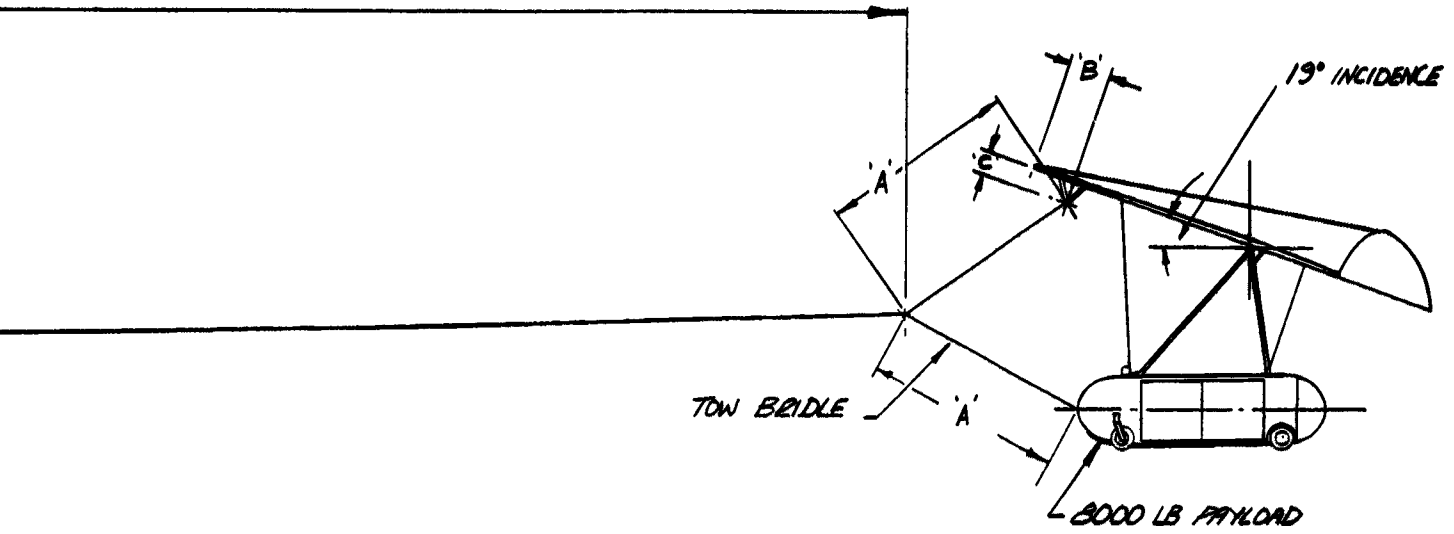


300 FT

TOW LINE

TOW

TOW BRIDLE & ATTACH. DIMENSIONS		
DIM.	* FT.	% KEEL LENGTH
A	22.5	46.0
B	4.6	9.4
C	2.2	4.45
* FOR 8000 LB. PAYLOAD GLIDER		



TOW BRIDLE & ATTACH. DIMENSIONS		
DIM.	* FT.	% KEEL LENGTH
A	22.5	46.0
B	4.6	9.4
C	2.2	4.45
* FOR 8000 LB. PAYLOAD GLIDER		

Figure 112 Helicopter/Glider Relationship Towed Cruise Configuration (B063-0032)

V. APPENDIX

A. RESULTS OF WING MEMBRANE FABRIC TESTS

The following Figures 113 through 119 indicate various exposure, notch and load tests for wing fabric materials.

Material	Total Weight Of Material (oz./sq. yd.)	Direction	Strength Before Exposure (lbs.)	Strength After Exposure (lbs.)	% Of Original Strength Remaining After Exposure
Dacron with Polyester Coating	7	Warp	178	172	96.6
		Fill	164	150	91.5
Dacron No Coating	5	Warp	198	148	74.8
		Fill	134	102	76.2
Fortisan- 36 No Coating	8	Fill	428	358	83.7
Nylon with Neoprene Coating	10	Warp	145	133	91.8
		Fill	104	84	80.8
Nylon with Neoprene	2	Fill	49	24	49.0

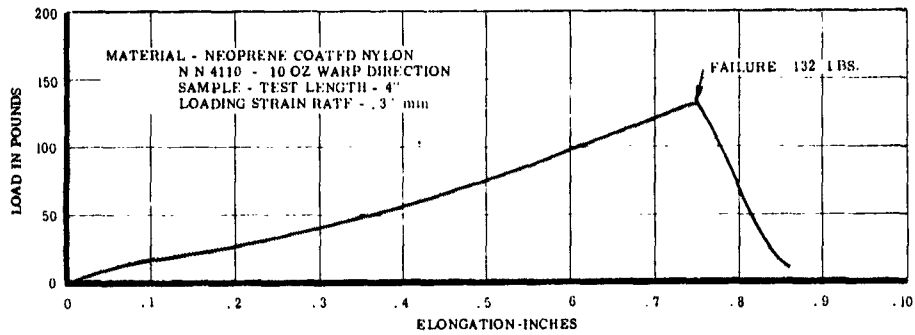
Exposure: 100 hours in weatherometer light equivalent to midday sun.

Strength: Tensile strength of 1" wide cut strip.

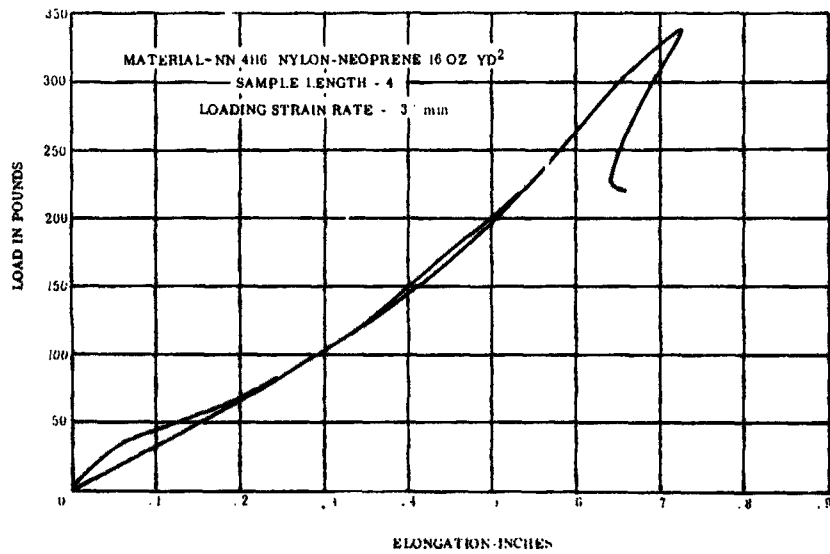
Figure 113 Results of Weatherometer Exposure Tests

Fabric	Coating	Total Wt./Sq. Yd.	Strength Lbs./In.	Notch Strength Lbs.	Notch to Un - Notched Ratio	St./Wt. Ratio
Fortisan-36	None	8 oz.	430	--	--	54
Nylon	Neoprene	16	250	40	.16	15.6
Nylon	Neoprene	10	150	--	--	15
Dacron	Mylar	7	185	75	.40	26.5
Dacron	None	4	150	60	.40	37.5
Dacron	None	3-1/4	90	37	.41	26.5
Dacron	None	5	150	53	.35	30
Dacron Scrim Weave	Mylar	3.3	75	35	.47	22.7
Nylon Rip Stop	Neoprene	2	50	16	.32	25
Dacron	Polyester	8	150	60	.40	19
Nylon	Polyester	7	140	34	.24	20

Figure 114 Fabric Tests

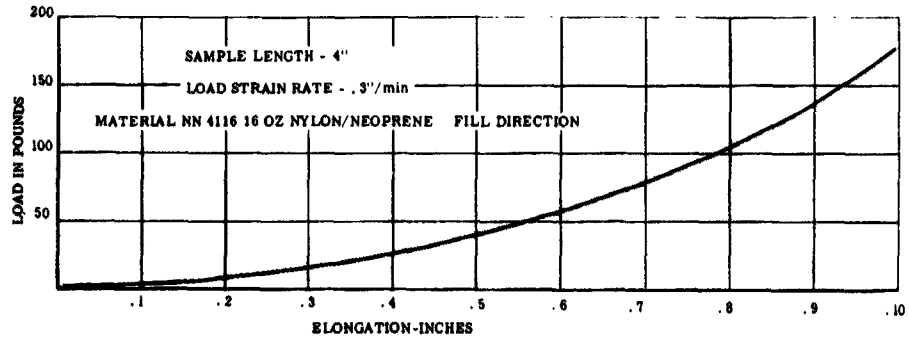


Test Load vs Elongation

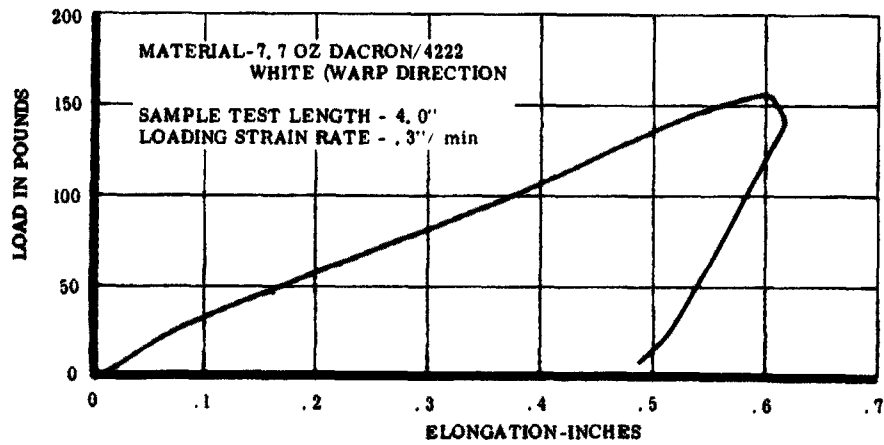


Test Load vs Elongation

Figure 115

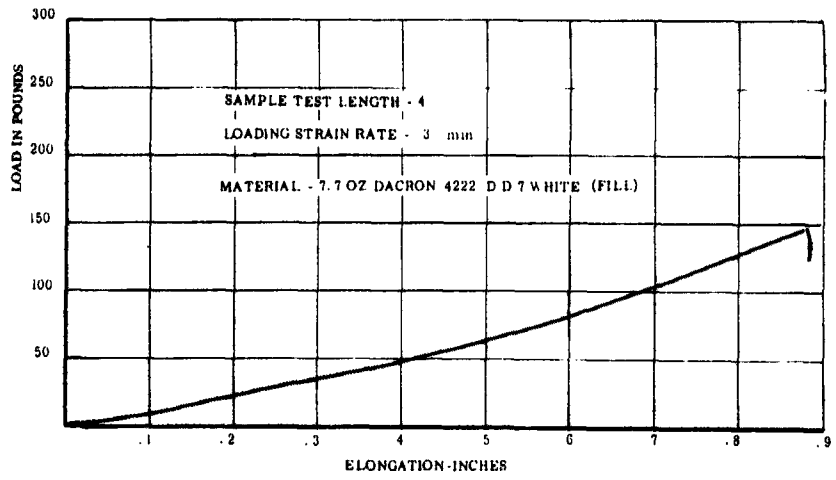


Test Load vs Elongation

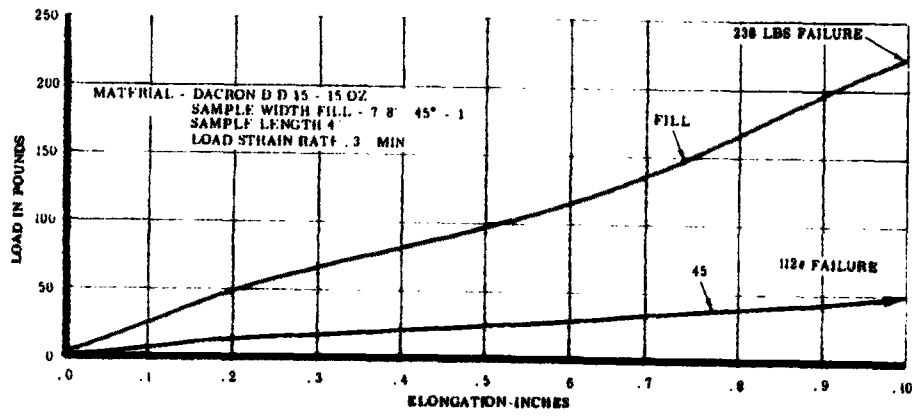


Test Load vs Elongation

Figure 116

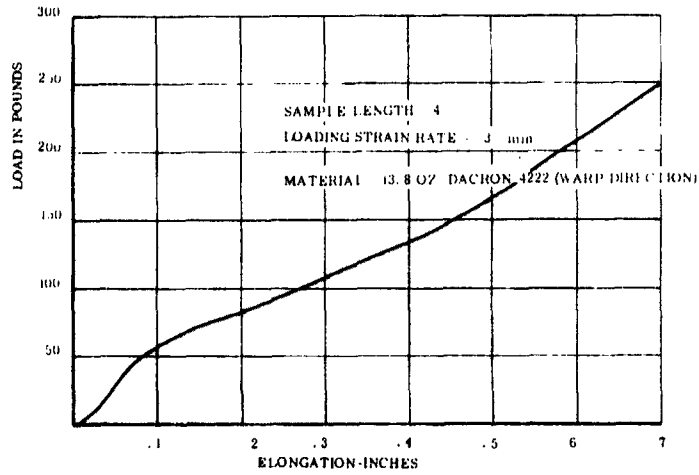


Test Load vs Elongation

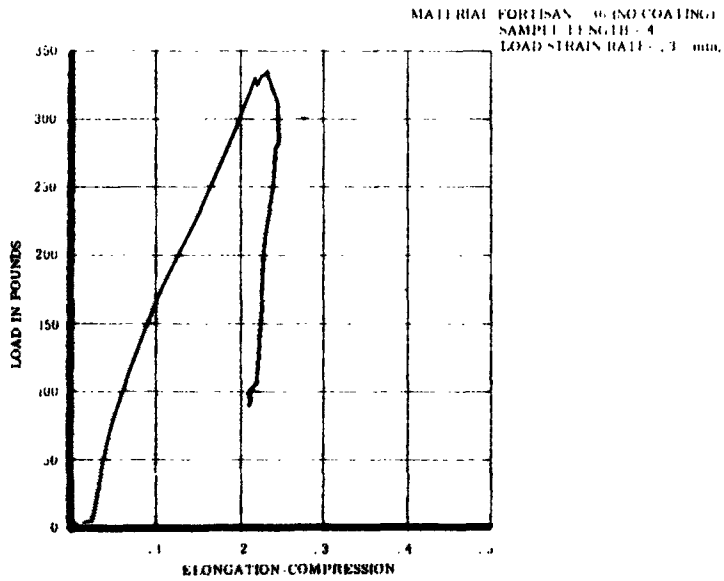


Test Load vs Elongation

Figure 117



Test Load vs Elongation



Test Load vs Elongation

Figure 118

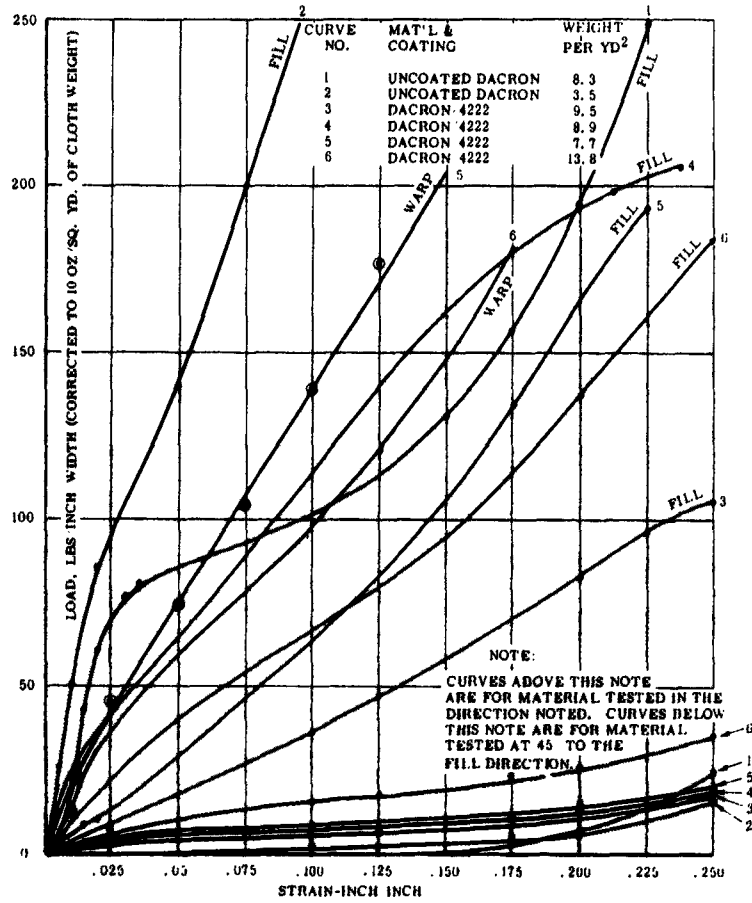


Figure 119 Test Load vs. Strain

**B. DIGITAL COMPUTER PROGRAM FOR FLEXIBLE WING CARGO  
GLIDER LANDING FLARE CALCULATIONS**

**Summary**

The flare portion of the landing approach of the unpowered glider is calculated on the IBM Type 650 MDDPM with a trapezoidal rule integration. Steady state, two degrees of freedom equations of motion are used, assuming that pitch-up has been accomplished prior to the flight segment under consideration. Velocity, altitude lost, and flight path angle are output. The integration is terminated at a desired input velocity. The grid variable is time.

**Development**

The assumption is made that the conditions are known after the transients resulting from the pitch-up to the landing attitude have subsided. The velocity and flight path angle sufficiently describe the flight condition in this case. From this point a constant  $C_L$  flare is accomplished, with the calculation arbitrarily terminated at a desired velocity, generally stalling speed.

From the diagram of forces in figure 1, the following equations may be written:

Summing forces along the flight path, with  $\gamma$  above horizontal:

$$-W \sin \gamma - D - M \frac{dv}{dt} = 0 \tag{1}$$

Summing forces normal to the flight path:

$$(L - W \cos \gamma) - (MV \frac{d\gamma}{dt}) = 0 \tag{2}$$

Equation (1) may be rewritten in differential form:

$$dv = - \frac{1}{m} (W \sin \gamma + D)dt \tag{3}$$

Integrating:

$$V_2 - V_1 = - \int_t^{t_2} (g \sin \gamma + \frac{D}{m}) dt$$

$$V_2 = V_1 - (g \sin \gamma + \frac{D}{m}) \Delta t \quad (4)$$

For finite values of  $\Delta t$  in equation (4) average values of  $\gamma$  and  $D$  must be used. To evaluate  $\gamma_2$ ,  $d\gamma/dt$  of equation (2) may be solved:

$$\frac{d\gamma}{dt} = \frac{L - W \cos \gamma}{mV} \quad (5)$$

$$\gamma_2 = \gamma_1 + (d\gamma/dt) \times (\Delta t) \quad (6)$$

Equation (6) is used to estimate a trial  $\gamma_2$  is based on the instantaneous  $d\gamma/dt$  at point 1. Having estimated  $\gamma_2$ , a first approximation to  $V_2$  may be solved with successive trials, until two such calculations agree to within a preestablished tolerance of the order of  $\pm 0.1\%$ .

Altitude lost and rate of sink follow without iteration.

$$R/S = (V_{avg}) (\sin \gamma) \times (60) \quad (7)$$

$$\Delta h = R/S \times (\Delta t/60) \quad (8)$$

#### Usage Information

The problem is executed in SOAP II mode on the IBM 650. The program is presented in the Appendix with both the SOAP II instructions, and the corresponding translated machine language commands.

Required in-put follows, and is punched in standard 650 Data card format 10 digit words, 8 to a card, floating point format.

Card	Word	Symbol	Item	Units
1	1	$\rho$	Atmospheric Density	Slugs/ft. 3
	2	$g$	Acceleration due to gravity	ft/sec <sup>2</sup>
	3	$k_1$	Velocity Conversion Factor to f. p. s.	f. p. s. /input

Card	Word	Symbol	Item	Units
	4	$\Delta t$	Time Increment	Secs.
	5	Sref.	Coefficient Reference Area	ft <sup>2</sup>
2	1	C <sub>L</sub>	Lift Coefficient	-
	2	C <sub>D</sub>	Drag Coefficient	-
	3	v <sub>S</sub>	Termination Velocity	(f. p. s.) x (k <sub>1</sub> )
2	4	V <sub>I</sub>	Initial Velocity	(f. p. s.) x (k <sub>1</sub> )
	5	$\gamma_I$	Initial Flight Path Angle	Degrees
	6	W	Weight	lbs.
	7	Tol	Integration Tolerance	-

Output is one card per integration step:

Alt. Lost Horiz. Dist. V R/S Lift Drag QS

The order in which equations are solved follows:

1.  $qS_1 = 1/2 \rho v_1^2 S_{ref}$
2.  $L_1 = C_L qS_1$
3.  $D_1 = C_D qS_1$
4.  $\dot{\gamma}_1 = \frac{L_1 - W \cos \gamma_1}{mV_1}$
5.  $\gamma_2 = \dot{\gamma}_1 \Delta t$
6.  $V_2 = V_1 - (g \sin \gamma + D/m) \Delta t$
7.  $qS_2 = 1/2 \rho V_2^2 S_{ref}$

8.  $L_2 = C_L qS_2$
9.  $D_2 = C_D qS_2$
10.  $\dot{\gamma}_2 = \frac{L_2 - W \cos \gamma_2}{mV_2}$
11.  $\gamma_2 = \frac{(\dot{\gamma}_1 + \dot{\gamma}_2)}{2} \times \Delta t$
12.  $V_2^1 = V_1 - \left[ g \sin \left( \frac{\gamma_1 + \gamma_2}{2} \right) - \left( \frac{D_1 + D_2}{2m} \right) \right] \times \Delta t$
13. Return to 7 until  $\frac{V_2^1 - V_2''}{V_2''} \leq \text{Tolerance}$  then go to 14
14.  $R/S = \left( \frac{V_2^1 + V_1}{2} \right) \sin \left( \frac{\gamma_2 + \gamma_1}{2} \right) \times 60$
15.  $\Delta h = \left( \frac{R/S}{60} \right) \times \Delta t$
16. Print Output
17. If  $V_2 \leq V_s$  Terminate. If  $V_2 > V_s$  go to 18
18. Set  $V_1 = V_2$
- Set  $\gamma_1 = \gamma_2$
- Return to Step 1.

C. MODEL SPECIFICATION - STRENGTH AND RIGIDITY, FLIGHT LOADS

1. SCOPE

1.1 This specification contains the strength and rigidity requirements for flight loading conditions applicable to procurement of airplanes.

2. APPLICABLE DOCUMENTS

2.1 The following specifications, of the issue in effect on the date of invitation for bids, form a part of this basic specification to the extent specified herein or as considered applicable:

SPECIFICATIONS

Military

MIL-S-5711	Structural Criteria, Piloted Airplanes, Structural Tests - Flight
MIL-D-8708	Demonstration Requirements for Airplanes
MIL-A-8860	Airplane Strength and Rigidity - General Specification for
MIL-A-8866	Airplane Strength and Rigidity - Reliability Requirements, Repeated Loads, and Fatigue
MIL-A-8867	Airplane Strength and Rigidity - Ground Tests
MIL-A-8868	Airplane Strength and Rigidity - Data and Reports

3. REQUIREMENTS

3.1 General - Except as otherwise specified, the requirements herein apply to the complete airplane structure. Within the specified ranges of center of gravity position, strength is required for the specified values of the parameters and any lesser or intermediate values which may be critical and which are practicable of attainment.

3.1.1 Gross weight - The design gross weights shall be as follows:

- For 250 lbs. payload - Gross weight 375 lbs.
- For 1,000 lbs. payload - Gross weight 1,500 lbs.
- For 4,000 lbs. payload - Gross weight 6,000 lbs.
- For 8,000 lbs. payload - Gross weight 11,000 lbs.

3.1.2 Center of gravity positions - Tolerances for C. G. location will have to be established inasmuch as the fuselage attitude is dependant on C. G. location.

3.1.3 Configurations - The configuration for design conditions shall be: the basic, high drag, landing approach and T. O.

3.1.3.1 Removable and disposable mass items - Not applicable - except for the cargo.

3.1.4 Airspeeds - The airspeeds shall be those specified in Appendix.

3.1.5 Altitudes - The altitudes for flight loading conditions shall be: S. L., 5000' and 10000'.

3.1.6 Power Settings - Not applicable.

3.1.7 Pressurization - Not applicable.

3.1.8 Air load distribution - The distributions of airloads used in the structural design shall be those determined by the use of acceptable analytic methods and by the use of aerodynamic data which are demonstrated to be applicable. These data shall include the effects of Mach number, aeroelasticity, and thermal effects.

3.1.9 Positions of adjustable fixed surfaces - Not applicable.

3.1.0 Positions of cockpit enclosures, bomb-bay doors, landing gear and doors, dive recovery devices, and cowl flaps - Not applicable.

3.1.11 Torque on primary control surfaces - Not applicable.

3.1.12 Tab loads - Not applicable.

3.1.13 Unsymmetrical horizontal tail loads - Not applicable.

3.1.14 Fail safe - So far as is practicable, the structure of VU, VR, VT, VO, VS, VW, and VP airplanes shall be designed to fail safe. Following a fatigue failure or obvious partial failure of a single principal structural element, at least half of the ultimate strength required for flight loads shall remain. These requirements supplement the repeated load and fatigue requirements of Specification MIL-A-8866 and the ground test requirements of Specification MIL-A-8867.

3.1.15 Deformation of doors, cowling, locks, and fasteners - Doors, locking mechanisms, such as landing gear up locks and down locks, and cowling fasteners shall not deflect adversely from their intended positions at loads up to design limit load for each loading condition for which limit loads are specified. Unlocking, unlatching, or release of coverings, and unlocking or unfastening of mechanisms shall not occur at loads up to and including design ultimate for loading conditions for which limit or ultimate loads are specified, and at loads up to and including maximum design loads for landings. Doors, other than passenger, cargo, or baggage doors; cowling, and other coverings shall remain in place under design ultimate flight loads if 10 percent of the fasteners are unfastened or if one quick release fastener selected at random on each edge of a door or panel secured by these fasteners is unfastened.

3.2 Symmetrical flight conditions -

3.2.1 Balanced maneuver - The airplane shall be in the basic and high drag configuration at all points on and within the maneuvering envelope bounded by O, A, B, C and O on the flight envelope as specified in Appendix. It shall be assumed that the pitching acceleration is zero.

3.2.2 Symmetrical maneuver with pitch - Not applicable.

3.2.3 Landing approach configuration pull-out - The vehicle shall be at the limit speed  $V_{LF}$  (See Spec. MIL-A-8860-6.2.3.9) in the landing-approach configuration. The load factors shall be all values from 0 to 2.0.

3.3 Unsymmetrical flight conditions - Not applicable due to the air loads being symmetrical about the center line of the wing.

3.4 Spins - Not applicable.

3.5 Vertical gusts - The vehicle shall be in the landing configuration at speeds up to  $V_{LF}$  and shall encounter at 50 FPS-EAS gust. The airplane shall be in the basic configuration at speed  $V_G$  (see below) and shall encounter a 66 FPS-EAS gust.

3.5.1 Speed for maximum gust intensity - The speed  $V_G$  shall be the speed given in the V-N diagram -- See Appendix.

3.5.2 The airplane resultant load shall be as specified in V-N diagram -- See Appendix.

3.5.3 Low altitude attack mission - Not applicable.

3.5.4 High altitude turns (USAF only) - Not applicable.

3.6 Horizontal gusts - The airspeeds, gust velocities, and other parameters of 3.5 shall apply, except that the gust factor shall be unity. A horizontal side gust shall be encountered.

#### 4. QUALITY ASSURANCE PROVISIONS

4.1 Design data - Structural design and analysis data shall be in accordance with Specification MIL-A-8868 modified to suit the peculiarities of the Flex Wing design.

4.2 Laboratory tests - Not applicable.

4.3 Flight tests - Not applicable.

#### 5. PREPARATION FOR DELIVERY

Not applicable.

#### 6. NOTES

6.1 Intended use - The requirements of this specification shall be used for the structural design and structural substantiation of Flex Wing Towed Logistic Vehicles.

D. MODEL SPECIFICATION - STRENGTH AND RIGIDITY, GROUND LOADS

1. SCOPE

1.1 This specification defines the strength and rigidity requirements for field-landing and ground-handling loads of land-based and carrier-based airplanes applicable to procurement of airplanes.

2. APPLICABLE DOCUMENTS

2.1 The following specifications and publication, of the issue in effect on the date of the invitation for bids, form a part of this basic specification to the extent specified herein:

SPECIFICATIONS

Military

MIL-W-5013	Wheel and Brake Assemblies; Aircraft
MIL-C-5041	Casings, Tire and Tubeless Tires; Aircraft Pneumatic
MIL-B-8584	Brake System, Wheel, Aircraft; Design of
MIL-A-8860	Airplane Strength and Rigidity - General Specification for
MIL-A-8863	Airplane Strength and Rigidity - Additional Loads for Carrier-Based Landplanes

PUBLICATION

AFTR 5815	Prediction of Dynamic Landing Loads
-----------	-------------------------------------

### 3. REQUIREMENTS

3.1 General - For conditions for which parameters or values of parameters are not completely specified to the extent necessary for the vehicle and its components to be in complete translation and rotational equilibrium, additional forces which are determined by a rational method or which are approved by the procuring activity shall be assumed to act in a manner such that the vehicle and its components are in equilibrium.

3.1.1 Weights - The design gross weights shall be as specified in Specification MIL-A-8860.

3.1.2 Weight distribution and center of gravity (CG) positions - Not applicable due to the peculiarity of the system using C. G. displacement for control.

3.1.3 Design loads - Limit and ultimate landing loads are not specified. The landing loads of 3.2 are design loads for which compliance with 3.1.4 of Specification MIL-A-8860 is required. For all other conditions the loads are limit loads.

3.1.4 Engine thrust - For the conditions of 3.2, the towing pull shall be all values from zero thrust to the maximum available.

3.1.5 Removable and disposable mass items - The load factors at store stations shall be those required at the appropriate design gross weight at the particular store location, multiplied by a factor commensurate with the elastic response of the structure.

#### 3.2 Landing

3.2.1 Landing loads analysis - The method of section 4 will be used. The effects of strut friction (where applicable) shall be included in the analysis. Conditions considered shall be all those critical throughout the landings and shall include at least the following:

- (a) Maximum spin-up load in combination with the vertical load occurring at the instant of maximum spin-up load.
- (b) Maximum spring-back load in combination with the vertical load occurring at the instant of maximum spring-back load.

(c) **Maximum vertical load in combination with the drag load occurring at the instant of maximum vertical load which drag load shall not be less than one quarter of the maximum vertical load.**

3.2.2 Spin-up and spring-back loads - Corresponding to touch down speed of  $1.2 V_L$  shall be used.

3.2.3 Tire pressures - Tire pressures shall be all values between 90 and 110 percent of the pressure that will be recommended in the erection and maintenance instructions.

3.2.4 Strut servicing - The air pressures shall be all values between 90 and 110 percent of the value that will be recommended in the erection and maintenance instructions. The oil volume shall be all values within 90 and 110 percent of the recommended volume except that if 110 percent is not attainable, the maximum attainable value shall apply.

3.2.5 Wing lift - The wing lift shall be the vehicle weight.

3.2.6 Overland landings - The vehicle design shall be such that the design landing-gear reactions are not exceeded when the vehicle is landed at a weight of 1.15 times the vehicle landing design gross weight but with a vehicle sinking speed of  $\sqrt{1/1.15}$  times the specified maximum design sinking speed.

3.2.7 Design sinking speed - Shall be 10 fps at design gross weight.

3.2.8 Symmetrical landings - The vehicle shall land in the following attitudes:

1. Front wheels touching first.
2. Rear wheels touching first.

3.2.9 Drift landing - The vehicle shall be in: (a) nose up, (b) nose down attitude. The vertical reaction on each gear shall be equal to one-half of the maximum vertical reaction obtained from two-point symmetrical landing. The side load on one gear shall consist of an inward acting load of 0.8 times the specified vertical reaction at that gear. Both side loads shall act simultaneously at the ground and be resisted by inertia of the vehicle. Drag loads shall be zero.

3.3 Taxiing.

3.3.1 Braking - For braking conditions, the landing gear and tires shall be in their static positions.

3.3.1.1 Two point braked roll - Not applicable.

3.3.1.2 Four-point braked roll - The vehicle shall be in the four-point attitude. The vertical load factor acting at C. G. shall be 1.2 at the vehicle gross weight. A drag reaction at each wheel in contact with the ground equipped with brakes, shall be assumed acting at the ground equal to .8 of the vertical reaction and shall be combined with the vertical reaction.

3.3.1.3 Unsymmetrical braking - Not applicable.

3.3.1.4 Reverse braking - The vehicle shall be in the three-point attitude. The vertical load factor at the C. G. shall be 1.0. a forward acting drag reaction, acting at the ground equal to .8 of the vertical reaction, shall be combined with the vertical reaction for each gear that is equipped with brakes.

3.3.1.5 Wheel, brakes, and tire heating - In the selection of wheels, brakes, and tires for Navy airplanes, the requirements of Specifications MIL-W-5013, MIL-B-8584, and MIL-C-5041 are applicable. The heat generated during braking shall not result in stresses which will cause explosion or failure of these components during and subsequent to prolonged and repeated brake application.

3.3.2 Turning - Not applicable.

3.3.3 Pivoting - Not applicable.

3.3.4 Taxiing - Not applicable.

3.3.5 Special tail-gear conditions - Not applicable.

3.3.6 Tail-gear obstruction - Not applicable.

3.4 Handling conditions -

3.4.1 Towing - The vehicle shall be in four-point attitude. The vertical reactions on all four wheels shall be static. The towing bar shall be attached to the fuselage flight towing point or, if applicable,

to a special ground towing point. The towing bar loads shall be established in a rational or conservative manner. The towing conditions shall be as specified below. The values of the towing load shall be defined by the formula:

$$T = .3W$$

Condition	Towing Load	
	Direction From Forward	Magnitude
I	0°, = 30° = 150°, 180°	.75 T
II	0° and 180°	T

3.4.2 Jacking - Jacking loads shall be those specified in table IV. The vertical load shall act singly and in combination with the longitudinal load, the lateral load, and both longitudinal and lateral loads. The horizontal loads at the jack points shall be reacted by inertia forces so as to cause no change in the vertical loads at the jack points.

Table IV  
Jacking Loads

Component	Landing gear 4-point attitude
Vertical	1.35F
Longitudinal	0.4F
Lateral	0.4F

F is the static vertical reaction at the jack point

3.4.3 Hoisting - The airplane shall be in the level attitude. The vertical component shall be 2.0W.

3.4.4 Mooring - With the airplane secured in the static attitude with the wing collapsed, Navy airplanes shall be subjected to a 100-knot wind from any horizontal direction; USAF and USA airplanes shall be subjected to a 65-knot wind from any horizontal direction.

3.5 Miscellaneous -

3.5.1 Rebound - With the landing gear fully extended and not in contact with the ground, a rebound load factor of -20.0 shall act on the unsprung weight of the landing gear along the line of motion of the strut as it approaches the fully extended position.

3.5.2 Extension and retraction of landing gear - Not applicable.

3.5.3 Braking wheels in air - Not applicable.

3.5.4 Load distribution on multiple wheels - Not applicable.

3.5.5 Tail bumper - Not applicable.

3.5.6 Turn-over - Not applicable.

3.6 Ski loads - Not applicable.

E. REFERENCES - Part I

1. Hoerner, Sighard F.: Fluid Dynamic Drag. Published in 1958 by the author.
2. Higdon, A. and Stiles, W. B.: Engineering Mechanics, Prentice-Hall, Inc., 1957.
3. Aircraft Characteristics United States Army. United States Transportation School, Fort Eustis, Virginia.
4. Pratt and Whitney Spec. No. An-2035 (Rev. 3), Engine model R-985-AN-1, Curve No. T-663.
5. Hartman, E. P. and Bierman, David: The Aerodynamic Characteristics of Full-scale Propellers having 2, 3, and 4 blades of Clark Y and R. A. F. 6 Airfoil Sections. NACA Technical Report No. 640.
6. Abbott, I. R. and von Doenhoff, A. E.: Theory of Wing Sections. McGraw - Hill, 1949.
7. Jones, Bradley: Elements of Practical Aerodynamics. John Wiley & Sons, Inc., New York, 1950.
8. Dommasch, D. O., Sherby, S. S. and Connolly, T. F.: Airplane Aerodynamics, Pitman Publishing Corp., New York, 1951.
9. Merkle, E. N.: Substantiating Data for the Standard Aircraft Characteristics Charts for the HU-1B Helicopter. Bell Helicopter Company, Report No. 204-099-763, 6 June 1961.
10. Gessow, Alfred, and Tapscott, Robert J.: Charts for Estimating Performance of High-Performance Helicopters. NACA Technical Report No. 1266, 1956.
11. Gessow, Alfred and Crim, Almer D.: An Extension of Lifting Rotor Theory to Cover Operation at Large Angles of Attack and High Inflow Conditions. NACA Technical Note 2665, 1952.
12. Reynard, D. L.: Hiller Aircraft Corp. Report No. 58-61, Characteristics and Performance, Model H-23D, 21 March 1958.

**REFERENCES - PART II**

- (1) NASA Wind Tunnel Data, Unpublished.
- (2) DeYoung, John, and Harper, Charles W. : Theoretical Span Loading at Subsonic Speeds for Wings Having Arbitrary Plan Form. NACA Report No. 921, 1948.
- (3) USAF Stability and Control Handbook, Volumes 1 and 2, Glenn L. Martin Company, August 1956 (M-03671), Confidential.
- (4) Toll, Thomas A, and Queijo, M. J. : Approximate Relations and Charts for Low Speed Stability Derivatives of Swept Wings. NACA Technical Note 1581, 1948.
- (5) DeYoung, John: Theoretical Antisymmetric Span Loading for Wings of Arbitrary Plan Form at Subsonic Speeds. NACA Technical Note 2140, 1950.
- (6) Jacks, Alvin H. : Aerodynamic Forces, Moments, and Stability Derivatives for Slender Bodies of General Cross Section. NACA Technical Note 3283, 1954.
- (7) Tobak, Murray Reese, David E., and Beam, Benjamin H. : Experimental Damping in Pitch of 45° Triangular Wings. NACA Research Memorandum A50J26, 1950.
- (8) Perkins, Courtland D., and Hage, Robert E. : Airplane Performance, Stability and Control. John Wiley and Sons, Inc., 1949.
- (9) Maggin, Bernard, and Shanks, Robert E. : Experimental Determination of the Lateral Stability of a Glider Towed by a Single Towline and Correlation with an approximate Theory. NACA Research Memorandum L8H23, 1948.
- (10) Amer, Kenneth B. : Method for Studying Helicopter Longitudinal Maneuver Stability. NACA Technical Note 3022, 1953.

MODEL SPECIFICATION  
AS APPLIED TO THE DESIGN OF  
THE FLEXIBLE WING VEHICLE

To 3.5.1 Speed for Max. Gust Intensity

$$V_S = \frac{295.2 \frac{W}{S}}{C_{L_{\max}}} = 16.36 \sqrt{\frac{W}{S}} \quad \text{Knots}$$

$$V_G = R V_S = 2.5 V_S = 40.9 \sqrt{\frac{W}{S}} \quad \text{Knots}$$

Where R = 2.5 is max. symmetrical flight limit load factor.

To 3.5.2

$$R_{\text{Gust}} = 1 + \rho_o \frac{V_e U_{de} m K_w}{2 w/s} = 1 - .002378 \frac{1.688 V_G (\text{knots})(66)2.64K_v}{2 w/s}$$

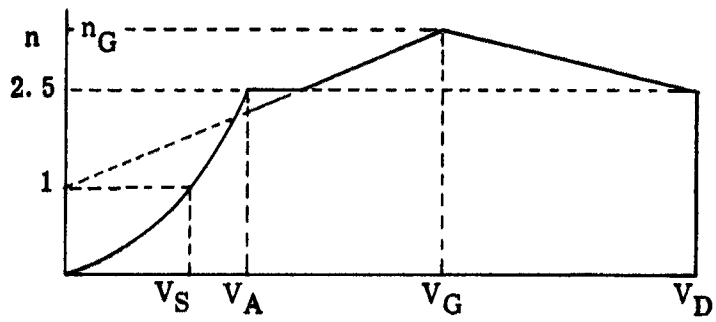
$$= 1 + .349 \frac{V_G K_w}{W/s}$$

In above Formula:  $V_{d_c} = 66 \text{ fps. } m = 2.64 \text{ RAD}^{-1} \text{ (Ref. 5 Fig. 1)}$

$$K_w = \frac{.88\mu}{5.3 + \mu} \quad \text{For } \mu = \frac{2 w/s}{g c m} \quad \text{(Ref. 2, Sec. 3.5.2)}$$

Where C = Average Chord =  $\frac{L}{2}$  (L = Keel Length)

$$\frac{4 W/s}{g L m}$$



V-n Diagram for Symm. Flight and Gusts

For values of  $V_S$ ,  $V_A$ ,  $V_G$  see Appendix II.

$V_D$  (preliminary - see Page 1 of this issue - to be later corrected for towing performance in descending flight).

E

7

MILITARY SPECIFICATION  
AS APPLIED TO THE DESIGN OF  
THE FLEXIBLE-WING VEHICLE

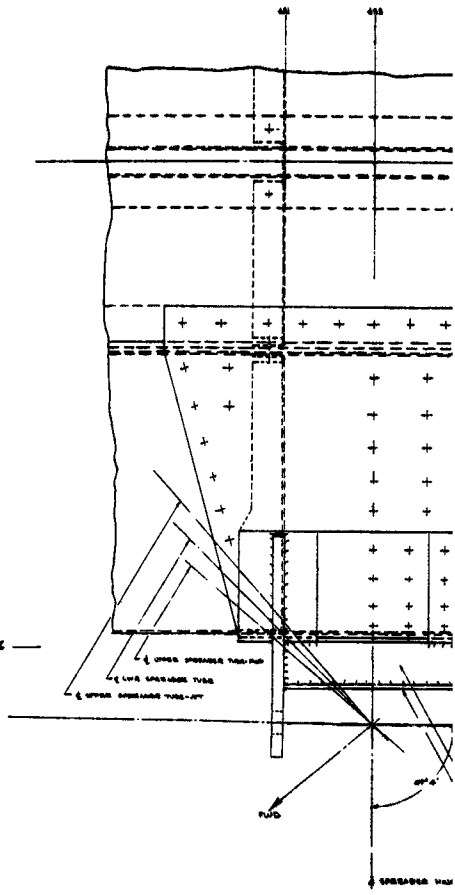
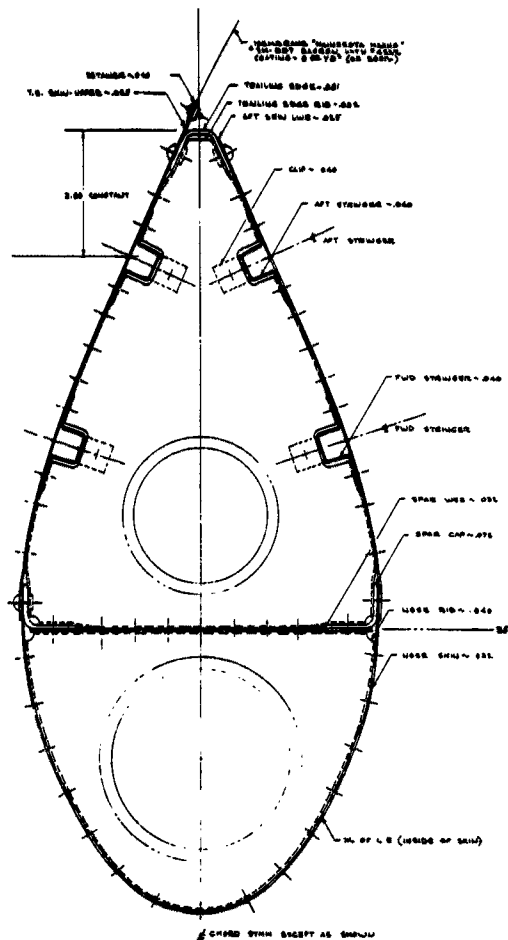
REFERENCES

1. MIL-A-8860
2. MIL-A-8861
3. MIL-A-8862
4. MIL-A-8868
5. Flexible-Wing Aerodynamic Characteristics - NASA Wind Tunnel Data of 4 April 1961.

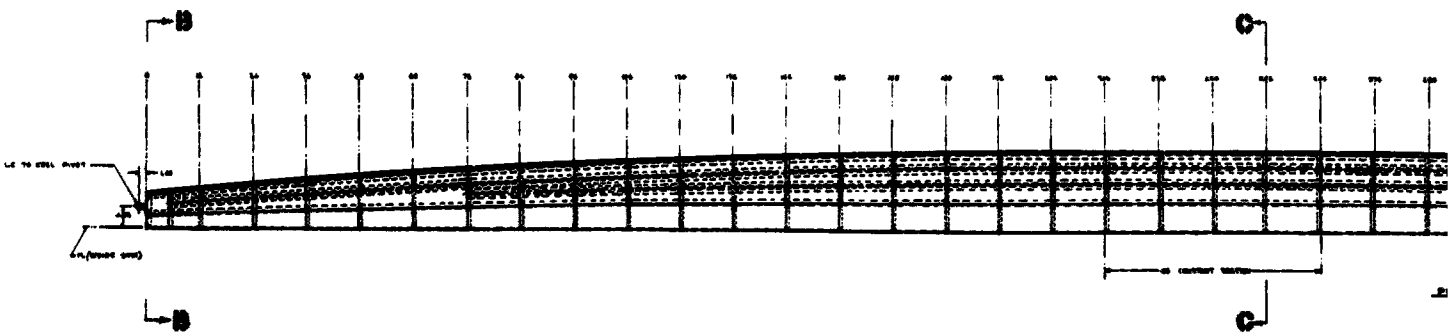
F. STUDY DRAWINGS

Various study configurations are indicated in the following Figures 120 through 127.

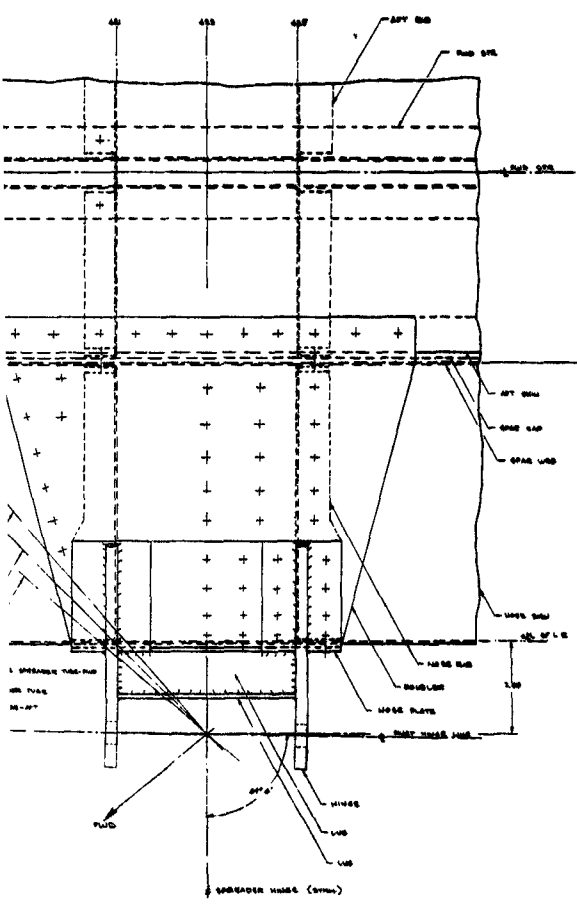
1



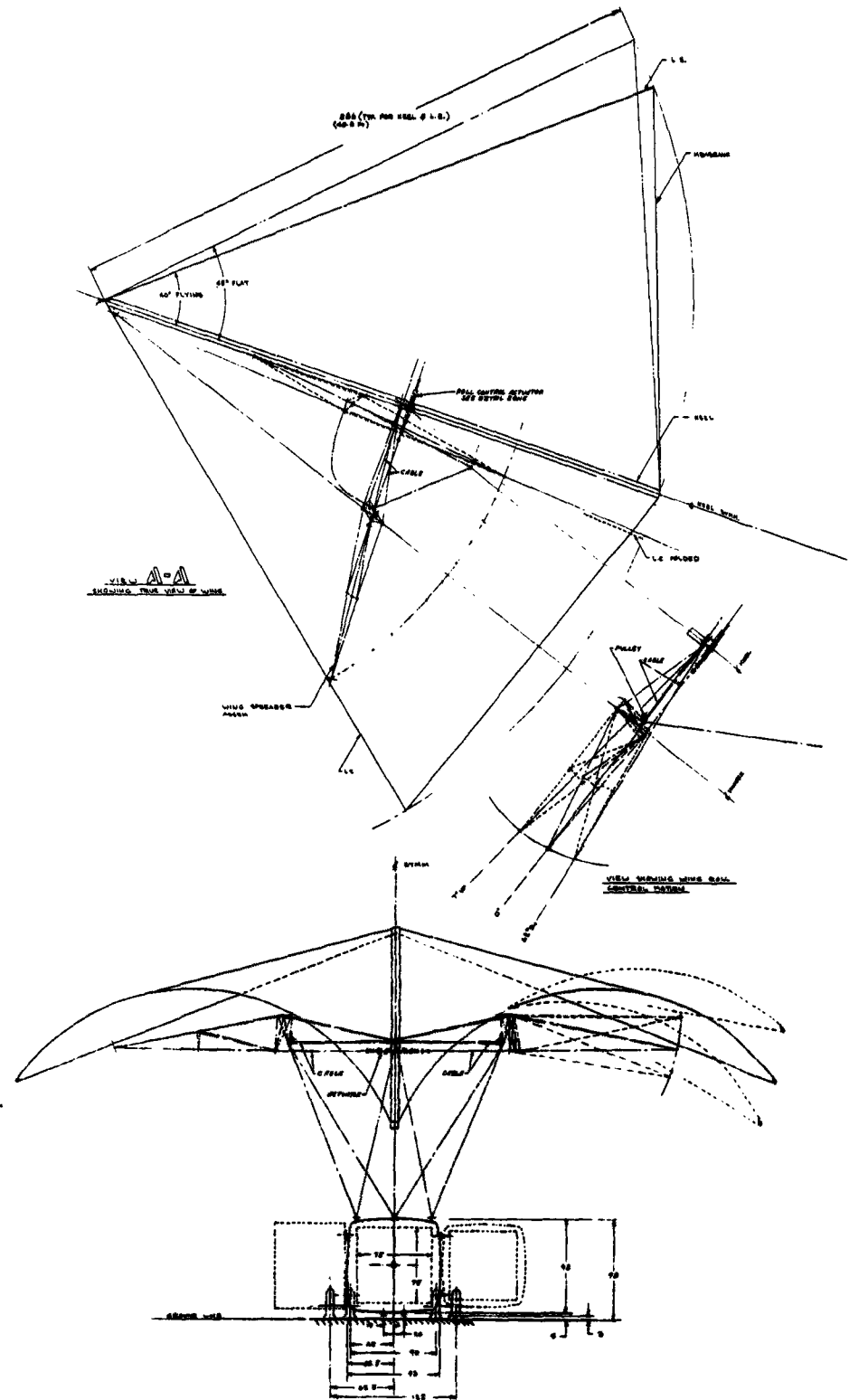
SECTION C-C  
TYPICAL  
FUS. SECTION



2



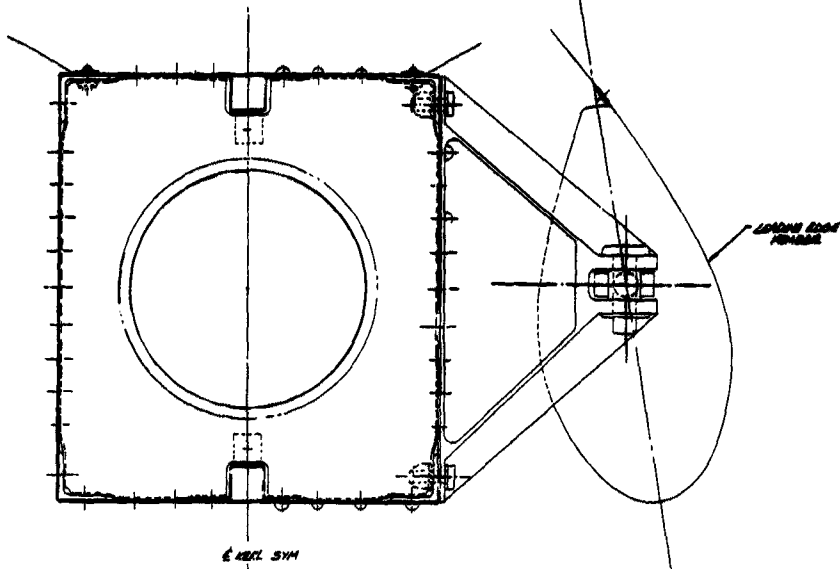




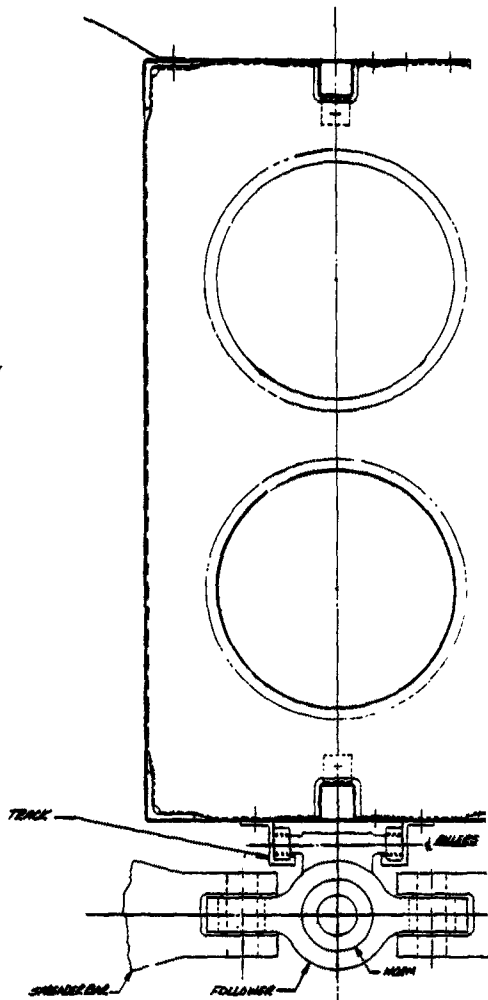
- DESIGN CRITERIA**
1. GROSS WEIGHT = 4000 LBS
  2. PAYLOAD = 8000 LBS
  3. WING AREA = 400 SQ FT
  4. WING SPAN = 100 FT
  5. WING CHORD = 40 FT
  6. WING WEIGHT = 1000 LBS
  7. WING BRACE = 100 LBS
  8. WING RIB = 100 LBS
  9. WING BRACE = 100 LBS
  10. WING RIB = 100 LBS
  11. WING BRACE = 100 LBS
  12. WING RIB = 100 LBS
  13. WING BRACE = 100 LBS
  14. WING RIB = 100 LBS
  15. WING BRACE = 100 LBS
  16. WING RIB = 100 LBS
  17. WING BRACE = 100 LBS
  18. WING RIB = 100 LBS
  19. WING BRACE = 100 LBS
  20. WING RIB = 100 LBS

Figure 120 Study - Flexible Wing Cargo Glider - 8000 Lb. Payload (B063-0009, Sheet 1 of 2)  
269

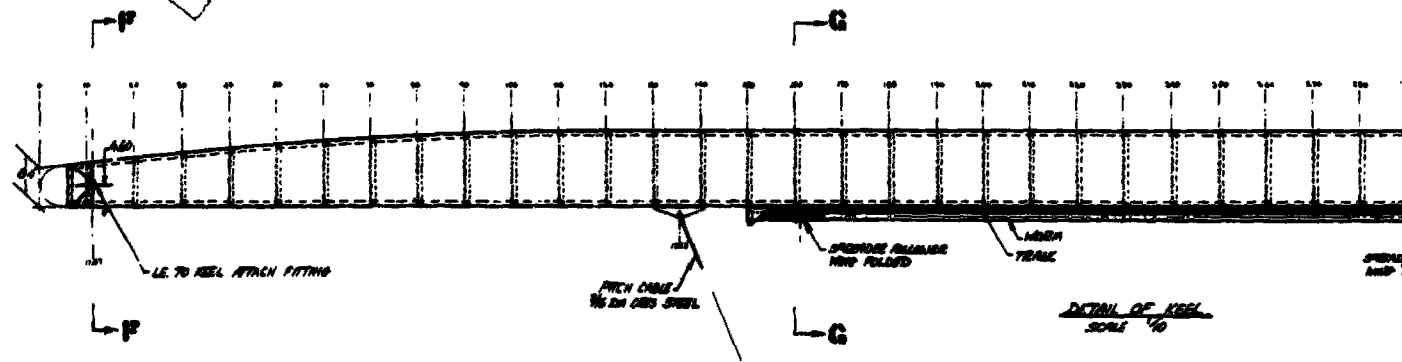
1



SECTION E-E  
LE TO REEL ATTACHMENT  
FULL SCALE

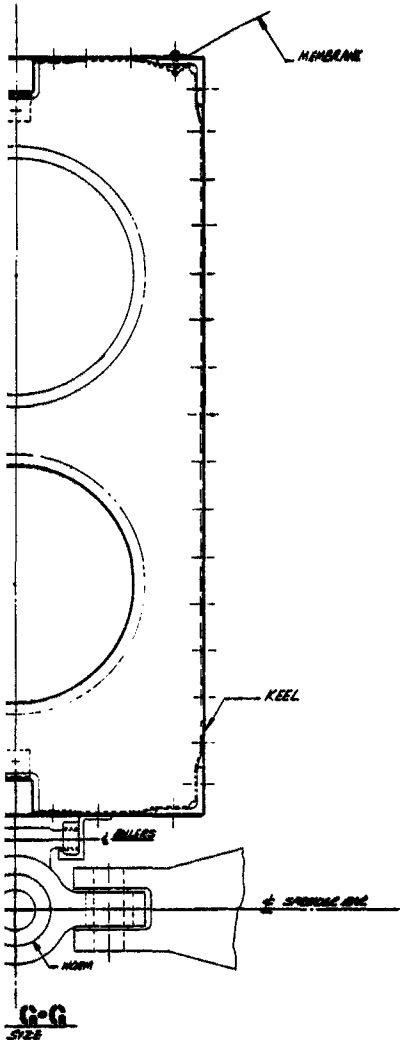


SECTION G-G  
FULL SIZE



DETAIL OF REEL  
SCALE 1/10

2



Note:  
1. For Keel Material and Gauges  
see Stress Report

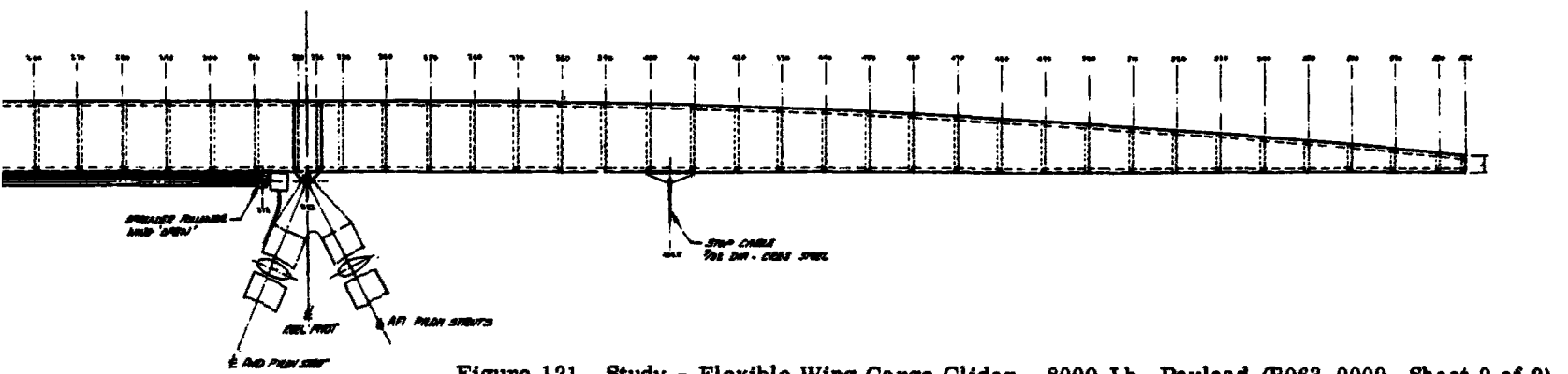
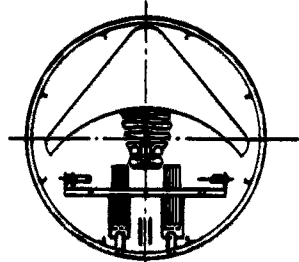


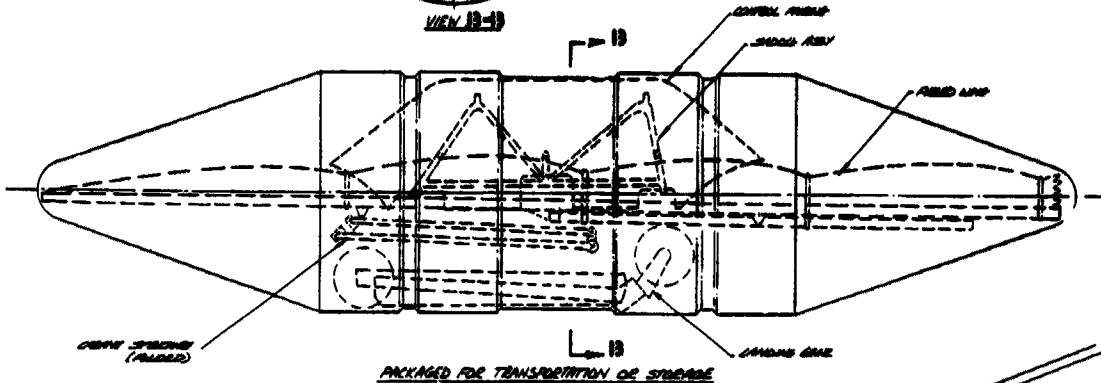
Figure 121 Study - Flexible Wing Cargo Glider - 8000 Lb. Payload (B063-0009, Sheet 2 of 2)  
271

1

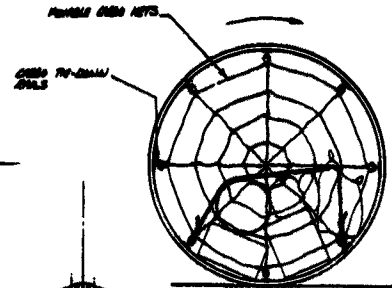
0280  
C28a



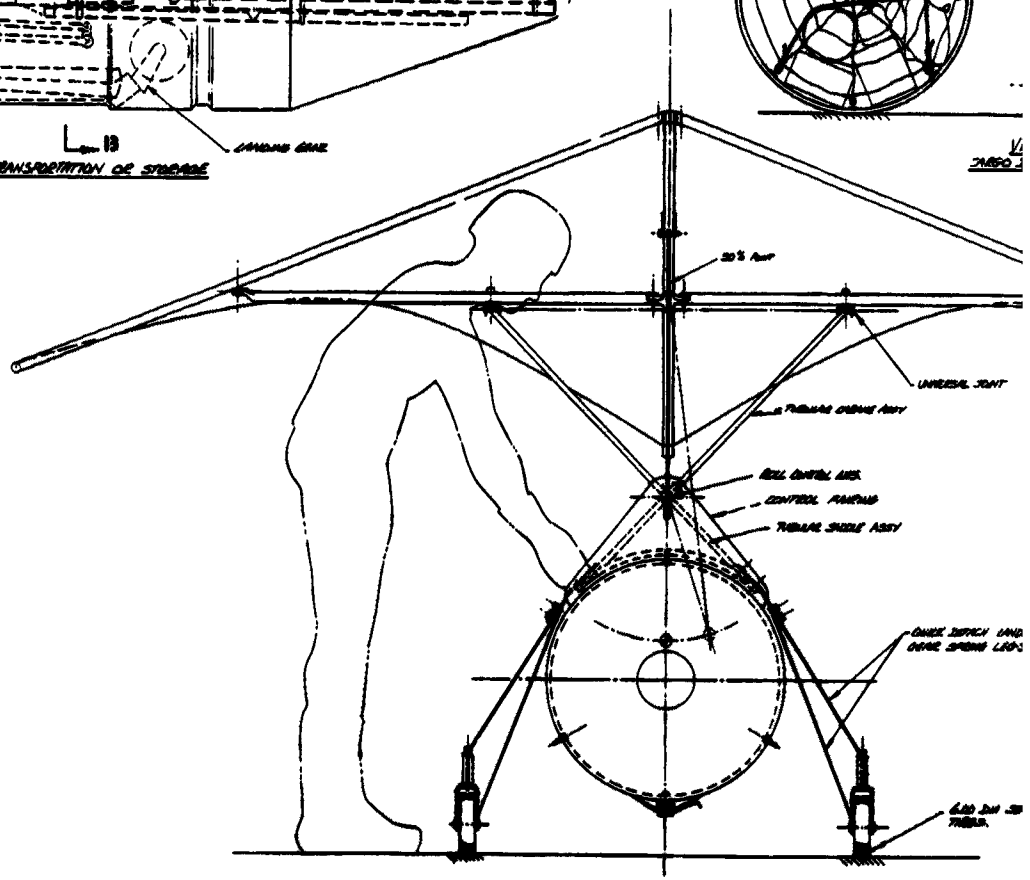
VIEW 13-13



PACKAGED FOR TRANSPORTATION OR STORAGE



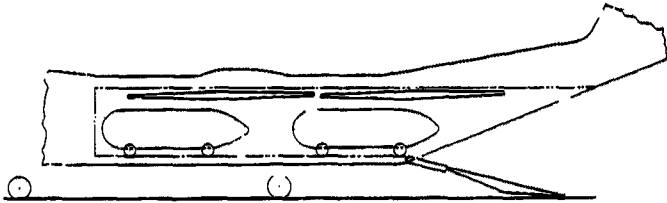
1/2  
PAGE 3



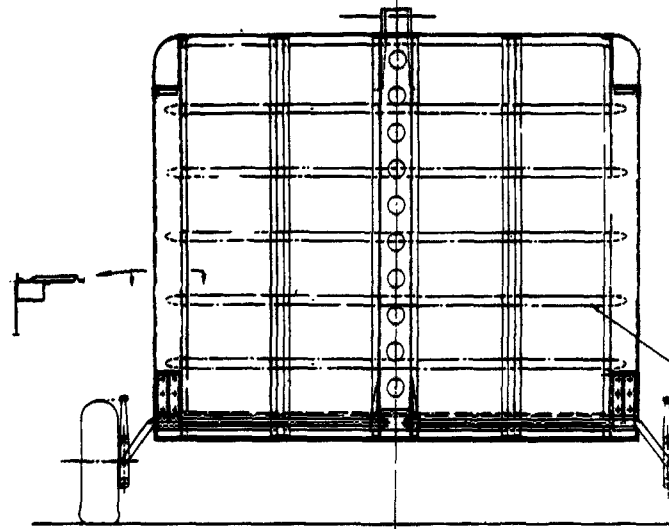




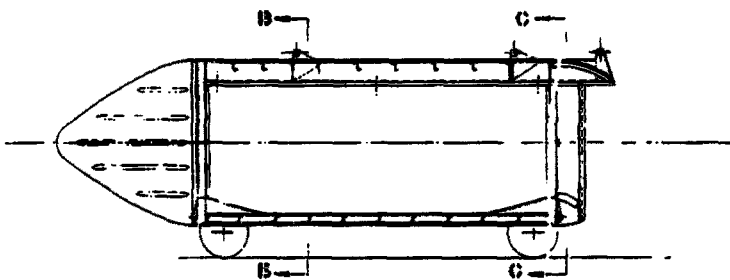
1



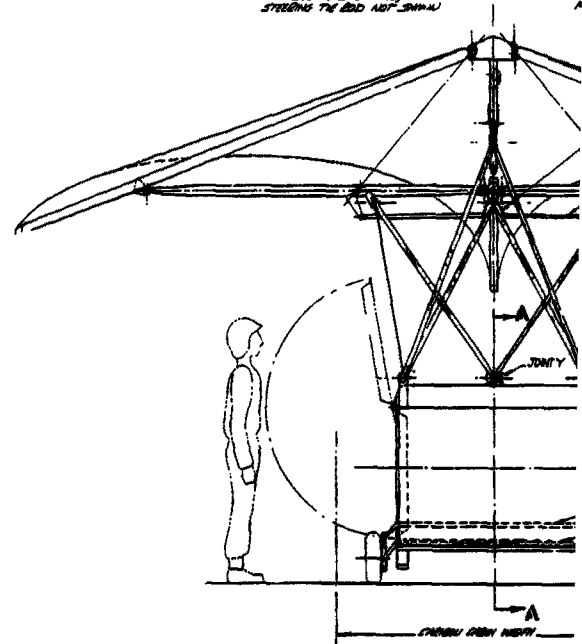
LOADED N.C.1 CARBON TUBE AIR DROP  
(1/8 SCALE)

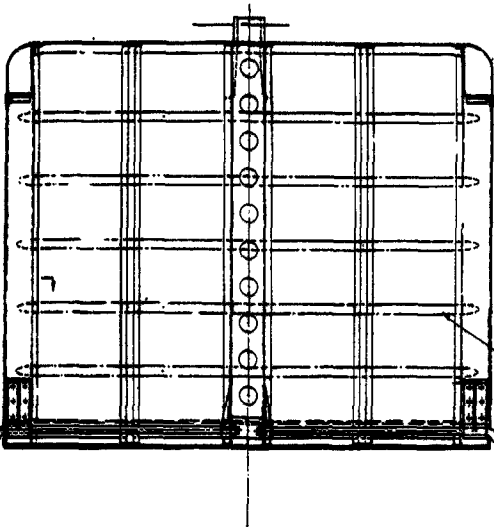


VIEW C-C (1/2 SCALE)  
FRONT BULKHEAD  
(NOT BULKHEAD SIMILAR)  
STEERING THE BODY NOT SHOWN

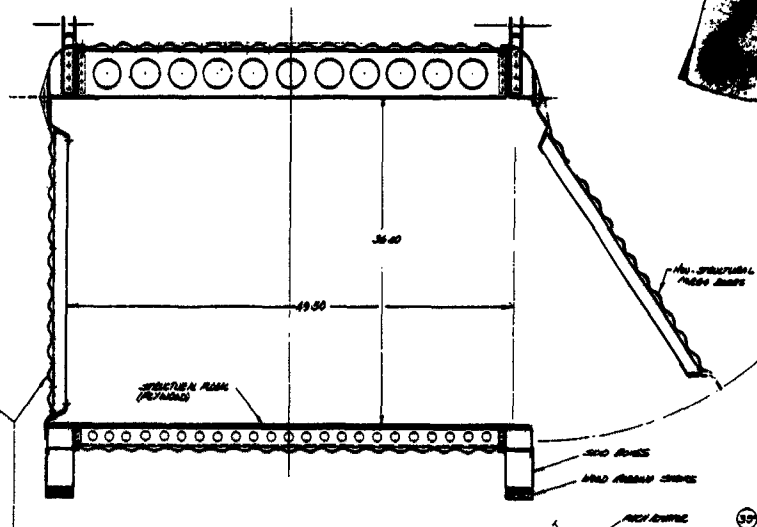


VIEW A-A  
SHOWING FRAME BODY STRUCTURE





VIEW G-G (+ SCALE)  
ROUNDED BULKHEAD  
(NOT BULKHEAD SIMILAR)  
STEEPNESS TO BE NOT SHOWN



VIEW B-B (+ SCALE)

SIMPLED STRUCTURE WITH MINIMUM WEIGHT OF  
CONNECTIONS, NEEDED STAYING BRACKETS ETC.  
MINIMUM NUMBER OF SUPPORTS  
MINIMUM OF OVERHANG, SPREADS OF JOINTS

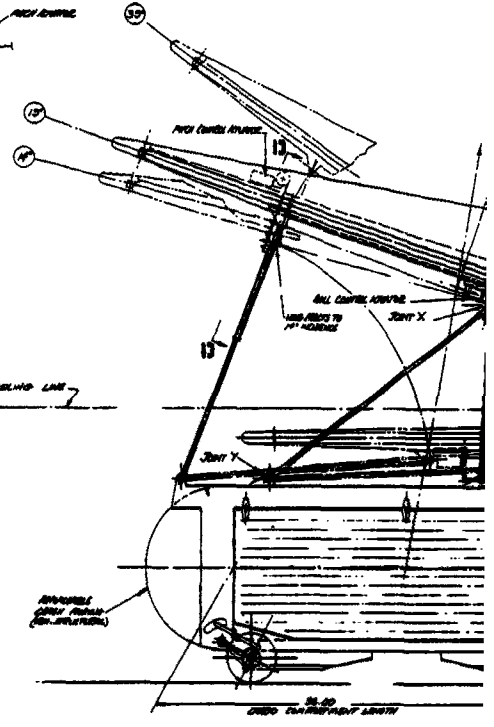
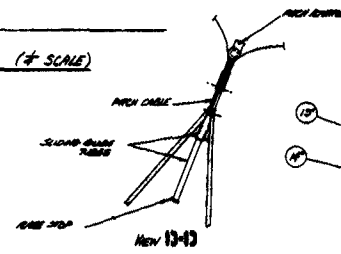
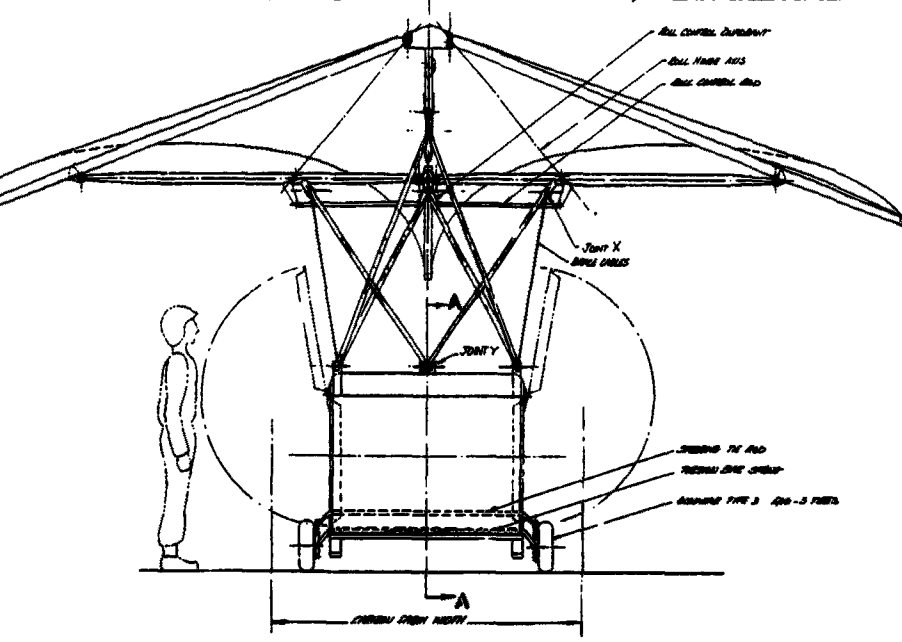
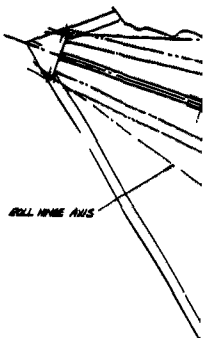
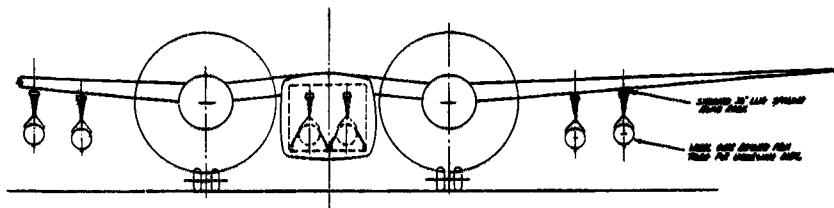


Figure 123 Detail Study - 1000 L

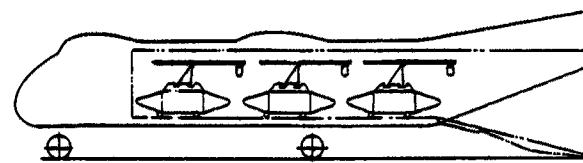


1

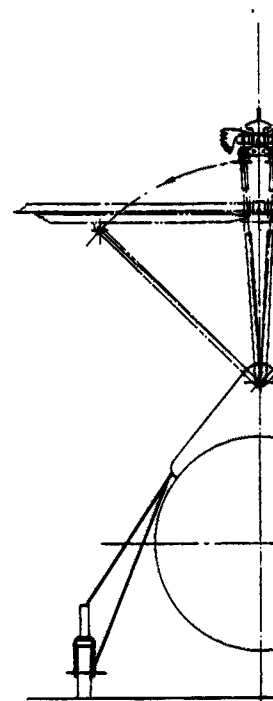


REMOVE ALL STRAPS  
FROM HERE

USE ONE STRAP FOR  
THEY ARE IDENTICAL



CARIBOU AIR-DRAG LOADING  
10 - 250 & HYPERBOL TRUSS  
1/4 SCALE





3

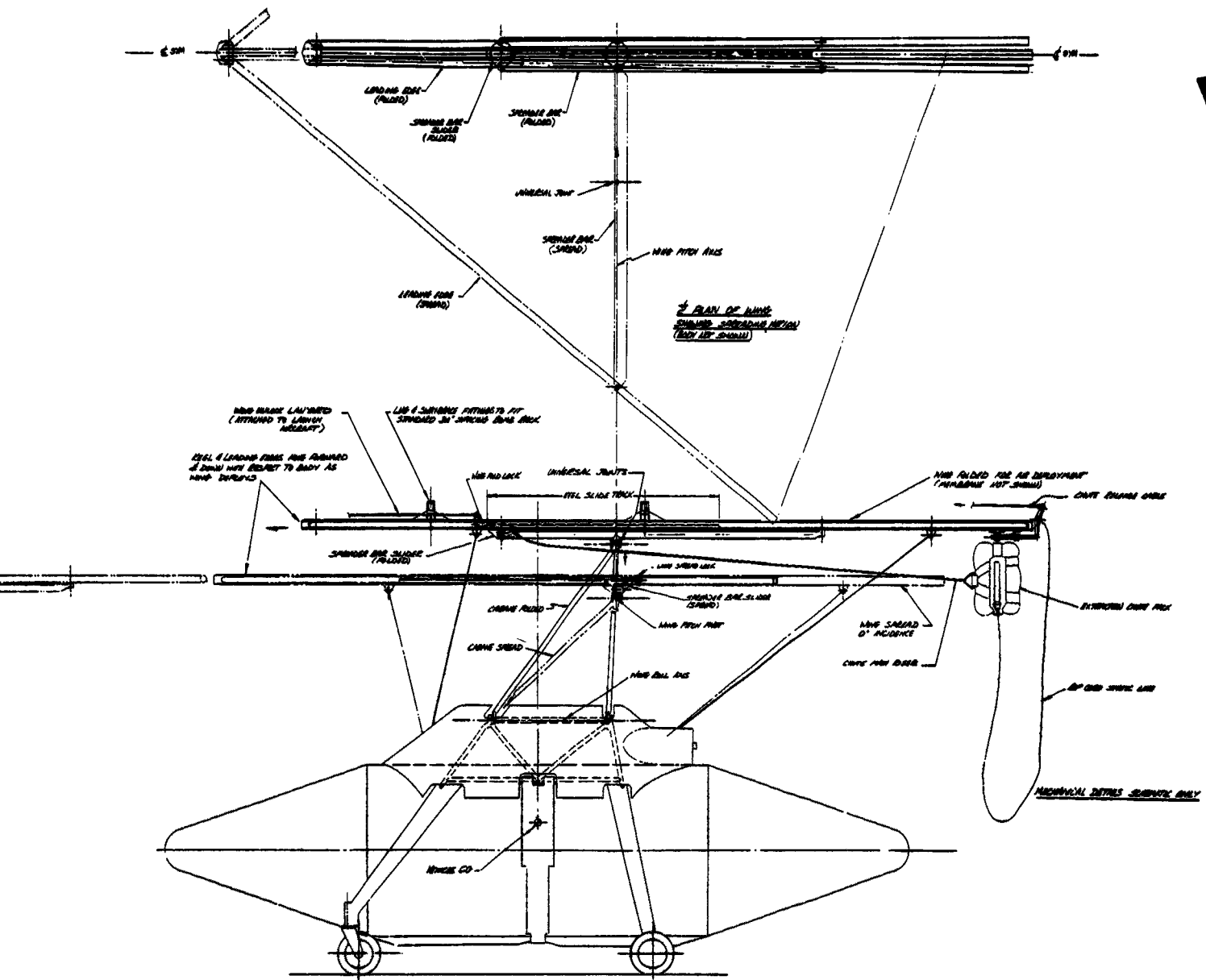


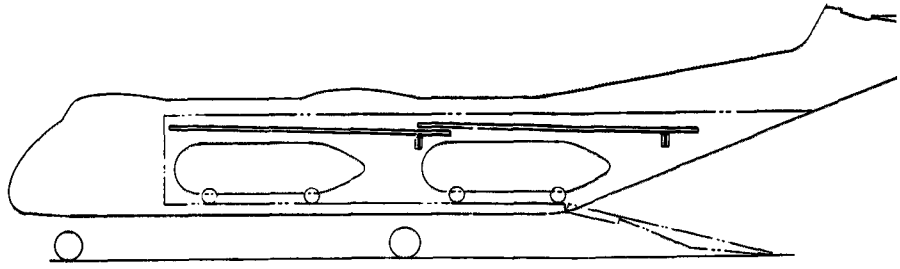
Figure 124 250 Lb. Payload Towed Glider Study - Air Drop Deployment (B063-0013)



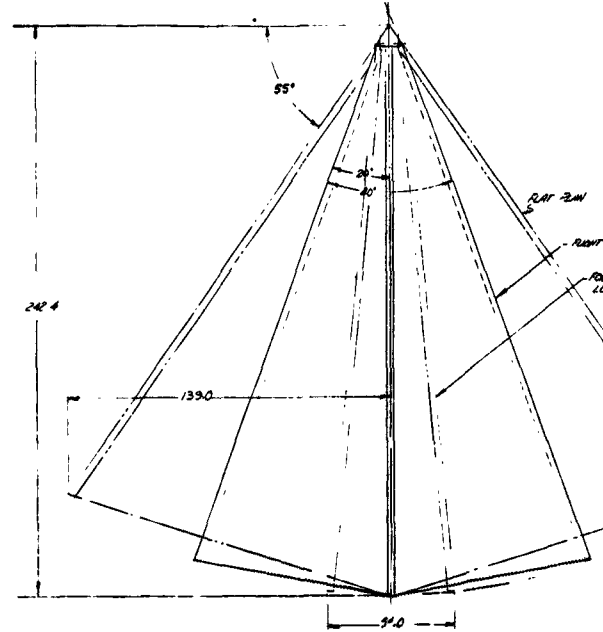
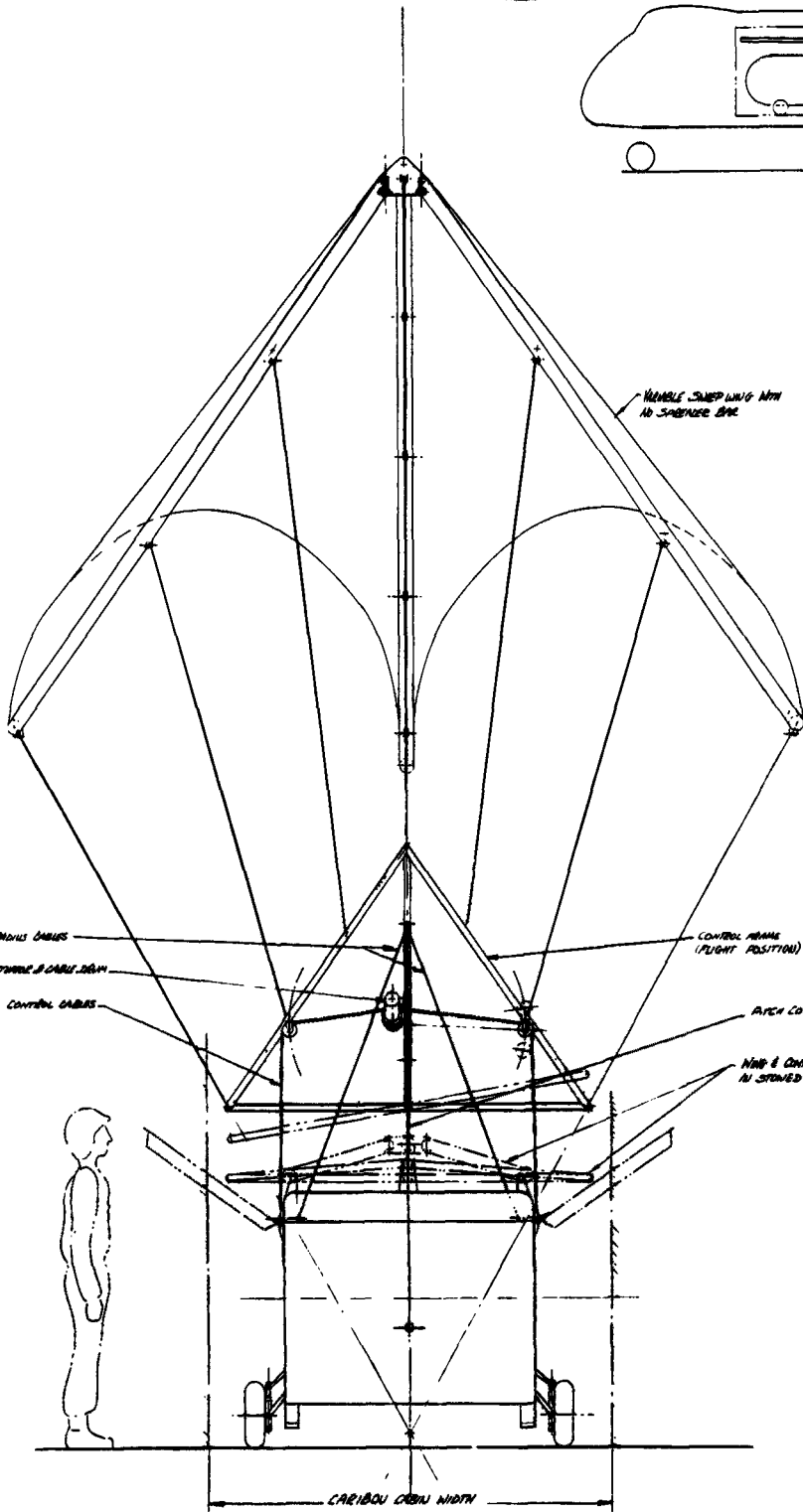




1



LOADED FOR CARIBOU AIRCRAFT (70)



BASIC WING GEOMETRY (KG)  
FLAT PLAN AREA 234 FT<sup>2</sup>

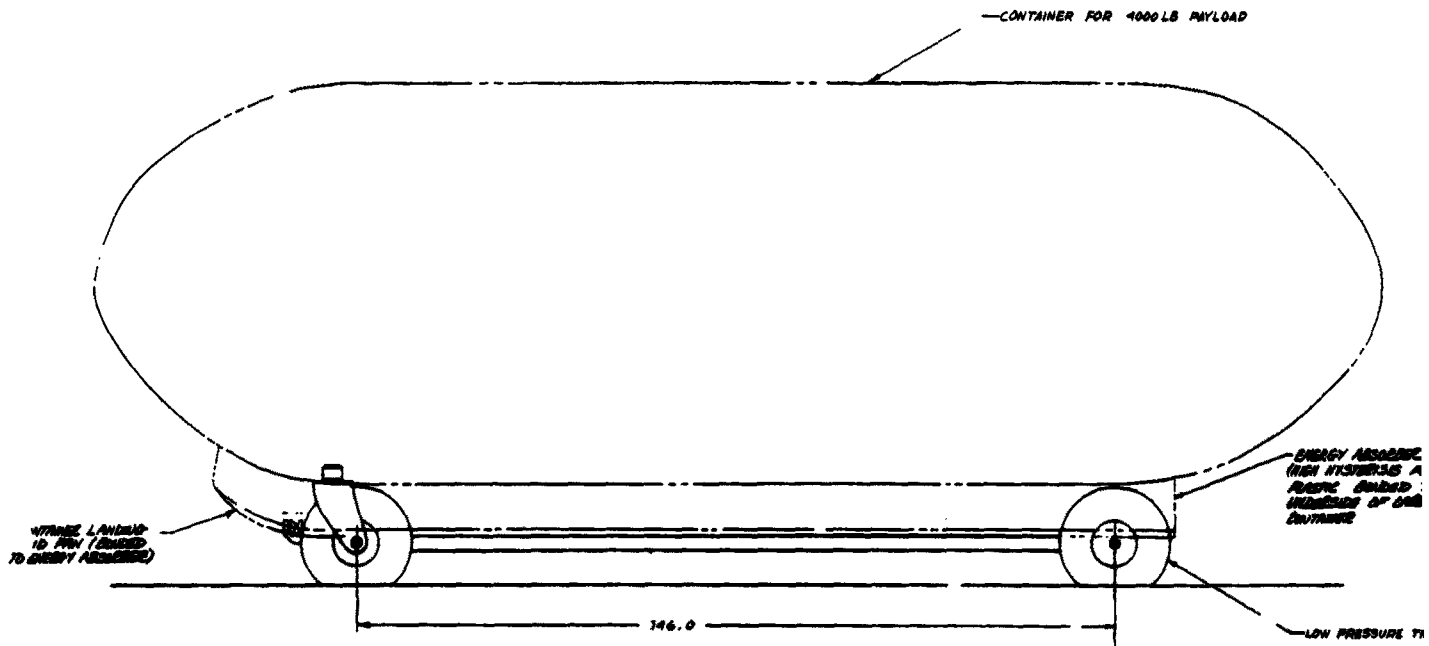
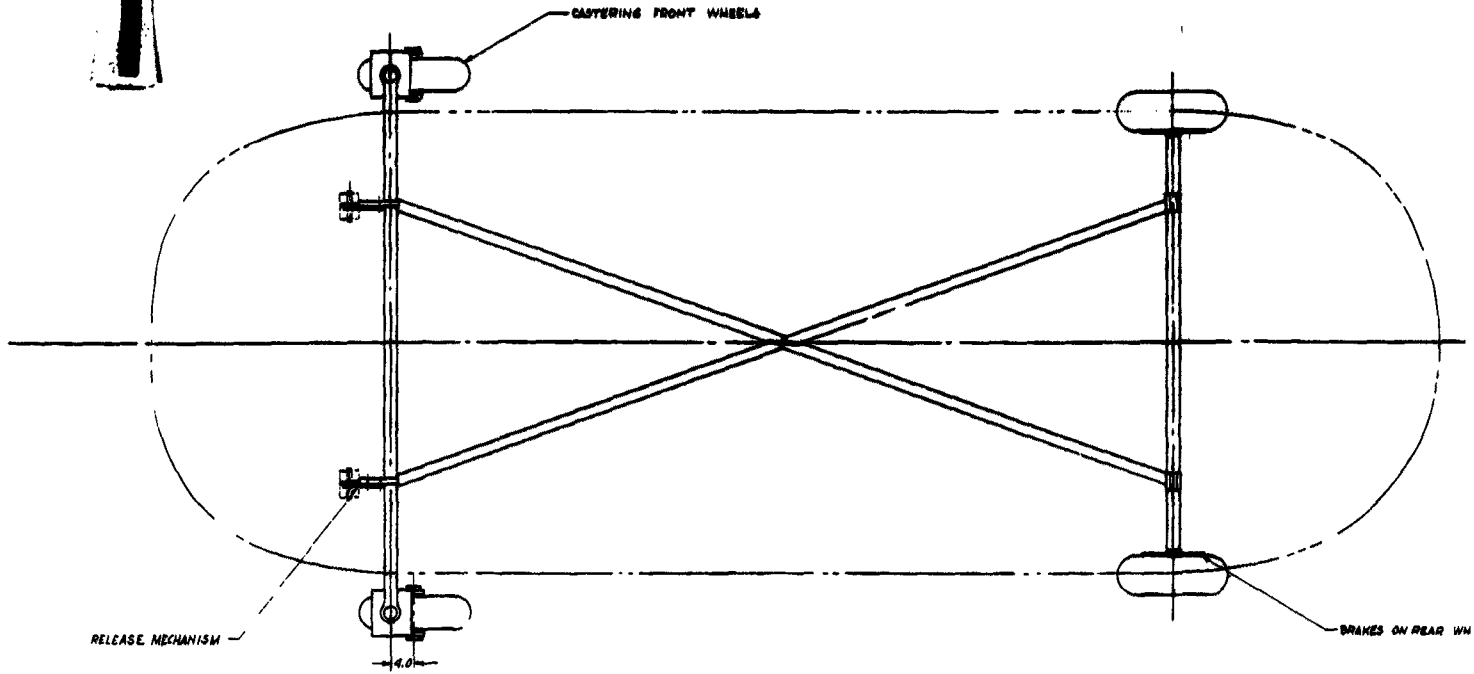
CARIBOU CEILING

View of  
in STD

- NOTE 1. WING CONFIGURATION & AERODYNAMIC DATA BASED ON APOLLO WIND TUNNEL TEST REPORT**
2. FOR BODY STRUCTURE PROPOSALS SEE 2065-0015
  3. GROSS WEIGHT 1400 LB
  4. PAYLOAD 1000 LB
  5. WING LENGTH 242.4 IN
  6. FLAT PLAN WING AREA 234 FT<sup>2</sup>
  7. WING LOADING 6.18/FT<sup>2</sup>
  8. CARGO VOLUME 36 FT<sup>3</sup>
  9. CARGO COMMITMENT DIMENSIONS 8 FT x 4 FT x 3 FT



1



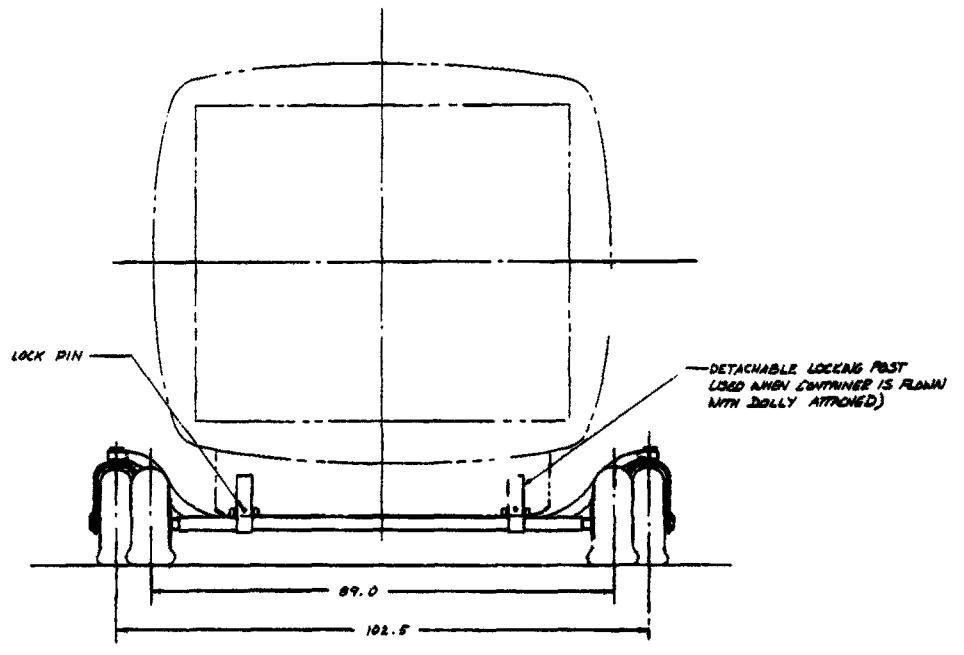
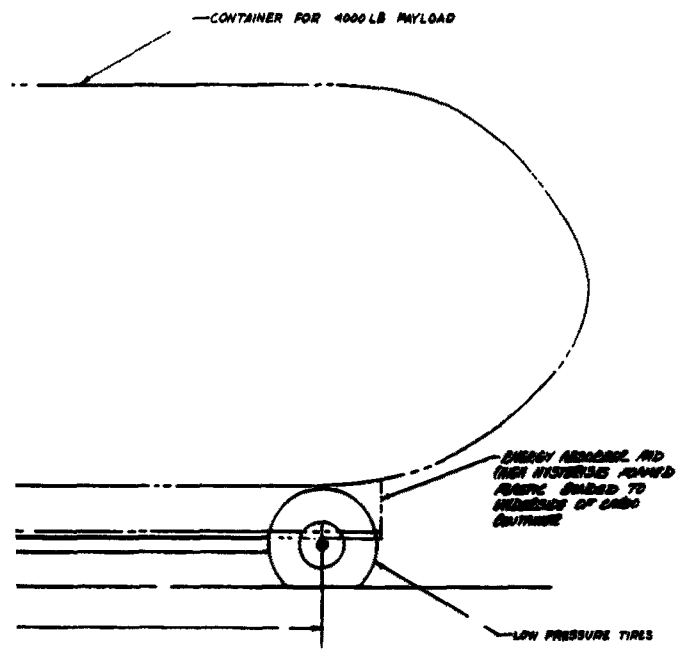
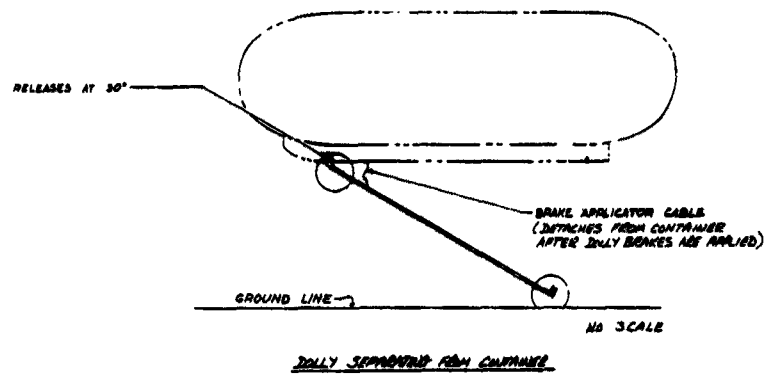
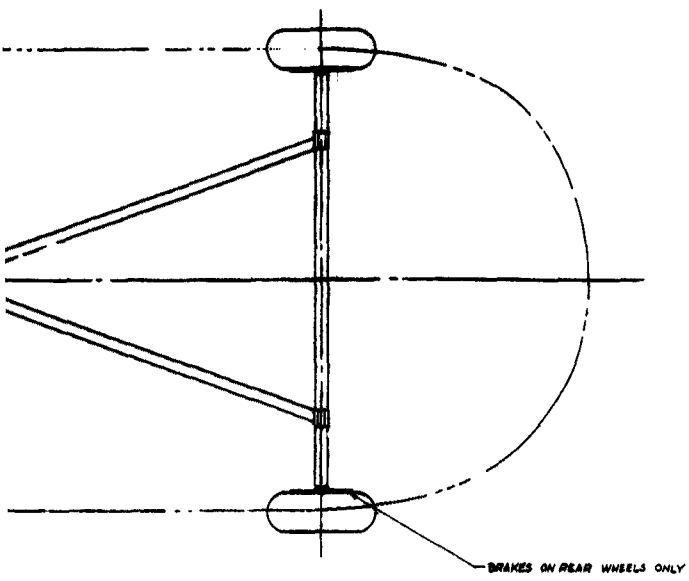


Figure 127 Study - Landing Gear  
283

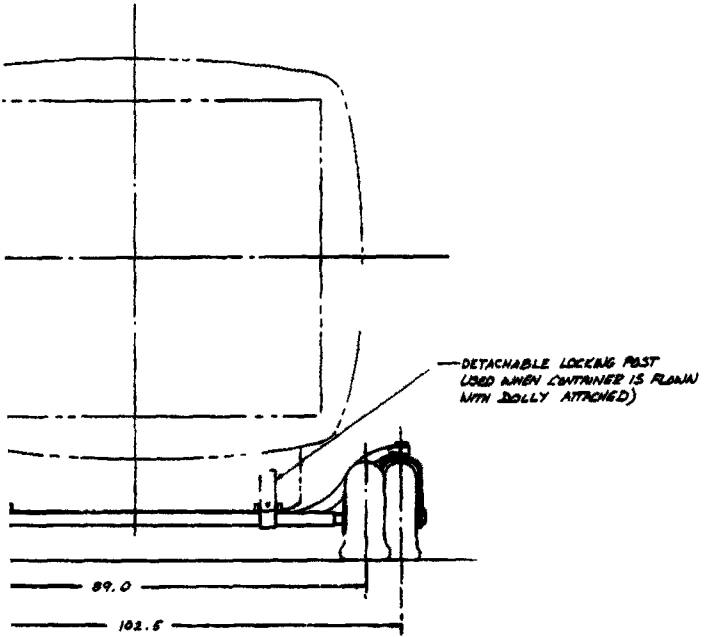
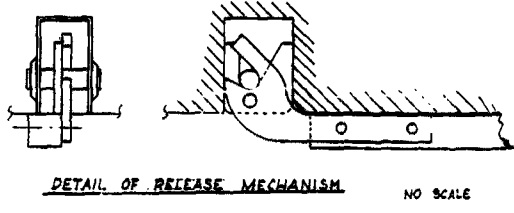
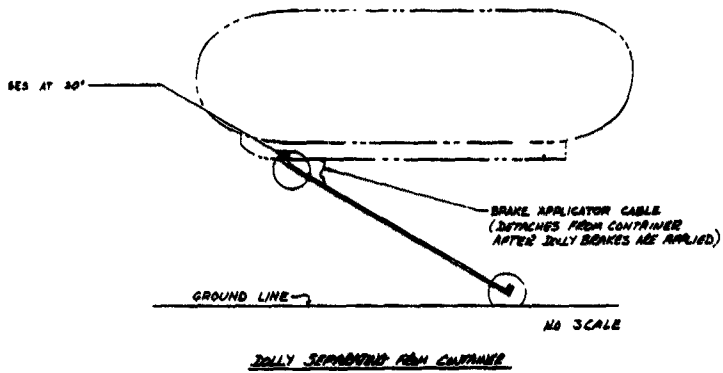


Figure 127 Study - Land

System (B063-0020)

## VI. DISTRIBUTION

USCONARC	3
First US Army	3
Second US Army	2
Third US Army	2
Fourth US Army	1
Sixth US Army	1
USAIC	2
USACGSC	1
USAWC	1
USAATBD	1
USA AVNS, CDO	1
USAARMBD	1
USAAVNBD	1
USATMC(FTZAT), ATO	1
DCSLOG	2
DCSOPS	1
Resch Anal Corp	1

USCDA	1
CofT	6
USATCDA	1
USATB	1
USATMC	20
USATC&FE	4
USATSCH	3
USATRECOM	48
USAEWES	1
USA Tri-Ser Proj Off	1
USATRECOM LO, USARD(EUR)	1
USATTCA	1
USATTCP	1
TCLO, USAABELCTBD	1
USACOMZEUR	3
USATDS	5
USARPAC	1

EUSA	1
USATAJ	6
USARYIS/IX CORPS	2
USARHAW	3
USARCARIB	4
ALFSEE	2
AFSC (SCS-3)	1
APGC (PGAPI)	1
Air Univ Lib	1
AFSC (Aero Sys Div)	2
CNR	3
BUWEPS, DN	5
ACRD(OW), DN	1
USNPGSCH	1
Day Tay Mod Bas	1
CMC	1
MCLFDC	1
MCEC	1

AMES RESEARCH CENTER, NASA	4
Lewis Rsch Cen, NASA	1
USASG, UK	1
BRAS, DAQMG (Mov & Tn)	4
ASTIA	10
HUMRRO	2
MOCOM	3
USSTRICOM	1
Ryan Aeronautical Company	20

AD \_\_\_\_\_ Accession No. \_\_\_\_\_  
Ryan Aeronautical Company, San Diego,  
California. Volume I. Flexible Wing Gliders,  
Final Program Summary Report. Volume II,  
Flexible Wing Cargo Gliders. Design Criteria  
and Aerodynamics.  
-- J. L. King, J. E. Fink, C. E. Craigo.

Report No. TCREC Tech. Report 62-3B  
September 15, 1962

\_\_\_\_\_pp (Contract DA-44-177-TC-779)

The final report of a study to determine the feasibility of the development of cargo gliders using the Rogallo type Flexible Membrane Wing. Designs are presented for configurations with payload capacities of 250, 1,000, 4,000 and 8,000 pounds each. Design and technical analysis of each configuration is presented. Requirements for the modification of standard air and rotor craft to be used for towing or air launching of the gliders are presented.

Unclassified

1. Flexible W  
Cargo Glid  
Design Cri  
and Aerod

2. Contract D  
177-TC-77

AD \_\_\_\_\_ Accession No. \_\_\_\_\_  
Ryan Aeronautical Company, San Diego,  
California. Volume I. Flexible Wing Gliders,  
Final Program Summary Report. Volume II,  
Flexible Wing Cargo Gliders. Design Criteria  
and Aerodynamics.  
-- J. L. King, J. E. Fink, C. E. Craigo.

Report No. TCREC Tech. Report 62-3B  
September 15, 1962

\_\_\_\_\_pp (Contract DA-44-177-TC-779)

The final report of a study to determine the feasibility of the development of cargo gliders using the Rogallo type Flexible Membrane Wing. Designs are presented for configurations with payload capacities of 250, 1,000, 4,000 and 8,000 pounds each. Design and technical analysis of each configuration is presented. Requirements for the modification of standard air and rotor craft to be used for towing or air launching of the gliders are presented.

AD \_\_\_\_\_ Accession No. \_\_\_\_\_  
Ryan Aeronautical Company, San Diego,  
California. Volume I. Flexible Wing Gliders,  
Final Program Summary Report. Volume II,  
Flexible Wing Cargo Gliders. Design Criteria  
and Aerodynamics.  
-- J. L. King, J. E. Fink, C. E. Craigo.

Report No. TCREC Tech. Report 62-3B  
September 15, 1962

\_\_\_\_\_pp (Contract DA-44-177-TC-779)

The final report of a study to determine the feasibility of the development of cargo gliders using the Rogallo type Flexible Membrane Wing. Designs are presented for configurations with payload capacities of 250, 1,000, 4,000 and 8,000 pounds each. Design and technical analysis of each configuration is presented. Requirements for the modification of standard air and rotor craft to be used for towing or air launching of the gliders are presented.

Unclassified

1. Flexible W  
Cargo Glid  
Design Crit  
and Aerody

2. Contract D  
177-TC-77

AD \_\_\_\_\_ Accession No. \_\_\_\_\_  
Ryan Aeronautical Company, San Diego,  
California. Volume I. Flexible Wing Gliders,  
Final Program Summary Report. Volume II,  
Flexible Wing Cargo Gliders. Design Criteria  
and Aerodynamics.  
-- J. L. King, J. E. Fink, C. E. Craigo.

Report No. TCREC Tech. Report 62-3B  
September 15, 1962

\_\_\_\_\_pp (Contract DA-44-177-TC-779)

The final report of a study to determine the feasibility of the development of cargo gliders using the Rogallo type Flexible Membrane W... Designs are presented for configurations with payload capacities of 250, 1,000, 4,000 and 8,000 pounds each. Design and technical analysis of each configuration is presented. Requirements for the modification of standard air and rotor craft to be used for towing or air launching of the gliders are presented.

Unclassified

1. Flexible Wing  
Cargo Gliders,  
Design Criteria  
and Aerodynamics

2. Contract DA 44-  
177-TC-779

Unclassified

1. Flexible Wing  
Cargo Gliders,  
Design Criteria  
and Aerodynamics

2. Contract DA 44-  
177-TC-779

<p>AD _____ Accession No. _____  Ryan Aeronautical Company, San Diego, California. Volume I, Flexible Wing Glider, Final Program Summary Report, Volume II, Flexible Wing Cargo Gliders, Design Criteria and Aerodynamics.  --J. L. King, J. E. Fink, C. E. Craigo.  Report No. TCREC Tech. Report 62-3A, December 28, 1961  _____pp (Contract DA-44-177-TC-779)</p> <p>The final report of a study to determine the feasibility of the development of cargo gliders using the Rogallo type Flexible Membrane Wing. Designs are presented for configurations with payload capacities of 250, 1,000, 4,000 and 8,000 pounds each. Design and technical analysis of each configuration is presented. Requirements for the modification of standard air and rotor craft to be used for towing or air launching of the gliders are presented.</p>	<p>Unclassified</p> <p>1. Flexible Wing Cargo Glider Final Program Summary</p> <p>2. Contract DA 44-177-TC-779</p>	<p>Accession No. _____  Ryan Aeronautical Company, San Diego, California. Volume I, Flexible Wing Glider, Final Program Summary Report, Volume II, Flexible Wing Cargo Gliders, Design Criteria and Aerodynamics.  King, J. E. Fink, C. E. Craigo.  o. TCREC Tech. Report 62-3A, December 28, 1961  (Contract DA-44-177-TC-779)</p> <p>report of a study to determine the feasibility of the development of cargo gliders using the Rogallo type Flexible Membrane Wing. Designs are presented for configurations with payload capacities of 250, 1,000, 4,000 and 8,000 pounds each. Design and technical analysis of each configuration is presented. Requirements for the modification of standard air and rotor craft to be used for towing or air launching of the gliders are presented.</p>	<p>Unclassified</p> <p>1. Flexible Wing Cargo Gliders, Final Program Summary</p> <p>2. Contract DA 44-177-TC-779</p>
<p>AD _____ Accession No. _____  Ryan Aeronautical Company, San Diego, California. Volume I, Flexible Wing Glider, Final Program Summary Report, Volume II, Flexible Wing Cargo Gliders, Design Criteria and Aerodynamics.  --J. L. King, J. E. Fink, C. E. Craigo.  Report No. TCREC Tech. Report 62-3A, December 28, 1961  _____pp (Contract DA-44-177-TC-779)</p> <p>The final report of a study to determine the feasibility of the development of cargo gliders using the Rogallo type Flexible Membrane Wing. Designs are presented for configurations with payload capacities of 250, 1,000, 4,000 and 8,000 pounds each. Design and technical analysis of each configuration is presented. Requirements for the modification of standard air and rotor craft to be used for towing or air launching of the gliders are presented.</p>	<p>Unclassified</p> <p>1. Flexible Wing Cargo Glider Final Program Summary</p> <p>2. Contract DA 44-177-TC-779</p>	<p>Accession No. _____  Ryan Aeronautical Company, San Diego, California. Volume I, Flexible Wing Glider, Final Program Summary Report, Volume II, Flexible Wing Cargo Gliders, Design Criteria and Aerodynamics.  King, J. E. Fink, C. E. Craigo.  o. TCREC Tech. Report 62-3A, December 28, 1961  (Contract DA-44-177-TC-779)</p> <p>report of a study to determine the feasibility of the development of cargo gliders using the Rogallo type Flexible Membrane Wing. Designs are presented for configurations with payload capacities of 250, 1,000, 4,000 and 8,000 pounds each. Design and technical analysis of each configuration is presented. Requirements for the modification of standard air and rotor craft to be used for towing or air launching of the gliders are presented.</p>	<p>Unclassified</p> <p>1. Flexible Wing Cargo Gliders, Final Program Summary</p> <p>2. Contract DA 44-177-TC-779</p>